

**THEORETICAL MODELS FOR MICROWAVE REMOTE SENSING
OF EARTH TERRAIN**

by

ROBERT TONG-IK SHIN

S.B., Massachusetts Institute of Technology
June 1977

S.M., Massachusetts Institute of Technology
February 1980

SUBMITTED IN PARTIAL FULFILLMENT OF THE
REQUIREMENTS FOR THE DEGREE OF

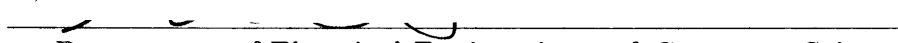
DOCTOR OF PHILOSOPHY

at the

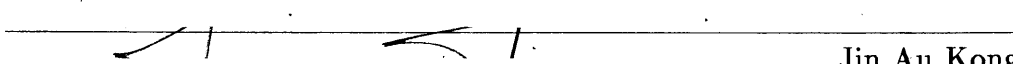
MASSACHUSETTS INSTITUTE OF TECHNOLOGY
September 1984

© Massachusetts Institute of Technology

Signature of Author


Department of Electrical Engineering and Computer Science
August 10, 1984

Certified by


Jin Au Kong
Thesis Supervisor

Accepted by


Arthur C. Smith
Chairman, Departmental Committee on Graduate Students

MASSACHUSETTS INSTITUTE
OF TECHNOLOGY

OCT 04 1984

LIBRARIES ARCHIVES



Room 14-0551
77 Massachusetts Avenue
Cambridge, MA 02139
Ph: 617.253.2800
Email: docs@mit.edu
<http://libraries.mit.edu/docs>

DISCLAIMER OF QUALITY

Due to the condition of the original material, there are unavoidable flaws in this reproduction. We have made every effort possible to provide you with the best copy available. If you are dissatisfied with this product and find it unusable, please contact Document Services as soon as possible.

Thank you.

Some pages in the original document contain pictures, graphics, or text that is illegible.

**THEORETICAL MODELS FOR MICROWAVE REMOTE SENSING
OF EARTH TERRAIN**

by

ROBERT TONG-IK SHIN

Submitted to the Department of Electrical Engineering and Computer Science
on August 10, 1984 in partial fulfillment of the requirements for the
Degree of Doctor of Philosophy

ABSTRACT

In the active and passive microwave remote sensing of earth terrain, scattering effects due to medium inhomogeneities and surface roughness play a dominant role in the determination of brightness temperatures and radar backscattering coefficients. The volume scattering effects are accounted for by modelling earth terrain either as a random medium or as a homogeneous medium containing discrete scatterers. The rough surface effects are studied with models of random and periodic rough surfaces. In order to more realistically model earth terrain, a composite model which accounts for volume and rough surface scattering is developed.

The volume scattering effects due to medium inhomogeneities are studied by characterizing earth terrain with a layered random medium model. The radiative transfer theory is used to calculate the backscattering and bistatic scattering coefficients from a two-layer random medium. Radiative transfer equations are solved numerically using the Fourier series expansion and the Gaussian quadrature method. In order to explain the scattering and emission characteristics of earth terrain which exhibit the effects of layered structure, the results are generalized to the case of multi-layered random medium. The complexity of the problem is kept at the same level as the two-layer cases by deriving effective boundary conditions which incorporate all the properties of the medium below that boundary.

The rough surface effects are studied with the models of random and periodic rough surfaces. The scattering and emission characteristics of randomly rough surface is studied by deriving bistatic scattering coefficients for the reflected and the transmitted waves with the Kirchhoff approach and the small perturbation method. The geometrical optics solution modified to incorporate the shadowing effect is used to study energy conservation and to derive the upper and lower bounds for the emissivities. The small perturbation method is modified with the use of a cumulant technique which is shown to have wider regions of validity. Active remote sensing of plowed fields is studied with the model of a randomly perturbed quasiperiodic surface and the Kirchhoff approach. The narrow-band Gaussian random variation around the spatial

frequency of the sinusoidal variation is used to introduce the quasiperiodicity. It is shown that there is a large difference between the cases where the incident wave vector is parallel or perpendicular to the row direction. When the incident wave vector is perpendicular to the row direction, the maximum value of the backscattering cross section does not necessarily occur at normal incidence. The scattering pattern is interpreted as a convolution of the scattering patterns for the sinusoidal and the random rough surfaces.

The composite model comprising an inhomogeneous layer over a homogeneous halfspace with rough boundaries is developed to study the scattering and emission characteristics of earth terrain. The radiative transfer theory is used. The random medium and discrete scatterer models are used to incorporate the volume scattering effects. To model rough top and bottom interfaces, the bistatic scattering coefficients for a randomly rough surface obtained using a combination of Kirchhoff theory and geometrical optics approach are used. Rough surface effects are incorporated into the radiative transfer theory by modifying the boundary conditions. Because the bistatic scattering coefficients for the rough surface violate energy conservation there is ambiguity in the emissivity. However, two alternate formulations are used to calculate the emissivity. By calculating the bistatic scattering coefficients of the scattering layer with rough top and bottom interfaces and integrating over the upper hemisphere an upper limit for the emissivity is obtained by invoking the principle of reciprocity. A lower limit for the emissivity is obtained by directly calculating thermal microwave emission and assuming that the same medium is at a uniform temperature. It is shown that the backscattering cross section for the angles of incidence near nadir is dominated by the rough surface effects whereas the large angle of incidence behavior is dominated by the volume scattering effects. The rough surface also causes the angular behavior of thermal emission to become flatter and displays smaller differences between horizontal and vertical polarizations due to more coupling of intensities at the boundaries.

Thesis Supervisor: Jin Au Kong
Title: Professor of Electrical Engineering

ACKNOWLEDGMENT

I would like to express my deepest appreciation to Professor Jin Au Kong for his consistent support and thoughtful guidance. Without his helpful advice and concern throughout every stage of my research, this thesis would never have materialized.

I would also like to thank my thesis readers Professors David H. Staelin and Jeffrey H. Shapiro for fruitful discussions, criticisms and suggestions.

Special debt of gratitude is due to Dr. David Briggs at Lincoln Laboratory for his consistent support over the past several years.

Many thanks are due to Drs. Leung Tsang, Weng Chew, Mike Zuniga, Shun-Lien Chuang, and Tarek Habashy for their helpful and lively discussions and suggestions which provided me with valuable insight.

I would also like to thank my colleagues Soon Yun Poh, Jay Kyoon Lee, Yaqiu Jin, Apo Sezginer, Sching Lin, Dongwook Park, Freeman Lin, Eric Yang, and Jeff Kiang for many enlightening discussions. I would especially like to thank Soon Poh for his friendship and concern over the past years.

I thank Ms. Cindy Kopf for her assistance in preparing my manuscripts.

I wish to express my profound gratitude to my wife Sangmi and to my brothers and sister for their support and encouragement.

Last, but certainly not least, my fondest thanks to my parents for their lifelong concern and faith in me. I credit all my accomplishment to their unwavering support.

DEDICATED
TO
MY PARENTS

TABLE OF CONTENTS

Title Page	1
Abstract	2
Acknowledgment	4
Dedication	5
Table of Contents	6
List of Figures	9
Chapter 1 Introduction	14
Chapter 2 Scattering and Emission by Random Rough Surfaces - Kirchhoff Approximation	26
2.1 Introduction	27
2.2 Formulation	29
2.3 Tangent Plane Approximation	31
2.4 Coherent and Incoherent Scattering Coefficients	37
2.5 Geometrical Optics Solution	47
Stationary Phase Method	48
Specular Surface Limit	55
Reciprocity and Conservation of Energy	57
Shadowing Effect	61
Emissivities	65
Chapter 3 Scattering and Emission by Random Rough Surfaces - Small Perturbation Method	73
3.1 Introduction	74
3.2 Formulation	76
3.3 Zeroth-Order Solution	80
3.4 First-Order Solution	83
3.5 Second-Order Solution	89
Appendices	93
Chapter 4 Scattering and Emission by Random Rough Surfaces - Modified Small Perturbation Method	95
4.1 Introduction	96

4.2	Formulation	98
4.3	Modified Small Perturbation Method	101
4.4	Bistatic Scattering Coefficients	105
4.5	Emissivities	109
Chapter 5	Scattering of Electromagnetic Waves from a Randomly Perturbed Quasiperiodic Surface	118
5.1	Introduction	119
5.2	Formulation	121
5.3	Coherent and Incoherent Scattering Coefficients	126
5.4	Geometrical Optics Solution	130
5.5	Results and Discussion	132
	Appendices	137
Chapter 6	Radiative Transfer Theory for Passive Remote Sensing of Multi-Layered Random Medium	159
6.1	Introduction	160
6.2	Formulation	162
6.3	Quadrature Method	164
6.4	Effective Boundary Conditions	169
6.5	Results and Discussion	174
	Appendix	175
Chapter 7	Radiative Transfer Theory for Active Remote Sensing of Two-Layer Random Medium	184
7.1	Introduction	185
7.2	Formulation	187
7.3	Fourier Series Expansion	190
7.4	Gaussian Quadrature Method	194
7.5	Results and Discussion	204
	Appendices	206
Chapter 8	Radiative Transfer Theory for Active Remote Sensing of Multi-Layered Random Medium	221
8.1	Introduction	222
8.2	Formulation	224
8.3	Numerical Solution	227
8.4	Effective Boundary Conditions	229
8.5	Results and Discussion	233

Chapter 9	Theory for Thermal Microwave Emission from a Homogeneous Layer with Rough Surfaces Containing Spherical Scatterers . . .	237
9.1	Introduction	238
9.2	Formulation	240
9.3	Boundary Conditions	242
9.4	Emissivity	245
9.5	Numerical Results and Discussion	248
	Appendices	251
Chapter 10	Theory for Active Remote Sensing of Two-Layer Random Medium with Rough Surfaces	270
10.1	Introduction	271
10.2	Formulation	273
10.3	Boundary Conditions	276
10.4	Fourier Series Expansion	280
10.5	Numerical Solution	285
10.6	Results and Discussion	288
	Appendices	290
Chapter 11	Conclusions and Recommendations for Future Studies	303
Bibliography	307
Biographical Note	319

LIST OF FIGURES

- Figure 2.1 Geometrical configuration of the problem.
- Figure 2.2 The shadowed area on the rough surface.
- Figure 2.3 Energy conservation for the geometrical optics solution.
- Figure 2.4 Energy conservation for the modified geometrical optics solution.
- Figure 4.1 Emissivities as a function of observation angle – Modified Small Perturbation Method.
- Figure 4.2 Emissivities as a function of observation angle – Kirchhoff Approximation.
- Figure 4.3 Emissivities as a function of observation angle – Modified Small Perturbation Method.
- Figure 4.4 Emissivities as a function of observation angle – Kirchhoff Approximation.
- Figure 4.5 Emissivities as a function of observation angle – Modified Small Perturbation Method.
- Figure 4.6 Emissivities as a function of observation angle – Kirchhoff Approximation.
- Figure 5.1 Geometrical configuration of the problem.
- Figure 5.2 $\sigma(\hat{k}_i)$ as a function of θ_i , for different frequencies with $\sigma = 1$ cm, $l = 10$ cm, $B = 10$ cm, $P = 100$ cm, $\sigma_r = 0$, and $\epsilon_1 = (6.0 + i0.6)\epsilon_{r,0}$.
- Figure 5.3 $\sigma(\hat{k}_i)$ as a function of θ_i , for different values of B at 5.0 GHz with $P = 100$ cm, $\sigma = 1$ cm, $l = 10$ cm, $\sigma_r = 0$, and $\epsilon_1 = (6.0 + i0.6)\epsilon_{r,0}$.
- Figure 5.4 $\sigma(\hat{k}_i)$ as a function of θ_i for different values of l at 1.4 GHz with $\sigma = 1$ cm, $B = 10$ cm, $P = 100$ cm, $\sigma_r = 0$, and $\epsilon_1 = (6.0 + i0.6)\epsilon_{r,0}$.
- Figure 5.5 $\sigma(\hat{k}_i)$ as a function of θ_i for different azimuthal angle of incidence ϕ_i at 1.4 GHz with $\sigma = 1$ cm, $l = 50$ cm, $B = 10$ cm, $P = 100$ cm, $\sigma_r = 0$, and $\epsilon_1 = (6.0 + i0.6)\epsilon_{r,0}$.

- Figure 5.6 (a) $\sigma(\hat{k}_i)$ as a function of θ_i for different values of l at 1.4 GHz with $\sigma = 1$ cm, $B = 10$ cm, $P = 100$ cm, $\sigma_x = 0$, and $\epsilon_1 = (6.0 + i0.6)\epsilon_0$.
 (b) Locations and amplitudes of the modes for $B = 10$ cm.
- Figure 5.7 (a) $\sigma(\hat{k}_i)$ as a function of θ_i for different values of B at 1.4 GHz with $\sigma = 1$ cm, $l = 50$ cm, $P = 100$ cm, $\sigma_x = 0$, and $\epsilon_1 = (6.0 + i0.6)\epsilon_0$.
 (b) Locations and amplitudes of the modes for $B = 7$ cm and $B = 5$ cm.
- Figure 5.8 $\sigma(\hat{k}_i)$ as a function of θ_i for different values of P at 1.4 GHz with $\sigma = 1$ cm, $l = 50$ cm, $B = 10$ cm, $P = 100$ cm, $\sigma_x = 0$, and $\epsilon_1 = (6.0 + i0.6)\epsilon_0$.
- Figure 5.9 (a) $\sigma(\hat{k}_i)$ as a function of θ_i for different values of σ at 1.4 GHz with $l = 50$ cm, $B = 10$ cm, $P = 100$ cm, $\sigma_x = 0$, and $\epsilon_1 = (6.0 + i0.6)\epsilon_0$.
 (b) $\sigma(\hat{k}_i)$ as a function of θ_i for different values of σ at 1.4 GHz with $l = 50$ cm, $B = 0$, $\sigma_x = 0$, and $\epsilon_1 = (6.0 + i0.6)\epsilon_0$.
- Figure 5.10 (a) $\sigma(\hat{k}_i)$ as a function of θ_i for different values of l at 1.4 GHz with $\sigma = 1$ cm, $B = 0$, $P = 100$ cm, $\sigma_x = 5$ cm, $l_x = 300$ cm, and $\epsilon_1 = (6.0 + i0.6)\epsilon_0$.
 (b) Locations and amplitudes of the modes for $\sigma_x = 5$ cm and $\sigma_x = 2$ cm.
- Figure 5.11 $\sigma(\hat{k}_i)$ as a function of θ_i for different values of l at 1.4 GHz with $\sigma = 1$ cm, $B = 10$ cm, $P = 100$ cm, $\sigma_x = 5$ cm, $l_x = 300$ cm, and $\epsilon_1 = (6.0 + i0.6)\epsilon_0$.
- Figure 5.12 $\sigma(\hat{k}_i)$ as a function of θ_i for different values of σ_x at 1.4 GHz with $\sigma = 1$ cm, $l = 50$ cm, $B = 10$ cm, $P = 100$ cm, $l_x = 300$ cm, and $\epsilon_1 = (6.0 + i0.6)\epsilon_0$.
- Figure 6.1 Geometrical configuration of the problem.
- Figure 6.2 Brightness temperature as a function of frequency.
- Figure 6.3 Brightness temperature as a function of observation angle at 5 GHz.
- Figure 6.4 Brightness temperature as a function of observation angle at 10.7 GHz.
- Figure 6.5 Brightness temperature as a function of observation angle at 18 GHz.
- Figure 6.6 Brightness temperature as a function of observation angle at 37 GHz.

- Figure 6.7 Brightness temperature as a function of frequency for a three-layer random medium.
- Figure 7.1 Geometrical configuration of the problem.
- Figure 7.2 Backscattering cross sections as a function of frequency.
- Figure 7.3 Backscattering cross sections as a function of incident angle at 10 GHz.
- Figure 7.4 Bistatic scattering coefficients γ_{hh} and γ_{vh} as a function of scattering angle θ_s at 10 GHz.
- Figure 7.5 Bistatic scattering coefficients γ_{hh} and γ_{vh} as a function of scattering angle θ_s at 10 GHz.
- Figure 7.6 Bistatic scattering coefficients γ_{hh} and γ_{vh} as a function of azimuthal scattering angle ϕ_s at 10 GHz.
- Figure 7.7 Bistatic scattering coefficients γ_{hh} and γ_{vv} as a function of azimuthal scattering angle ϕ_s at 10 GHz.
- Figure 7.8 Bistatic scattering coefficients γ_{hh} and γ_{vh} as a function of azimuthal scattering angle ϕ_s at 10 GHz.
- Figure 7.9 Bistatic scattering coefficients γ_{hh} and γ_{vv} as a function of azimuthal scattering angle ϕ_s at 10 GHz.
- Figure 8.1 Geometrical configuration of the problem.
- Figure 8.2 Backscattering cross section for horizontally polarized like-like return σ_{hh} as a function of frequency for a three-layer random medium.
- Figure 8.3 Backscattering cross section for depolarized return σ_{vh} as a function of frequency for a three-layer random medium.
- Figure 9.1 Geometrical configuration of the problem.
- Figure 9.2 Brightness temperature as a function of angle for rough surface at bottom boundary.

- Figure 9.3 Brightness temperature as a function of angle for rough surface at bottom boundary with $\epsilon_2 = 15\epsilon_{0r}$.
- Figure 9.4 Brightness temperature as a function of angle for rough surface at bottom boundary with $s^2 = 0.1$.
- Figure 9.5 Brightness temperature as a function of angle for rough surface at bottom boundary with $\epsilon_1 = (3.0 + i0.0018)\epsilon_{0r}$.
- Figure 9.6 Brightness temperature as a function of angle for rough surface at top boundary.
- Figure 9.7 Brightness temperature as a function of angle for rough surface at top boundary with $s^2 = 0.1$.
- Figure 9.8 Brightness temperature as a function of angle for rough surfaces at top and bottom boundaries.
- Figure 9.9 Brightness temperature as a function of angle for rough surface at bottom boundary with volume scattering.
- Figure 9.10 Brightness temperature as a function of angle for rough surface at top boundary with volume scattering.
- Figure 9.11 Brightness temperature as a function of angle for rough surface at top and bottom boundaries with volume scattering.
- Figure 9.12 Brightness temperature as a function of angle at 18 GHz for vertical polarization.
- Figure 9.13 Brightness temperature as a function of angle at 18 GHz for horizontal polarization.
- Figure 10.1 Geometrical configuration of the problem.
- Figure 10.2 Backscattering cross sections as a function of incident angle for rough surface and volume scattering at 5 GHz.

Figure 10.3 Backscattering cross sections as a function of incident angle for volume scattering, rough surface scattering, and combined volume and rough surface scattering at 5 GHz.

Figure 10.4 Backscattering cross sections as a function of frequency for $\theta_i = 4.2^\circ$.

Figure 10.5 Backscattering cross sections as a function of frequency for $\theta_i = 32^\circ$.

CHAPTER 1

Introduction

The remote sensing of the earth and the elements of its environment at microwave frequencies have been found to contain many practical applications. The primary advantage inherent in remote sensing at microwave frequencies over optical and infrared frequencies is in its all-weather, day-and-night operational capabilities. Active and passive microwave remote sensing with both radar and radiometer have been investigated in areas of snow and ice covered land or water [Rouse, 1969; Waite and McDonald, 1969; Johnson and Farmer, 1971; Meier and Edgerton, 1971; Gloersen *et al.*, 1973; Ketchum and Tooma, 1973; Elachi *et al.*, 1976; Kunzi *et al.*, 1976; Parashar *et al.*, 1977; Ulaby *et al.*, 1977; Zwally, 1977; Hofer and Schanda, 1978; Hofer and Good, 1979; Rango *et al.*, 1979], vegetation canopy [Ulaby, 1975; Ulaby *et al.*, 1975; Bush and Ulaby, 1976, 1978], cloud and rainfall [Grody, 1976; Tsang *et al.*, 1977], and soil moisture studies [Dickey *et al.*, 1974; Schmugge *et al.*, 1974; Ulaby and Batlivala, 1976a,b; Njoku and Kong, 1977; Newton and Rouse, 1980; Wang *et al.*, 1980; Jackson and Schmugge, 1981; Njoku and O'Neill, 1981; Wang *et al.*, 1983]. While extensive effort has been concentrated in the measurement and collection of voluminous experimental data, theoretical models that are useful in interpreting these data have not been satisfactorily developed, especially where combinations of absorption, scattering, layering and rough surface are important factors. Although past theoretical emphasis

has been largely concentrated on rough surface scattering, recent theoretical models have been proposed to account for volume scattering effects.

The scattering of electromagnetic waves from a randomly rough surface has been studied extensively for many years. Two basic analytical approaches have been the Kirchhoff approach (KA) [Beckmann and Spizzichino, 1963; Kodis, 1966; Stogryn, 1967; Sancer, 1969; Smith, 1967; Sung and Holzer, 1976; Tsang and Kong, 1980a] and the small perturbation method (SPM) [Rice, 1963; Valenzuela, 1967, 1968]. The KA approximates the surface fields using the tangent plane approximation. Under the tangent plane approximation, the fields at any point of the surface are approximated by the fields that would be present on the tangent plane at that point. Thus, the tangent plane approximation requires a large radius of curvature relative to the incident wavelength at every point on the surface. The SPM assumes that the surface variations are much smaller than the incident wavelength and the slopes of the rough surface are relatively small. The bistatic scattering coefficients for the reflected and transmitted waves have been derived using both the KA and SPM.

The Kirchhoff approximated diffraction integral for a dielectric rough surface is still difficult to evaluate analytically and further approximations are usually made. The integrands which depend on the local surface slopes can be expanded in slope terms about zero slope, and then can be integrated by parts discarding the edge effect [Leader, 1971; Tsang and Newton, 1982]. The integrals can then be evaluated by keeping only a few terms of the expansion. In the high frequency limit, the geometrical optics solution can be obtained using the method of stationary phase. The geometrical optics solution is independent of frequency and states that the scattered intensity is proportional to the probability of the occurrence of the slopes which will specularly reflect or transmit the incident wave into the direction of observation [Barrick, 1968].

The scattering of electromagnetic waves from a slightly rough surface can be studied using a perturbation method. In the SPM due to Rice [1963], it is assumed that the surface variations are much smaller than the incident wavelength and the slopes of the rough surface are relatively small. The Rayleigh hypothesis is used to express the reflected and transmitted fields into upward and downward going waves. The field amplitudes are determined from the boundary conditions and the divergence relations. The extended boundary condition (EBC) method may also be used with the perturbation method to solve for the scattered fields [Agarwal, 1977; Nieto-Vesperinas, 1982]. In the EBC method, the surface currents on the rough surface are first calculated. The scattered fields then can be calculated from the diffraction integral by making use of the calculated surface fields. Both of the perturbation methods yield the same expansions for the scattered fields, because the expansions of the amplitudes of the scattered fields are unique within their circles of convergence [Maradudin, 1983]. The SPM has been used to calculate the scattered fields up to the second-order. The zeroth-order solutions are just reflected and transmitted fields from a flat surface. The first-order solution gives the lowest-order incoherent transmitted and reflected intensities. However, the first-order solution does not give the depolarization effect in the backscattering direction. The second-order solution gives the lowest-order correction due to the rough surface to the coherent reflection and transmission coefficients. Also, the depolarization of the backscattering power is illustrated with the second-order solution.

Scattering of electromagnetic waves from a periodic rough surface is of interest in the remote sensing of plowed vegetation fields with row structures. The variations of the radar scattering coefficients and the radiometric brightness temperatures due to change in the look direction relative to the row direction are observed to be significant [Wang

et al., 1980; Ulaby *et al.*, 1981]. The extended boundary condition (EBC) method has been used to solve for the scattered fields from periodic surfaces [Waterman, 1975; Chuang and Kong, 1981, 1982]. The method is based on Green's theorem relating the amplitudes of the incident plane waves to the Fourier components of the fields on the periodic surface, which in turn gives the amplitudes of the diffracted Floquet waves. Thus the amplitudes of the diffracted Floquet waves can be solved in terms of the amplitudes of the incident plane waves directly by a transition matrix. After obtaining the scattered field amplitudes the emissivity of the periodic surface can be calculated using the principles of reciprocity and energy conservation. Because of the exact nature of the theory, the reciprocity relation and the energy conservation have been shown to hold exactly and the unambiguous emissivity of the periodic rough surface has been obtained [Kong *et al.*, 1984].

Scattering of electromagnetic waves from a randomly perturbed sinusoidal surface is of interest in the active remote sensing of plowed fields. The variation of the radar scattering coefficients due to the change in the look direction relative to the row direction have been well documented [Batlivala and Ulaby, 1976; Ulaby and Bare, 1979; Fenner *et al.*, 1980]. In the past, the problem of electromagnetic wave scattering from periodic or random rough surface has been extensively studied. The problem of scattering by randomly perturbed periodic surface has been studied by assuming that the periodic surface causes a tilting effect [Ulaby *et al.*, 1982]. In this approach the scattering coefficients of the random rough surfaces obtained using the Kirchhoff approximation or small perturbation method is averaged over the change in local incidence angle due to the periodic surface. This approach has also been used to solve the scattering from a composite random rough surface with small and large scale variations [Semenov, 1966; Wu and Fung, 1972].

In the active and passive microwave remote sensing of earth terrain, the scattering effects due to medium inhomogeneities and rough interfaces play a dominant role in the determination of brightness temperatures and radar backscattering coefficients. The effects of volume scattering have been treated with two theoretical models for the terrain media: (1) the random medium model where scattering effects can be accounted for by introducing a randomly fluctuating part in the permittivities, and (2) the discrete scatterer model where discrete scatterers are imbedded in a homogeneous background medium.

In the theoretical developments for passive remote sensing the effect of volume scattering due to medium inhomogeneity was first accounted for by Gurvich *et al.* [1973]. They derived expressions for the brightness temperature of a halfspace random medium with a laminar structure, assuming uniform temperature distribution. Tsang and Kong [1975] solved the problem of thermal microwave emission from a halfspace random medium with a laminar structure and nonuniform temperature distribution using the radiative transfer theory. England [1974] first examined thermal microwave emission from a uniform low-loss dielectric medium containing randomly distributed isotropic scatterers, with a radiative transfer approach. He [1975] then considered the more general case of a scattering layer over a homogeneous halfspace, using the radiative transfer theory and a Rayleigh scattering model. Tsang and Kong [1977a] derived a more general result than that of England for both the halfspace and two-layer case, using a Mie scattering model. With the Born approximation, Tsang and Kong [1976a] obtained the emissivity of a halfspace random medium with a three-dimensional variation.

In active remote sensing, Stogryn [1974] first calculated the bistatic scattering coefficients for a random medium with a spherical correlation function using a pertur-

bation approach. Leader [1975] studied scattering from Rayleigh scatterers imbedded in a dielectric slab using the matrix doubling method. Using the Born approximation, Tsang and Kong [1976a] studied scattering of electromagnetic waves by a halfspace random medium. They [1978] also developed the radiative transfer theory to calculate the bistatic scattering coefficients from a halfspace random medium. An iterative approach is used to obtain results to the second order, in order to exhibit depolarization of backscattered power. Using the first-order renormalization method, Fung and Fung [1977] obtained the bistatic scattering coefficients from a vegetation-like halfspace random medium. Fung [1979] then extended the result to the case of a vegetation-like layer over a homogeneous halfspace. Zuniga and Kong [1980] studied the scattering from a slab of random medium using the Born approximation. Then, Zuniga *et al.* [1980] extended the result to the second order in albedo to show the depolarization effect in the backscattering direction.

The radiative transfer theory has been useful in the interpretation of remote sensing data [Kong *et al.*, 1979]. Even though it deals only with the intensities of the field quantities and neglects their coherent nature, it accounts for the multiple scattering and obeys energy conservation. The modified radiative transfer (MRT) theory [Tsang and Kong, 1976c; Zuniga and Kong, 1980, 1981] which takes into account the partial coherent effects due to the boundaries has been derived for the cases when the interference effects become important [Blinn *et al.*, 1972]. The MRT equations have been developed for a two-layer random medium with laminar structure by applying the nonlinear approximation to Dyson's equation and the ladder approximation to the Bethe-Salpeter equation [Tsang and Kong, 1976c]. Then, the MRT equations for electromagnetic wave propagation in a two-layer medium with three-dimensional permittivity fluctuations are derived [Zuniga and Kong, 1980, 1981]. The MRT equa-

tions are then solved with the first order renormalization approximation to obtain the backscattering cross sections.

In the microwave remote sensing of earth terrain, the multi-layered models have shown to be more realistic in the interpretation of the data. In the passive remote sensing the radiative transfer theory has been used to study thermal microwave emission from a multi-layered random medium with laminar structures [Djermakoye and Kong, 1979]. The propagation matrix formalism is applied to obtain closed-form solutions. For the inhomogeneous slab random medium with non-uniform scattering, absorption and a temperature profile in the vertical direction, the method of invariant imbedding has been used [Tsang and Kong, 1977b]. The boundary value problem of the radiative transfer equations is converted to an initial value problem starting at zero slab thickness. Thermal microwave emission from a three-layer random medium with three-dimensional variations has also been studied using the radiative transfer theory [Tsang and Kong, 1980b]. The quadrature method is used and the results are found to be useful in the interpretation of snow data exhibiting diurnal change [Hofer and Shanda, 1978; Stiles and Ulaby, 1980]. In the active remote sensing, the scattering from multi-layered random medium has been solved using the Born approximation and the propagation matrix formalism [Zuniga *et al.*, 1979]. The radiative transfer theory also has been applied to scattering from multi-layer of Rayleigh scatterers where the iterative approach is used to obtain solutions to first-order [Shin, 1980; Karam and Fung, 1982].

Most of the previous work on volume scattering all assumed planar boundaries, and the effect of rough surface scattering was neglected. However, in order to understand in a more meaningful way the problems of radar backscattering and thermal microwave emission from natural terrains, a composite model that can account for

both the volume and surface scattering effects must be studied. Recently, the Rayleigh scattering model has been used with the radiative transfer equations to study the combined volume and rough surface scattering effects [Fung and Chen, 1981a,b; Fung and Eom, 1981].

In Chapters 2 and 3, the scattering and emission from random rough surface are studied. The scattering of electromagnetic waves from a randomly rough surface has been studied extensively for many years. Two basic analytical approaches have been the Kirchhoff approach (KA) and the small perturbation method (SPM). The KA approximates the surface fields using the tangent plane approximation. Under the tangent plane approximation, the fields at any point of the surface are approximated by the fields that would be present on the tangent plane at that point. The SPM assumes that the surface variations are much smaller than the incident wavelength and the slopes of the rough surface are relatively small. The bistatic scattering coefficients derived under the KA and SPM are reviewed and summarized in Chapters 2 and 3, respectively. The bistatic scattering coefficients for the transmitted fields are also derived using KA and SPM in order to study the energy conservation of the various approximations. The emissivity of the random rough surface are calculated by integrating the bistatic scattering coefficients over the upper hemisphere. The geometrical optics solutions are modified using the shadowing functions. The upper and lower limit of the emissivity are obtained using the modified geometrical optics solutions.

In Chapter 4, the cumulant technique is used to modify the SPM solutions. The resulting modified SPM solution are shown to have a wider region of validity than the conventional SPM results and to agree with the KA results for all values of the variance of the surface heights in the limit of large correlation lengths. The bistatic scattering coefficients for the reflected waves are calculated. The emissivities are also calculated by

integrating over the upper hemisphere the reflected coherent and incoherent scattering coefficients.

In Chapter 5, the Kirchhoff approximation is used to study the scattering of electromagnetic waves from a randomly perturbed quasiperiodic surface. In order to more realistically model the plowed fields we characterize the rough surface as a composite surface with a Gaussian random variation, a sinusoidal variation and a narrow-band Gaussian random variation around the same spatial frequency. Introduction of the narrow-band random variation causes the surface to be quasi-periodic. The physical optics integral obtained with the Kirchhoff approximation is evaluated to obtain the coherent and incoherent bistatic coefficients. In the geometrical optics limit, the stationary phase method is used to further simplify the results. In this limit it is shown that the bistatic scattering coefficients are proportional to the probability of the occurrence of the slopes which will specularly reflect the incident wave into the observation direction. The theoretical results are illustrated for the various cases by plotting the backscattering cross sections as a function of the angle of incidence with the incident wave vector either parallel or perpendicular to the row direction. The appearances of peaks are explained in terms of the scattering patterns for sinusoidal surfaces.

In Chapter 6, the problem of thermal microwave emission from a multi-layered random medium on top of homogeneous halfspace is solved using the radiative transfer theory. The brightness temperatures are calculated using a numerical approach. The radiative transfer equations are solved using a quadrature method where the integrals are replaced by the summation over the discrete quadrature angles. The resulting system of first-order differential equations are solved by obtaining eigenvalues and eigenvectors and matching the boundary conditions. The effective boundary conditions are derived in terms of the effective reflection matrices and the effective source vectors

to reduce the complexity of the problem to that of a two-layer problem. The effective reflection matrices and the effective source vectors are solved recursively by considering only one layer at a time. The numerical solutions are illustrated by plotting brightness temperatures as functions of frequency and observation angle for multi-layered cases.

In Chapter 7, the problem of scattering from a multi-layer random medium is solved using the radiative transfer theory. Using all four Stokes parameters, the bistatic scattering coefficients of two-layer random medium are first calculated using a numerical approach which provides a valid solution for both small and large albedos. A Fourier-series expansion in the azimuthal direction is used to eliminate the azimuthal ϕ -dependence from the radiative transfer equations. Then, the set of equations without the ϕ -dependence is solved using the method of Gaussian quadrature. The integrals in the radiative transfer equations are replaced by a Gaussian quadrature and the resulting system of first-order differential equations is solved by obtaining eigenvalues and eigenvectors and matching the boundary conditions. The order of system of eigen-equations is reduced for more efficient computation by making use of the symmetry properties of the scattering function matrix. Then in Chapter 8, the results are generalized to the case of scattering from multi-layered random medium. The effective boundary conditions are derived in terms of the effective reflection matrices to reduce the complexity of the problem to that of a two-layer problem. The effective reflection matrices are solved recursively by considering only one layer at a time. The numerical results are illustrated by plotting backscattering cross sections and the bistatic scattering coefficients as functions of frequency, incident angle, and the scattering angles.

In Chapter 9, the radiative transfer theory is used to solve the problem of thermal microwave emission from a scattering layer overlying a homogeneous halfspace with rough interfaces at the top and bottom boundaries. Mie scattering phase func-

tion is used for volume scattering, and the bistatic scattering coefficients of a Gaussian random surface, obtained using a combination of the Kirchhoff approximation and a geometrical optics approach, is used for rough surface scattering. The rough surface effects are incorporated into the radiative transfer equations by modifying the boundary conditions satisfied by the intensities at the top and bottom interfaces. The radiative transfer equations are solved numerically, using the Gaussian quadrature method. Because the bistatic coefficients of the rough surface violate energy conservation there is ambiguity in the emissivity. However, using two alternate formulations, the upper and lower limits of the emissivity are calculated. By calculating the bistatic coefficients of a scattering layer with rough top and bottom interfaces and integrating over the scattering angles in the upper hemisphere we can obtain an upper limit for the emissivity by invoking the principle of reciprocity. A lower limit for the emissivity is obtained by directly calculating thermal microwave emission and assuming that the same medium is at a uniform temperature. The theoretical results are illustrated by plotting the brightness temperatures as functions of observation angles and polarizations.

In Chapter 10, the problem of scattering from a two-layer random medium with rough boundaries is solved using the radiative transfer theory. The rough surface effects are incorporated into the radiative transfer equations by modifying the boundary conditions. The reflected and transmitted bistatic scattering coefficients derived with the randomly rough surface models are used to derive the boundary conditions satisfied by the intensities at the top and bottom interfaces. The radiative transfer equations are solved numerically using the Fourier-series expansion and the Gaussian quadrature method. The order of system of eigen-equations is reduced for more efficient computation by making use of the symmetry properties of the scattering function matrix. The theoretical results are illustrated by plotting the backscattering cross sections as

functions of frequency and incident angle.

In Chapter 11, various theoretical models developed in this thesis for microwave remote sensing of earth terrain are summarized and the recommendations for future studies are made.

CHAPTER 2

Scattering and Emission by Random Rough Surfaces –

Kirchhoff Approximation

The scattering of electromagnetic waves from a random rough surface is studied using the Kirchhoff approximation. The tangent plane approximation is used to approximate the surface fields. The bistatic scattering coefficients for the reflected and transmitted waves are derived. The integrands which depend on the local surface slopes are expanded in slope terms and the integrals are evaluated by keeping only a few terms of the expansion. In the high frequency limit, the geometrical optics solution is obtained using the method of stationary phase. The geometrical optics solution is independent of frequency and states that the scattered intensity is proportional to the probability of the occurrence of the slopes which will specularly reflect or transmit the incident wave into the direction of observation. The bistatic scattering coefficients are modified to incorporate the shadowing effects. The sum of reflected and transmitted intensities is shown to be always less than the incident intensity and this is used to derive the upper and lower bounds for the correct emissivity of the rough surface in the geometrical optics limit.

2.1 Introduction

The scattering of electromagnetic waves from a randomly rough surface has been studied extensively for many years. Two basic analytical approaches have been the Kirchhoff approach (KA) [Beckmann and Spizzichino, 1963; Semenov, 1965; Kodis, 1966; Stogryn, 1967; Barrick, 1968; Fung and Chan, 1969; Sancer, 1969; Lynch and Wagner, 1970; Leader, 1971; Sung and Holzer, 1976; Sung and Ekerhardt, 1978; Tsang and Kong, 1980a,b; Bass and Fuks, 1979; Ulaby *et al.*, 1981] and the small perturbation method (SPM) [Rice, 1963; Valenzuela, 1967, 1968; Agarwal, 1977; Nieto-Vesperina, 1982]. The KA approximates the surface fields using the tangent plane approximation. Under the tangent plane approximation, the fields at any point of the surface are approximated by the fields that would be present on the tangent plane at that point. Thus, the tangent plane approximation requires a large radius of curvature relative to the incident wavelength at every point on the surface. The SPM assumes that the surface variations are much smaller than the incident wavelength and the slopes of the rough surface are relatively small.

In this chapter we derive the bistatic scattering coefficients for the reflected and transmitted waves using the KA. The Kirchhoff approximated diffraction integral for a dielectric rough surface is still difficult to evaluate analytically and further approximations are usually made. The integrands which depend on the local surface slopes can be expanded in slope terms about zero slopes, and then can be integrated by part discarding the edge effect. The integrals can then be evaluated by keeping only a few terms of the expansion. In the high frequency limit, the geometrical optics solution can be obtained using the method of stationary phase. The geometrical optics solution is independent of frequency and states that the scattered intensity is proportional to the

probability of the occurrence of the slopes which will specularly reflect or transmit the incident wave into the direction of observation. The bistatic scattering coefficients are modified to incorporate the shadowing effects. The sum of reflected and transmitted intensities is then shown to be always less than the incident intensity. This used to derive the upper and lower bounds for the correct emissivity of the rough surface in the geometrical optics limit.

2.2 Formulation

Consider a plane wave incident upon a random rough surface [Fig. 2.1]. The electric field of the incident wave is given by

$$\bar{E}_i = \hat{e}_i E_0 e^{i\bar{k}_i \cdot \bar{r}} \quad (1)$$

where \bar{k}_i denotes the incident wave vector and \hat{e}_i the polarization of the electric field vector. The rough surface is characterized by a random height distribution $z = f(\bar{r}_\perp)$ where $f(\bar{r}_\perp)$ is a Gaussian random variable with zero mean, $\langle f(\bar{r}_\perp) \rangle = 0$. The scattered and the transmitted fields are given by the diffraction integral. From Huygens' principle, which expresses the field at an observation point in terms of fields at the boundary surface, the following expressions are obtained for the scattered fields in region 0 and the transmitted fields in region 1 [Kong, 1975].

$$\bar{E}_s(\bar{r}) = \int_{S'} dS' \left\{ i\omega\mu_0 \bar{G}(\bar{r}, \bar{r}') \cdot [\hat{n} \times \bar{H}(\bar{r}')] + \nabla \times \bar{G}(\bar{r}, \bar{r}') \cdot [\hat{n} \times \bar{E}(\bar{r}')] \right\} \quad (2a)$$

$$\bar{E}_t(\bar{r}) = \int_{S'} dS' \left\{ i\omega\mu_0 \bar{G}_1(\bar{r}, \bar{r}') \cdot [\hat{n}_d \times \bar{H}(\bar{r}')] - \nabla \times \bar{G}_1(\bar{r}, \bar{r}') \cdot [\hat{n}_d \times \bar{E}(\bar{r}')] \right\} \quad (2b)$$

where S' denotes the rough surface on which the surface integration is to be carried out, \hat{n} and \hat{n}_d are the unit vectors normal to the rough surface and pointing into the reflected and transmitted regions, respectively [Fig. 2]. The dyadic Green's function for homogenous space of the region 0 and 1, $\bar{G}(\bar{r}, \bar{r}')$ and $\bar{G}_1(\bar{r}, \bar{r}')$, are

$$\bar{G}(\bar{r}, \bar{r}') = \left[\bar{I} + \frac{\nabla \nabla}{k^2} \right] \frac{e^{ik|\bar{r}-\bar{r}'|}}{4\pi|\bar{r}-\bar{r}'|} \quad (3a)$$

and

$$\bar{\bar{G}}_1(\bar{r}, \bar{r}') = \left[\bar{I} + \frac{\nabla \nabla}{k_1^2} \right] \frac{e^{ik_1 |\bar{r} - \bar{r}'|}}{4\pi |\bar{r} - \bar{r}'|} \quad (3b)$$

where $k = \omega \sqrt{\mu, \epsilon_0}$ and $k_1 = \omega \sqrt{\mu, \epsilon_1}$. If the observation point is in the far field region, then the dyadic Green's functions simplify to

$$\bar{\bar{G}}(\bar{r}, \bar{r}') \simeq (\bar{I} - \hat{k}_s \hat{k}_s) \frac{e^{ikr}}{4\pi r} e^{-i\bar{k} \cdot \bar{r}'} \quad (4)$$

$$\bar{\bar{G}}_1(\bar{r}, \bar{r}') \simeq (\bar{I} - \hat{k}_t \hat{k}_t) \frac{e^{ik_1 r}}{4\pi r} e^{-i\bar{k}_t \cdot \bar{r}'} \quad (5)$$

where \hat{k}_s and \hat{k}_t denotes the scattered and transmitted direction in region 0 and region 1, respectively.

Substituting (4) and (5) into the diffraction integral (2), we obtain, in the reflected direction \hat{k}_s and transmitted direction \hat{k}_t ,

$$\bar{E}_s(\bar{r}) = \frac{ik e^{ikr}}{4\pi r} (\bar{I} - \hat{k}_s \hat{k}_s) \cdot \int_{S'} dS' \left\{ \hat{k}_s \times [\hat{n} \times \bar{E}(\bar{r}')] + \eta [\hat{n} \times \bar{H}(\bar{r}')] \right\} e^{-i\bar{k}_s \cdot \bar{r}'} \quad (6a)$$

$$\bar{E}_t(\bar{r}) = \frac{ik_1 e^{ik_1 r}}{4\pi r} (\bar{I} - \hat{k}_t \hat{k}_t) \cdot \int_{S'} dS' \left\{ \hat{k}_t \times [\hat{n}_d \times \bar{E}(\bar{r}')] + \eta_1 [\hat{n}_d \times \bar{H}(\bar{r}')] \right\} e^{-i\bar{k}_t \cdot \bar{r}'} \quad (6b)$$

where η and η_1 are the wave impedances in the regions 0 and 1, respectively.

2.3 Tangent Plane Approximation

In the Kirchhoff approach, an approximate expression for the surface fields is obtained under the tangent plane approximation. Under the tangent plane approximation, the fields at any point of the surface are approximated by the fields that would be present on the tangent plane at that point. Thus, the tangent plane approximation requires a large radius of curvature relative to the incident wavelength at every point on the surface [Beckman and Spizzichino, 1963].

First we form an orthonormal system $(\hat{p}_i, \hat{q}_i, \hat{k}_i)$ at the point \bar{r}' , with

$$\hat{q}_i = \frac{\hat{k}_i \times \hat{n}}{|\hat{k}_i \times \hat{n}|} \quad (7)$$

$$\hat{p}_i = \hat{q}_i \times \hat{k}_i \quad (8)$$

where, $\hat{n}(\bar{r}') = -\hat{n}_d(\bar{r}')$, is the normal to the surface at the point \bar{r}' pointing into the region 0. The unit vectors \hat{q}_i and \hat{p}_i are the local perpendicular and parallel polarization vectors at the point \bar{r}' . In applying the tangent plane approximation, we solve the boundary value problem for the TE and TM polarization of a wave incident onto an infinite planar interface taking the tangent plane to be the interface. We decompose the incident field into locally perpendicular and parallel polarization fields.

The perpendicular component of the incident field is

$$(\hat{e}_i \cdot \hat{q}_i) \hat{q}_i E_{\perp} e^{i\vec{k}_i \cdot \bar{r}'}$$

so that the local reflected field is

$$(\hat{e}_i \cdot \hat{q}_i) \hat{q}_i E_{\perp} R_{\perp} e^{i\vec{k}_i \cdot \bar{r}'}$$

where R_h is the local Fresnel reflection coefficient

$$R_h = \frac{k \cos \theta_{li} - \sqrt{k_1^2 - k^2 \sin^2 \theta_{li}}}{k \cos \theta_{li} + \sqrt{k_1^2 - k^2 \sin^2 \theta_{li}}} \quad (9a)$$

with θ_{li} as the local angle of incident at the point \bar{r}' . The magnetic fields associated with the above are

$$\frac{1}{\eta} \hat{k}_i \times (\hat{e}_i \cdot \hat{q}_i) \hat{q}_i E_{\perp} e^{i\bar{k}_i \cdot \bar{r}'}$$

and

$$\frac{1}{\eta} \hat{k}_r \times (\hat{e}_i \cdot \hat{q}_i) \hat{q}_i E_{\perp} R_h e^{i\bar{k}_r \cdot \bar{r}'}$$

where \hat{k}_r is the local reflected direction and is related to the incident direction by

$$\hat{k}_r = \hat{k}_i - 2\hat{n}(\hat{n} \cdot \hat{k}_i)$$

Hence the tangential electric field of this perpendicular component is

$$\hat{n} \times \bar{E} = (\hat{n} \times \hat{q}_i)(\hat{e}_i \cdot \hat{q}_i)(1 + R_h) E_{\perp} e^{i\bar{k}_i \cdot \bar{r}'}$$

and the associated magnetic field is

$$\begin{aligned} \hat{n} \times \bar{H} &= \frac{1}{\eta} (\hat{e}_i \cdot \hat{q}_i) \hat{n} \times \left[(\hat{k}_i \times \hat{q}_i) + R_h (\hat{k}_r \times \hat{q}_i) \right] E_{\perp} e^{i\bar{k}_i \cdot \bar{r}'} \\ &= -(1 - R_h) (\hat{n} \cdot \hat{k}_i) \frac{(\hat{e}_i \cdot \hat{q}_i)}{\eta} \hat{q}_i E_{\perp} e^{i\bar{k}_i \cdot \bar{r}'} \end{aligned}$$

where we have made use of the relations $\hat{n} \cdot \hat{q}_i = 0$ and $\hat{n} \cdot \hat{k}_r = -\hat{n} \cdot \hat{k}_i$. The calculations can be repeated for local parallel polarized component with local reflection coefficient for vertical polarization.

$$R_v = \frac{\epsilon_1 k \cos \theta_{li} - \epsilon_{\perp} \sqrt{k_1^2 - k^2 \sin^2 \theta_{li}}}{\epsilon_1 k \cos \theta_{li} + \epsilon_{\perp} \sqrt{k_1^2 - k^2 \sin^2 \theta_{li}}} \quad (9b)$$

Summing up the local parallel and perpendicular polarized components, we obtain

$$\hat{n} \times \overline{E}(\vec{r}') = E_{\parallel} \left\{ (\hat{\epsilon}_i \cdot \hat{q}_i)(\hat{n} \times \hat{q}_i)(1 + R_{\parallel}) + (\hat{\epsilon}_i \cdot \hat{p}_i)(\hat{n} \cdot \hat{k}_i)\hat{q}_i(1 - R_{\perp}) \right\} e^{i\vec{k} \cdot \vec{r}'} \quad (10a)$$

$$\hat{n} \times \overline{H}(\vec{r}') = \frac{E_{\parallel}}{\eta} \left\{ -(\hat{\epsilon}_i \cdot \hat{q}_i)(\hat{n} \cdot \hat{k}_i)\hat{q}_i(1 - R_{\parallel}) + (\hat{\epsilon}_i \cdot \hat{p}_i)(\hat{n} \times \hat{q}_i)(1 + R_{\perp}) \right\} e^{i\vec{k} \cdot \vec{r}'} \quad (10b)$$

The local angle of incident can be calculated from the formula

$$\cos \theta_{li} = -\hat{n} \cdot \hat{k}_i \quad (11)$$

The normal vector at the point \vec{r}' is given by

$$\hat{n}(\vec{r}') = \frac{-\alpha \hat{x} - \beta \hat{y} + \hat{z}}{\sqrt{1 + \alpha^2 + \beta^2}} \quad (12)$$

where α and β are the local slopes in the x and y directions,

$$\alpha = \frac{\partial f(x', y')}{\partial x'} \quad (13a)$$

$$\beta = \frac{\partial f(x', y')}{\partial y'} \quad (13b)$$

Substituting (10) into (6), we obtain, after some algebraic manipulations,

$$\overline{E}_s(\vec{r}) = \frac{ik e^{ikr}}{4\pi r} E_{\parallel} (\vec{I} - \hat{k}_s \hat{k}_s) \cdot \int_A d\vec{r}'_{\perp} \overline{F}(\alpha, \beta) e^{i(\vec{k}_{\perp} - \vec{k}_{s\perp}) \cdot \vec{r}'} \quad (14a)$$

$$\overline{E}_t(\vec{r}) = -\frac{ik_t e^{ik_s r}}{4\pi r} E_{\parallel} (\vec{I} - \hat{k}_t \hat{k}_t) \cdot \int_A d\vec{r}'_{\perp} \overline{N}(\alpha, \beta) e^{i(\vec{k}_{\perp} - \vec{k}_{t\perp}) \cdot \vec{r}'} \quad (14b)$$

where

$$\begin{aligned} \bar{F}(\alpha, \beta) = & (1 + \alpha^2 + \beta^2)^{1/2} \left\{ -(\hat{\epsilon}_i \cdot \hat{q}_i)(\hat{n} \cdot \hat{k}_i)\hat{q}_i(1 - R_h) + (\hat{\epsilon}_i \cdot \hat{p}_i)(\hat{n} \times \hat{q}_i)(1 + R_v) \right. \\ & \left. - (\hat{\epsilon}_i \cdot \hat{q}_i)(\hat{k}_s \times (\hat{n} \times \hat{q}_i))(1 + R_h) + (\hat{\epsilon}_i \cdot \hat{p}_i)(\hat{n} \cdot \hat{k}_i)(\hat{k}_s \times \hat{q}_i)(1 - R_v) \right\} \end{aligned} \quad (15a)$$

$$\begin{aligned} \bar{N}(\alpha, \beta) = & (1 + \alpha^2 + \beta^2)^{1/2} \left\{ -\frac{\eta_1}{\eta}(\hat{\epsilon}_i \cdot \hat{q}_i)(\hat{n} \cdot \hat{k}_i)\hat{q}_i(1 - R_h) + \frac{\eta_1}{\eta}(\hat{\epsilon}_i \cdot \hat{p}_i)(\hat{n} \times \hat{q}_i)(1 + R_v) \right. \\ & \left. + (\hat{\epsilon}_i \cdot \hat{q}_i)(\hat{k}_t \times (\hat{n} \times \hat{q}_i))(1 + R_h) + (\hat{\epsilon}_i \cdot \hat{p}_i)(\hat{n} \cdot \hat{k}_i)(\hat{k}_t \times \hat{q}_i)(1 - R_v) \right\} \end{aligned} \quad (15b)$$

The orthonormal systems for the incident, reflected and transmitted fields are given respectively by $(\hat{v}_i, \hat{h}_i, \hat{k}_i)$, $(\hat{v}_s, \hat{h}_s, \hat{k}_s)$ and $(\hat{v}_t, \hat{h}_t, \hat{k}_t)$ with

$$\hat{k}_i = \hat{x} \sin \theta_i \cos \phi_i + \hat{y} \sin \theta_i \sin \phi_i - \hat{z} \cos \theta_i \quad (16a)$$

$$\hat{h}_i = -\hat{x} \sin \phi_i + \hat{y} \cos \phi_i \quad (16b)$$

$$\hat{v}_i = -\hat{x} \cos \theta_i \cos \phi_i - \hat{y} \cos \theta_i \sin \phi_i - \hat{z} \sin \theta_i \quad (16c)$$

$$\hat{k}_s = \hat{x} \sin \theta_s \cos \phi_s + \hat{y} \sin \theta_s \sin \phi_s + \hat{z} \cos \theta_s \quad (17a)$$

$$\hat{h}_s = -\hat{x} \sin \phi_s + \hat{y} \cos \phi_s \quad (17b)$$

$$\hat{v}_s = \hat{x} \cos \theta_s \cos \phi_s + \hat{y} \cos \theta_s \sin \phi_s - \hat{z} \sin \theta_s \quad (17c)$$

$$\hat{k}_t = \hat{x} \sin \theta_t \cos \phi_t + \hat{y} \sin \theta_t \sin \phi_t - \hat{z} \cos \theta_t \quad (18a)$$

$$\hat{h}_t = -\hat{x} \sin \phi_t + \hat{y} \cos \phi_t \quad (18b)$$

$$\hat{v}_t = -\hat{x} \cos \theta_t \cos \phi_t - \hat{y} \cos \theta_t \sin \phi_t - \hat{z} \sin \theta_t \quad (18c)$$

We note that except for the phase factors, the expressions in the integrands of the diffraction integral, (14), are not explicit functions of \bar{r}' . They are explicit functions of the slopes α and β which are functions of \bar{r}' . The tangent plane approximated diffraction integrals, as expressed in (14), do not take into account the effects of shadowing and multiple scattering.

At this point the question of shadowing comes in naturally. When the direction of incidence is not normal to the $x - y$ plane, some points on the rough surface will not be illuminated directly [Fig. 2.2]. For some points [point 1, Fig. 2.2] the local angle of incidence θ_{li} is not defined since

$$\cos \theta_{li} = -\hat{n} \cdot \hat{k}_i < 0 \quad (19)$$

All the points on the rough surface with such local slopes will not be illuminated directly. Some other points [point 2, Fig. 2] are not directly illuminated, even though the local angle of incidence is well defined, because of the height of rough surface at that point relative to the heights of the surrounding points. However, even without the complication due to shadowing the diffraction integrals for the scattered fields are difficult to evaluate analytically. This is because the local reflection coefficients R_v and R_h are functions of the surface slopes. One solution would be to evaluate the integrals numerically for a given realization of the random rough surface. Then, the shadowing effect can be incorporated directly during the numerical integration. In the limiting case of a perfectly conducting random rough surface, the local reflection coefficients R_v and R_h are 1 and -1 , respectively, and do not depend on the local surface slopes. Then, by neglecting the shadowing effect so that at all the points of the rough surface, $\hat{n} \times \bar{E} = 0$ and $\hat{n} \times \bar{H} = 2\hat{n} \times \bar{H}_i$ (even at the points with slopes such that they cannot be directly illuminated), the diffraction integrals can be cast into a well-defined integral.

For the dielectric random rough surface, various approximations have been applied to the Kirchhoff approximated diffraction integrals. The integrands which depend on the local surface slopes can be expanded in slope terms about zero slopes, and, then integrated by parts discarding the edge effect [Leader, 1971]. Usually only a few terms of the expansion are kept. In the high frequency limit the geometrical optics solution can be obtained from (14) with the stationary phase method. The geometrical optics solution is independent of frequency and states that the scattered intensity is proportional to the probability of the occurrence of the slopes which will specularly reflect or transmit the incident wave into the direction of observation [Barrick, 1968].

In the calculation of the reflected fields, the expression for the diffraction integral, (14a), contains the total field (incident and reflected) on the surface. The scattered field in region 0 evaluated from (14a) are the same whether one uses the total field or the reflected field on the surface of rough interface. However, when the integrand $\bar{F}(\alpha, \beta)$ is approximated the results using total or reflected surface fields may not give the same result [Holzer and Sung, 1978]. For the case when shadowing is present, using the total field or the reflected field on the illuminated region, while assuming no incident wave for the shadowed region, corresponds to different approximations and the results obtained for the scattered fields are different. The geometrical optics solution is independent of whether total or reflected field is used since the integrand $\bar{F}(\alpha, \beta)$ is evaluated at the stationary phase points $\alpha_{..}$ and $\beta_{..}$.

2.4 Coherent and Incoherent Scattering Coefficients

The scattered intensities from a random rough surface can in general be decomposed into coherent and incoherent components. Coherent components only contribute in the specular reflected or transmitted directions while incoherent components contribute in all directions. In the limiting case of flat surface the scattered intensity consists of only the specularly reflected and transmitted coherent intensities. In the other limiting case of a very rough surface, the coherent components almost vanish and intensities are incoherently scattered. In this section we solve for the coherent and incoherent scattered intensities by further approximating the integrands in the Kirchhoff approximated diffraction integrals.

One commonly used approximation is to expand the integrands $\bar{F}(\alpha, \beta)$ and $\bar{N}(\alpha, \beta)$ in slope terms about the zero slopes and to keep only the lowest few terms [Leader, 1971]. Expanding \bar{F} and \bar{N} we obtain

$$\bar{F}(\alpha, \beta) = \bar{F}(0, 0) + \alpha \left. \frac{\partial \bar{F}}{\partial \alpha} \right|_{\alpha, \beta=0} + \beta \left. \frac{\partial \bar{F}}{\partial \beta} \right|_{\alpha, \beta=0} + \dots \quad (20a)$$

$$\bar{N}(\alpha, \beta) = \bar{N}(0, 0) + \alpha \left. \frac{\partial \bar{N}}{\partial \alpha} \right|_{\alpha, \beta=0} + \beta \left. \frac{\partial \bar{N}}{\partial \beta} \right|_{\alpha, \beta=0} + \dots \quad (20b)$$

where $\bar{F}(0, 0)$ is $\bar{F}(\alpha, \beta)$ evaluated at $\alpha = \beta = 0$, etc. For angle of incidence near normal and for surfaces with small mean square surface slope, the Fresnel reflection coefficients only vary slightly with the change of local angle of incidence. Thus, we shall keep only the first terms in (20) in our subsequent calculations. Thus, from (14), we have

$$\bar{E}_s = \frac{ike^{ikr}}{4\pi r} E_{s, (\bar{I} - \hat{k}_s \hat{k}_s) \cdot \bar{F}(0, 0) I} \quad (21a)$$

$$\bar{E}_t = \frac{ik_1 e^{ik_1 r}}{r} E_{\perp} (\bar{I} - \hat{k}_t \hat{k}_t) \cdot \bar{N}(0, 0) I_t \quad (21b)$$

where the integrals I and I_t are given by

$$I = \int_A e^{i(\bar{k}_s - \bar{k}_t) \cdot \bar{r}'} d\bar{r}'_{\perp} \quad (22a)$$

$$I_t = \int_{A_{\perp}} e^{i(\bar{k}_s - \bar{k}_t) \cdot \bar{r}'} d\bar{r}'_{\perp} \quad (22b)$$

The scattered fields are now separated into a mean field and a fluctuating part of the field

$$\bar{E}_s(\bar{r}) = \bar{E}_{sm}(\bar{r}) + \bar{\mathcal{E}}_s(\bar{r}) \quad (23a)$$

$$\bar{E}_t(\bar{r}) = \bar{E}_{tm}(\bar{r}) + \bar{\mathcal{E}}_t(\bar{r}) \quad (23b)$$

with

$$\langle \bar{\mathcal{E}}_s(\bar{r}) \rangle = \langle \bar{\mathcal{E}}_t(\bar{r}) \rangle = 0 \quad (24)$$

and

$$\langle \bar{E}_s(\bar{r}) \rangle = \bar{E}_{sm}(\bar{r}) \quad (25a)$$

$$\langle \bar{E}_t(\bar{r}) \rangle = \bar{E}_{tm}(\bar{r}) \quad (25b)$$

The total scattered intensity is then a sum of coherent and incoherent intensities

$$\langle |\bar{E}_s(\bar{r})|^2 \rangle = |\bar{E}_{sm}|^2 + \langle |\bar{\mathcal{E}}_s(\bar{r})|^2 \rangle \quad (26a)$$

$$\langle |\bar{E}_t(\bar{r})|^2 \rangle = |\bar{E}_{tm}|^2 + \langle |\bar{\mathcal{E}}_t(\bar{r})|^2 \rangle \quad (26b)$$

In view of (21) and (22), we have

$$|\overline{E}_{sm}(\bar{r})|^2 = \frac{k^2 |E_0|^2}{16\pi^2 r^2} \left[|(\hat{v}_s \cdot \overline{F}(0,0))|^2 + |(\hat{h}_s \cdot \overline{F}(0,0))|^2 \right] |I|^2 \quad (27a)$$

$$\langle |\overline{E}_s(\bar{r})|^2 \rangle = \frac{k^2 |E_0|^2}{16\pi^2 r^2} \left[|(\hat{v}_s \cdot \overline{F}(0,0))|^2 + |(\hat{h}_s \cdot \overline{F}(0,0))|^2 \right] D_I \quad (27b)$$

$$|\overline{E}_{tm}(\bar{r})|^2 = \frac{k_1^2 |E_0|^2}{16\pi^2 r^2} \left[|(\hat{v}_t \cdot \overline{N}(0,0))|^2 + |(\hat{h}_t \cdot \overline{N}(0,0))|^2 \right] |I_t|^2 \quad (28a)$$

$$\langle |\overline{E}_t(\bar{r})|^2 \rangle = \frac{k_1^2 |E_0|^2}{16\pi^2 r^2} \left[|(\hat{v}_t \cdot \overline{N}(0,0))|^2 + |(\hat{h}_t \cdot \overline{N}(0,0))|^2 \right] D_{I_t} \quad (28b)$$

where

$$D_I = \langle |I|^2 \rangle - |I|^2 \quad (29a)$$

$$D_{I_t} = \langle |I_t|^2 \rangle - |I_t|^2 \quad (29b)$$

At this point, we need to further specify the height distribution $f(\bar{r}_\perp)$. The rough surface is assumed to be a Gaussian process. The probability for $f(\bar{r}_\perp)$ is independent of the position \bar{r}_\perp on the rough surface and has gaussian distribution

$$p(f(\bar{r}_\perp)) = \frac{1}{\sqrt{2\pi}\sigma} e^{-f^2/2\sigma^2} \quad (30)$$

where σ is the standard deviation of the surface height. For two points on the surface, $\bar{r}_{\perp 1}$ and $\bar{r}_{\perp 2}$, the joint probability density [Davenport and Root, 1958] is

$$p(f_1(\bar{r}_{\perp 1}), f_2(\bar{r}_{\perp 2})) = \frac{1}{2\pi\sigma^2\sqrt{1-C^2}} \exp \left[-\frac{f_1^2 - 2Cf_1f_2 + f_2^2}{2\sigma^2(1-C^2)} \right] \quad (31)$$

where C is the correlation coefficient between the two points and is a function of $\bar{r}_{\perp 1}$ and $\bar{r}_{\perp 2}$. For a statistically homogeneous isotropic surface, it is only a function of $\rho = \sqrt{(x_1 - x_2)^2 + (y_1 - y_2)^2}$.

$$\langle f(\bar{r}_{\perp 1})f(\bar{r}_{\perp 2}) \rangle = \sigma^2 C(\rho) \quad (32)$$

$$C(0) = 1 \quad (33a)$$

$$C(\infty) = 0 \quad (33b)$$

$$|C(\rho)| \leq 1 \quad (33c)$$

It can now easily be shown that

$$\langle e^{i\nu f(\bar{r}_{\perp})} \rangle = \int_{-\infty}^{\infty} df p(f) e^{i\nu f} = \exp \left[-\frac{1}{2} \sigma^2 \nu^2 \right] \quad (34)$$

where $\langle \rangle$ denotes the ensemble average. Similarly,

$$\begin{aligned} \langle e^{i\nu(f_1(\bar{r}_{\perp 1}) - f_2(\bar{r}_{\perp 2}))} \rangle &= \int_{-\infty}^{\infty} \int_{-\infty}^{\infty} df_1 df_2 p(f_1, f_2) e^{i\nu(f_1 - f_2)} \\ &= \exp \left[-\sigma^2 \nu^2 (1 - C(\rho)) \right] \end{aligned} \quad (35)$$

The expressions for $|\langle I \rangle|^2$, $D_I |\langle I_t \rangle|^2$ and D_{I_t} can now be derived in terms of the statistical moments of the height distribution.

The integral I is given by

$$I = \int_A e^{i\bar{k}_{\perp 1} \cdot \bar{r}_{\perp}} e^{ik_{\perp 2} f(\bar{r}_{\perp})} d\bar{r}_{\perp} \quad (36)$$

where

$$\bar{k}_d = \bar{k}_i - \bar{k}_s = k_{dx}\hat{x} + k_{dy}\hat{y} + k_{dz}\hat{z} \quad (37)$$

The ensemble average of I is given by

$$\langle I \rangle = \int_{A'} e^{i\bar{k}_{dz}\bar{r}'_{\perp}} \langle e^{ik_{dz}J(\bar{r}'_{\perp})} \rangle d\bar{r}'_{\perp} \quad (38)$$

In view of (34), we obtain, after carrying out the $d\bar{r}'_{\perp}$ integration,

$$\langle I \rangle = 4L_x L_y \exp \left[-\frac{1}{2} k_{dz}^2 \sigma^2 \right] \text{sinc}(k_{dx}L_x) \text{sinc}(k_{dy}L_y) \quad (39)$$

where $\text{sinc } x = \sin x/x$, $2L_x$ and $2L_y$ are the lengths of rough surface in the x and y directions, respectively so that

$$A' = 4L_x L_y \quad (40)$$

Therefore,

$$|\langle I \rangle|^2 = 16L_x^2 L_y^2 \exp[-k_{dz}^2 \sigma^2] \text{sinc}^2(k_{dx}L_x) \text{sinc}^2(k_{dy}L_y) \quad (41)$$

By allowing L_x and L_y to approach infinity in the above expression, we obtain

$$|\langle I \rangle|^2 = 4\pi^2 A' \exp[-k_{dz}^2 \sigma^2] \delta(k_{dx}) \delta(k_{dy}) \quad (42)$$

where δ is the Dirac delta function and we made use of the following identity:

$$\lim_{L_x, L_y \rightarrow \infty} \frac{L_x L_y}{\pi^2} \text{sinc}^2(k_{dx}L_x) \text{sinc}^2(k_{dy}L_y) = \delta(k_{dx}) \delta(k_{dy}) \quad (43)$$

The integral for $\langle II' \rangle$ is given by

$$\langle II' \rangle = \int_A d\bar{r}_\perp \int_A d\bar{r}'_\perp e^{i\bar{k}_\perp \cdot (\bar{r}_\perp - \bar{r}'_\perp)} \langle e^{ik_{dx}(f(\bar{r}_\perp) - f(\bar{r}'_\perp))} \rangle \quad (44)$$

Using (35) and making the usual change of variables of the difference and half the sum of coordinates, we obtain

$$\langle II' \rangle = \int_{-2L_x}^{2L_x} dx \int_{-2L_y}^{2L_y} dy (2L_x - |x|)(2L_y - |y|) \exp(ik_{dx}x + ik_{dy}y) \exp[-k_{dz}^2 \sigma^2 (1 - C(\rho))] \quad (45)$$

The correlation function $C(\rho)$ is assumed to have a gaussian form [Barrick, 1970]

$$C(\rho) = e^{-\rho^2/l^2} \quad (46)$$

where l is the correlation length for the random variable $f(\bar{r}_\perp)$ in the transverse plane. The expression for the standard deviation of the integral I can now be evaluated in closed form. We first note that $|\langle I \rangle|^2$ can be also be expressed as

$$|\langle I \rangle|^2 = \int_{-2L_x}^{2L_x} dx \int_{-2L_y}^{2L_y} dy (2L_x - |x|)(2L_y - |y|) \exp(ik_{dx}x + ik_{dy}y) \exp(-\sigma^2 k_{dz}^2) \quad (47)$$

Combining (45) and (47) and in view of (46), we note that the contribution of the integral of $\langle II' \rangle - |\langle I \rangle|^2$ come from $|x|$ and $|y|$ of the same order of l and the integrand is practically zero for $\rho = (x^2 + y^2)^{1/2}$ larger then a few l 's. Assuming the illuminated rough surface contains many correlation lengths $L_x, L_y \gg l$, we obtain

$$\begin{aligned} D_I &= \langle II' \rangle - |\langle I \rangle|^2 \\ &= A_0 \int_{-\infty}^{\infty} dx \int_{-\infty}^{\infty} dy \left\{ \exp[-\sigma^2 k_{dz}^2 (1 - C(\rho))] - \exp[-\sigma^2 k_{dz}^2] \right\} \exp[ik_{dx}x + ik_{dy}y] \quad (48) \end{aligned}$$

Converting the integral in (48) to cylindrical coordinates and carrying out the integral in $d\phi$ gives a Bessel function in the integrand. We further make a power series expansion

$$\exp(-\sigma^2 k_{dz}^2(1 - C(\rho))) - \exp(-\sigma^2 k_{dz}^2) = \exp(-\sigma^2 k_{dz}^2) \left[\sum_{m=1}^{\infty} \frac{(\sigma^2 k_{dz}^2)^m}{m!} \exp\left(-\frac{m\rho^2}{l^2}\right) \right] \quad (49)$$

and make use of the integral identity

$$\int_0^{\infty} d\rho \rho J_m(k_\rho \rho) e^{-m\rho^2/l^2} = \frac{l^2}{2m} \exp\left(-\frac{k_\rho l^2}{4m}\right) \quad (50)$$

Using (49)-(50) in (48), we obtain [Gradshteyn and Ryzhik, 1965]

$$\begin{aligned} D_I &= \langle II^* \rangle - \langle I \rangle^2 \\ &= \pi A_{..} \sum_{m=1}^{\infty} \frac{(k_{dz}^2 \sigma^2)^m}{m!m} l^2 \exp\left[-\frac{(k_{dx}^2 + k_{dy}^2)l^2}{4m}\right] \exp[-\sigma^2 k_{dz}^2] \end{aligned} \quad (51)$$

In a similar manner, the expressions for $\langle |I_t|^2 \rangle$ and D_{I_t} may be derived. They are

$$\langle |I_t|^2 \rangle = 4\pi^2 A_{..} \exp[-\sigma^2 k_{tdz}^2] \delta(k_{tdx}) \delta(k_{tdy}) \quad (52)$$

and

$$D_{I_t} = \pi A_{..} \sum_{m=1}^{\infty} \frac{(k_{tdz}^2 \sigma^2)^m}{m!m} l^2 \exp\left[-\frac{(k_{tdx}^2 + k_{tdy}^2)l^2}{4m}\right] \exp[-\sigma^2 k_{tdz}^2] \quad (53)$$

where

$$\bar{k}_{td} = \bar{k}_i - \bar{k}_t = k_{tdx} \hat{x} + k_{tdy} \hat{y} + k_{tdz} \hat{z} \quad (54)$$

The bistatic scattering coefficients for the reflected intensities are defined as

$$\gamma_{ln}^r(\hat{k}_s, \hat{k}_i) = \frac{4\pi r^2 (S_r)_l}{A_{..} \cos \theta_i (S_{..})_n} \quad (a, b = v, h) \quad (55)$$

where subscript a represents the polarization of the incident wave, subscript b the polarization of the scattered wave, S_i the Poynting power density of the incident wave, S_r the Poynting power density of the scattered wave, A_i the area of the rough surface projected to the $x - y$ plane, and θ_i the incident angle. From (21), we calculate the vertically and horizontally polarized coherent and incoherent scattered intensities for the cases of vertically and horizontally polarized incident fields according to (27). Let

$$\bar{F}_b(0, 0) = \bar{F}(0, 0) \Big|_{i_i=b_i} \quad (56)$$

$\bar{F}(0, 0)$ can be calculated by setting $\alpha = \beta = 0$ in (12) and (15a). Next we take the dot product with \hat{v}_s and \hat{h}_s .

$$\hat{h}_s \cdot \bar{F}_h(0, 0) = [(1 - R_{h..}) \cos \theta_i - (1 + R_{h..}) \cos \theta_s] \cos(\phi_s - \phi_i) \quad (57a)$$

$$\hat{v}_s \cdot \bar{F}_h(0, 0) = [(1 - R_{h..}) \cos \theta_i \cos \theta_s - (1 + R_{h..})] \sin(\phi_s - \phi_i) \quad (57b)$$

$$\hat{h}_s \cdot \bar{F}_v(0, 0) = [(1 + R_{v..}) - (1 - R_{v..}) \cos \theta_i \cos \theta_s] \sin(\phi_s - \phi_i) \quad (57c)$$

$$\hat{v}_s \cdot \bar{F}_v(0, 0) = [-(1 + R_{v..}) \cos \theta_s + (1 - R_{v..}) \cos \theta_i] \cos(\phi_s - \phi_i) \quad (57d)$$

The $R_{v..}$ and $R_{h..}$ of the above equations are respectively the Fresnel reflection coefficients of a smooth surface for vertically and horizontally polarized incident waves, and are equal to the expressions in (9a) and (9b) with θ_{i_i} replaced by θ_i .

In view of (27), the bistatic scattering coefficients γ_{ab}^r can be decomposed into a coherent part $\gamma_{ab}^{r,c}$ and an incoherent part $\gamma_{ab}^{r,i}$.

$$\gamma_{ab}^r(\hat{k}_s, \hat{k}_i) = \gamma_{ab}^{r,c}(\hat{k}_s, \hat{k}_i) + \gamma_{ab}^{r,i}(\hat{k}_s, \hat{k}_i) \quad (58)$$

where

$$\gamma_{c_{ab}}^r(\hat{k}_s, \hat{k}_i) = \frac{k^2}{4\pi A_{i, \cos \theta_i}} |\hat{a}_s \cdot \bar{F}_b(0, 0)|^2 |I|^2 \quad (59a)$$

$$\gamma_{i_{ab}}^r(\hat{k}_s, \hat{k}_i) = \frac{k^2}{4\pi A_{i, \cos \theta_i}} |\hat{a}_s \cdot \bar{F}_b(0, 0)|^2 D_I \quad (59b)$$

The coherent scattered wave only exists in the specular direction. Thus, using (42) and (57), and since

$$\delta(k_{dx})\delta(k_{dy}) = \delta(\theta_s - \theta_i)\delta(\phi_s - \phi_i)/(k^2 \sin \theta_i \cos \theta_i)$$

we find that

$$\gamma_{c_{ab}}^r(\hat{k}_s, \hat{k}_i) = \begin{cases} \frac{4\pi |I_{i, \perp}|^2}{\sin^2 \theta_i} \exp(-4k^2 \sigma^2 \cos^2 \theta_i) \delta(\theta_s - \theta_i) \delta(\phi_s - \phi_i) & \text{if } a = b \\ 0 & \text{if } a \neq b \end{cases} \quad (60)$$

By the same token, we define the bistatic scattering coefficients for the transmitted intensities to be,

$$\gamma_{i_{ab}}^t(\hat{k}_t, \hat{k}_i) = \frac{4\pi r^2 (S_t)_b}{A_{i, \cos \theta_i} (S_{i, \perp})_a} \quad (61)$$

where S_t is the Poynting power density of the transmitted wave. Following exactly the same procedure we obtain

$$\gamma_{ab}^t(\hat{k}_t, \hat{k}_i) = \gamma_{c_{ab}}^t(\hat{k}_t, \hat{k}_i) + \gamma_{i_{ab}}^t(\hat{k}_t, \hat{k}_i) \quad (62)$$

where

$$\gamma_{c_{ab}}^t(\hat{k}_t, \hat{k}_i) = \frac{k_1^2}{4\pi A_{i, \cos \theta_i}} \frac{\eta}{\eta_1} |\hat{a}_t \cdot \bar{N}_b(0, 0)|^2 |I_t|^2 \quad (63a)$$

$$\gamma_{i_{ab}}^t(\hat{k}_t, \hat{k}_i) = \frac{k_1^2}{4\pi A_{i, \cos \theta_i}} \frac{\eta}{\eta_1} |\hat{a}_t \cdot \bar{N}_b(0, 0)|^2 D_I \quad (63b)$$

with

$$\bar{N}_{l,(0,0)} = \bar{N}(0,0)_{i,l=l_i} \quad (64)$$

and

$$\hat{h}_t \cdot \bar{N}_h(0,0) = \left[\frac{\eta_1}{\eta} (1 - R_{h..}) \cos \theta_t - (1 - R_{h..}) \cos \theta_t \right] \cos(\phi_t - \phi_i) \quad (65a)$$

$$\hat{v}_t \cdot \bar{N}_h(0,0) = \left[-\frac{\eta_1}{\eta} (1 - R_{h..}) \cos \theta_t \cos \theta_t - (1 + R_{h..}) \right] \sin(\phi_t - \phi_i) \quad (65b)$$

$$\hat{h}_t \cdot \bar{N}_v(0,0) = \left[\frac{\eta_1}{\eta} (1 + R_{v..}) + (1 - R_{v..}) \cos \theta_t \cos \theta_t \right] \sin(\phi_t - \phi_i) \quad (65c)$$

$$\hat{v}_t \cdot \bar{N}_v(0,0) = \left[\frac{\eta_1}{\eta} (1 + R_{v..}) \cos \theta_t + (1 - R_{v..}) \cos \theta_t \right] \cos(\phi_t - \phi_i) \quad (65d)$$

Again, the coherent component only exists in the specular transmission direction, and we find

$$\gamma_{c_{h..}}^t(\hat{k}_t, \hat{k}_i) = 4\pi \frac{\eta_1 \cos \theta_{1i}}{\eta \cos \theta_i} \frac{|1 + R_{v..}|^2}{\sin \theta_{1i}} \exp[-(k_1 \cos \theta_{1i} - k \cos \theta_i)^2 \sigma^2] \delta(\theta_t - \theta_{1i}) \delta(\phi_t - \phi_i) \quad (66a)$$

$$\gamma_{c_{h..}}^t(\hat{k}_t, \hat{k}_i) = 4\pi \frac{\eta \cos \theta_{1i}}{\eta_1 \cos \theta_i} \frac{|1 + R_{h..}|^2}{\sin \theta_{1i}} \exp[-(k_1 \cos \theta_{1i} - k \cos \theta_i)^2 \sigma^2] \delta(\theta_t - \theta_{1i}) \delta(\phi_t - \phi_i) \quad (66b)$$

and

$$\gamma_{c_{a..}}(\hat{k}_t, \hat{k}_i) = 0 \quad \text{for } a \neq b \quad (66)$$

where θ_{1i} is related to θ_i by the Snell's law

$$k_1 \sin \theta_{1i} = k \sin \theta_i \quad (67)$$

We note that the coherent component is only nonzero in the specular direction. Also as $k\sigma$ increases, the coherent component diminishes exponentially.

2.5 Geometrical Optics Solution

Under the geometric optics limit as $k \rightarrow \infty$, the asymptotic solution to the Kirchhoff approximated diffraction integrals can be derived using the method of stationary phase. The coherent component of the scattered fields will vanish in this limit and only incoherent component will remain. The bistatic scattering coefficients for the reflected and transmitted fields are derived and shown to be proportional to the probability of the occurrence of the slopes which will specularly reflected or transmit the incident wave into the observation direction. The bistatic scattering coefficients satisfy reciprocity but violates energy conservation. This is due to the neglect of the effects of multiple scattering and shadowing. The scattering coefficients are modified to incorporate the shadowing effects. The sum of reflected and transmitted intensities are then shown to be always less than the incident intensity since only the single scattering solution is used. However, this will be made use of in the next section to derive the upper and lower bounds for the correct emissivity of a rough surface in the geometrical optics limit.

Stationary Phase Method

The diffraction integrals are evaluated using the method of stationary phase. The reflected fields are first calculated. From (14), the exponential phase factor is

$$\psi = \bar{k}_d \bar{r}' = k_{dx} x' + k_{dy} y' + k_{dz} f(x', y') \quad (68)$$

To determine the stationary phase point, we set

$$\frac{\partial \psi}{\partial x'} = 0 = k_{dx} + k_{dz} \alpha_{..} \quad (69)$$

so that at the stationary phase point

$$\alpha_{..} = -\frac{k_{dx}}{k_{dz}} \quad (70)$$

Similarly by differentiating the phase term ψ with respect to y' we get

$$\beta_{..} = -\frac{k_{dy}}{k_{dz}} \quad (71)$$

Thus, the slopes α and β assume values of $\alpha_{..}$ and $\beta_{..}$ at the stationary phase point. The slopes $\alpha_{..}$ and $\beta_{..}$ are such that the incident and scattered wave direction form a specular reflection. This can be seen from the fact that from (12) we have

$$\hat{n}(\alpha_{..}, \beta_{..}) = \frac{(\bar{k}_s - \bar{k}_i)}{|\bar{k}_d|} \quad (72)$$

Replacing the surface slopes $\bar{\alpha}$ and $\bar{\beta}$ by $\alpha_{..}$ and $\beta_{..}$, we obtain, from (14),

$$\bar{E}_s(\bar{r}) = \frac{ik e^{ikr}}{4\pi r} E_{..}(\bar{J} - \hat{k}_s \hat{k}_s) \bar{F}(\alpha_{..}, \beta_{..}) \int_A d\bar{r}'_{\perp} e^{i\bar{k}_{\perp} \cdot \bar{r}'_{\perp}} \quad (73)$$

The scattered intensity is

$$\langle |\bar{E}_s|^2 \rangle = \frac{k^2 |E_{..}|^2}{16\pi^2 r^2} \left| (\bar{J} - \hat{k}_s \hat{k}_s) \cdot \bar{F}(\alpha_{..}, \beta_{..}) \right|^2 \langle II' \rangle \quad (74)$$

where

$$\langle II' \rangle = \left\langle \int_A d\bar{r}_{\perp} \int_A d\bar{r}'_{\perp} e^{i\bar{k}_{\perp} \cdot (\bar{r}_{\perp} - \bar{r}'_{\perp})} e^{ik_{\perp z} (f(\bar{r}_{\perp}) - f(\bar{r}'_{\perp}))} \right\rangle \quad (75)$$

The above integral can be solved by the method of asymptotics. For large k , contributions of the integral come from regions where (x', y') is close to (x, y) . Expanding $f(x', y')$ about (x, y) ,

$$\begin{aligned} f(x', y') &= f(x, y) + \alpha(x' - x) + \beta(y' - y) \\ &+ \sum_{n=0}^{\infty} \sum_{\substack{m=0 \\ n+m \neq 0,1}}^{\infty} \frac{1}{n!m!} \frac{\partial^{m+n} f}{\partial x^n \partial y^m} (x' - x)^n (y' - y)^m \end{aligned} \quad (76)$$

and replacing the integration variables by

$$u = k(x - x') \quad (77a)$$

$$v = k(y - y') \quad (77b)$$

we obtain

$$\begin{aligned} \langle II' \rangle &= \left\langle \frac{1}{k^2} A_{..} \int \int du dv \exp \left[iu(q_x + \alpha q_z) + iv(q_y + \beta q_z) + O\left(\frac{1}{k}\right) \right] \right\rangle \\ &= \frac{4\pi^2 A_{..}}{k^2} \langle \delta(q_x + \alpha q_z) \delta(q_y + \beta q_z) \rangle \end{aligned} \quad (78)$$

where

$$\bar{q} = \frac{\bar{k}_l}{k} \quad (79)$$

Therefore,

$$\langle \lim_{k \rightarrow \infty} II^* \rangle = \frac{4\pi^2 A_{..}}{k^2} \int_{-\infty}^{\infty} \int_{-\infty}^{\infty} d\alpha d\beta \delta(q_x \alpha q_z) \delta(q_y + \beta q_z) p(\alpha, \beta) \quad (80)$$

where $p(\alpha, \beta)$ is the probability density function for the slopes at the surface. Thus,

$$\langle \lim_{k \rightarrow \infty} II^* \rangle = \frac{4\pi^2 A_{..}}{k_{dz}^2} p\left(-\frac{k_{dx}}{k_{dz}}, -\frac{k_{dy}}{k_{dz}}\right) \quad (81)$$

For the gaussian random rough surface

$$p(\alpha, \beta) = \frac{1}{2\pi\sigma^2 |C'''(0)|} \exp\left[-\frac{\alpha^2 + \beta^2}{2\sigma^2 |C'''(0)|}\right] \quad (82)$$

where σ is the standard deviation of the height of rough surface and $C'''(0)$ is the double derivative of the correlation function at $\rho = 0$. Thus, $\sigma |C'''(0)|$ is the mean square surface slope ε^2 and for the gaussian correlation function with correlation length l

$$\varepsilon^2 = \sigma^2 |C'''(0)| = 2 \frac{\sigma^2}{l^2} \quad (83)$$

Hence

$$\langle II^* \rangle = \frac{2\pi A_{..}}{k_{dz}^2 \sigma^2 |C'''(0)|} \exp\left[-\frac{k_{dx}^2 + k_{dy}^2}{2k_{dz}^2 \sigma^2 |C'''(0)|}\right] \quad (84)$$

Another way to evaluate $\langle II^* \rangle$ is to perform the ensemble average first, and then to approximate the integral. From (45) and (75)

$$\langle II^* \rangle = \int_{-2L_x}^{2L_x} dx \int_{-2L_y}^{2L_y} dy (2L_x - |x|)(2L_y - |y|) e^{i\bar{k}_{dx} \bar{r}_x + i\bar{k}_{dy} \bar{r}_y} \exp[-k_{dz}^2 \sigma^2 (1 - C(\rho))] \quad (85)$$

Since $k_{dz}^2 \sigma^2 \gg 1$, most of the contribution comes from around the origin. Thus expanding the integrand about the origin we have $1 - C(\rho) \approx \rho^2 |C'''(0)|/2$ and substituting into (84), the integral can be evaluated readily by making use of the integral identity

$$\int_0^\infty d\rho \rho J_0(k\rho) \exp(-\alpha\rho^2) = \frac{1}{2\alpha} \exp\left[-\frac{k^2}{4\alpha}\right] \quad (86)$$

The final result for $\langle II' \rangle$ is the same as (84).

For an incident field with polarization b_i , the scattered intensity for polarization a_s is given by

$$\langle |E_s(\bar{r})|^2 \rangle = \frac{k^2 |E_0|^2}{16\pi^2 r^2} |\hat{a}_s \cdot \bar{F}_l(\alpha_s, \beta_s)|^2 \langle II' \rangle \quad (87)$$

where

$$\bar{F}_l(\alpha_s, \beta_s) = \bar{F}(\alpha_s, \beta_s)|_{i=b_i} \quad (88)$$

and using (15a), we find that

$$|\hat{a}_s \cdot \bar{F}_l(\alpha_s, \beta_s)|^2 = \frac{|\bar{k}_d|^{14}}{k^2 |\hat{k}_i \times \hat{k}_s|^4 k_{dz}^2} f_{lss} \quad (89)$$

with

$$f_{vv} = \left| (\hat{h}_s \cdot \hat{k}_i)(\hat{h}_i \cdot \hat{k}_s) R_h + (\hat{v}_s \cdot \hat{k}_i)(\hat{v}_i \cdot \hat{k}_s) R_v \right|^2 \quad (90a)$$

$$f_{hv} = \left| (\hat{v}_s \cdot \hat{k}_i)(\hat{h}_i \cdot \hat{k}_s) R_h - (\hat{h}_s \cdot \hat{k}_i)(\hat{v}_i \cdot \hat{k}_s) R_v \right|^2 \quad (90b)$$

$$f_{vh} = \left| (\hat{h}_s \cdot \hat{k}_i)(\hat{v}_i \cdot \hat{k}_s) R_h - (\hat{v}_s \cdot \hat{k}_i)(\hat{h}_i \cdot \hat{k}_s) R_v \right|^2 \quad (90c)$$

$$f_{hh} = \left| (\hat{v}_s \cdot \hat{k}_i)(\hat{v}_i \cdot \hat{k}_s) R_h + (\hat{h}_s \cdot \hat{k}_i)(\hat{h}_i \cdot \hat{k}_s) R_v \right|^2 \quad (90d)$$

and R_r and R_h are evaluated at

$$\hat{n} = \frac{k_{d,r}/k_{d,z}\hat{x} + k_{d,y}/k_{d,z}\hat{y} + \hat{z}}{\sqrt{k_{d,r}^2/k_{d,z}^2 + k_{d,y}^2/k_{d,z}^2 + 1}} \quad (91)$$

Then, the bistatic scattering coefficients for the reflected intensities are, in view of (55) and (84)

$$\gamma_{ab}^r(\hat{k}_s, \hat{k}_i) = \frac{|\bar{k}_d|^4}{\cos \theta_i |\hat{k}_i \times \hat{k}_s|^4 k_{d,z}^4} \frac{1}{2\sigma^2 |C'''(0)|} \exp \left[-\frac{k_{d,r}^2 + k_{d,y}^2}{2k_{d,z}^2 \sigma^2 |C'''(0)|} \right] f_{ab} \quad (92)$$

We note that, from (90), the geometrical optics solution does not depend on whether the total or scattered field is used in the diffraction integral because $\bar{F}(\alpha, \beta)$ is evaluated at the stationary phase point [Holzer and Sung, 1978].

In the backscattering direction $\hat{k}_s = -\hat{k}_i$. The backscattering cross sections are defined to be

$$\sigma_{ab}(\hat{k}_i) = \cos \theta_i \gamma_{ab}^r(-\hat{k}_i, \hat{k}_i) \quad (93)$$

From (92), we obtain

$$\sigma_{hh}(\theta_i) = \sigma_{vv}(\theta_i) = \frac{|R|^2}{\cos^4 \theta_i 2\sigma^2 |C'''(0)|} \exp \left[-\frac{\tan^2 \theta_i}{2\sigma^2 |C'''(0)|} \right] \quad (94)$$

$$\sigma_{vh}^r(\theta_i) = \sigma_{hv}^r(\theta_i) = 0 \quad (95)$$

where R is the reflection coefficient at normal incidence. We note from (95) that there is no depolarization in the backscattering direction.

The bistatic scattering coefficients for the transmitted waves can be derived in a similar manner. The stationary phase method is used to evaluate the diffraction integral for the transmitted fields. The stationary phase points are given by

$$\alpha_{..} = -\frac{k_{t,d,r}}{k_{t,d,z}} \quad (96a)$$

$$\beta_{..} = -\frac{k_{t,dy}}{k_{t,dz}} \quad (96b)$$

where $\alpha_{..}$ and $\beta_{..}$ are the values that the slopes α and β assume at the stationary phase point. We note that at the stationary phase point

$$\hat{n} = \frac{k_{t,dx}/k_{t,dz}\hat{x} + k_{t,dy}/k_{t,dz}\hat{y} + \hat{z}}{\sqrt{k_{t,dx}^2/k_{t,dz}^2 + k_{t,dy}^2/k_{t,dz}^2 + 1}} \quad (97)$$

and it can be shown

$$\bar{k}_i - (\bar{k}_i \cdot \hat{n})\hat{n} = \bar{k}_t - (\bar{k}_t \cdot \hat{n})\hat{n} \quad (98)$$

which is a statement of Snell's law that the tangential components of the wave vectors \bar{k}_i and \bar{k}_t must be equal. Thus, the slopes $\alpha_{..}$ and $\beta_{..}$ are such that incident and transmitted wave directions form a specular transmission.

The transmitted field is obtained from (14) by replacing α and β by $\alpha_{..}$ and $\beta_{..}$.

$$\bar{E}_t(\bar{r}) = -\frac{ik_1 e^{ik_1 r}}{4\pi r} E_{..} (\bar{I} - \hat{k}_t \hat{k}_t) \cdot \bar{N}(\alpha_{..}, \beta_{..}) \int_A d\bar{r}'_{\perp} e^{i\bar{k}_{t,\perp} \cdot \bar{r}'} \quad (99)$$

The transmitted intensity is

$$\langle |\bar{E}_t|^2 \rangle = \frac{k_1^2 |E_{..}|^2}{16\pi^2 r^2} \left| (\bar{I} - \hat{k}_t \hat{k}_t) \cdot \bar{N}(\alpha_{..}, \beta_{..}) \right|^2 \langle I_t I_t^* \rangle \quad (100)$$

where

$$\langle I_t I_t^* \rangle = \left\langle \int_{A_{..}} d\bar{r}'_{\perp} \int_{A_{..}} d\bar{r}''_{\perp} e^{ik_{t,dx}(\bar{r}'_{\perp} - \bar{r}''_{\perp})} e^{ik_{t,dz}(f(\bar{r}'_{\perp}) - f(\bar{r}''_{\perp}))} \right\rangle \quad (101)$$

Again the above integral is solved by the method of asymptotics to yield

$$\langle I_t I_t^* \rangle = \frac{2\pi A_{..}}{k_{t,dz}^2 \sigma^2 |C'''(0)|} \exp \left[-\frac{k_{t,dx}^2 + k_{t,dy}^2}{2k_{t,dz}^2 \sigma^2 |C'''(0)|} \right] \quad (102)$$

The bistatic scattering coefficients for the transmitted intensities are, in view (61)

$$\gamma_{ab}^t(\hat{k}_t, \hat{k}_i) = \frac{2k_1^2 |\bar{k}_{td}|^2 (\hat{n} \cdot \hat{k}_t)^2}{\cos \theta_i |\hat{k}_i \times \hat{k}_t|^4 k_{tdz}^4} \frac{\eta}{\eta_1} \frac{1}{\sigma^2 |C''(0)|} \exp \left[-\frac{k_{tdx}^2 - k_{tdy}^2}{2k_{tdz}^2 \sigma^2 |C''(0)|} \right] W_{ab} \quad (103)$$

with

$$W_{vv} = \left| (\hat{h}_t \cdot \hat{k}_i)(\hat{h}_i \cdot \hat{k}_t)(1 + R_h) + (\hat{v}_t \cdot \hat{k}_i)(\hat{v}_i \cdot \hat{k}_t) \frac{\eta_1}{\eta} (1 + R_v) \right|^2 \quad (104a)$$

$$W_{hv} = \left| -(\hat{v}_t \cdot \hat{k}_i)(\hat{h}_i \cdot \hat{k}_t)(1 + R_h) + (\hat{h}_t \cdot \hat{k}_i)(\hat{v}_i \cdot \hat{k}_t) \frac{\eta_1}{\eta} (1 + R_v) \right|^2 \quad (104b)$$

$$W_{vh} = \left| (\hat{h}_t \cdot \hat{k}_i)(\hat{v}_i \cdot \hat{k}_t)(1 + R_h) - (\hat{v}_t \cdot \hat{k}_i)(\hat{h}_i \cdot \hat{k}_t) \frac{\eta_1}{\eta} (1 + R_v) \right|^2 \quad (104c)$$

$$W_{hh} = \left| (\hat{v}_t \cdot \hat{k}_i)(\hat{v}_i \cdot \hat{k}_t)(1 + R_h) + (\hat{h}_t \cdot \hat{k}_i)(\hat{h}_i \cdot \hat{k}_t) \frac{\eta_1}{\eta} (1 + R_v) \right|^2 \quad (104d)$$

The reflection coefficients R_h and R_v are to be taken at the stationary phase point so that

$$R_h = \frac{k(\hat{n} \cdot \hat{k}_i) - k_1(\hat{n} \cdot \hat{k}_t)}{k(\hat{n} \cdot \hat{k}_i) + k_1(\hat{n} \cdot \hat{k}_t)} \quad (105a)$$

$$R_v = \frac{k_1(\hat{n} \cdot \hat{k}_i) - k(\hat{n} \cdot \hat{k}_t)}{k_1(\hat{n} \cdot \hat{k}_i) + k(\hat{n} \cdot \hat{k}_t)} \quad (105b)$$

Specular Surface Limit

In the limit $\sigma^2 C'''(0) \rightarrow 0$, which means that the variance of the slope goes to zero, a specular surface is obtained. In such a limit

$$\lim_{\sigma^2 |C'''(0)| \rightarrow 0} \frac{1}{2\sigma^2 |C'''(0)|} \exp \left[-\frac{k_{dx}^2 + k_{dy}^2}{2k_{dz}^2 \sigma^2 |C'''(0)|} \right] = \pi \delta \left(\frac{k_{dx}}{k_{dz}}, \frac{k_{dy}}{k_{dz}} \right) \quad (106)$$

In terms of angular variable θ, ϕ

$$\delta \left(\frac{k_{dx}}{k_{dz}}, \frac{k_{dy}}{k_{dz}} \right) = 4 \frac{\cos \theta_i}{\sin \theta_i} \delta(\theta_s - \theta_i) \delta(\phi_s - \phi_i) \quad (107)$$

which implies that it is nonvanishing only at $\theta_s = \theta_i$ and $\phi_s = \phi_i$. Then, the bistatic scattering coefficients for the reflected intensities simplify to

$$\gamma_{vv}^r(\hat{k}_s, \hat{k}_i) = \frac{4\pi}{\sin \theta_i} |R_{vv}|^2 \delta(\theta_s - \theta_i) \delta(\phi_s - \phi_i) \quad (108a)$$

$$\gamma_{hh}^r(\hat{k}_s, \hat{k}_i) = \frac{4\pi}{\sin \theta_i} |R_{hh}|^2 \delta(\theta_s - \theta_i) \delta(\phi_s - \phi_i) \quad (108b)$$

$$\gamma_{hv}^r(\hat{k}_s, \hat{k}_i) = \gamma_{vh}^r(\hat{k}_s, \hat{k}_i) = 0 \quad (108c)$$

where R_{vv} and R_{hh} are the Fresnel reflection coefficients of a flat surface. In a similar manner, the bistatic scattering coefficients for the transmitted intensities simplify to

$$\gamma_{vv}^t(\hat{k}_t, \hat{k}_i) = \frac{4\pi}{\sin \theta_{1t}} (1 - |R_{vv}|^2) \delta(\theta_t - \theta_{1t}) \delta(\phi_t - \phi_i) \quad (109a)$$

$$\gamma_{hh}^t(\hat{k}_t, \hat{k}_i) = \frac{4\pi}{\sin \theta_{1t}} (1 - |R_{hh}|^2) \delta(\theta_t - \theta_{1t}) \delta(\phi_t - \phi_i) \quad (109b)$$

$$\gamma_{hv}^t(\hat{k}_t, \hat{k}_i) = \gamma_{vh}^t(\hat{k}_t, \hat{k}_i) = 0 \quad (109c)$$

where

$$\theta_{1i} = \sin^{-1} \left(\frac{k}{k_1} \sin \theta_i \right) \quad (110)$$

Therefore, all the scattered intensities are scattered into the specular reflection and transmission directions of a flat surface.

The bistatic scattering coefficients obtained in this section are single scattering solutions which neglect the multiple scattering and shadowing effects. In this present form, they satisfy the principle of reciprocity but violate the energy conservation. In the next section we will investigate the reciprocity and energy conservation relations. Then the bistatic coefficients are modified to incorporate the shadowing effects and later used to study the emissivity of a rough surface in the geometrical optics limit.

Reciprocity and Conservation of Energy

We note that a reciprocity relation exists for the bistatic transmission and reflection coefficients obtained in (92) and (103). Consider two media 1 and 2 with indices of refraction n_1 and n_2 and with wave numbers k_1 and k_2 . The two media are separated by a rough surface. Then the bistatic transmission coefficient $\gamma_{ab}^{t21}(\hat{k}_2, \hat{k}_1)$ signifies a wave incident from angle (θ_1, ϕ_1) with polarization b onto angle (θ_2, ϕ_2) in medium 2 with polarization a . This is obtained from (103) by substituting $(\theta_i, \phi_i) = (\theta_1, \phi_1)$, $(\theta_t, \phi_t) = (\theta_2, \phi_2)$, $k_t = k_2$, and $k = k_1$. Similarly $\gamma_{ab}^{t12}(\hat{k}_1, \hat{k}_2)$ is for an incident wave from medium 2 and can be obtained by substituting in (103) $(\theta_i, \phi_i) = (\theta_2, \phi_2)$, $(\theta_t, \phi_t) = (\theta_1, \phi_1)$, $k_t = k_1$ and $k = k_2$. The following reciprocity relation is seen to hold for the bistatic transmission coefficients.

$$n_1^2 \cos \theta_1 \gamma_{ab}^{t21}(\hat{k}_2, \hat{k}_1) = n_2^2 \cos \theta_2 \gamma_{ab}^{t12}(\hat{k}_1, \hat{k}_2) \quad (111)$$

For the bistatic reflection coefficients, we similarly obtain the following reciprocity relations

$$\cos \theta_s \gamma_{ab}^{r11}(\hat{k}_i, \hat{k}_s) = \cos \theta_i \gamma_{ba}^{r11}(\hat{k}_s, \hat{k}_i) \quad (112)$$

and

$$\cos \theta_s \gamma_{ab}^{r22}(\hat{k}_i, \hat{k}_s) = \cos \theta_i \gamma_{ba}^{r22}(\hat{k}_s, \hat{k}_i) \quad (113)$$

where $\gamma_{ab}^{r11}(\hat{k}_s, \hat{k}_i)$ and $\gamma_{ab}^{r22}(\hat{k}_s, \hat{k}_i)$ are the bistatic reflection coefficients in media 1 and 2 between an incident wave with polarization b and a scattered wave with polarization a .

In the definition for the bistatic scattering coefficients we note that $S_{i,A} \cos \theta_i$ is the power intercepted by the surface area normal to the direction of the incident wave. The total power reflected back is $r^2 S_r$ integrated over the upper hemisphere. Similarly,

the total transmitted power is $r^2 S_t$ integrated over the lower hemisphere. We define the reflectivity

$$r_h(\theta_i) = \frac{1}{4\pi} \sum_a \int_{\dots}^{\pi/2} d\theta_s \sin \theta_s \int_{\dots}^{2\pi} d\phi_s \gamma_{ab}^r(\hat{k}_s, \hat{k}_i) \quad (114a)$$

and the transmissivity

$$t_h(\theta_i) = \frac{1}{4\pi} \sum_a \int_{\dots}^{\pi/2} d\theta_t \sin \theta_t \int_{\dots}^{2\pi} d\phi_t \gamma_{ab}^t(\hat{k}_t, \hat{k}_i) \quad (114b)$$

where the summation a is over both the vertical and horizontal polarizations.

Making use of (90)-(92), we find the reflectivities for the vertical and horizontal polarizations to be

$$\begin{aligned} r_v(\theta_i) &= \int_{\dots}^{\pi/2} d\theta_s \sin \theta_s \int_{\dots}^{2\pi} d\phi_s \frac{1}{2\pi\sigma^2|C''(0)|} \exp \left[-\frac{k_{dx}^2 + k_{dy}^2}{2k_{dz}^2\sigma^2|C''(0)|} \right] \\ &\quad \times \frac{|\bar{k}_d|^4}{4 \cos \theta_i |\hat{k}_i \times \hat{k}_s|^2 k_{dz}^4} \left[(\hat{h}_i \cdot \hat{k}_s)^2 |R_h|^2 + (\hat{v}_i \cdot \hat{k}_s)^2 |R_v|^2 \right] \end{aligned} \quad (115a)$$

$$\begin{aligned} r_h(\theta_i) &= \int_{\dots}^{\pi/2} d\theta_s \sin \theta_s \int_{\dots}^{2\pi} d\phi_s \frac{1}{2\pi\sigma^2|C''(0)|} \exp \left[-\frac{k_{dx}^2 + k_{dy}^2}{2k_{dz}^2\sigma^2|C''(0)|} \right] \\ &\quad \times \frac{|\bar{k}_d|^4}{4 \cos \theta_i |\hat{k}_i \times \hat{k}_s|^2 k_{dz}^4} \left[(\hat{v}_i \cdot \hat{k}_s)^2 |R_h|^2 + (\hat{h}_i \cdot \hat{k}_s)^2 |R_v|^2 \right] \end{aligned} \quad (115b)$$

where we made use of the fact that

$$|\hat{k}_i \times \hat{k}_s|^2 = (\hat{v}_i \cdot \hat{k}_s)^2 + (\hat{h}_i \cdot \hat{k}_s)^2 = (\hat{h}_s \cdot \hat{k}_i)^2 + (\hat{v}_s \cdot \hat{k}_i)^2 \quad (116)$$

Similarly, making use of (104)-(106), the transmissivities for the vertical and horizontal polarizations are found to be

$$\begin{aligned} t_v(\theta_i) &= \int_{\dots}^{\pi/2} d\theta_t \sin \theta_t \int_{\dots}^{2\pi} d\phi_t \frac{1}{2\pi\sigma^2|C''(0)|} \exp \left[-\frac{k_{tdx}^2 + k_{tdy}^2}{2k_{tdz}^2\sigma^2|C''(0)|} \right] \\ &\quad \times \frac{k_i^2 |\bar{k}_t|^2 (\hat{n} \cdot \hat{k}_i)(\hat{n} \cdot \hat{k}_t)}{\cos \theta_i |\hat{k}_i \times \hat{k}_t|^2 k_{tdz}^4} \left[(\hat{h}_i \cdot \hat{k}_t)^2 (1 - |R_h|^2) + (\hat{v}_i \cdot \hat{k}_t)^2 (1 - |R_v|^2) \right] \end{aligned} \quad (117a)$$

$$\begin{aligned}
t_h(\theta_i) = & \int_{..}^{\pi/2} d\theta_t \sin \theta \int_{..}^{2\pi} \phi_t \frac{1}{2\pi\sigma^2|C'''(0)|} \exp \left[-\frac{k_{t,dx}^2 + k_{t,dy}^2}{2k_{t,dz}^2\sigma^2|C'''(0)|} \right] \\
& \times \frac{k_i^2|\bar{k}_{t,d}|^2(\hat{n} \cdot \hat{k}_i)(\hat{n} \cdot \hat{k}_t)}{\cos \theta_i|\hat{k}_i \times \hat{k}_t|^2k_{t,dz}^4} \left[(\hat{v}_i \cdot \hat{k}_t)^2(1 - |R_h|^2) + (\hat{h}_i \cdot \hat{k}_t)^2(1 - |R_v|^2) \right] \quad (117b)
\end{aligned}$$

where we made use of

$$|\hat{k}_i \times \hat{k}_t|^2 = (\hat{h}_i \cdot \hat{k}_i)^2 + (\hat{v}_i \cdot \hat{k}_i)^2 = (\hat{h}_i \cdot \hat{k}_t)^2 + (\hat{v}_i \cdot \hat{k}_t)^2 \quad (118)$$

$$|1 + R_h|^2 = (1 - |R_h|^2) \frac{(\hat{n} \cdot \hat{k}_i)}{n_t(\hat{n} \cdot \hat{k}_t)} \quad (119a)$$

$$\frac{|1 + R_v|^2}{n_i^2} = (1 - |R_v|^2) \frac{(\hat{n} \cdot \hat{k}_i)}{n_t(\hat{n} \cdot \hat{k}_t)} \quad (119b)$$

with

$$n_t = \frac{k_t}{k} \quad (120)$$

Conservation of energy relations should also exist for the reflectivity and transmissivity functions. However, as pointed out before, because shadowing and multiple scattering effects are ignored, conservation of energy is only approximately satisfied [Lynch and Wagner, 1970]. To investigate the violation of the conservation of energy, we define

$$\Delta_h(\theta_i) = 1 - r_h(\theta_i) - t_h(\theta_i) \quad (121a)$$

$$\Delta_v(\theta_i) = 1 - r_v(\theta_i) - t_v(\theta_i) \quad (121b)$$

In Fig. 2.3, $\Delta_h(\theta_i)$ and $\Delta_v(\theta_i)$ are plotted as a function of incident angle. We see that energy loss becomes severe as incident angle increases. However, as incident angle is further increased, the trend reverses and the sum of reflected and transmitted energy

becomes greater than unity. Near the normal angle of incidence there is little shadowing and most of the rough surface is illuminated. Therefore, since we only have the single scattering solution there is loss of energy. At higher angle of incidence, the multiple scattering solutions are still left out. However, the shadowing effect dominates and the single scattering solution is blowing up as incident angle is increased. In the next section we modify the bistatic scattering coefficients to include the effect of shadowing and show that in doing so the sum of reflected and transmitted energy is always less than unity.

Shadowing Effect

The bistatic scattering coefficients are now modified to account for the shadowing effect. The modified scattering coefficients satisfy reciprocity but still do not conserve energy since multiple scattering effects are neglected. The sum of reflected and transmitted energy is shown to be always less than unity. The modified bistatic scattering coefficients will be used in the next section to derive the upper and lower bound for the correct emissivity of the rough surface.

The bistatic reflection coefficients are first considered. The diffraction integral for the reflected field, (14), is modified with the addition of an illumination function $L(\hat{k}_i, \hat{k}_s, \bar{r}')$, as follows:

$$\bar{E}_s(\bar{r}) = \frac{ik e^{ikr}}{4\pi} E_o (\bar{I} - \hat{k}_s \hat{k}_s) \cdot \int_A d\bar{r}'_{\perp} \bar{F}(\alpha, \beta) L(\hat{k}_i, \hat{k}_s, \bar{r}') e^{ik_{\perp} \cdot \bar{r}'} \quad (122)$$

where $L(\hat{k}_i, \hat{k}_s, \bar{r}') = 1$ if a ray having a direction \hat{k}_i is not intersected by the surface and illuminates the point \bar{r}' and if the line drawn from the point \bar{r}' in the direction \hat{k}_s does not strike the surface, and $L(\hat{k}_i, \hat{k}_s, \bar{r}') = 0$ otherwise [Sancer, 1969]. The above integral is evaluated by the method of stationary phase. The scattered intensity is, from (74),

$$\langle |\bar{E}_s|^2 \rangle = \frac{k^2 |E_o|^2}{16\pi^2 r^2} \left| (\bar{I} - \hat{k}_s \hat{k}_s) \cdot \bar{F}(\alpha_o, \beta_o) \right|^2 \langle II' \rangle \quad (123)$$

where $\langle II' \rangle$ is now modified to include shadowing

$$\langle II' \rangle = \left\langle \int_{A..} d\bar{r}'_{\perp} \int_{A..} d\bar{r}''_{\perp} e^{i\bar{k}_{\perp} \cdot (\bar{r} - \bar{r}')} L(\hat{k}_i, \hat{k}_s, \bar{r}'_{\perp}) L(\hat{k}_i, \hat{k}_s, \bar{r}''_{\perp}) e^{ik_{\perp} \cdot (f(\bar{r}'_{\perp}) - f(\bar{r}''_{\perp}))} \right\rangle \quad (124)$$

The above integral is solved by the method of asymptotics as in (76)-(82). We also note that as $k \rightarrow \infty$,

$$\begin{aligned} \lim_{k \rightarrow \infty} L(\hat{k}_i, \hat{k}_s, \bar{r}_\perp) L(\hat{k}_i, \hat{k}_s, \bar{r}'_\perp) &= L(\hat{k}_i, \hat{k}_s, \bar{r}_\perp) L\left(\hat{k}_i, \hat{k}_s, \tau - \frac{u}{k}, y - \frac{v}{k}\right) \\ &= L^2(\hat{k}_i, \hat{k}_s, \bar{r}_\perp) \end{aligned} \quad (125)$$

Hence we obtain the following expression analogous to (81).

$$\langle \lim_{k \rightarrow \infty} II^* \rangle = \frac{A_s 4\pi^2}{k_{dz}^2} \int dL p(\alpha, \beta, L) \Big|_{\alpha = -\frac{k_{dx}}{k_{dz}}, \beta = -\frac{k_{dy}}{k_{dz}}} L^2(\hat{k}_i, \hat{k}_s, \bar{r}_\perp) \quad (126)$$

where $p(\alpha, \beta, L)$ is the joint probability density function for α, β and L . Since the process is homogeneous the result above is independent of \bar{r} . Representing in terms of the conditional probability density

$$p(\alpha, \beta, L) = p(\alpha, \beta) p(L | \alpha, \beta) \quad (127)$$

where

$$p(L | \alpha, \beta) = P_L(\hat{k}_i, \hat{k}_s | \alpha, \beta) \delta(L - 1) + \left[1 - P_L(\hat{k}_i, \hat{k}_s | \alpha, \beta)\right] \delta(L) \quad (128)$$

with $P_L(\hat{k}_i, \hat{k}_s | \alpha, \beta)$ the probability that a point will be illuminated by rays having the directions \hat{k}_i and $-\hat{k}_s$ given the value of the slope at the point. Thus, using (82)

$$\langle II^* \rangle = \frac{A_s 4\pi^2}{k_{dz}^2} \frac{1}{2\pi\sigma^2 |C'''(0)|} \exp\left[-\frac{k_{dx}^2 + k_{dy}^2}{2k_{dz}^2 \sigma^2 |C'''(0)|}\right] P_L\left(\hat{k}_i, \hat{k}_s \mid -\frac{k_{dx}}{k_{dz}}, -\frac{k_{dy}}{k_{dz}}\right) \quad (129)$$

The bistatic reflection coefficients are modified to

$$\gamma_{i,b}^{m,r}(\hat{k}_s, \hat{k}_i) = \gamma_{i,b}^r(\hat{k}_s, \hat{k}_i) P_L\left(\hat{k}_i, \hat{k}_s \mid -\frac{k_{dx}}{k_{dz}}, -\frac{k_{dy}}{k_{dz}}\right) \quad (130)$$

There have been many works on incorporating the shadowing effect into the bistatic scattering coefficients [Beckman, 1965; Wagner, 1967; Smith, 1967a, b; Sancer, 1969]. We use the shadowing function derived by Smith and Sancer to modify the bistatic scattering coefficients.

$$P_L \left(\hat{k}_t, \hat{k}_s \mid -\frac{k_{dx}}{k_{dz}}, -\frac{k_{dy}}{k_{dz}} \right) = S(\theta_s, \theta_i) \quad (131)$$

where

$$S(\hat{k}_s, \hat{k}_i) = \begin{cases} \frac{1}{1+\Lambda(\mu_s)} & \phi_s = \phi_i + \pi, \theta_s \geq \theta_i \\ \frac{1}{1+\Lambda(\mu_i)} & \phi_s = \phi_i + \pi, \theta_i \geq \theta_s \\ \frac{1}{1+\Lambda(\mu_s)+\Lambda(\mu_i)} & \text{otherwise} \end{cases} \quad (132)$$

and

$$\mu = \cot \theta \quad (133)$$

$$\Lambda(\mu) = \frac{1}{2} \left[\sqrt{\frac{2}{\pi}} \frac{s}{\mu} e^{-\mu^2/2s^2} - \operatorname{erfc} \left(\frac{\mu}{\sqrt{2}s} \right) \right] \quad (134)$$

s^2 is the mean square surface slope

$$s^2 = \sigma^2 |C''(0)| \quad (135)$$

and erfc is the complementary error function. The bistatic transmission coefficients can be modified in a similar fashion. Thus

$$\gamma_{ub}^{m_i}(\hat{k}_t, \hat{k}_i) = \gamma_{ub}^i(\hat{k}_t, \hat{k}_i) S_t(\theta_t, \theta_i) \quad (136)$$

where

$$S_t(\theta_t, \theta_i) = \frac{1}{1 + \Lambda(\mu_t) + \Lambda(\mu_i)} \quad (137)$$

The modified reflectivity and transmissivity functions $r_i''(\theta_i)$ and $t_i''(\theta_i)$ are obtained from (114) by substituting in the modified bistatic scattering coefficients into the equation. The energy conservation is again studied by plotting Δ_r and Δ_t . In Fig. 2.4, we can see that the sum of reflected and transmitted energy are always less than unity.

Emissivities

The emissivity of a rough surface can be calculated from the bistatic reflection coefficients. It is defined to be [Peake, 1959]

$$\epsilon_n(\theta_i, \phi_i) = 1 - \frac{1}{4\pi} \sum_{l=v,h} \int_{\theta''}^{\pi/2} d\theta_s \sin \theta_s \int_{\phi''}^{2\pi} d\phi_s \gamma_{ln}^r(\theta_s, \phi_s; \theta_i, \phi_i) \quad (138)$$

The coherent and incoherent bistatic reflection coefficients derived from the Kirchhoff approximated diffraction integrals in (59) are used to calculate the emissivity of the rough surface. In terms of the coherent and incoherent reflectivity functions, the emissivity is given by

$$\epsilon_n(\theta_i) = 1 - r_{c_n}(\theta_i) - r_{i_n}(\theta_i) \quad (139)$$

where, for $\alpha = c$ or i

$$r_{\alpha_n}(\theta_i) = \frac{1}{4\pi} \sum_{l=v,h} \int_{\theta''}^{\pi/2} d\theta_s \sin \theta_s \int_{\phi''}^{2\pi} d\phi_s \gamma_{\alpha n}^r(\theta_s, \phi_s; \theta_i, \phi_i) \quad (140)$$

In the above equation the dependence on the azimuthal angle of incidence ϕ_i is dropped since the rough surface is isotropic and the results are independent of ϕ_i . After substituting in the explicit expressions for the bistatic scattering coefficients and carrying out the angular integration, we obtain

$$r_{c_n}(\theta_i) = |R_{nn}|^2 \exp[-4k^2\sigma^2 \cos^2 \theta_i] \quad (141)$$

$$\begin{aligned} r_{i_n}(\theta_i) = & \frac{k^2 l^2}{8 \cos \theta_i} \int_{\theta''}^{\pi/2} d\theta_s \sin \theta_s \exp[-\sigma^2 k_{dz}^2] \sum_{m=1}^{\infty} \frac{(k\sigma(\cos \theta_s + \cos \theta_i))^{2m}}{m!m} e^{-y_m} \\ & \times \left\{ \left| (1 + R_{nn}) - (1 - R_{nn}) \cos \theta_i \cos \theta_s \right|^2 \frac{I_1(x_m)}{x_m} \right. \\ & \left. + \left| -(1 + R_{nn}) \cos \theta_s + (1 - R_{nn}) \cos \theta_i \right|^2 \left(I_0(x_m) - \frac{I_1(x_m)}{x_m} \right) \right\} \quad (142) \end{aligned}$$

where $a = v, h$ and

$$y_m = \frac{k^2 l^2 (\sin^2 \theta_i + \sin^2 \theta_s)}{4m} \quad (143)$$

$$x_m = \frac{k^2 l^2 \sin \theta_i \sin \theta_s}{2m} \quad (144)$$

and I_0 and I_1 are the zeroth and first-order modified Bessel functions. We note that if the reflected field is used instead of the total field in the diffraction integral, then, for $a = v$ or h

$$\begin{aligned} r_{v,h}(\theta_i) = & |R_{uv}|^2 \frac{k^2 l^2}{8 \cos \theta_i} \int_{\theta_s}^{\pi/2} d\theta_s \sin \theta_s \exp[-\sigma^2 k_{dz}^2] \sum_{m=1}^{\infty} \frac{(k\sigma(\cos \theta_s + \cos \theta_i))^{2m}}{m!m} e^{-y_m} \\ & \times \left\{ (1 + \cos \theta_i \cos \theta_s)^2 \frac{I_1(x_m)}{x_m} + (\cos \theta_s + \cos \theta_i)^2 \left(I_0(x_m) - \frac{I_1(x_m)}{x_m} \right) \right\} \end{aligned} \quad (145)$$

The difference between the incoherent reflectivities obtained using the total or the reflected field in the diffraction integral is due to the approximation made on the integrand $\bar{F}(\alpha, \beta)$. If the next order term in the expansion of $\bar{F}(\alpha, \beta)$ in slope terms about the zero slopes are kept in (20b) while neglecting the shadowing effect, then the results obtained using the total and the reflected field can be shown to be the same. Note that in neglecting the shadowing effect, we are applying the tangent plane approximation even to the points on the rough surface that cannot be directly illuminated. The above model has some success in matching brightness temperature measurements from soils with rough surfaces [Tsang and Newton, 1982; Schmugge, 1983]. The model with coherent reflectivity alone is discussed in Choudhury *et al.* [1979].

The emissivity may also be calculated in terms of the bistatic transmission coefficients from medium 1 to medium 0, in view of (113)

$$e_u(\theta_i, \phi_i) = \frac{1}{4\pi} \sum_{h=v,h} \int_{\theta_s}^{\pi/2} d\theta_1 \sin \theta_1 \int_{\phi_s}^{2\pi} d\phi_1 \gamma_{uv}^{t(1)}(\theta_i, \phi_i; \theta_1, \phi_1) \frac{n_1^2 \cos \theta_1}{n_0^2 \cos \theta_i} \quad (146)$$

The emissivities calculated using (138) and (146) are only the same if the bistatic scattering coefficients satisfy the principles of reciprocity and energy conservation. Thus we are obtaining the approximated solution for the emissivity using (138), since the scattering coefficients that we made use of satisfy the reciprocity relation and energy conservation only approximately at best.

The emissivity of a random rough surface in the high frequency limit can be calculated using the bistatic scattering coefficients derived in the geometrical optics limit. The modified scattering coefficients, given by (130) and (136), which incorporate the shadowing effect are used. As stated before, a well defined emissivity of a medium depends on (1) the satisfaction of reciprocity relations, and (2) the satisfaction of conservation of energy by bistatic scattering coefficients. The modified scattering coefficients satisfy the reciprocity but violate the energy conservation since only the single scattering solution is used. Thus there is ambiguity and the results obtained using (138) and (146) are not the same. However, the sum of reflected and transmitted intensity is shown to be always less than unity and this fact can be made use of to derive the upper and lower limits of the correct emissivity.

The emissivity calculated using (138) represents the upper limit of the correct solution since the bistatic reflection coefficients are obtained using only the single scattering solution. If the higher-order scattering effects are included, the net reflected intensity will be higher and the emissivity will always be lower. Thus, in view of (141) and (145), the upper bound solution for the emissivity is given by

$$e_{ii}^u(\theta_i) = 1 - r_i^m(\theta_i) \quad (147)$$

where m denotes modified reflectivity with incorporation of shadowing effects according to (130). The emissivity calculated using (146) represents the lower limit of the correct

solution. If the higher-order scattering effects at the rough boundary are included, the bistatic transmission coefficients will always increase. Consequently, more thermal emission from the medium 1 will be transmitted, and the emissivity will always increase. Using the reciprocity relations satisfied by the bistatic transmission coefficients, (111), the lower bound solution for the emissivity is given by in view of (141),

$$e_n^l(\theta_i) = t_n^m(\theta_i) \quad (148)$$

Therefore, the two solutions given by (147) and (148) represent the upper and lower limits of the correct solution, and the ambiguity is due to the violation of energy conservation.

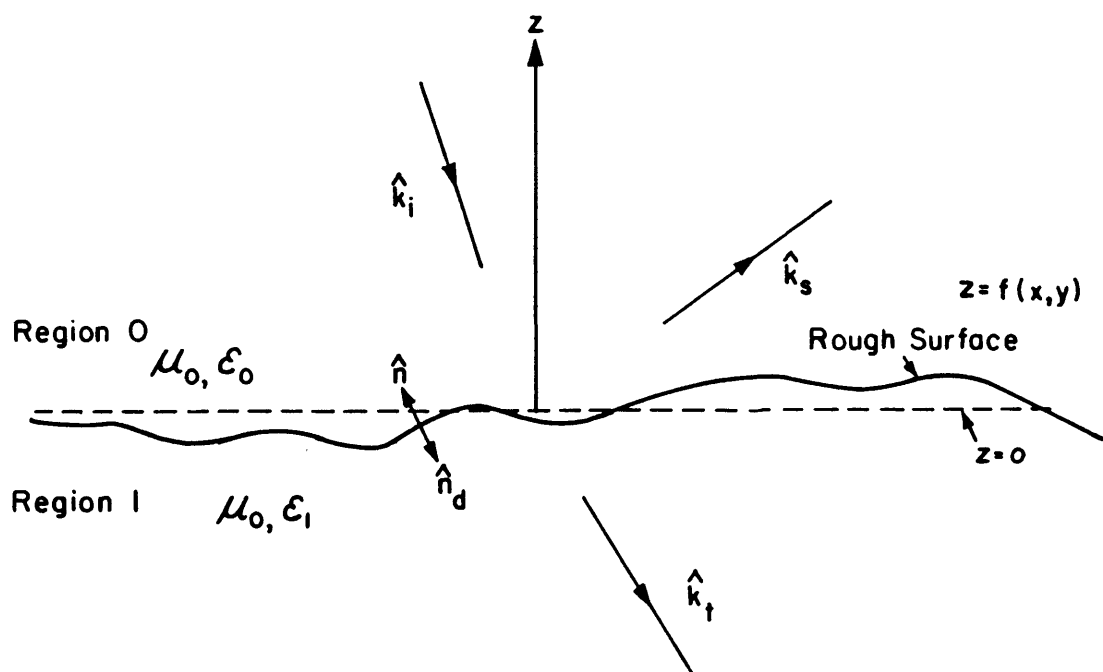


Figure 2.1 Geometrical configuration of the problem.

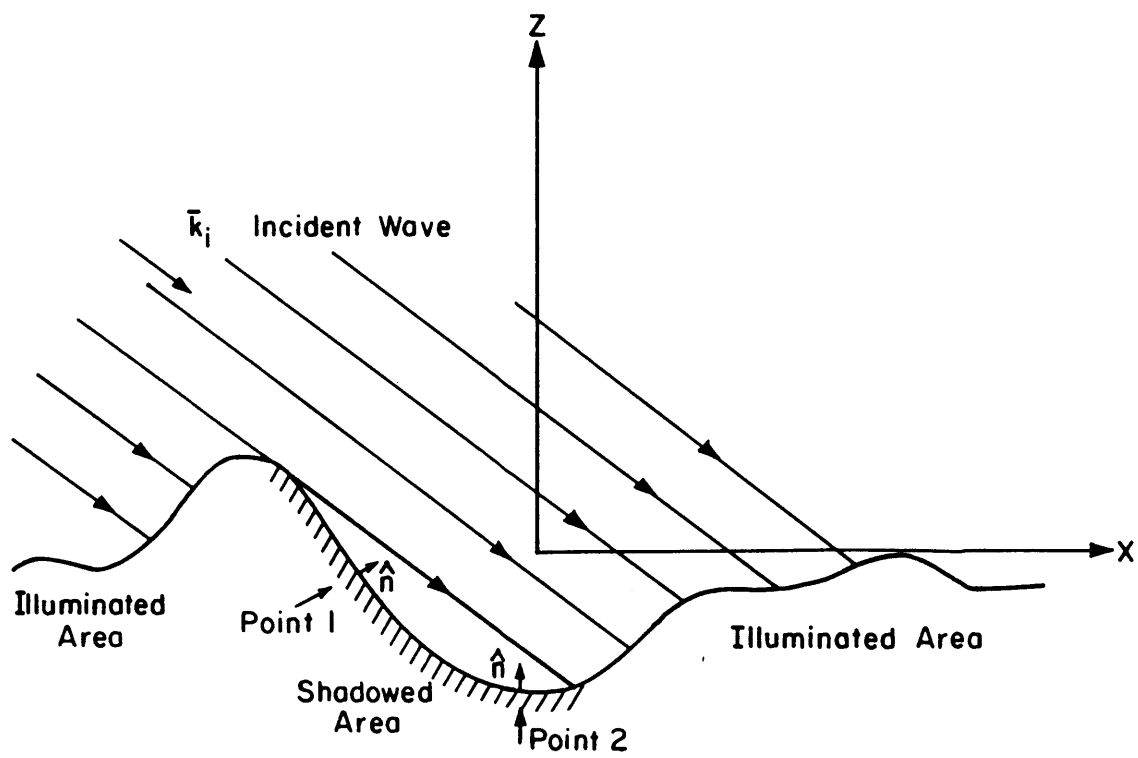


Figure 2.2 The shadowed area on the rough surface.

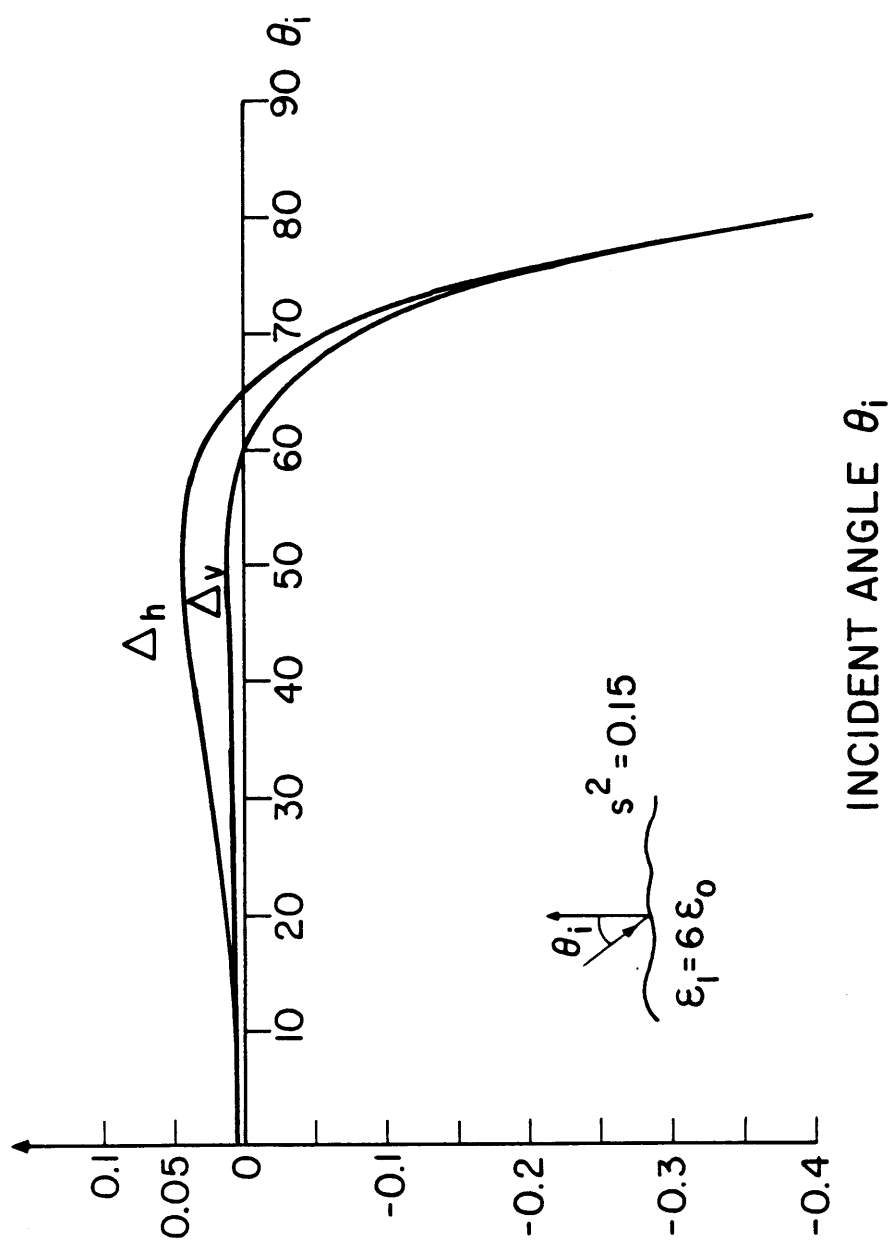


Figure 2.3 Energy conservation for the geometrical optics solution.

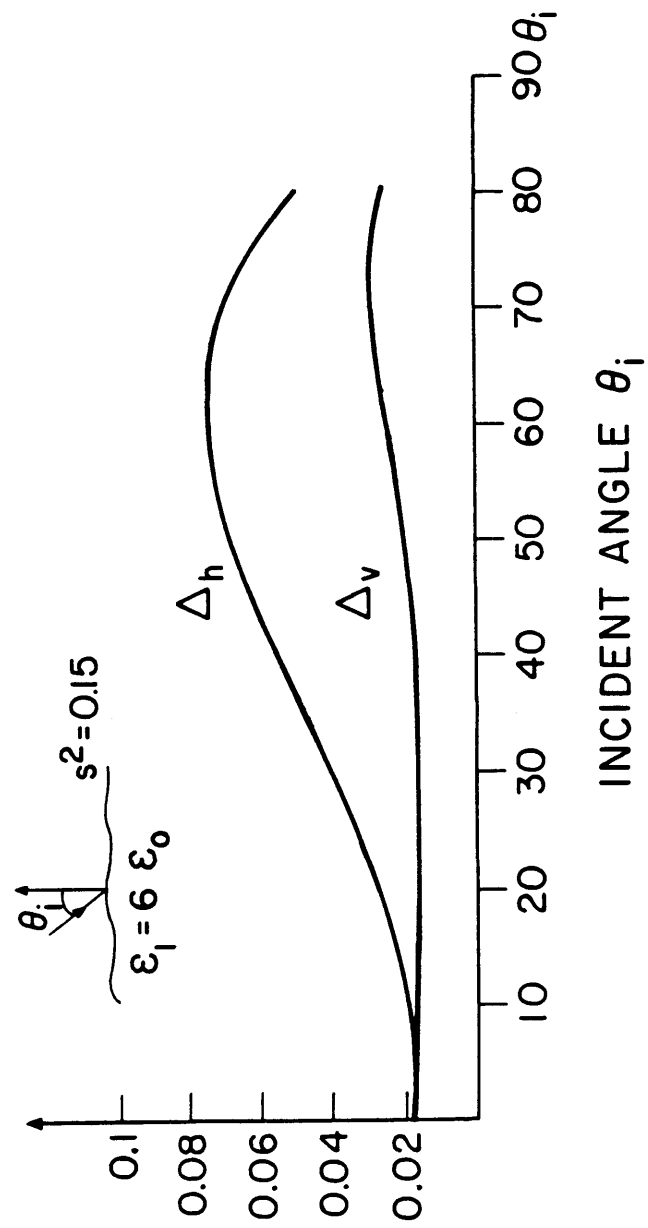


Figure 2.4 Energy conservation for the modified geometrical optics solution.

CHAPTER 3

Scattering and Emission by Random Rough Surfaces – Small Perturbation Method

The scattering of electromagnetic waves from a slightly rough surface is studied using a perturbation method. The extended boundary condition method is used with the perturbation method to solve for the scattered and transmitted fields to the second order. The zeroth-order solutions are just the reflected and transmitted fields of a flat surface. The first-order solutions give the lowest-order incoherent reflected and transmitted intensities. The second-order solution gives the lowest-order correction to the coherent reflection and transmission coefficients and the depolarization in the backscattered power.

3.1 Introduction

The scattering of electromagnetic waves from a slightly rough surface can be studied using a perturbation method. In the small perturbation method (SPM) due to Rice [1963], it is assumed that the surface variations are much smaller than the incident wavelength and the slopes of the rough surface are relatively small. The SPM makes use of Rayleigh hypothesis to express the reflected and transmitted fields into upward and downward going waves, respectively. The field amplitudes are then determined from the boundary conditions and the divergence relations. The extended boundary condition (EBC) method may also be used with the perturbation method to solve for the scattered fields [Agarwal, 1977; Nieto-Vesperina, 1982]. In the EBC method, the surface currents on the rough surface are first calculated. The scattered fields then can be calculated from the diffraction integral by making use of the calculated surface fields. Both perturbation methods yield the same expansions for the scattered fields, because the expansions of the amplitudes of the scattered fields are unique within their circles of convergence [Maradudin, 1983].

In this chapter we derive the bistatic scattering coefficients for the reflected and transmitted waves using the SPM. The EBC method is used to formulate the problem. Even though the Rayleigh method is simpler in the sense that the scattered fields amplitudes are obtained directly, the EBC method is conceptually consistent with the previous chapter on scattering from random rough surface with the Kirchhoff approach. The SPM is used to calculate the scattered fields up to the second-order. The zeroth-order solutions are just the reflected and transmitted fields of a flat surface. The first-order solutions give the lowest-order incoherent transmitted and reflected intensities. However, the first-order solution does not give the depolarization effect in the

backscattering direction. The second-order solution gives the lowest-order correction to the coherent reflection and transmission coefficients and the depolarization in the backscattering power.

3.2 Formulation

Consider a plane wave in free space with electric field $\bar{E}_i = \hat{e}_i E_0 \exp(i\bar{k}_i \cdot \bar{r})$ incident upon a slightly rough surface of a medium with permittivity ϵ_1 . The rough surface is characterized by a random height distribution $z = f(\bar{r}_\perp)$ where $f(\bar{r}_\perp)$ is a random variable with zero mean, $\langle f(\bar{r}_\perp) \rangle = 0$. Let f_{min} and f_{max} be the minimum and maximum values of the surface profile $f(\bar{r}_\perp)$. From Huygens' principle, the total field $\bar{E}(\bar{r})$ in free space and the transmitted field $\bar{E}_1(\bar{r})$ in the dielectric medium satisfy

$$\begin{aligned} \bar{E}_i(\bar{r}) + \int_{S'} dS' \left\{ i\omega\mu_0 \bar{G}(\bar{r}, \bar{r}') \cdot [\hat{n} \times \bar{H}(\bar{r}')] + \nabla \times \bar{G}(\bar{r}, \bar{r}') \cdot [\hat{n} \times \bar{E}(\bar{r}')] \right\} \\ = \begin{cases} \bar{E}(\bar{r}) & z > f(\bar{r}_\perp) \\ 0 & z < f(\bar{r}_\perp) \end{cases} \end{aligned} \quad \begin{array}{l} (1a) \\ (1b) \end{array}$$

$$\begin{aligned} \int_{S'} dS' \left\{ i\omega\mu_1 \bar{G}_1(\bar{r}, \bar{r}') \cdot [\hat{n}_d \times \bar{H}_1(\bar{r}')] + \nabla \times \bar{G}_1(\bar{r}, \bar{r}') \cdot [\hat{n}_d \times \bar{E}_1(\bar{r}')] \right\} \\ = \begin{cases} 0 & z > f(\bar{r}_\perp) \\ \bar{E}_1(\bar{r}) & z < f(\bar{r}_\perp) \end{cases} \end{aligned} \quad \begin{array}{l} (2a) \\ (2b) \end{array}$$

where S' denotes the rough surface in which the surface integration is to be carried out, \hat{n} and \hat{n}_d are the unit vectors normal to the rough surface and pointing into the free space and the dielectric medium, respectively, and $\bar{G}(\bar{r}, \bar{r}')$ and $\bar{G}_1(\bar{r}, \bar{r}')$ are respectively the dyadic Green's functions for free space and homogeneous dielectric of region 1. We make use of the integral representation of dyadic Green's function [Appendix A].

Since tangential fields are continuous, we can define surface field unknowns

$$dS' \eta \hat{n} \times \bar{H}(\bar{r}') = d\bar{r}'_\perp \bar{a}(\bar{r}'_\perp) = dS' \frac{\eta}{\eta_1} \eta_1 \hat{n} \times \bar{H}_1(\bar{r}') \quad (3a)$$

$$dS' \hat{n} \times \bar{E}(\bar{r}') = d\bar{r}'_{\perp} \bar{b}(\bar{r}'_{\perp}) = dS' \hat{n} \times \bar{E}_1(\bar{r}') \quad (3b)$$

Evaluating (1b) for $z < f_{min}$ and (2a) for $z > f_{max}$ we obtain

$$\begin{aligned} \bar{E}_i(\bar{r}) &= \frac{1}{8\pi^2} \int d\bar{k}_{\perp} e^{i\bar{k}_{\perp} \cdot \bar{r}_{\perp}} e^{-ik_z z} \frac{k}{k_z} \int d\bar{r}'_{\perp} e^{-i\bar{k}_{\perp} \cdot \bar{r}'_{\perp}} e^{ik_z f(\bar{r}'_{\perp})} \\ &\times \left\{ \left[\hat{e}(-k_z) \hat{e}(-k_z) + \hat{h}(-k_z) \hat{h}(-k_z) \right] \cdot \bar{a}(\bar{r}'_{\perp}) \right. \\ &\quad \left. + \left[-\hat{h}(-k_z) \hat{e}(-k_z) + \hat{e}(-k_z) \hat{h}(-k_z) \right] \cdot \bar{b}(\bar{r}'_{\perp}) \right\} \end{aligned} \quad (4a)$$

$$\begin{aligned} 0 &= \frac{1}{8\pi^2} \int d\bar{k}_{\perp} e^{i\bar{k}_{\perp} \cdot \bar{r}_{\perp}} e^{ik_{1z} z} \frac{k_{\perp}}{k_{1z}} \int d\bar{r}'_{\perp} e^{-i\bar{k}_{\perp} \cdot \bar{r}'_{\perp}} e^{-ik_{1z} f(\bar{r}'_{\perp})} \\ &\times \left\{ \frac{k}{k_1} \left[\hat{e}_1(k_{1z}) \hat{e}_1(k_{1z}) + \hat{h}_1(k_{1z}) \hat{h}_1(k_{1z}) \right] \cdot \bar{a}(\bar{r}'_{\perp}) \right. \\ &\quad \left. + \left[-\hat{h}_1(k_{1z}) \hat{e}_1(k_{1z}) + \hat{e}_1(k_{1z}) \hat{h}_1(k_{1z}) \right] \cdot \bar{b}(\bar{r}'_{\perp}) \right\} \end{aligned} \quad (4b)$$

where f_{min} and f_{max} are the minimum and maximum values of the surface profile $f(\bar{r}'_{\perp})$.

The above equations are the extended boundary conditions, which can be used to solve for the surface fields along with the following equations which are results of (3a) and (3b)

$$\hat{n}(\bar{r}'_{\perp}) \cdot \bar{a}(\bar{r}'_{\perp}) = 0 \quad (5a)$$

$$\hat{n}(\bar{r}'_{\perp}) \cdot \bar{b}(\bar{r}'_{\perp}) = 0 \quad (5b)$$

The unit normal vector to the rough surface $\hat{n}(\bar{r}'_{\perp})$ is given by

$$\hat{n} = \frac{-\hat{x} \partial f(\bar{r}'_{\perp}) / \partial x' - \hat{y} \partial f(\bar{r}'_{\perp}) / \partial y' + \hat{z}}{\sqrt{1 + (\partial f / \partial x')^2 + (\partial f / \partial y')^2}} \quad (6)$$

Thus, (5) can be rewritten as

$$a_z(\bar{r}'_\perp) = \left(\hat{x} \frac{\partial f(\bar{r}'_\perp)}{\partial x'} + \hat{y} \frac{\partial f(\bar{r}'_\perp)}{\partial y'} \right) \cdot \bar{a}_\perp(\bar{r}'_\perp) \quad (7a)$$

$$b_z(\bar{r}'_\perp) = \left(\hat{x} \frac{\partial f(\bar{r}'_\perp)}{\partial x'} + \hat{y} \frac{\partial f(\bar{r}'_\perp)}{\partial y'} \right) \cdot \bar{b}_\perp(\bar{r}'_\perp) \quad (7b)$$

with a_z and b_z as the z components of \bar{a} and \bar{b} respectively.

Once the surface fields are obtained, then the scattered field in free space and the transmitted field in medium 1 can be derived from the diffraction integrals. Thus, evaluating (1a) and (2b) for $z > f_{max}$ and $z < f_{min}$ respectively, we obtain

$$\begin{aligned} \bar{E}_s(\bar{r}) = & -\frac{1}{8\pi^2} \int d\bar{k}_\perp e^{i\bar{k}_\perp \cdot \bar{r}_\perp} e^{ik_z z} \frac{k}{k_z} \int d\bar{r}'_\perp e^{-i\bar{k}_\perp \cdot \bar{r}'_\perp} e^{-ik_z f(\bar{r}'_\perp)} \\ & \times \left\{ \left[\hat{\epsilon}(k_z) \hat{\epsilon}(k_z) + \hat{h}(k_z) \hat{h}(k_z) \right] \cdot \bar{a}(\bar{r}'_\perp) + \left[-\hat{h}(k_z) \hat{\epsilon}(k_z) + \hat{\epsilon}(k_z) \hat{h}(k_z) \right] \cdot \bar{b}(\bar{r}'_\perp) \right\} \quad (8a) \end{aligned}$$

$$\begin{aligned} \bar{E}_t(\bar{r}) = & \frac{1}{8\pi^2} \int d\bar{k}_\perp e^{i\bar{k}_\perp \cdot \bar{r}_\perp} e^{-i\bar{k}_{1z} z} \frac{k_1}{k_{1z}} \int d\bar{r}'_\perp e^{-i\bar{k}_\perp \cdot \bar{r}'_\perp} e^{ik_{1z} f(\bar{r}'_\perp)} \\ & \times \left\{ \frac{k}{k_1} \left[\hat{\epsilon}_1(-k_{1z}) \hat{\epsilon}_1(-k_{1z}) + \hat{h}_1(-k_{1z}) \hat{h}_1(-k_{1z}) \right] \cdot \bar{a}(\bar{r}'_\perp) \right. \\ & \left. + \left[-\hat{h}_1(-k_{1z}) \hat{\epsilon}_1(-k_{1z}) + \hat{\epsilon}_1(-k_{1z}) \hat{h}_1(-k_{1z}) \right] \cdot \bar{b}(\bar{r}'_\perp) \right\} \quad (8b) \end{aligned}$$

Therefore, the objective is to solve for the surface fields using (4) and (7), and then to solve for the scattered fields using (8).

The surface fields are calculated by making a perturbation expansion. We let

$$\bar{a}(\bar{r}'_\perp) = \sum_m \frac{\bar{a}^{(m)}(\bar{r}'_\perp)}{m!} \quad (9a)$$

$$\bar{b}(\bar{r}'_{\perp}) = \sum_m \frac{\bar{b}^{(m)}(\bar{r}'_{\perp})}{m!} \quad (9b)$$

where \bar{a}^m and \bar{b}^m are respectively the m -th order solution of \bar{a} and \bar{b} . We also have

$$e^{\pm ik_z f(\bar{r}'_{\perp})} = \sum_m \frac{(\pm ik_z f(\bar{r}'_{\perp}))^m}{m!} \quad (10a)$$

$$e^{\pm ik_{1z} f(\bar{r}'_{\perp})} = \sum_m \frac{(\pm ik_{1z} f(\bar{r}'_{\perp}))^m}{m!} \quad (10b)$$

The above expansions can be substituted into (4) to obtain the set of equations for the different order solutions with f regarded as a small parameter. Also, from (7) and (9)

$$a_z^{(0)}(\bar{r}'_{\perp}) = b_z^{(0)}(\bar{r}'_{\perp}) = 0 \quad (11)$$

$$a_z^{(m)}(\bar{r}'_{\perp}) = m \left(\hat{x} \frac{\partial f(\bar{r}'_{\perp})}{\partial x'} + \hat{y} \frac{\partial f(\bar{r}'_{\perp})}{\partial y'} \right) \cdot \bar{a}_{\perp}^{(m-1)}(\bar{r}'_{\perp}) \quad (12a)$$

$$b_z^{(m)}(\bar{r}'_{\perp}) = m \left(\hat{x} \frac{\partial f(\bar{r}'_{\perp})}{\partial x'} + \hat{y} \frac{\partial f(\bar{r}'_{\perp})}{\partial y'} \right) \cdot \bar{b}_{\perp}^{(m-1)}(\bar{r}'_{\perp}) \quad (12b)$$

Thus, we are assuming

$$k_z f(\bar{r}'_{\perp}), k_{1z} f(\bar{r}'_{\perp}), \frac{\partial f}{\partial x'}, \frac{\partial f}{\partial y'} \ll 1 \quad (13)$$

Substituting (9)-(10) into (4) and (7) and equating the same order terms we can calculate the surface fields to zeroth-order, first-order, etc. Then, from (8), the scattered fields can be obtained to different order. In the following sections we solve for the surface fields, and then the scattered field up to the second-order. The zeroth-order solution is just the reflected and transmitted fields of a flat surface. The first-order solution gives the lowest-order incoherent scattered intensities. However, the first-order solution does not give the depolarization effect in the backscattering direction. The second-order solution gives the lowest-order correction to the coherent reflection and transmission coefficients. Also, depolarization of the backscattered power is manifested.

3.3 Zeroth-Order Solution

The zeroth-order solution can be obtained by keeping only the lowest-order terms in the expansion of (7) and (8). We first define the orthonormal system $(\hat{f}_i, \hat{g}_i, \hat{z}_i)$, which are given by

$$\hat{g}_i = \hat{x} \frac{k_{yi}}{k_{\rho i}} - \hat{y} \frac{k_{xi}}{k_{\rho i}} = \hat{e}(k_{zi}) \quad (14a)$$

$$\hat{f}_i = \hat{x} \frac{k_{xi}}{k_{\rho i}} + \hat{y} \frac{k_{yi}}{k_{\rho i}} \quad (14b)$$

$$\hat{z}_i = \hat{z} \quad (14c)$$

where $k_{\rho i}^2 = k_{xi}^2 + k_{yi}^2$ and let

$$\bar{a}(\bar{\mathbf{r}}'_\perp) = \hat{g}_i a_q(\bar{\mathbf{r}}'_\perp) + \hat{f}_i a_p(\bar{\mathbf{r}}'_\perp) + \hat{z}_i a_z(\bar{\mathbf{r}}'_\perp) \quad (15a)$$

$$\bar{b}(\bar{\mathbf{r}}'_\perp) = \hat{g}_i b_q(\bar{\mathbf{r}}'_\perp) + \hat{f}_i b_p(\bar{\mathbf{r}}'_\perp) + \hat{z}_i b_z(\bar{\mathbf{r}}'_\perp) \quad (15b)$$

To solve for the-zeroth order solution, we note that

$$\begin{aligned} \bar{E}_i(\bar{\mathbf{r}}) &= \hat{e}_i E_{ii} e^{i\bar{k}_\perp \cdot \bar{\mathbf{r}}_\perp - ik_{zi}z} \\ &= \hat{e}_i \frac{1}{4\pi^2} E_{ii} \int d\bar{k}_\perp e^{i\bar{k}_\perp \cdot \bar{\mathbf{r}}_\perp - ik_{zi}z} \int d\bar{\mathbf{r}}'_\perp e^{i\bar{k}_\perp \cdot \bar{\mathbf{r}}'_\perp - i\bar{k}_\perp \cdot \bar{\mathbf{r}}'_\perp} \end{aligned} \quad (16)$$

Using (16) in (4a), we note that the $d\bar{\mathbf{r}}'_\perp$ integration in (4a) must produce a Dirac delta function of the form $\delta(\bar{k}_\perp - \bar{k}_{\perp i})$. Hence

$$\begin{aligned} \hat{e}_i e^{i\bar{k}_\perp \cdot \bar{\mathbf{r}}'_\perp} &= \frac{k}{2k_{zi}} \left\{ \left[\hat{e}(-k_{zi})\hat{e}(-k_{zi}) + \hat{h}(-k_{zi})\hat{h}(-k_{zi}) \right] \cdot \bar{a}^{(0)}(\bar{\mathbf{r}}'_\perp) \right. \\ &\quad \left. + \left[-\hat{h}(-k_{zi})\hat{e}(-k_{zi}) + \hat{e}(-k_{zi})\hat{h}(-k_{zi}) \right] \cdot \bar{b}^{(0)}(\bar{\mathbf{r}}'_\perp) \right\} \end{aligned} \quad (17a)$$

Hence from (4b), we have

$$\begin{aligned} & \left[\hat{\epsilon}_1(k_{1zi}) \hat{\epsilon}_1(k_{1zi}) + \hat{h}_1(k_{1zi}) \hat{h}_1(k_{1zi}) \right] \cdot \bar{a}^{(0)}(\bar{\mathbf{r}}'_\perp) \frac{k}{k_1} \\ & - \left[-\hat{h}_1(k_{1zi}) \hat{\epsilon}_1(k_{1zi}) - \hat{\epsilon}_1(k_{1zi}) \hat{h}_1(k_{1zi}) \right] \cdot \bar{b}^{(0)}(\bar{\mathbf{r}}'_\perp) = 0 \end{aligned} \quad (17b)$$

Using (11) and (15) in (17) and noting that the dot products of \hat{p}_i and \hat{q}_i with $\hat{\epsilon}$ and \hat{h} can be calculated from (14), (A4) and (A5), we have from (17a)

$$\hat{\epsilon}_i e^{i\bar{k}_\perp \cdot \bar{\mathbf{r}}} = \frac{k}{2k_{zi}} \left\{ \hat{\epsilon}(-k_{zi}) \left(a_q^{(0)}(\bar{\mathbf{r}}') + \frac{k_{zi}}{k} b_p^{(0)}(\bar{\mathbf{r}}'_\perp) \right) + \hat{h}(-k_{zi}) \left(\frac{k_{zi}}{k} a_p^{(0)}(\bar{\mathbf{r}}'_\perp) - b_q^{(0)}(\bar{\mathbf{r}}'_\perp) \right) \right\} \quad (18a)$$

Using (17b), we have

$$k a_q^{(0)}(\bar{\mathbf{r}}') - k_{1zi} b_p^{(0)}(\bar{\mathbf{r}}') = 0 \quad (18b)$$

$$\frac{k k_{1zi}}{k_1^2} a_p^{(0)}(\bar{\mathbf{r}}') + b_q^{(0)}(\bar{\mathbf{r}}') = 0 \quad (18c)$$

Since (18a) contains two scalar equations, (18) provides four equations for the four unknowns $a_p^{(0)}$, $a_q^{(0)}$, $b_p^{(0)}$, and $b_q^{(0)}$. Solving them and substituting back into $\bar{a}^{(0)}(\bar{\mathbf{r}}'_\perp)$ and $\bar{b}^{(0)}(\bar{\mathbf{r}}'_\perp)$ gives

$$\bar{a}^{(0)}(\bar{\mathbf{r}}'_\perp) = \bar{a}^{(0)}(\bar{k}_\perp i) e^{i\bar{k}_\perp \cdot \bar{\mathbf{r}}'_\perp} \quad (19a)$$

$$\bar{b}^{(0)}(\bar{\mathbf{r}}'_\perp) = \bar{b}^{(0)}(\bar{k}_\perp i) e^{i\bar{k}_\perp \cdot \bar{\mathbf{r}}'_\perp} \quad (19b)$$

where

$$\bar{a}_q^{(0)}(\bar{k}_\perp i) = (\hat{\epsilon}(-k_{zi}) \cdot \hat{\epsilon}_i) \frac{k_{zi}}{k} (1 - R_{h..}) \quad (20a)$$

$$\bar{a}_p^{(0)}(\bar{k}_\perp i) = (\hat{h}(-k_{zi}) \cdot \hat{\epsilon}_i) (1 + R_{v..}) \quad (20b)$$

$$\bar{b}_q^{(0)}(\bar{k}_\perp i) = -(\hat{h}(-k_{zi}) \cdot \hat{\epsilon}_i) \frac{k_{zi}}{k} (1 - R_{v..}) \quad (20c)$$

$$\bar{b}_p^{(0)}(\bar{k}_\perp i) = (\hat{\epsilon}(-k_{zi}) \cdot \hat{\epsilon}_i) (1 + R_{h..}) \quad (20d)$$

and $R_{h..}$ and $R_{v..}$ are the Fresnel reflection coefficients for the TE and TM waves

$$R_{h..} = \frac{k_{zi} - k_{1zi}}{k_{zi} + k_{1zi}} \quad (21a)$$

$$R_{v..} = \frac{\epsilon_1 k_{zi} - \epsilon.. k_{1zi}}{\epsilon_1 k_{zi} + \epsilon.. k_{1zi}} \quad (21b)$$

The unit vectors $\hat{e}(-k_{zi})$ and $\hat{h}(-k_{zi})$ are related to the previously used unit vectors \hat{h}_i and \hat{v}_i as

$$\hat{e}(-k_{zi}) = -\hat{h}_i \quad (22a)$$

$$\hat{h}(-k_{zi}) = -\hat{v}_i \quad (22b)$$

Therefore, from (8), the reflected and transmitted fields are given by

$$\bar{E}_r^{(0)} = \left\{ R_{h..}(\hat{e}(-k_{zi}) \cdot \hat{e}_i)\hat{e}(k_{zi}) + R_{v..}(\hat{h}(-k_{zi}) \cdot \hat{e}_i)\hat{h}(k_{zi}) \right\} E_o e^{i\bar{k}_{i\perp} \cdot \bar{r}_\perp + ik_{zi}z} \quad (23a)$$

$$\bar{E}_t^{(0)} = \left\{ (1 + R_{h..})(\hat{e}(-k_{zi}) \cdot \hat{e}_i)\hat{e}_1(-k_{1zi}) + \frac{k}{k_1}(1 + R_{v..})(\hat{h}(-k_{zi}) \cdot \hat{e}_i)\hat{h}_1(-k_{1zi}) \right\} E_o e^{i\bar{k}_{i\perp} \cdot \bar{r}_\perp - ik_{1zi}z} \quad (23b)$$

which are just the reflected and transmitted fields from a flat surface.

3.4 First-Order Solution

The first-order solution for the surface fields can be obtained by substituting (9)-(10) into (4), (7), (12) and equating first-order terms. From (12a) and (19a)

$$a_z^{(1)}(\bar{r}'_\perp) = \left(\hat{x} \frac{\partial f(\bar{r}'_\perp)}{\partial x'} + \hat{y} \frac{\partial f(\bar{r}'_\perp)}{\partial y'} \right) \cdot \bar{a}_\perp^{(0)}(\bar{k}_\perp) e^{i\bar{k}_\perp \cdot \bar{r}'_\perp} \quad (24)$$

To simplify (24), we introduce the Fourier transforms

$$F(\bar{k}_\perp) = \frac{1}{(2\pi)^2} \int d\bar{r}'_\perp f(\bar{r}'_\perp) e^{-i\bar{k}_\perp \cdot \bar{r}'_\perp} \quad (25)$$

$$\bar{A}^{(1)}(\bar{k}_\perp) = \frac{1}{(2\pi)^2} \int d\bar{r}'_\perp \bar{a}^{(1)}(\bar{r}'_\perp) e^{-i\bar{k}_\perp \cdot \bar{r}'_\perp} \quad (26a)$$

$$\bar{B}^{(1)}(\bar{k}_\perp) = \frac{1}{(2\pi)^2} \int d\bar{r}'_\perp \bar{b}^{(1)}(\bar{r}'_\perp) e^{-i\bar{k}_\perp \cdot \bar{r}'_\perp} \quad (26b)$$

and multiply equation (24) by $\exp[-i\bar{k}_\perp \cdot \bar{r}'_\perp]/(2\pi)^2$ and integrate over $d\bar{r}'_\perp$. We obtain, by expressing $\partial f(\bar{r}'_\perp)/\partial x'$ and $\partial f(\bar{r}'_\perp)/\partial y'$ in terms of $F(\bar{k}_\perp)$,

$$A_z^{(1)}(\bar{k}_\perp) = \left\{ \left(\frac{k_x k_{yi} - k_y k_{xi}}{k_{\rho i}} \right) a_q^{(0)}(\bar{k}_\perp) + \left(\frac{k_x k_{xi} + k_y k_{yi}}{k_{\rho i}} - k_{\rho i} \right) a_p^{(0)}(\bar{k}_\perp) \right\} iF(\bar{k}_\perp - \bar{k}_\perp) \quad (27a)$$

Similarly from (12b)

$$B_z^{(1)}(\bar{k}_\perp) = \left\{ \left(\frac{k_x k_{yi} - k_y k_{xi}}{k_{\rho i}} \right) b_q^{(0)}(\bar{k}_\perp) + \left(\frac{k_x k_{xi} + k_y k_{yi}}{k_{\rho i}} - k_{\rho i} \right) b_p^{(0)}(\bar{k}_\perp) \right\} iF(\bar{k}_\perp - \bar{k}_\perp) \quad (27b)$$

Next we match both sides of equation (4a) to first order. We note that

$$\begin{aligned} & \left[\int d\bar{r}'_\perp e^{-i\bar{k}_\perp \cdot \bar{r}'_\perp} e^{ik_z f(\bar{r}'_\perp)} \right]_{\text{first order}} \\ &= \int d\bar{r}'_\perp e^{-i\bar{k}_\perp \cdot \bar{r}'_\perp} \left[ik_z f(\bar{r}'_\perp) \bar{a}^{(0)}(\bar{k}_\perp) e^{i\bar{k}_\perp \cdot \bar{r}'_\perp} + \bar{a}^{(1)}(\bar{r}'_\perp) \right] \\ &= (2\pi)^2 \left[ik_z F(\bar{k}_\perp - \bar{k}_\perp) \bar{a}^{(0)}(\bar{k}_\perp) + \bar{A}^{(1)}(\bar{k}_\perp) \right] \end{aligned} \quad (28)$$

Hence the first order equation from (4a) is

$$\begin{aligned}
0 = & \int d\bar{k}_\perp e^{i\bar{k}_\perp \cdot \bar{r}_\perp} e^{-ik_z z} \frac{k}{k_z} \\
& \times \left\{ \left[\hat{\varepsilon}(-k_z) \hat{\varepsilon}(-k_z) + \hat{h}(-k_z) \hat{h}(-k_z) \right] \cdot \left[\bar{A}^{(1)}(\bar{k}_\perp) + ik_z \bar{a}^{(0)}(\bar{k}_{\perp i}) F(\bar{k}_\perp - \bar{k}_{\perp i}) \right] \right. \\
& \left. + \left[-\hat{h}(-k_z) \hat{\varepsilon}(-k_z) + \hat{\varepsilon}(-k_z) \hat{h}(-k_z) \right] \cdot \left[\bar{B}^{(1)}(\bar{k}_\perp) + ik_z \bar{b}^{(0)}(\bar{k}_{\perp i}) F(\bar{k}_\perp - \bar{k}_{\perp i}) \right] \right\} \quad (29a)
\end{aligned}$$

and from (4b), in a similar fashion, we obtain

$$\begin{aligned}
0 = & \int d\bar{k}_\perp e^{i\bar{k}_\perp \cdot \bar{r}_\perp} e^{ik_{1z} z} \frac{k_1}{k_{1z}} \\
& \times \left\{ \frac{k}{k_1} \left[\hat{\varepsilon}_1(k_{1z}) \hat{\varepsilon}_1(k_{1z}) + \hat{h}_1(k_{1z}) \hat{h}_1(k_{1z}) \right] \cdot \left[\bar{A}^{(1)}(\bar{k}_\perp) - ik_{1z} \bar{a}^{(0)}(\bar{k}_{\perp i}) F(\bar{k}_\perp - \bar{k}_{\perp i}) \right] \right. \\
& \left. + \left[-\hat{h}_1(k_{1z}) \hat{\varepsilon}_1(k_{1z}) + \hat{\varepsilon}_1(k_{1z}) \hat{h}_1(k_{1z}) \right] \cdot \left[\bar{B}^{(1)}(\bar{k}_\perp) - ik_{1z} \bar{b}^{(0)}(\bar{k}_{\perp i}) F(\bar{k}_\perp - \bar{k}_{\perp i}) \right] \right\} \quad (29b)
\end{aligned}$$

Equations (29a) and (29b) are vector equations so that there are four scalar equations contained in them. Hence (27) and (29) are six scalar equations for the six unknowns $A_q^{(1)}(\bar{k}_\perp)$, $A_p^{(1)}(\bar{k}_\perp)$, $A_z^{(1)}(\bar{k}_\perp)$, $B_q^{(1)}(\bar{k}_\perp)$, $B_p^{(1)}(\bar{k}_\perp)$, $B_z^{(1)}(\bar{k}_\perp)$. After much algebraic manipulation, we obtain

$$\bar{A}_\perp^{(1)}(\bar{k}_\perp) = iF(\bar{k}_\perp - \bar{k}_{\perp i}) \bar{A}_\perp^{(0)}(\bar{k}_{\perp i}) \quad (30a)$$

$$\bar{B}_\perp^{(1)}(\bar{k}_\perp) = iF(\bar{k}_\perp - \bar{k}_{\perp i}) \bar{B}_\perp^{(0)}(\bar{k}_{\perp i}) \quad (30b)$$

where the explicit expansions for $\tilde{A}_q^{(1)}$, $\tilde{A}_p^{(1)}$, $\tilde{B}_q^{(1)}$ and $\tilde{B}_p^{(1)}$ are given in Appendix B.

The first-order scattered fields can now be obtained from (8). To first-order, we obtain

$$\begin{aligned}
\bar{E}_s^{(1)} = & -\frac{1}{2} \int d\bar{k}_\perp e^{i\bar{k}_\perp \cdot \bar{r}_\perp} e^{ik_z z} \frac{k}{k_z} \\
& \times \left\{ \left[\hat{\varepsilon}(k_z) \hat{\varepsilon}(k_z) + \hat{h}(k_z) \hat{h}(k_z) \right] \cdot \left[\bar{A}^{(1)}(\bar{k}_\perp) - ik_z F(\bar{k}_\perp - \bar{k}_{\perp i}) \bar{a}^{(0)}(\bar{k}_{\perp i}) \right] \right. \\
& \left. + \left[-\hat{h}(k_z) \hat{\varepsilon}(k_z) + \hat{\varepsilon}(k_z) \hat{h}(k_z) \right] \cdot \left[\bar{B}^{(1)}(\bar{k}_\perp) - ik_z F(\bar{k}_\perp - \bar{k}_{\perp i}) \bar{b}^{(0)}(\bar{k}_{\perp i}) \right] \right\} \quad (31a)
\end{aligned}$$

$$\begin{aligned}
\bar{E}_i^{(1)} &= \frac{1}{2} \int d\bar{k}_\perp e^{i\bar{k}_\perp \cdot \bar{r}_\perp} e^{-ik_{1z}} \frac{k_1}{k_{1z}} \\
&\times \left\{ \frac{k}{k_1} \left[\hat{\epsilon}_1(-k_{1z}) \hat{\epsilon}_1(-k_{1z}) + \hat{h}_1(-k_{1z}) \hat{h}_1(-k_{1z}) \right] \cdot \left[\bar{A}^{(1)}(\bar{k}_\perp) + ik_{1z} F(\bar{k}_\perp - \bar{k}_{\perp i}) \bar{a}^{(1)}(\bar{k}_{\perp i}) \right] \right. \\
&\left. + \left[-\hat{h}_1(-k_{1z}) \hat{\epsilon}_1(-k_{1z}) + \hat{\epsilon}_1(-k_{1z}) \hat{h}_1(-k_{1z}) \right] \cdot \left[\bar{B}^{(1)}(\bar{k}_\perp) + ik_{1z} F(\bar{k}_\perp - \bar{k}_{\perp i}) \bar{b}^{(1)}(\bar{k}_{\perp i}) \right] \right\} \quad (31b)
\end{aligned}$$

In view of (30) and the fact that

$$\langle \bar{F}(\bar{k}_\perp) \rangle = \frac{1}{(2\pi)^2} \int d\bar{r}'_\perp e^{i\bar{k}_\perp \cdot \bar{r}'_\perp} \langle f(\bar{r}'_\perp) \rangle = 0 \quad (32)$$

we have

$$\langle \bar{E}_s^{(1)} \rangle = \langle \bar{E}_i^{(1)} \rangle = 0$$

Thus, the first-order solution does not modify the coherent reflection and transmission coefficients and we have to calculate the second-order solution to see the correction terms due to rough surface.

The lowest-order incoherent scattering coefficients can be derived from (31), by considering the vertically and horizontally polarized incident field and calculating the vertically and horizontally polarized scattered fields. We first calculate the scattered fields in the free space. For an incident field with polarization \hat{a}_i the scattered intensity with polarization \hat{b}_s is given by

$$\begin{aligned}
\langle |E_s^{(1)}|^2 \rangle &= \int d\bar{k}_\perp f'_{lm} W(|\bar{k}_\perp - \bar{k}_{\perp i}|) \\
&= \int d\Omega_s k^2 \cos \theta_s f'_{lm} W(|\bar{k}_\perp - \bar{k}_{\perp i}|) \quad (33)
\end{aligned}$$

where $W(|\bar{k}_\perp - \bar{k}_{\perp i}|)$ is the Fourier transform of the correlation function and

$$f'_{hh} = \left| E_s (k_1^2 - k^2) \frac{2k_{z_i}}{(k_z + k_{1z})(k_{z_i} + k_{1z_i})} \left(\frac{k_x k_{xi} + k_y k_{yi}}{k_\rho k_{\rho i}} \right) \right|^2 \quad (34a)$$

$$f'_{vh} = \left[E_{\nu}(k_1^2 - k^2) \frac{2kk_{1z}k_{zi}}{(k_1^2k_z + k^2k_{1z})(k_{zi} + k_{1zi})} \left(\frac{k_xk_{yi} - k_yk_{xi}}{k_xk_{yi}} \right) \right]^2 \quad (34b)$$

$$f'_{hv} = \left[E_{\nu}(k_1^2 - k^2) \frac{2kk_{1z}k_{zi}}{(k_z + k_{1z})(k_1^2k_{zi} + k^2k_{1zi})} \left(\frac{k_xk_{xi} - k_yk_{yi}}{k_xk_{yi}} \right) \right]^2 \quad (34c)$$

$$f'_{vv} = \left[E_{\nu}(k_1^2 - k^2) \frac{2k_1^2k_{zi}}{(k_1^2k_z + k^2k_{1z})(k_1^2k_{zi} + k^2k_{1zi})} \left[-k_xk_{xi} - \frac{k^2}{k_1^2}k_{1z}k_{1zi} \left(\frac{k_xk_{xi} + k_yk_{yi}}{k_xk_{yi}} \right) \right] \right]^2 \quad (34d)$$

In deriving (33), we made use of

$$\langle F(\bar{k}'_{\perp})F(\bar{k}_{\perp}) \rangle = \delta(\bar{k}'_{\perp} - \bar{k}_{\perp})W(|\bar{k}'_{\perp}|) \quad (35)$$

For a Gaussian correlation function we have

$$W(|\bar{k}_{\perp} - \bar{k}'_{\perp}|) = \frac{1}{4\pi} \sigma^2 l^2 \exp \left[- (k_{dx}^2 + k_{dy}^2) \frac{l^2}{4} \right] \quad (36)$$

where

$$\bar{k}_{d\perp} = \bar{k}_{\perp} - \bar{k}'_{\perp} \quad (37)$$

and σ is the standard deviation of the surface height and l is the correlation length for $f(\bar{r}_{\perp})$ in the transverse plane.

The bistatic scattering coefficients $\gamma_{lm}^r(\hat{k}_s, \hat{k}_i)$ are defined as the ratio of scattered power of polarization b_s per unit solid angle in direction \hat{k}_s and the intercepted power of polarization a_i in direction \hat{k}_i averaged over 4π radians. Therefore, in view of (33),

$$\gamma_{lm}^r(\hat{k}_s, \hat{k}_i) = 4\pi \frac{k^2 \cos \theta_s f'_{lm} W(|\bar{k}_{\perp} - \bar{k}'_{\perp}|)}{\cos \theta_i |E_{\nu}|^2} \quad (38)$$

Substituting (34) and (36) into the above equation and rearranging terms, we obtain

$$\gamma_{lm}^r(\hat{k}_s, \hat{k}_i) = \frac{4k^4 \sigma^2 l^2 \cos^2 \theta_s \cos^2 \theta_i}{\cos \theta_i} f_{lm} \exp \left[-k_{d\perp}^2 \frac{l^2}{4} \right] \quad (39)$$

where

$$k_{t,i'}^2 = k^2 (\sin^2 \theta_s + \sin^2 \theta_i - 2 \sin \theta_s \sin \theta_i \cos(\phi_s - \phi_i)) \quad (40)$$

and

$$f_{hh} = \left| \frac{(k_1^2 - k^2)}{(k_z + k_{1z})(k_{zi} + k_{1zi})} \right|^2 \cos^2(\phi_s - \phi_i) \quad (41a)$$

$$f_{vh} = \left| \frac{(k_1^2 - k^2)k k_{1z}}{(k_1^2 k_z + k^2 k_{1z})(k_{zi} + k_{1zi})} \right|^2 \sin^2(\phi_s - \phi_i) \quad (41b)$$

$$f_{hv} = \left| \frac{(k_1^2 - k^2)k k_{1zi}}{(k_z + k_{1z})(k_1^2 k_{zi} + k^2 k_{1zi})} \right|^2 \sin^2(\phi_s - \phi_i) \quad (41c)$$

$$f_{vv} = \left| \frac{(k_1^2 - k^2)}{(k_1^2 k_z + k^2 k_{1z})(k_1^2 k_{zi} + k^2 k_{1zi})} [k_1^2 k^2 \sin \theta_s \sin \theta_i - k^2 k_{1z} k_{1zi} \cos(\phi_s - \phi_i)] \right|^2 \quad (41d)$$

In the backscattering direction $\hat{k}_s = -\hat{k}_i$. The backscattering cross section per unit area are

$$\sigma_{hh}(\theta_i) = 4k^4 \sigma^2 l^2 \cos^4 \theta_i |R_{ho}|^2 \exp[-k^2 l^2 \sin^2 \theta_i] \quad (42a)$$

$$\sigma_{vv}(\theta_i) = 4k^2 \sigma^2 l^2 \cos^4 \theta_i \left| \frac{(k_1^2 - k^2)(k_1^2 k^2 \sin^2 \theta_i + k^2 k_{1z} k_{1zi})}{(k_1^2 k_{zi} + k^2 k_{1zi})^2} \right|^2 \exp[-k^2 l^2 \sin^2 \theta_i] \quad (42b)$$

$$\sigma_{vh}(\theta_i) = \sigma_{hv}(\theta_i) = 0 \quad (42c)$$

Therefore, there is no depolarization in the backscattering direction.

The bistatic scattering coefficients for the transmitted fields in the medium 1 can be obtained from (31b). Following the same procedure we obtain

$$\gamma_{lm}^\dagger(\hat{k}_t, \hat{k}_i) = \frac{4k_1^2 k^2 \sigma^2 l^2 \cos^2 \theta_t \cos^2 \theta_i}{\cos \theta_i} \frac{\eta}{\eta_1} W_{lm} \exp\left[-k_{t,i'}^2 \frac{l^2}{4}\right] \quad (43)$$

where

$$k_{t,i'}^2 = k_1^2 \sin \theta_t + k^2 \sin^2 \theta_i - 2k_1 k \sin \theta_t \sin \theta_i \cos(\phi_t - \phi_i) \quad (44)$$

and

$$W_{hh} = \left[\frac{(k_1^2 - k^2)}{(k_z + k_{1z})(k_{z1} - k_{1z1})} \right]^2 \cos^2(\phi_t - \phi_i) \quad (45a)$$

$$W_{rh} = \left[\frac{(k_1^2 - k^2)kk_z}{(k_1^2k_z + k^2k_{1z})(k_{z1} + k_{1z1})} \right]^2 \sin^2(\phi_t - \phi_i) \quad (45b)$$

$$W_{hr} = \left[\frac{(k_1^2 - k^2)kk_{1z1}}{(k_z + k_{1z})(k_1^2k_{z1} + k^2k_{1z1})} \right]^2 \sin^2(\phi_t - \phi_i) \quad (45c)$$

$$W_{rr} = \left[\frac{(k_1^2 - k^2)k_1k}{(k_1^2k_z + k^2k_{1z})(k_1^2k_{z1} + k^2k_{1z1})} |k_1k \sin \theta_t \sin \theta_i + k_zk_{1z1} \cos(\phi_t - \phi_i)| \right]^2 \quad (45d)$$

The first-order solution gives the lowest order incoherent scattered intensities. The bistatic reflection and transmission coefficients can be easily shown to satisfy the principle of reciprocity. However, in the first-order solution, there is no depolarization effect in the backscattering direction and the coherent reflection and transmission coefficients are not modified. Therefore, to calculate corrections to coherent reflection and transmission coefficients, we need to calculate the second-order solution.

3.5 Second-Order Solution

The second-order solution for the surface fields and the scattered fields can be obtained from (4), (7) and (8) by collecting and equating the second-order terms. We will first consider the case of a horizontally polarized incident wave, $\hat{e}_i = \hat{e}(-k_{zi})$. The second-order scattered field in $\hat{e}(k_z)$ and $\hat{h}(k_z)$ polarizations, which corresponds to horizontally and vertically polarized scattered fields, respectively, can be calculated to be

$$\begin{aligned}
 E_{n,z}^{(2)}(\bar{r}) &= \int d\bar{k}_\perp e^{i\bar{k}_\perp \cdot \bar{r}_\perp} e^{ik_{zz}} \int d\bar{k}'_\perp F(\bar{k}'_\perp - \bar{k}_{\perp i}) F(\bar{k}_\perp - \bar{k}'_\perp) \\
 &\quad \times \left\{ \frac{k_1^2 - k^2}{k_z + k_{1z}} \left(\frac{k_y k_{xi} - k_x k_{yi}}{k_\rho k_{\rho i}} \right) \tilde{B}'_q^{(1)}(\bar{k}'_\perp) - \frac{k_1^2 - k^2}{k_z + k_{1z}} \left(\frac{k_x k_{xi} + k_y k_{yi}}{k_\rho k_{\rho i}} \right) \tilde{B}'_{p'}^{(1)}(\bar{k}'_\perp) \right. \\
 &\quad \left. + \frac{1}{2} \frac{k_1^2 - k^2}{k_z + k_{1z}} (k_{1z} - k_{1zi}) \left(\frac{k_x k_{xi} + k_y k_{yi}}{k_\rho k_{\rho i}} \right) b_{p'}^{(0)}(\bar{k}_{\perp i}) \right\} \quad (46a)
 \end{aligned}$$

$$\begin{aligned}
 E_{n,s}^{(2)}(\bar{r}) &= \int d\bar{k}_\perp e^{i\bar{k}_\perp \cdot \bar{r}_\perp} e^{ik_{zz}} \int d\bar{k}'_\perp F(\bar{k}'_\perp - \bar{k}_{\perp i}) F(\bar{k}_\perp - \bar{k}'_\perp) \\
 &\quad \times \left\{ -\frac{k_1^2 - k^2}{k_1^2 k_z + k^2 k_{1z}} k_\rho k'_\rho \left[\frac{k'_x k_{yi} - k'_y k_{xi}}{k'_\rho k_{\rho i}} \tilde{A}'_q^{(1)}(\bar{k}'_\perp) + \left(\frac{k'_x k_{xi} + k'_y k_{yi}}{k'_\rho k_{\rho i}} \right) \tilde{A}'_{p'}^{(1)}(\bar{k}'_\perp) \right] \right. \\
 &\quad - \frac{(k_1^2 - k^2) k k_{1z}}{k_1^2 k_z + k^2 k_{1z}} \left(\frac{k_x k_{xi} + k_y k_{yi}}{k_\rho k_{\rho i}} \right) \tilde{B}'_q^{(1)}(\bar{k}'_\perp) - \frac{(k_1^2 - k^2) k k_{1z}}{k_1^2 k_z + k^2 k_{1z}} \left(\frac{k_y k_{xi} - k_x k_{yi}}{k_\rho k_{\rho i}} \right) \tilde{B}'_{p'}^{(1)}(\bar{k}'_\perp) \\
 &\quad \left. + \frac{1}{2} \frac{(k_1^2 - k^2) k}{k_1^2 k_z + k^2 k_{1z}} (k_1^2 - k_{1z} k_{1zi}) \left(\frac{k_y k_{xi} - k_x k_{yi}}{k_\rho k_{\rho i}} \right) b_q^{(0)}(\bar{k}_{\perp i}) \right\} \quad (46b)
 \end{aligned}$$

where

$$b_{p'}^{(0)}(\bar{k}_{\perp i}) = 1 + R_{n..} \quad (47)$$

$$\begin{aligned}
 \tilde{A}'_q^{(1)}(\bar{k}_\perp) &= \left\{ \frac{k_\rho k_{\rho i}}{k} \left(\frac{k_x k_{xi} + k_y k_{yi}}{k_\rho k_{\rho i}} \right) - \frac{k k_1^2}{k_z k_{1z} + k_1^2} \left(\frac{k_x k_{yi} - k_y k_{xi}}{k_\rho k_{\rho i}} \right)^2 \right. \\
 &\quad \left. + \frac{k_z k_{1z} + k_1^2}{k} \left(\frac{k_x k_{xi} + k_y k_{yi}}{k_\rho k_{\rho i}} \right)^2 \right\} b_{p'}^{(0)}(\bar{k}_{\perp i}) \quad (48a)
 \end{aligned}$$

$$\begin{aligned} \tilde{A}_p^{(1)}(\bar{k}_\perp) = & \left\{ \frac{k_p k_{pi}}{k} \left(\frac{k_x k_{xi} + k_y k_{yi}}{k_p k_{pi}} \right) + \left(\frac{k k_1^2}{k_z k_{1z} + k_p^2} - \frac{k_z k_{1z} + k^2}{k} \right) \right. \\ & \left. \times \left(\frac{k_x k_{xi} + k_y k_{yi}}{k_p k_{pi}} \right) \left(\frac{k_y k_{xi} - k_x k_{yi}}{k_p k_{pi}} \right) \right\} b_p^{(0)}(\bar{k}_{\perp i}) \end{aligned} \quad (48b)$$

$$\dot{B}_p^{(1)}(\bar{k}_\perp) = \frac{k_1^2 - k^2}{k_1^2 k_z + k^2 k_{1z}} k_p^2 \left(\frac{k_x k_{xi} - k_y k_{yi}}{k_p k_{pi}} \right) \left(\frac{k_x k_{yi} - k_y k_{xi}}{k_p k_{pi}} \right) b_p^{(0)}(\bar{k}_{\perp i}) \quad (48c)$$

$$\ddot{B}_p^{(1)}(\bar{k}_\perp) = \left\{ -k_{1zi} + \frac{(k_1^2 - k^2)}{(k_z + k_{1z})} - \frac{(k_1^2 - k^2)}{(k_1^2 k_z + k^2 k_{1z})} k_p^2 \left(\frac{k_y k_{xi} - k_x k_{yi}}{k_p k_{pi}} \right)^2 \right\} b_p^{(0)}(\bar{k}_{\perp i}) \quad (48d)$$

Thus, by taking ensemble average of (48), we obtain the lowest order correction to the coherent reflection coefficients. By making use of

$$\langle F(\bar{k}'_\perp - \bar{k}_{\perp i}) F(\bar{k}_\perp - \bar{k}'_\perp) \rangle = \delta(\bar{k}_\perp - \bar{k}_{\perp i}) W(|\bar{k}'_\perp - \bar{k}_{\perp i}|) \quad (49)$$

we obtain

$$\langle E_{hs}^{(2)} \rangle = e^{i\bar{k}_{\perp i} \cdot \bar{r}_\perp} e^{ik_{zi} z} (k_{zi} - k_{1zi}) \int d\bar{k}'_\perp \ddot{B}_p^{(1)}(\bar{k}'_\perp) W(|\bar{k}'_\perp - \bar{k}_{\perp i}|) \quad (50)$$

$$\langle E_{vs}^{(2)} \rangle = 0 \quad (51)$$

There is no depolarization of the coherent waves on the specular direction since we have an isotropic rough surface. In view of (20a), the modified reflection coefficient for the horizontal polarization is,

$$\begin{aligned} R_{01} = & R_{hs} + k_{zi} \frac{(k_1^2 - k^2)}{(k_{zi} + k_{1zi})^2} \sigma^2 l^2 \int_0^\infty k_p dk_p \exp \left[-\frac{1}{4} (k_p^2 + k_{pi}^2) l^2 \right] \\ & \times \left\{ \left[-\frac{(k_1^2 - k^2)}{(k_z + k_{1z})} \frac{k_z k_{1z}}{k_p^2 + k_z k_{1z}} + k_{1zi} \right] I_0(x) + \frac{k_1^2 - k^2}{k_z + k_{1z}} \frac{k_p^2}{k_p^2 + k_z k_{1z}} \left(I_0(x) - \frac{I_1(x)}{x} \right) \right\} \end{aligned} \quad (52)$$

where

$$x = \frac{1}{2} k_p k_{pi} l^2 \quad (53)$$

and I_0 and I_1 are the zeroth and first order modified Bessel functions.

The modified reflection coefficient for the vertical polarization can also be obtained by considering a vertically polarized incident field and calculating for the scattered fields. Following the same procedure we obtain

$$\begin{aligned}
S_{01} = R_{v..} - k_{zi} \frac{(k_1^2 - k^2)}{(k^2 k_{1zi} + k_1^2 k_{zi})^2} k^2 k_1^2 \sigma^2 l^2 \int_0^\infty k_\rho dk_\rho \exp \left[-\frac{1}{4}(k_\rho^2 + k_{\rho i}^2) l^2 \right] \\
\left\{ k_{1zi} \left[I_0(x) - 2 \frac{k_\rho k_{\rho i}}{k_\rho^2 + k_z k_{1z}} I_1(x) \right] - \frac{k_1^2 - k^2}{k_z + k_{1z}} \frac{k_{1zi}^2}{k_1^2} I_0(x) \right. \\
\left. + \frac{k_1^2 - k^2}{k_z + k_{1z}} \frac{k_{1zi}^2}{k_1^2} \frac{k_\rho^2}{k_\rho^2 + k_z k_{1z}} \left[I_0(x) - \frac{I_1(x)}{x} \right] - \frac{k_1^2 - k^2}{k_z + k_{1z}} \frac{k_\rho^2 k_{\rho i}^2}{k_\rho^2 + k_z k_{1z}} \frac{1}{k^2} I_0(x) \right\} \quad (54)
\end{aligned}$$

The modified coherent transmission coefficients for the horizontal and vertical polarization can be calculated similarly to give

$$\begin{aligned}
X_{01} = 1 + R_{h..} + k_{zi} \frac{(k_1^2 - k^2)}{(k_{zi} + k_{1zi})^2} \sigma^2 l^2 \int_0^\infty k_\rho dk_\rho \exp \left[-\frac{1}{4}(k_\rho^2 + k_{\rho i}^2) l^2 \right] \\
\times \left\{ (k_z - k_{1z}) \left[I_0(x) - \frac{k_\rho^2}{k_\rho^2 + k_z k_{1z}} \frac{I_1(x)}{x} \right] - \frac{1}{2}(k_{zi} - k_{1zi}) I_0(x) \right\} \quad (55a)
\end{aligned}$$

and

$$\begin{aligned}
Y_{01} = 1 + R_{v..} + k_{zi} \frac{(k_1^2 - k^2)}{(k_1^2 k_{zi} + k^2 k_{1zi})^2} k_1^2 \sigma^2 l^2 \int_0^\infty k_\rho dk_\rho \exp \left[-\frac{1}{4}(k_\rho^2 + k_{\rho i}^2) l^2 \right] \\
\times \left\{ -\frac{1}{2}(k^2 k_{1zi} - k_1^2 k_{zi}) I_0(x) - (k_1^2 - k^2) \frac{k_\rho^2 k_{\rho i}^2}{(k_1^2 k_z + k^2 k_{1z})} I_0(x) \right. \\
- \frac{k_1^2 - k^2}{k_z + k_{1z}} k_{zi} k_{1zi} I_0(x) + (k_1^2 - k^2) \frac{k_\rho^2 k_{zi} k_{1zi}}{(k_1^2 k_z + k^2 k_{1z})} \left(I_0(x) - \frac{I_1(x)}{x} \right) \\
\left. + \frac{k_z + k_{1z}}{k_1^2 k_z + k^2 k_{1z}} k_\rho k_{\rho i} (k^2 k_{1zi} - k_1^2 k_{zi}) I_1(x) \right\} \quad (55b)
\end{aligned}$$

The depolarization scattered intensity in the backscattering direction can be obtained by considering a horizontally polarized incident field and calculating the vertically polarized scattered intensity or vice versa. From reciprocity the two solutions

σ_{vh} and σ_{hv} can be shown to be the same. The second-order scattered field for a horizontally polarized incident field is given by (48b). Keeping only the terms that do not vanish in the backscattering direction and calculating the scattered intensity in the backscattering direction, the depolarized backscattering cross section per unit area can be calculated to be

$$\begin{aligned} \sigma_{hv}(\theta_i) = \sigma_{vh}(\theta_i) = & 8\pi k^2 \cos^2 \theta_i \left| \frac{2k(k_1^2 - k^2)^2 k_{1zi} k_{zi}}{(k_1^2 k_{zi} + k^2 k_{1zi})(k_{zi} - k_{1zi})} \right|^2 \\ & \times \int d\bar{k}'_{\perp} \left| \frac{(k_{xi} k'_y - k_{yi} k'_x)(k_{xi} k'_x + k_{yi} k'_y)}{k_{zi}^2 (k^2 k'_{zi} + k_1^2 k'_{1zi})} \right|^2 W(|\bar{k}'_{\perp} - \bar{k}_{\perp i}|) W(|\bar{k}'_{\perp} + \bar{k}_{\perp i}|) \quad (56a) \end{aligned}$$

After carrying out the $d\phi'$ -integration the above equation simplifies to

$$\begin{aligned} \sigma_{hv}(\theta_i) = \sigma_{vh}(\theta_i) = & \frac{1}{2} k^6 \cos^4 \theta_i \sigma^4 l^4 \left| \frac{(k_1^2 - k^2)^2 k_{1zi}}{(k_1^2 k_{zi} + k^2 k_{1zi})(k_{zi} + k_{1zi})} \right|^2 \exp \left[-\frac{1}{2} k_{zi}^2 l^2 \right] \\ & \times \int_0^{\infty} dk'_{zi} \frac{k_{zi}^3}{|k^2 k'_{zi} + k_1^2 k'_{1zi}|^2} \exp \left[-\frac{1}{2} k_{zi}^2 l^2 \right] \quad (56b) \end{aligned}$$

Therefore, by obtaining the second-order solution we can show the depolarization effect in the backscattered direction.

Appendix A: Integral Representation of Dyadic Green's Function

The integral representation of the free space dyadic Green's function is given by

$$\bar{\bar{G}}(\bar{r}, \bar{r}') = -\hat{z}\hat{z} \frac{\delta(\bar{r}, \bar{r}')}{k_z^2} + \begin{cases} \frac{1}{\delta\pi^2} \int d\bar{k}_\perp \frac{1}{k_z} \left[\hat{e}(k_z)\hat{e}(k_z) + \hat{h}(k_z)\hat{h}(k_z) \right] e^{i\bar{k}_\perp \cdot (\bar{r} - \bar{r}')} & z > z' \\ \frac{1}{\delta\pi^2} \int d\bar{k}_\perp \frac{1}{k_z} \left[\hat{e}(-k_z)\hat{e}(-k_z) + \hat{h}(-k_z)\hat{h}(-k_z) \right] e^{i\bar{K}_\perp \cdot (\bar{r} - \bar{r}')} & z < z' \end{cases} \quad (\text{A1})$$

where

$$\bar{k} = k_x \hat{x} + k_y \hat{y} + k_z \hat{z} \quad (\text{A2})$$

$$\bar{K} = k_x \hat{x} + k_y \hat{y} - k_z \hat{z} \quad (\text{A3})$$

$$\hat{e}(k_z) = \hat{k} \times \hat{z} / |\hat{k} \times \hat{z}| = \frac{1}{k_\rho} (\hat{x}k_y - \hat{y}k_x) \quad (\text{A4})$$

$$\hat{h}(k_z) = \frac{1}{k_z} \hat{e} \times \bar{k} = \frac{-k_z}{k_z k_\rho} (\hat{x}k_x + \hat{y}k_y) + \frac{k_\rho}{k_z} \hat{z} \quad (\text{A5})$$

$$\hat{e}(-k_z) = \hat{e}(k_z) \quad (\text{A6})$$

$$\hat{h}(-k_z) = \frac{1}{k_z} \hat{e} \times \bar{K} = \frac{k_z}{k_z k_\rho} (\hat{x}k_x - \hat{y}k_y) + \frac{k_\rho}{k_z} \hat{z} \quad (\text{A6})$$

Appendix B: Explicit Expressions for $\tilde{A}_q^{(1)}(\bar{k}_\perp)$, $\tilde{A}_p^{(1)}(\bar{k}_\perp)$, $\tilde{B}_q^{(1)}(\bar{k}_\perp)$, and $\tilde{B}_p^{(1)}(\bar{k}_\perp)$

$$\begin{aligned}
\tilde{A}_q^{(1)}(\bar{k}_\perp) &= \frac{(k_1^2 - k^2)}{(k_1^2 k_z + k^2 k_{1z})} k_\rho k_{\rho i} \left(\frac{k_x k_{yi} - k_y k_{xi}}{k_\rho k_{\rho i}} \right) a_p^{(0)}(\bar{k}_{\perp i}) - \frac{k_\rho k_{\rho i}}{k} \left(\frac{k_x k_{xi} + k_y k_{yi}}{k_\rho k_{\rho i}} \right) b_p^{(0)}(\bar{k}_{\perp i}) \\
&+ \left(\frac{k k_1^2}{k_z k_{1z} + k_\rho^2} - \frac{k_z k_{1z} - k_\rho^2}{k} \right) \left(\frac{k_x k_{xi} - k_y k_{yi}}{k_\rho k_{\rho i}} \right) \left(\frac{k_x k_{yi} - k_y k_{xi}}{k_\rho k_{\rho i}} \right) b_q^{(0)}(\bar{k}_{\perp i}) \\
&- \left[\frac{k k_1^2}{k_z k_{1z} + k_\rho^2} \left(\frac{k_x k_{yi} - k_y k_{xi}}{k_\rho k_{\rho i}} \right)^2 + \frac{k_z k_{1z} + k_\rho^2}{k} \left(\frac{k_x k_{xi} + k_y k_{yi}}{k_\rho k_{\rho i}} \right)^2 \right] b_p^{(0)}(\bar{k}_{\perp i}) \quad (B1)
\end{aligned}$$

$$\begin{aligned}
\tilde{A}_p^{(1)}(\bar{k}_\perp) &= \frac{(k_1^2 - k^2)}{(k_1^2 k_z + k^2 k_{1z})} k_\rho k_{\rho i} \left(\frac{k_y k_{xi} + k_x k_{yi}}{k_\rho k_{\rho i}} \right) a_p^{(0)}(\bar{k}_{\perp i}) + \frac{k_\rho k_{\rho i}}{k} \left(\frac{k_y k_{xi} - k_x k_{yi}}{k_\rho k_{\rho i}} \right) b_p^{(0)}(\bar{k}_{\perp i}) \\
&+ \left[\frac{k k_1^2}{k_z k_{1z} + k_\rho^2} \left(\frac{k_x k_{xi} + k_y k_{yi}}{k_\rho k_{\rho i}} \right)^2 + \left(\frac{k_z k_{1z} + k_\rho^2}{k} \right) \left(\frac{k_x k_{yi} - k_y k_{xi}}{k_\rho k_{\rho i}} \right) \right] b_q^{(0)}(\bar{k}_{\perp i}) \\
&+ \left[\frac{k k_1^2}{k_z k_{1z} + k_\rho^2} - \frac{k_z k_{1z} + k_\rho^2}{k} \right] \left(\frac{k_x k_{xi} + k_y k_{yi}}{k_\rho k_{\rho i}} \right) \left(\frac{k_y k_{xi} - k_x k_{yi}}{k_\rho k_{\rho i}} \right) b_p^{(0)}(\bar{k}_{\perp i}) \quad (B2)
\end{aligned}$$

$$\begin{aligned}
\tilde{B}_q^{(1)}(\bar{k}_\perp) &= k a_p^{(0)}(\bar{k}_\perp) - \frac{k}{k_z k_{1z} + k_\rho^2} k_\rho k_{\rho i} \left(\frac{k_x k_{xi} + k_y k_{yi}}{k_\rho k_{\rho i}} \right) a_p^{(0)}(\bar{k}_{\perp i}) \\
&+ \left[\frac{(k_1^2 - k^2)}{(k_z + k_{1z})} - \frac{(k_1^2 - k^2)}{(k_1^2 k_z + k^2 k_{1z})} k_\rho^2 \left(\frac{k_x k_{xi} + k_y k_{yi}}{k_\rho k_{\rho i}} \right)^2 \right] b_q^{(0)}(\bar{k}_{\perp i}) \\
&+ \frac{(k_1^2 - k^2)}{(k_1^2 k_z + k^2 k_{1z})} k_\rho^2 \left(\frac{k_x k_{xi} + k_y k_{yi}}{k_\rho k_{\rho i}} \right) \left(\frac{k_x k_{yi} - k_y k_{xi}}{k_\rho k_{\rho i}} \right) b_p^{(0)}(\bar{k}_{\perp i}) \quad (B3)
\end{aligned}$$

$$\begin{aligned}
\tilde{B}_p^{(1)}(\bar{k}_\perp) &= -k a_q^{(0)}(\bar{k}_{\perp i}) \frac{k}{k_z k_{1z} + k_\rho^2} k_\rho k_{\rho i} \left(\frac{k_y k_{xi} - k_x k_{yi}}{k_\rho k_{\rho i}} \right) a_p^{(0)}(\bar{k}_{\perp i}) \\
&- \frac{(k_1^2 - k^2)}{(k_1^2 k_z + k^2 k_{1z})} k_\rho^2 \left(\frac{k_x k_{xi} + k_y k_{yi}}{k_\rho k_{\rho i}} \right) \left(\frac{k_y k_{xi} - k_x k_{yi}}{k_\rho k_{\rho i}} \right) b_q^{(0)}(\bar{k}_{\perp i}) \\
&+ \left[\frac{(k_1^2 - k^2)}{(k_z + k_{1z})} - \frac{(k_1^2 - k^2)}{(k_1^2 k_z + k^2 k_{1z})} k_\rho^2 \left(\frac{k_x k_{xi} - k_y k_{yi}}{k_\rho k_{\rho i}} \right)^2 \right] b_p^{(0)}(\bar{k}_{\perp i}) \quad (B4)
\end{aligned}$$

CHAPTER 4

Scattering and Emission by Random Rough Surfaces – Modified Small Perturbation Method

The scattering of electromagnetic waves from a randomly rough dielectric surface is studied using a modified small perturbation method. The extended boundary condition method is used to solve for the scattered and transmitted fields. The small perturbation method (SPM) is modified with the use of cumulant technique. The coherent reflectivities and the bistatic scattering coefficients are derived using the modified SPM and are shown to have wider regions of validity than the conventional SPM result. The emissivity of the rough surface is then calculated by integrating the bistatic scattering coefficients over the upper hemisphere.

4.1 Introduction

Over the years, extensive theoretical and experimental investigations have been performed on scattering and emission of random rough surfaces and applied to sea, planetary and soil surfaces. Most of the work utilized either the Kirchhoff approach [Beckmann and Spizzichino, 1963; Semenov, 1965; Kodis, 1966; Stogryn, 1967; Barrick, 1968; Fung and Chan, 1969; Sancer, 1969; Lynch and Wagner, 1970; Leader, 1971; Sung and Holzer, 1976; Sung and Ekerhardt, 1978; Tsang and Kong, 1980a,b; Bass and Fuks, 1979; Ulaby *et al.*, 1981] or the small perturbation method [Rice, 1963; Valenzuela, 1967, 1968; Agarwal, 1977; Nieto-Vesperina, 1982]. The small perturbation method is used to study the rough surface with the height small compared with a wavelength and the slope much smaller than unity. The Kirchhoff approach has been used to study rough surfaces with large radius of curvatures. In recent years, there has been considerable interest in the development of more general theories which can bridge these two limiting methods. The full wave approach [Bahar, 1978; Bahar and Barrick, 1983] has been used for composite surfaces which cannot be decomposed into small-scale perturbations and large-scale surfaces. It has also been used to study depolarization effects. The diagrammatic approach [Zipfel and DeSanto, 1972; DeSanto, 1974; DeSanto, 1983] makes use of the Feynman diagram and has been used to obtain the coherent intensity beyond the Kirchhoff approximation and compared with some experimental data.

In this chapter we study the problem of scattering and emission from a randomly rough dielectric surface using the modified SPM. The extended boundary condition method is used to solve for the scattered and transmitted fields. The small perturbation method is modified with the use of cumulant technique to derive the coherent reflection

coefficients and the bistatic scattering coefficients. The results are shown to have wider regions of validity than the conventional SPM results. The emissivity is obtained by integrating the bistatic scattering coefficients over the upper hemisphere. The results are illustrated by comparing with the emissivities obtained with the KA for the various cases.

4.2 Formulation

Consider a plane wave in free space with electric field $\bar{E}_i = \hat{\varepsilon}_i \exp(i\bar{k}_i \cdot \bar{r})$ incident upon a randomly rough surface with permittivity ε_1 . The rough surface is characterized by a height distribution $z = f(\bar{r}_\perp)$ where $f(\bar{r}_\perp)$ is a random variable with zero mean, $\langle f(\bar{r}_\perp) \rangle = 0$. Let f_{min} and f_{max} be the minimum and maximum values of the surface profile $f(\bar{r}_\perp)$. From Huygen's principle, the total field $\bar{E}(\bar{r})$ in free space, and the transmitted field $\bar{E}_1(\bar{r})$ in the dielectric medium satisfy

$$\begin{aligned} \bar{E}_i(\bar{r}) + \int_{S'} dS' \left\{ i\omega\mu_0 \bar{\bar{G}}(\bar{r}, \bar{r}') \cdot [\hat{n} \times \bar{H}(\bar{r}')] + \nabla \times \bar{\bar{G}}(\bar{r}, \bar{r}') \cdot [\hat{n} \times \bar{E}(\bar{r}')] \right\} \\ = \begin{cases} \bar{E}(\bar{r}) & z > f(\bar{r}_\perp) & (1a) \\ 0 & z < f(\bar{r}_\perp) & (1b) \end{cases} \end{aligned}$$

$$\begin{aligned} \int_{S'} dS' \left\{ i\omega\mu_1 \bar{\bar{G}}_1(\bar{r}, \bar{r}') \cdot [\hat{n}_d \times \bar{H}_1(\bar{r}')] + \nabla \times \bar{\bar{G}}_1(\bar{r}, \bar{r}') \cdot [\hat{n}_d \times \bar{E}_1(\bar{r}')] \right\} \\ = \begin{cases} 0 & z > f(\bar{r}_\perp) & (2a) \\ \bar{E}_1(\bar{r}) & z < f(\bar{r}_\perp) & (2b) \end{cases} \end{aligned}$$

where S' denotes the rough surface over which the surface integration is to be carried out, \hat{n} and \hat{n}_d are the unit vectors normal to the rough surface and pointing into the free space and the dielectric medium, respectively, and $\bar{\bar{G}}(\bar{r}, \bar{r}')$ and $\bar{\bar{G}}_1(\bar{r}, \bar{r}')$ are respectively the dyadic Green's functions for free space and the homogeneous dielectric of region 1.

Evaluating (1b) for $z < f_{min}$ and (2a) for $z > f_{max}$, we obtain the extended boundary conditions which can be solved for the surface fields [Chapter 3, Sec 3.2]. Once the surface fields are obtained, then the scattered field in free space and the transmitted

field in medium 1 can be derived from the diffraction integrals. Thus, evaluating (1a) and (2b) for $z > f_{max}$ and $z < f_{min}$ respectively, we obtain

$$\begin{aligned} \bar{E}_s(\bar{r}) = & -\frac{1}{8\pi^2} \int d\bar{k}_\perp e^{i\bar{k}_\perp \cdot \bar{r}_\perp} e^{ik_z z} \frac{k}{k_z} \int d\bar{r}'_\perp e^{-i\bar{k}_\perp \cdot \bar{r}'_\perp} e^{-ik_z f(\bar{r}'_\perp)} \\ & \times \left\{ \left[\hat{e}(k_z) \hat{e}(k_z) + \hat{h}(k_z) \hat{h}(k_z) \right] \cdot \bar{a}(\bar{r}'_\perp) + \left[-\hat{h}(k_z) \hat{e}(k_z) + \hat{e}(k_z) \hat{h}(k_z) \right] \cdot \bar{b}(\bar{r}'_\perp) \right\} \end{aligned} \quad (3a)$$

$$\begin{aligned} \bar{E}_t(\bar{r}) = & \frac{1}{8\pi^2} \int d\bar{k}_\perp e^{i\bar{k}_\perp \cdot \bar{r}_\perp} e^{-i\bar{k}_{1z} z} \frac{k_1}{k_{1z}} \int d\bar{r}'_\perp e^{-i\bar{k}_\perp \cdot \bar{r}'_\perp} e^{ik_{1z} f(\bar{r}'_\perp)} \\ & \times \left\{ \frac{k}{k_1} \left[\hat{e}_1(-k_{1z}) \hat{e}_1(-k_{1z}) + \hat{h}_1(-k_{1z}) \hat{h}_1(-k_{1z}) \right] \cdot \bar{a}(\bar{r}'_\perp) \right. \\ & \left. + \left[-\hat{h}_1(-k_{1z}) \hat{e}_1(-k_{1z}) + \hat{e}_1(-k_{1z}) \hat{h}_1(-k_{1z}) \right] \cdot \bar{b}(\bar{r}'_\perp) \right\} \end{aligned} \quad (3b)$$

where

$$d\bar{r}'_\perp \bar{a}(\bar{r}'_\perp) = dS' \eta \hat{n} \times \bar{H}(\bar{r}') = dS' \frac{\eta}{\eta_1} \eta_1 \hat{n} \times \bar{H}_1(\bar{r}') \quad (4a)$$

$$d\bar{r}'_\perp \bar{b}(\bar{r}'_\perp) = dS' \hat{n} \times \bar{E}(\bar{r}') = dS' \hat{n} \times \bar{E}_1(\bar{r}') \quad (4b)$$

In Chapter 2 we used the Kirchhoff approximation to solve for the scattered fields from the above diffraction integrals by making use of tangent plane approximation for the surface fields. In Chapter 3 we used the small perturbation method to calculate the surface fields and the scattered fields by making a perturbation expansion. In this chapter we will modify the SPM with the cumulant average technique and solve for the scattered fields.

We will consider the case of horizontally polarized scattered field due to the horizontally polarized incident wave in detail to illustrate the modified SPM. The SPM and KA results are derived in Chapters 2 and 3. The coherent reflected field with the

lowest order correction due to the rough surface, obtained with the SPM [Chapter 3, Sec. 3.5] is given by

$$\langle E_{hs} \rangle = R_{hs} e^{i\bar{k}_\perp \cdot \bar{r}_\perp} e^{ik_{z1}z} \left\{ 1 + (k_{z1} - k_{1z1}) \int d\bar{k}'_\perp \hat{B}_p^{(1)}(\bar{k}'_\perp) W(\bar{k}'_\perp - \bar{k}_\perp) \right\} \quad (5)$$

where R_{hs} is the Fresnel reflection coefficient for the TE wave. In the limit $l \rightarrow \infty$, where l is the correlation length for $f(\bar{r}_\perp)$ in the transverse plane, the above expression simplifies to

$$\langle E_{hs} \rangle = R_{hs} [1 - 2k_{z1}^2 \sigma^2] e^{i\bar{k}_\perp \cdot \bar{r}_\perp} e^{ik_{z1}z} \quad (6)$$

The coherent reflected wave under the Kirchhoff Approximation is derived in Chapter 2 to be

$$\langle E_{hs} \rangle = R_{hs} e^{-2k_{z1}^2 \sigma^2} e^{i\bar{k}_\perp \cdot \bar{r}_\perp} e^{ik_{z1}z} \quad (7)$$

In the limit $k_{z1}\sigma \ll 1$, the above expression reduces to

$$\langle E_{hs} \rangle = R_{hs} [1 - 2k_{z1}^2 \sigma^2] e^{i\bar{k}_\perp \cdot \bar{r}_\perp} e^{ik_{z1}z} \quad (8)$$

which checks with the SPM result in the $l \rightarrow \infty$ limit. In the next section we will modify the SPM with the cumulant technique such that in the limit $l \rightarrow \infty$ the KA result given by (7) is obtained and in the limit $k_{z1}\sigma \ll 1$, the SPM result given by (5) is obtained.

4.3 Modified Small Perturbation Method

The horizontally polarized scattered field for the incident wave with horizontal polarization has been derived in Chapter 3 using SPM by making a perturbation expansion. The expressions for the second-order solution is given by

$$E_{h,s}^{(0)}(\bar{r}) = R_{h,s} e^{i\bar{k}_\perp \cdot \bar{r}_\perp} e^{ik_z z} \quad (9)$$

$$E_{h,s}^{(1)}(\bar{r}) = - \int d\bar{k}_\perp e^{i\bar{k}_\perp \cdot \bar{r}_\perp} e^{ik_z z} iF(\bar{k}_- - \bar{k}_{\perp i}) (k_z - k_{1z}) \left(\frac{k_x k_{xi} + k_y k_{yi}}{k_\rho k_{\rho i}} \right) b_p^{(0)}(\bar{k}_{\perp i}) \quad (10)$$

$$\begin{aligned} E_{h,s}^{(2)}(\bar{r}) = & \int d\bar{k}_\perp e^{i\bar{k}_\perp \cdot \bar{r}_\perp} e^{ik_z z} \int d\bar{k}'_\perp F(\bar{k}'_\perp - \bar{k}_{\perp i}) F(\bar{k}_- - \bar{k}'_\perp) \\ & \times \left\{ \frac{k_1^2 - k^2}{k_z + k_{1z}} \left(\frac{k_y k_{xi} - k_x k_{yi}}{k_\rho k_{\rho i}} \right) \tilde{B}_q^{(1)}(\bar{k}'_\perp) - \frac{k_1^2 - k^2}{k_z + k_{1z}} \left(\frac{k_x k_{xi} + k_y k_{yi}}{k_\rho k_{\rho i}} \right) \tilde{B}_p^{(1)}(\bar{k}'_\perp) \right. \\ & \left. + \frac{1}{2} \frac{k_1^2 - k^2}{k_z + k_{1z}} (k_{1z} - k_{1zi}) \left(\frac{k_x k_{xi} + k_y k_{yi}}{k_\rho k_{\rho i}} \right) b_p^{(0)}(\bar{k}_{\perp i}) \right\} \quad (11) \end{aligned}$$

where

$$F(\bar{k}_\perp) = \frac{1}{4\pi^2} \int d\bar{r}'_\perp f(\bar{r}'_\perp) e^{-i\bar{k}_\perp \cdot \bar{r}'_\perp} \quad (12)$$

$$\tilde{B}_q^{(1)}(\bar{k}_\perp) = \frac{k_1^2 - k^2}{k_1^2 k_z + k^2 k_{1z}} k_\rho^2 \left(\frac{k_x k_{xi} + k_y k_{yi}}{k_\rho k_{\rho i}} \right) \left(\frac{k_x k_{yi} - k_y k_{xi}}{k_\rho k_{\rho i}} \right) b_p^{(0)}(\bar{k}_{\perp i}) \quad (13)$$

$$\tilde{B}_p^{(1)}(\bar{k}_\perp) = \left\{ -k_{1zi} + \frac{(k_1^2 - k^2)}{(k_z + k_{1z})} - \frac{(k_1^2 - k^2)}{(k_1^2 k_z + k^2 k_{1z})} k_\rho^2 \left(\frac{k_y k_{xi} - k_x k_{yi}}{k_\rho k_{\rho i}} \right)^2 \right\} b_p^{(0)}(\bar{k}_{\perp i}) \quad (14)$$

$$b_p^{(0)}(\bar{k}_{\perp i}) = 1 + R_{h,s} \quad (15)$$

In the modified SPM we first assume that the scattered field can be expressed in the following form:

$$\begin{aligned} E_{h,s}(\bar{r}) = & -\frac{1}{8\pi^2} \int d\bar{k}_\perp e^{i\bar{k}_\perp \cdot \bar{r}_\perp} e^{ik_z z} \frac{2}{k_z + k_{zi}} (k_{1z} - k_z) (1 + R_{h,s}) \int d\bar{r}'_\perp e^{-i(\bar{k}_\perp - \bar{k}_{\perp i}) \cdot \bar{r}'_\perp} \\ & \times \left\{ \left(\frac{k_x k_{xi} + k_y k_{yi}}{k_\rho k_{\rho i}} \right) e^{(k_z + k_{zi})h_s(\bar{r}'_\perp)} + \left(\frac{k_x k_{yi} - k_y k_{xi}}{k_\rho k_{\rho i}} \right) \left(e^{(k_z + k_{zi})h_s(\bar{r}'_\perp)} - 1 \right) \right\} \quad (16) \end{aligned}$$

where $h_r(\bar{r}'_\perp)$ and $h_s(\bar{r}'_\perp)$ are the unknown functions to be determined by making a perturbation expansion. We let

$$h_r(\bar{r}_\perp) = \sum_{m=1}^{\infty} \frac{h_r^{(m)}(\bar{r}_\perp)}{m!} \quad h_s(\bar{r}_\perp) = \sum_{m=1}^{\infty} \frac{h_s^{(m)}(\bar{r}_\perp)}{m!} \quad (17)$$

Substituting the above expansion into (16) and further expanding the equation for the scattered field, we can solve for $h_r^{(m)}$ and $h_s^{(m)}$ by comparing with the SPM result. The first-order result is given by

$$H_r^{(1)}(\bar{k}_\perp) = -iF(\bar{k}_\perp - \bar{k}_{\perp i}) \quad H_s^{(1)}(\bar{k}_\perp) = 0 \quad (18)$$

where

$$H_r^{(m)}(\bar{k}_\perp) = \frac{1}{4\pi^2} \int d\bar{r}'_\perp h_r^{(m)}(\bar{r}'_\perp) e^{-i\bar{k}_\perp \cdot \bar{r}'_\perp} \quad (19)$$

Thus, we have

$$h_r^{(1)}(\bar{r}'_\perp) = -if(\bar{r}'_\perp) \quad h_s^{(1)}(\bar{r}'_\perp) = 0 \quad (20)$$

The second-order results are given by

$$\begin{aligned} H_r^{(2)}(\bar{k}_\perp - \bar{k}_{\perp i}) &= -(k_z + k_{zi}) \int d\bar{k}'_\perp H_r^{(1)}(\bar{k}_\perp - \bar{k}'_\perp) H_r^{(1)}(\bar{k}'_\perp - \bar{k}_{\perp i}) \\ &+ \int d\bar{k}'_\perp F(\bar{k}_\perp - \bar{k}'_\perp) F(\bar{k}'_\perp - \bar{k}_{\perp i}) \left\{ (k_{1z} - k_{1zi}) + 2 \frac{\tilde{B}_p^{(1)}(\bar{k}'_\perp)}{b_p^{(0)}(\bar{k}_{\perp i})} \right\} \end{aligned} \quad (21a)$$

$$H_s^{(2)}(\bar{k}_\perp - \bar{k}'_\perp) = \int d\bar{k}'_\perp F(\bar{k}_\perp - \bar{k}'_\perp) F(\bar{k}'_\perp - \bar{k}_{\perp i}) \frac{\tilde{B}_p^{(1)}(\bar{k}'_\perp)}{b_p^{(0)}(\bar{k}_{\perp i})} \quad (21b)$$

The coherent reflected field is obtained by taking the ensemble average of (16).

We have

$$\langle \mathbf{E}_{h_s}(\bar{r}) \rangle = R_{h_s} \langle e^{2k_z h_s(\bar{r}'_\perp)} \rangle e^{i\bar{k}_\perp \cdot \bar{r}_\perp} e^{ik_z z} \quad (22)$$

If we make the regular perturbation expansion of the above expression and take the ensemble average, then we obtain the same result as the SPM. Thus, we make use of cumulant average technique [Shen and Maradudin, 1980; Kubo, 1962] in performing the ensemble average in (16). The cumulant average is defined such that

$$\langle e^{2k_{zi}h_c(\bar{r}'_{\perp})} \rangle = \exp \left[\langle e^{2k_{zi}h_c(\bar{r}'_{\perp})} - 1 \rangle_c \right] \quad (23)$$

where $\langle \dots \rangle_c$ stands for cumulant average. For a random variable χ , there is an exact relationship between the cumulant average $\langle \chi^n \rangle_c$ and the moments $\langle \chi^m \rangle$ for $m \leq n$ [Kubo, 1962]. The first two relations are given by

$$\langle \chi \rangle_c = \langle \chi \rangle \quad (24a)$$

$$\langle \chi^2 \rangle_c = \langle \chi^2 \rangle - \langle \chi \rangle^2 \quad (24b)$$

The left-hand-side of (23) is normally evaluated by making the power series expansion:

$$\langle e^{2k_{zi}h_c(\bar{r}'_{\perp})} \rangle = 1 + \langle 2k_{zi}h_c(\bar{r}'_{\perp}) \rangle + \frac{1}{2} \langle (2k_{zi}h_c(\bar{r}'_{\perp}))^2 \rangle + \dots \quad (25)$$

Similarly, we expand

$$\langle e^{2k_{zi}h_c(\bar{r}'_{\perp})} - 1 \rangle_c = \langle 2k_{zi}h_c(\bar{r}'_{\perp}) \rangle_c + \frac{1}{2} \langle (2k_{zi}h_c(\bar{r}'_{\perp}))^2 \rangle_c + \dots \quad (26)$$

Note that by substituting (25) and (26) into (23) and by further expanding the right-hand-side of (23), the relation between the cumulant average and moments of the random variable can be obtained by equating the same order terms.

We evaluate (26) using the perturbation expansion for $h_r(\bar{r}_\perp)$. We have, by keeping the terms to the second order,

$$\begin{aligned} \langle e^{2k_{zi}h_r(\bar{r}'_\perp)} - 1 \rangle_r &\simeq \langle 2k_{zi}h_r^{(1)}(\bar{r}'_\perp) \rangle_r - \frac{1}{2} \langle (2k_{zi}h_r^{(2)}(\bar{r}'_\perp))^2 \rangle_r - \frac{1}{2} \langle (2k_{zi}h_r^{(1)}(\bar{r}'_\perp))^2 \rangle_r \\ &= k_{zi} \langle h_r^{(2)}(\bar{r}'_\perp) \rangle + 2k_{zi}^2 \langle h_r^{(1)}(\bar{r}'_\perp) \rangle \end{aligned} \quad (27)$$

where we made use of the fact $\langle h_r^{(1)}(\bar{r}'_\perp) \rangle = 0$. Thus, the coherent reflected field for the horizontal polarization is given by

$$\langle E_{h^*} \rangle = R_{h^*} e^{i\bar{k}_\perp \cdot \bar{r}_\perp} e^{ik_{zi}z} \exp \left[(k_{zi} + k_{1zi}) \int d\bar{k}'_\perp \hat{B}_r^{(1)}(\bar{k}'_\perp) W(|\bar{k}'_\perp - \bar{k}_{\perp i}|) \right] \quad (28)$$

We note that the above result agree with the SPM result and the KA result, given by (5) and (7), in the respective limits of $k_{zi}\sigma \ll 1$ and $l \rightarrow \infty$.

4.4 Bistatic Scattering Coefficients

The bistatic scattering coefficients can be derived by calculating the incoherent scattered intensities. From (16) we have, by making use of cumulant average technique,

$$\begin{aligned} \gamma_{hh}(\bar{k}_\perp, \bar{k}_{\perp i}) &= \frac{4\pi}{\cos \theta_i} k_z^2 k_{zi}^2 \frac{4}{(k_z + k_{zi})^2} \left| \frac{k_1^2 - k^2}{(k_z + k_{1z})(k_{zi} + k_{1zi})} \right|^2 \left(\frac{k_x k_{xi} + k_y k_{yi}}{k_\rho k_{\rho i}} \right)^2 \\ &\times \exp \left[-2 \operatorname{Re} \{ M_{hi}(\bar{k}_\perp, \bar{k}_{\perp i}) \} \right] \frac{1}{4\pi^2} \int d\bar{r}'_\perp e^{-i(\bar{k}_\perp - \bar{k}_{\perp i}) \cdot \bar{r}'_\perp} \left\{ \exp \left[(k_z + k_{zi})^2 C(\bar{r}'_\perp) \right] - 1 \right\} \end{aligned} \quad (29)$$

where

$$M_{hi}(\bar{k}_\perp, \bar{k}_{\perp i}) = \frac{1}{2}(k_z^2 - k_{zi}^2)\sigma^2 + \frac{(k_z + k_{zi})}{2k_{zi}} M_{hi}(\bar{k}_{\perp i}, \bar{k}_{\perp i}) \quad (30)$$

with

$$M_{hi}(\bar{k}_{\perp i}, \bar{k}_{\perp i}) = 2k_{zi} \int d\bar{k}'_\perp \left\{ k_{1zi} - \frac{(k_1^2 - k^2)}{k'_z + k'_{1z}} - \frac{(k_1^2 - k^2)k_{\rho i}^2}{k_1^2 k'_z + k^2 k'_{1z}} \left(\frac{k'_y k_{xi} - k'_x k_{yi}}{k'_\rho k_{\rho i}} \right)^2 \right\} W(|\bar{k}'_\perp - \bar{k}_{\perp i}|) \quad (31)$$

For the correlation function $C(\bar{r}'_\perp)$ with the gaussian dependence, the integrals in (29) and (31) can be carried out. We have

$$\begin{aligned} \gamma_{hh}(\bar{k}_\perp, \bar{k}_{\perp i}) &= \frac{1}{\cos \theta_i} k_z^2 k_{zi}^2 \frac{4}{(k_z + k_{zi})^2} \left| \frac{k_1^2 - k^2}{(k_z + k_{1z})(k_{zi} + k_{1zi})} \right|^2 \cos^2(\phi - \phi_i) \\ &\times \exp \left[-2 \operatorname{Re} \{ M_{hi}(\bar{k}_\perp, \bar{k}_{\perp i}) \} \right] \sum_{m=1}^{\infty} \frac{[(k_z + k_{zi})\sigma]^{2m}}{m! m} \exp \left[-\frac{k_{d\rho}^2 l^2}{4m} \right] \end{aligned} \quad (32)$$

$$\begin{aligned} M_{hi}(\bar{k}_{\perp i}, \bar{k}_{\perp i}) &= k_{zi} \sigma^2 l^2 \int_0^\infty k'_\rho dk'_\rho \exp \left[-(k_{\rho i}^2 + k_{\rho i}^2) \frac{l^2}{4} \right] \\ &\times \left\{ \left[k_{1zi} - \frac{(k_1^2 - k^2)}{k'_z + k'_{1z}} \right] I_0(x) + \frac{(k_1^2 - k^2)}{k_1^2 k'_z + k^2 k'_{1z}} k_{\rho i}^2 \frac{I_1(x)}{x} \right\} \end{aligned} \quad (33)$$

where

$$k_{d\rho}^2 = k_\rho^2 + k_{\rho i}^2 - 2k_\rho k_{\rho i} \cos(\phi - \phi_i) \quad (34)$$

$$x = \frac{1}{2} k'_p k_{\rho i} l^2 \quad (35)$$

and I_0 and I_1 are the zeroth and first order modified Bessel functions.

The vertically polarized scattered field for the horizontally polarized incident field is obtained in a similar manner. We assume that the scattered fields can be expressed in the following form:

$$\begin{aligned} E_{vs}(\bar{r}) = & -\frac{1}{8\pi^2} \int d\bar{k}_\perp e^{i\bar{k}_\perp \cdot \bar{r}_\perp} e^{ik_z z} \frac{2}{k_z + k_{z1}} k k_{1z} \frac{k_1^2 - k^2}{k_1^2 k_z + k^2 k_{1z}} (1 + R_{hv}) \int d\bar{r}'_\perp e^{-i(\bar{k}_\perp - \bar{k}'_\perp) \cdot \bar{r}'_\perp} \\ & \times \left\{ \left(e^{(k_z + k_{z1})v \cdot (\bar{r}'_\perp)} - 1 \right) + \left(\frac{k_x k_{xi} + k_y k_{yi}}{k_p k_{\rho i}} \right) \left(e^{(k_z + k_{z1})v \cdot (\bar{r}'_\perp)} - 1 \right) \right. \\ & \left. + \left(\frac{k_x k_{yi} - k_y k_{xi}}{k_p k_{\rho i}} \right) \left(e^{(k_z + k_{z1})v \cdot (\bar{r}'_\perp)} - 1 \right) \right\} \quad (36) \end{aligned}$$

Then the bistatic scattering coefficient can be derived by following exactly the same procedure. We have

$$\begin{aligned} \gamma_{vh}(\bar{k}_\perp, \bar{k}'_\perp) = & \frac{4\pi}{\cos \theta_i} k_z^2 k_{z1}^2 \frac{4}{(k_z + k_{z1})^2} \left| \frac{k k_{1z} (k_1^2 - k^2)}{(k_1^2 k_z + k^2 k_{1z})(k_{z1} + k_{1z1})} \right|^2 \left(\frac{k_y k_{xi} - k_x k_{yi}}{k_p k_{\rho i}} \right)^2 \\ & \times \exp[-2 \operatorname{Re}\{M'_{hi}(\bar{k}_\perp, \bar{k}'_\perp)\}] \frac{1}{4\pi^2} \int d\bar{r}'_\perp e^{-i(\bar{k}_\perp - \bar{k}'_\perp) \cdot \bar{r}'_\perp} \left\{ \exp[(k_z + k_{z1})^2 C(\bar{r}'_\perp)] - 1 \right\} \quad (37) \end{aligned}$$

where

$$M'_{hi}(\bar{k}_\perp, \bar{k}'_\perp) = \frac{1}{2} (k_z^2 - k_{z1}^2) \sigma^2 + \frac{1}{2} (k_z + k_{z1}) \frac{k_{\rho i}^2}{k_{1z1}} \sigma^2 + \frac{(k_z + k_{z1})}{2k_{z1}} M_{hi}(\bar{k}_\perp, \bar{k}'_\perp) \quad (38)$$

The bistatic scattering coefficients for the vertically polarized incident wave can also be derived following exactly the same procedure as outlined in the previous section. For the vertically and horizontally polarized scattered fields we assume the following

form:

$$\begin{aligned}
E_{v..}(\bar{r}) = & -\frac{1}{8\pi^2} \int d\bar{k}_\perp e^{i\bar{k}_\perp \cdot \bar{r}_\perp} e^{ik_z z} \frac{2}{k_z + k_{zi}} \frac{k_1^2 - k^2}{k_1^2 k_z + k^2 k_{1z}} (1 + R_{v..}) \int d\bar{r}'_\perp e^{-i(\bar{k}_\perp - \bar{k}'_\perp) \cdot \bar{r}'_\perp} \\
& \times \left\{ k_\rho k_{\rho i} e^{(k_z + k_{zi})r'_\perp(\bar{r}'_\perp)} - \frac{k^2}{k_1^2} k_{1z} k_{1zi} \left(\frac{k_x k_{xi} + k_y k_{yi}}{k_\rho k_{\rho i}} \right) e^{(k_z + k_{zi})r'_\perp(\bar{r}'_\perp)} \right. \\
& \left. - \frac{k^2}{k_1^2} k_{1z} k_{1zi} \left(\frac{k_y k_{xi} - k_x k_{yi}}{k_\rho k_{\rho i}} \right) \left(e^{(k_z + k_{zi})r'_\perp(\bar{r}'_\perp)} - 1 \right) \right\} \quad (39)
\end{aligned}$$

$$\begin{aligned}
E_{h..}(\bar{r}) = & -\frac{1}{8\pi^2} \int d\bar{k}_\perp e^{i\bar{k}_\perp \cdot \bar{r}_\perp} e^{ik_z z} \frac{2}{k_z + k_{zi}} \frac{k k_{1zi}}{k_1^2} \frac{k_1^2 - k^2}{k_z + k_{1z}} (1 + R_{h..}) \int d\bar{r}'_\perp e^{-i(\bar{k}_\perp - \bar{k}'_\perp) \cdot \bar{r}'_\perp} \\
& \times \left\{ \left(\frac{k_y k_{xi} - k_x k_{yi}}{k_\rho k_{\rho i}} \right) \left(e^{(k_z + k_{zi})r'_\perp(\bar{r}'_\perp)} - 1 \right) - \left(\frac{k_x k_{xi} + k_y k_{yi}}{k_\rho k_{\rho i}} \right) \left(e^{(k_z + k_{zi})r'_\perp(\bar{r}'_\perp)} - 1 \right) \right\} \quad (40)
\end{aligned}$$

where $R_{v..}$ is the Fresnel reflection coefficient for the vertical polarization. Then, the bistatic scattering coefficients are calculated to be

$$\begin{aligned}
\gamma_{vv}(\bar{k}_\perp, \bar{k}'_\perp) = & \frac{4\pi}{\cos \theta_i} k_z^2 k_{zi}^2 \frac{4}{(k_z + k_{zi})^2} \left| \frac{k_1^2 (k_1^2 - k^2)}{(k_1^2 k_z + k^2 k_{1z})(k_1^2 k_{zi} + k^2 k_{1zi})} \right|^2 \\
& \times \left| k_\rho k_{\rho i} \exp[-M'_{vi}(\bar{k}_\perp, \bar{k}'_\perp)] - \frac{k^2}{k_1^2} k_{1z} k_{1zi} \exp[-M''_{vi}(\bar{k}_\perp, \bar{k}'_\perp)] \left(\frac{k_x k_{xi} + k_y k_{yi}}{k_\rho k_{\rho i}} \right) \right|^2 \\
& \times \frac{1}{4\pi^2} \int d\bar{r}'_\perp e^{-i(\bar{k}_\perp - \bar{k}'_\perp) \cdot \bar{r}'_\perp} \left\{ \exp[(k_z + k_{zi})^2 C(\bar{r}'_\perp)] - 1 \right\} \quad (41)
\end{aligned}$$

$$\begin{aligned}
\gamma_{hv}(\bar{k}_\perp, \bar{k}'_\perp) = & \frac{4\pi}{\cos \theta_i} k_z^2 k_{zi}^2 \frac{4}{(k_z + k_{zi})^2} \left| \frac{k k_{1zi} (k_1^2 - k^2)}{(k_z + k_{1z})(k_1^2 k_{zi} + k^2 k_{1zi})} \right|^2 \left(\frac{k_y k_{xi} - k_x k_{yi}}{k_\rho k_{\rho i}} \right)^2 \\
& \times \exp[-2 \operatorname{Re}\{M'_{vi}(\bar{k}_\perp, \bar{k}'_\perp)\}] \frac{1}{4\pi^2} \int d\bar{r}'_\perp e^{-i(\bar{k}_\perp - \bar{k}'_\perp) \cdot \bar{r}'_\perp} \left\{ \exp[(k_z + k_{zi})^2 C(\bar{r}'_\perp)] - 1 \right\} \quad (42)
\end{aligned}$$

where

$$M'_{vi}(\bar{k}_\perp, \bar{k}'_\perp) = \frac{1}{2}(k_z^2 - k_{zi}^2)\sigma^2 + \frac{(k_z + k_{zi})}{2k_{zi}} M''_{vi}(\bar{k}_\perp, \bar{k}'_\perp) \quad (43a)$$

$$M''_{vi}(\bar{k}_\perp, \bar{k}'_\perp) = \frac{1}{2}(k_z^2 - k_{zi}^2)\sigma^2 + \frac{(k_z + k_{zi})}{2k_{zi}} M'_{vi}(\bar{k}_\perp, \bar{k}'_\perp) \quad (43b)$$

$$M'_{vi}(\bar{k}_\perp, \bar{k}_{\perp i}) = \frac{1}{2}(k_z^2 - k_{zi}^2)\sigma^2 - \frac{1}{2}(k_z + k_{zi})\frac{k_{\rho i}^2}{k_{1zi}}\sigma^2 + \frac{(k_z + k_{zi})}{2k_{zi}}M''_{vi}(\bar{k}_\perp, \bar{k}_{\perp i}) \quad (43c)$$

with

$$M''_{vi}(\bar{k}_\perp, \bar{k}_{\perp i}) = -2\frac{k_{zi}}{k_{\rho i}} \int d\bar{k}'_\perp k'_\rho \left\{ \frac{k_1^2 - k^2}{k_1^2 k'_z + k^2 k'_{1z}} k'_\rho k_{\rho i} - \frac{k^2 k_{1zi}}{k_{\rho i}^2 + k'_z k'_{1z}} \left(\frac{k'_x k_{xi} + k'_y k_{yi}}{k'_\rho k_{\rho i}} \right) \right\} \mathcal{W}(|\bar{k}'_\perp - \bar{k}_{\perp i}|) \quad (44a)$$

$$M''_{vi}(\bar{k}_\perp, \bar{k}_{\perp i}) = 2k_{zi} \int d\bar{k}'_\perp \left\{ \frac{k_1^2}{k_{1zi}} - \frac{(k_1^2 - k^2)}{k'_z + k'_{1z}} - \frac{k_1^2}{k_{1zi}} \frac{k'_\rho k_{\rho i}}{k_{\rho i}^2 + k'_z k'_{1z}} \left(\frac{k'_x k_{xi} + k'_y k_{yi}}{k'_\rho k_{\rho i}} \right) + \frac{(k_1^2 - k^2)}{k_1^2 k'_z + k^2 k'_{1z}} k_{\rho i}^2 \left(\frac{k'_x k_{xi} + k'_y k_{yi}}{k'_\rho k_{\rho i}} \right)^2 \right\} \mathcal{W}(|\bar{k}'_\perp - \bar{k}_{\perp i}|) \quad (44b)$$

The coherent reflected field for vertical polarization is given by

$$\begin{aligned} \langle \mathbf{E}_{v,s} \rangle &= e^{i\bar{k}_\perp \cdot \bar{r}_\perp} e^{ik_{zi}z} \frac{1}{2k_{zi}} (1 + R_{v,v}) \frac{k_1^2 - k^2}{k_1^2 k_{zi} + k^2 k_{1zi}} \\ &\times \left\{ -k_{\rho i}^2 \exp[-M''_{vi}(\bar{k}_\perp, \bar{k}_{\perp i})] + \frac{k^2}{k_1^2} k_{1zi}^2 \exp[-M''_{vi}(\bar{k}_\perp, \bar{k}_{\perp i})] \right\} \quad (45) \end{aligned}$$

For Gaussian correlation function, we have

$$M''_{vi}(\bar{k}_\perp, \bar{k}_{\perp i}) = k_{zi} \sigma^2 l^2 \int_0^\infty k'_\rho dk'_\rho e^{-y} \left\{ -\frac{k_1^2 - k^2}{k_1^2 k'_z + k^2 k'_{1z}} k_{\rho i}^2 I_{\rho\rho}(x) + \frac{k^2 k_{1zi}}{k_{\rho i}^2 + k'_z k'_{1z}} \frac{k'_\rho}{k_{\rho i}} I_1(x) \right\} \quad (46a)$$

$$\begin{aligned} M''_{vi}(\bar{k}_\perp, \bar{k}_{\perp i}) &= 2k_{zi} \int_0^\infty k'_\rho dk'_\rho e^{-y} \left\{ \left(\frac{k_1^2}{k_{1zi}} - \frac{(k_1^2 - k^2)}{k'_z + k'_{1z}} \right) I_{\rho\rho}(x) - \frac{k_1^2}{k_{1zi}} \frac{k'_\rho k_{\rho i}}{k_{\rho i}^2 + k'_z k'_{1z}} I_1(x) \right. \\ &\quad \left. + \frac{(k_1^2 - k^2)}{k_1^2 k'_z + k^2 k'_{1z}} k_{\rho i}^2 \left(I_{\rho\rho}(x) - \frac{I_1(x)}{x} \right) \right\} \quad (46b) \end{aligned}$$

4.5 Emissivities

By using energy conservation and reciprocity arguments, the emissivity can be expressed in the following form [Peake, 1959]:

$$\epsilon_{\mu}(\theta_i) = 1 - r_{\mu}^c(\theta_i) - r_{\mu}^i(\theta_i) \quad \beta = v, h \quad (47)$$

where r_{μ}^c is the coherent reflectivity and r_{μ}^i is the incoherent reflectivity. The reflectivities are given by

$$r_{\mu}^c(\theta_i) = |R_{\mu}|^2 \quad (48)$$

$$r_{\mu}^i(\theta_i) = \frac{1}{4\pi} \sum_{\alpha=v,h} \int_0^{2\pi} d\phi \int_0^{\pi/2} d\theta \sin \theta \gamma_{\alpha\mu}(\theta, \phi; \theta_i, \phi_i) \quad (49)$$

where R_{μ} is the coherent reflection coefficient.

The coherent reflection coefficients of the rough surface derived with the modified SPM is given by

$$R_h = R_{h0} \exp[M_{hi}(\bar{k}_{\perp i}, \bar{k}_{\perp i})] \quad (50a)$$

$$R_v = \frac{1}{2k_{zi}} (1 + R_{v0}) \frac{k_1^2 - k^2}{k_1^2 k_{zi} + k^2 k_{1zi}} \left\{ -k_{\mu}^2 \exp[-M'_{vi}(\bar{k}_{\perp i}, \bar{k}_{\perp i})] + \frac{k^2}{k_1^2} k_{1zi}^2 \exp[-M''_{vi}(\bar{k}_{\perp i}, \bar{k}_{\perp i})] \right\} \quad (50b)$$

The emissivities can be obtained by making use of the expressions for the bistatic scattering coefficients derived in the previous section. For the correlation function with Gaussian dependence we obtain, after carrying out the $d\phi$ -integration,

$$\begin{aligned} r_h^i(\theta_i) &= \frac{1}{\cos \theta_i} \int_0^{\pi/2} d\theta \sin \theta k_z^2 k_{zi}^2 l^2 \frac{2}{(k_z + k_{zi})^2} \left| \frac{k_1^2 - k^2}{(k_z + k_{1z})(k_{zi} + k_{1zi})} \right|^2 \\ &\quad \times \exp[-2 \operatorname{Re}\{M_{hi}(\bar{k}_{\perp}, \bar{k}_{\perp i})\}] \sum_{m=1}^{\infty} \frac{[(k_z + k_{zi})\sigma]^{2m}}{m! m} e^{-y_m} \left[I_0(x_m) - \frac{I_1(x_m)}{x_m} \right] \\ &+ \frac{1}{\cos \theta_i} \int_0^{\pi/2} d\theta \sin \theta k_z^2 k_{zi}^2 l^2 \frac{2}{(k_z + k_{zi})^2} \left| \frac{k k_{iz}(k_1^2 - k^2)}{(k_1^2 k_z + k^2 k_{1z})(k_{zi} + k_{1zi})} \right|^2 \\ &\quad \times \exp[-2 \operatorname{Re}\{M'_{hi}(\bar{k}_{\perp}, \bar{k}_{\perp i})\}] \sum_{m=1}^{\infty} \frac{[(k_z + k_{zi})\sigma]^{2m}}{m! m} e^{-y_m} \frac{I_1(x_m)}{x_m} \end{aligned} \quad (51a)$$

$$\begin{aligned}
r_r^i(\theta_i) = & \frac{1}{\cos \theta_i} \int_0^{\pi/2} d\theta \sin \theta k_z^2 k_{zi}^2 l^2 \frac{2}{(k_z + k_{zi})^2} \left| \frac{k_1^2 - k^2}{(k_1^2 k_z + k^2 k_{1z})(k_1^2 k_{zi} + k^2 k_{1zi})} \right|^2 \\
& \times \sum_{m=1}^{\infty} \frac{[(k_z + k_{zi})\sigma]^{2m}}{m! m} e^{-y_m} \left\{ |k_r k_{r'} k_1^2|^2 \exp[-2 \operatorname{Re}\{M_{r'i}''(\bar{k}_\perp, \bar{k}_{\perp i})\}] I_0(x_m) \right. \\
& \quad + |k^2 k_{1z} k_{1zi}|^2 \exp[-2 \operatorname{Re}\{M_{r'i}''(\bar{k}_\perp, \bar{k}_{\perp i})\}] \left[I_0(x_m) - \frac{I_1(x_m)}{x_m} \right] \\
& \quad \left. - 2 \operatorname{Re} \left\{ k_1^2 k_r k_{r'} k^2 k_{1z} k_{1zi} \exp[-M_{r'i}''(\bar{k}_\perp, \bar{k}_{\perp i})] \exp[-M_{r'i}''(\bar{k}_\perp, \bar{k}_{\perp i})] \right\} I_1(x_m) \right\} \\
& + \frac{1}{\cos \theta_i} \int_0^{\pi/2} d\theta \sin \theta k_z^2 k_{zi}^2 l^2 \frac{2}{(k_z + k_{zi})^2} \left| \frac{k k_{1zi} (k_1^2 - k^2)}{(k_z + k_{1z})(k_1^2 k_{zi} + k^2 k_{1zi})} \right|^2 \\
& \times \exp[-2 \operatorname{Re}\{M_{r'i}'(\bar{k}_\perp, \bar{k}_{\perp i})\}] \sum_{m=1}^{\infty} \frac{[(k_z + k_{zi})\sigma]^{2m}}{m! m} e^{-y_m} \frac{I_1(x_m)}{x_m} \tag{51b}
\end{aligned}$$

where

$$y_m = (k_r^2 + k_{r'}^2) \frac{l^2}{4m} \quad x_m = k_r k_{r'} \frac{l^2}{2m} \tag{52}$$

The emissivities calculated using the modified SPM is illustrated and compared with the result obtained using the KA [Chap. 2, Eqs. (141) and (145)] for the various cases. In Fig. 4.1 we illustrate the effect of standard deviation of the surface height σ . As σ is increased there is an increase in the emissivities except at large observation angles for vertical polarization. Also, the difference between vertical and horizontal polarizations becomes smaller. In Fig. 4.2 the KA result for the same set of parameters are illustrated. The KA result is not valid for large angles of observation. For angles near nadir there is increase in the emissivities which is larger than the modified SPM results. In Figs. 4.3 and 4.4 the effect of increasing the correlation length l is illustrated. There is a decrease in the emissivities near nadir as l is increased. We note that as $l \rightarrow \infty$ the emissivity of the rough surface approaches that of the flat surface since the sum of coherent and incoherent reflected intensities is equal to the reflected intensity of the flat surface. In Figs. 4.5 and 4.6 we increase σ and l by the same ratio, which

is equivalent to increasing the frequency for the same parameters. We note that while there is a slight increase in the emissivity near nadir angles for KA, there is a decrease for MSPM. We note that the coherent reflectivities obtained using the KA does not depend on the correlation length l while the modified SPM results is a function of both σ and l .

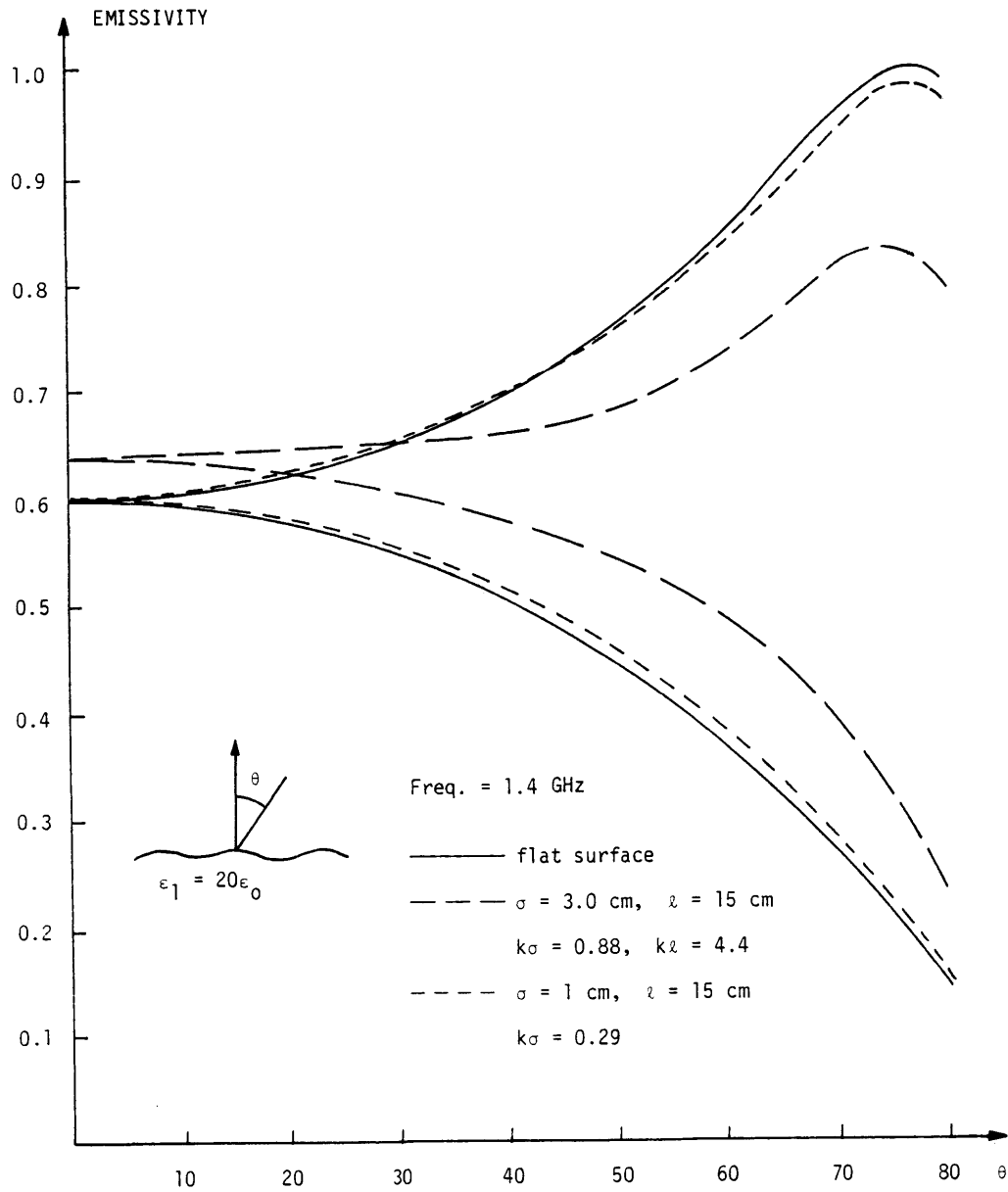


Figure 4.1 Emissivities as a function of observation angle – Modified Small Perturbation Method.

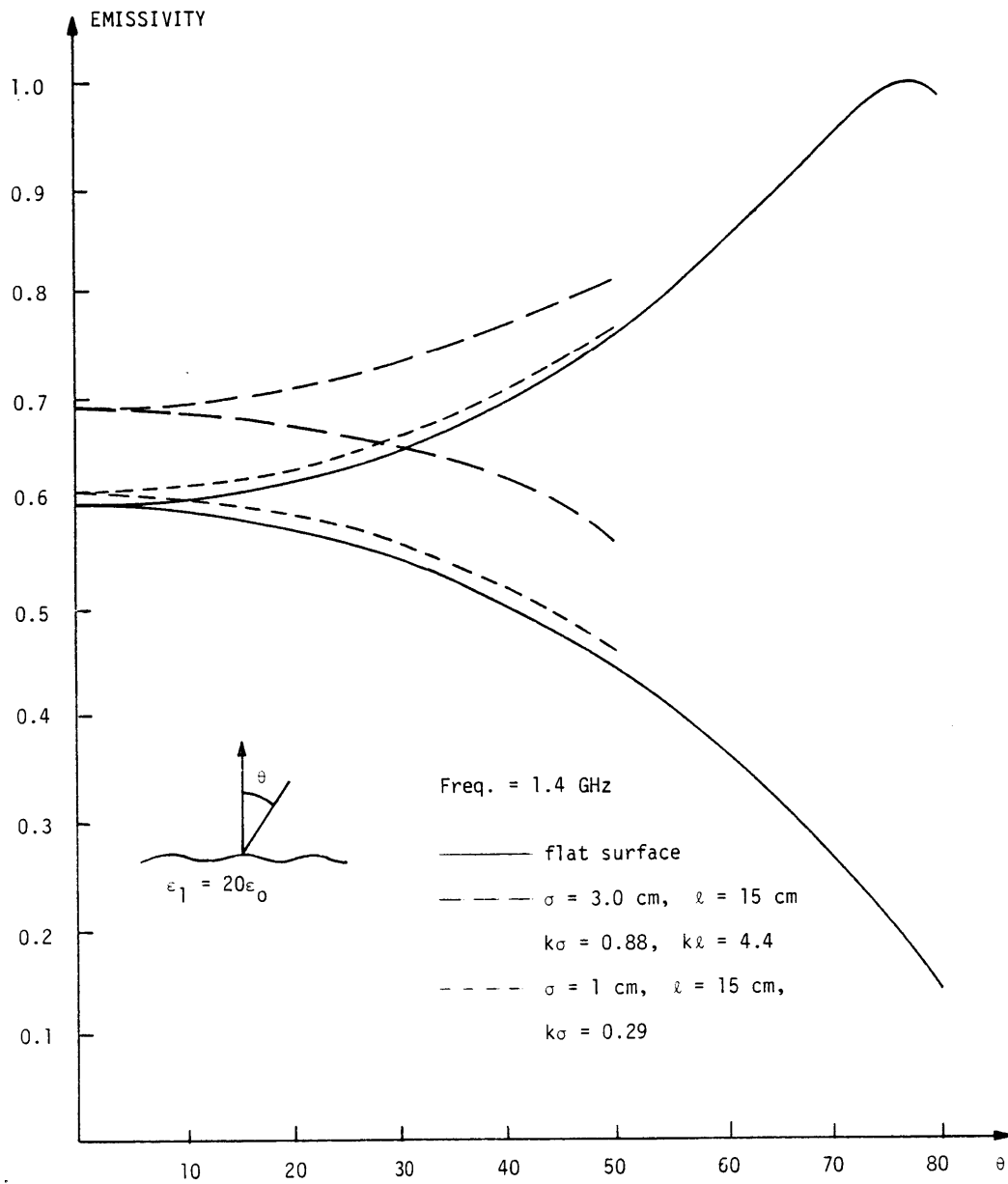


Figure 4.2 Emissivities as a function of observation angle – Kirchhoff Approximation.

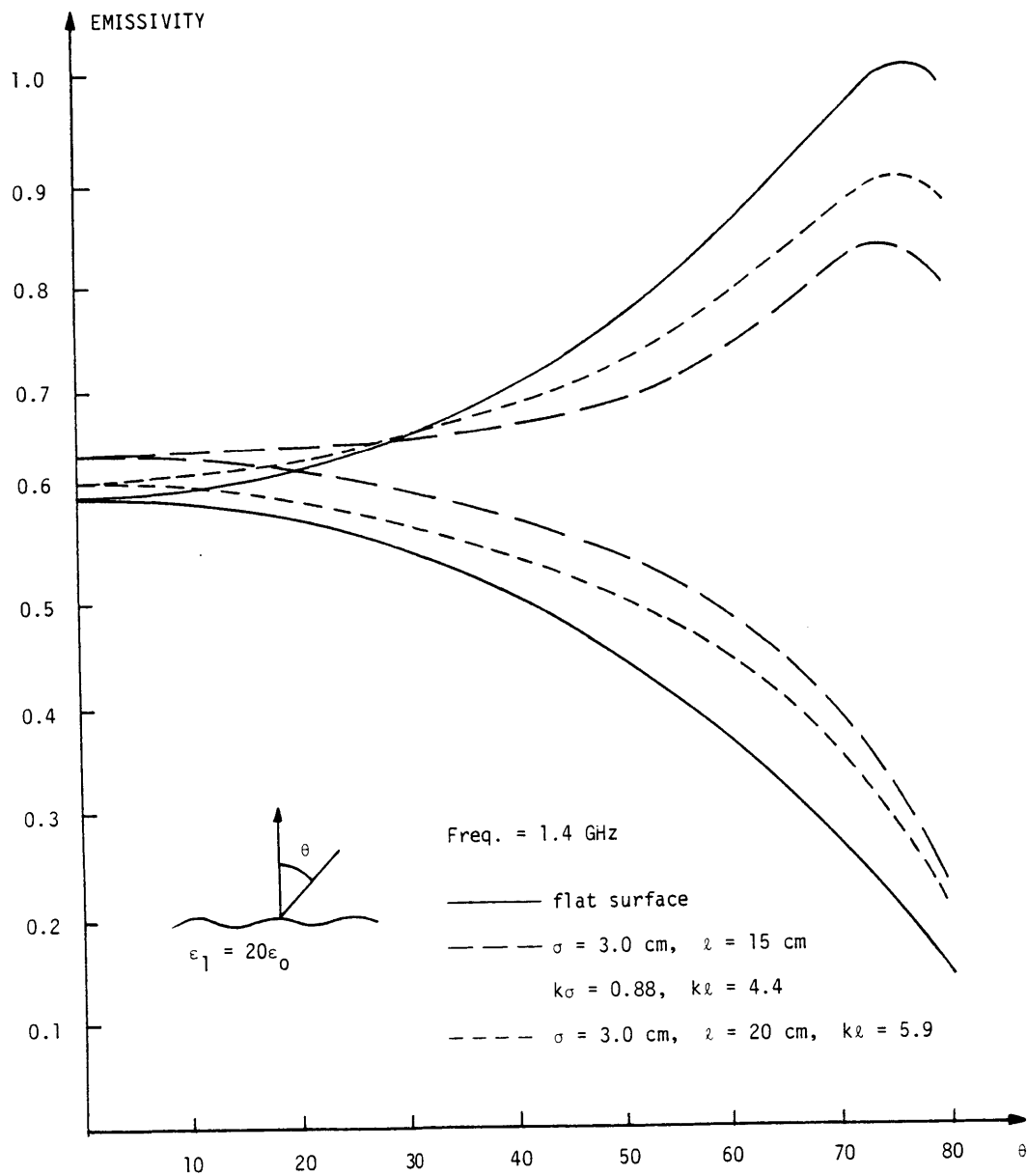


Figure 4.3 Emissivities as a function of observation angle – Modified Small Perturbation Method.

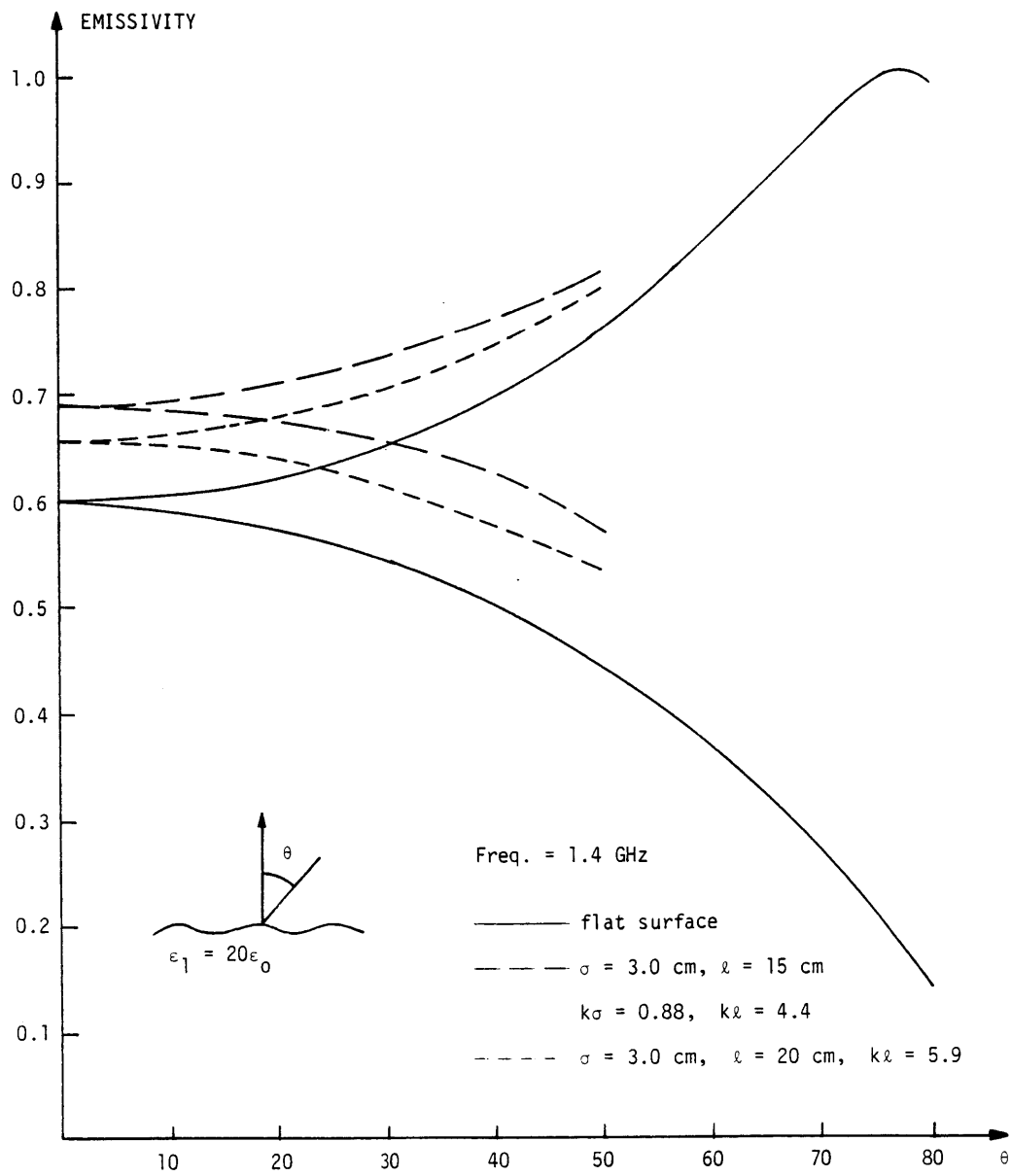


Figure 4.4 Emissivities as a function of observation angle – Kirchhoff Approximation.

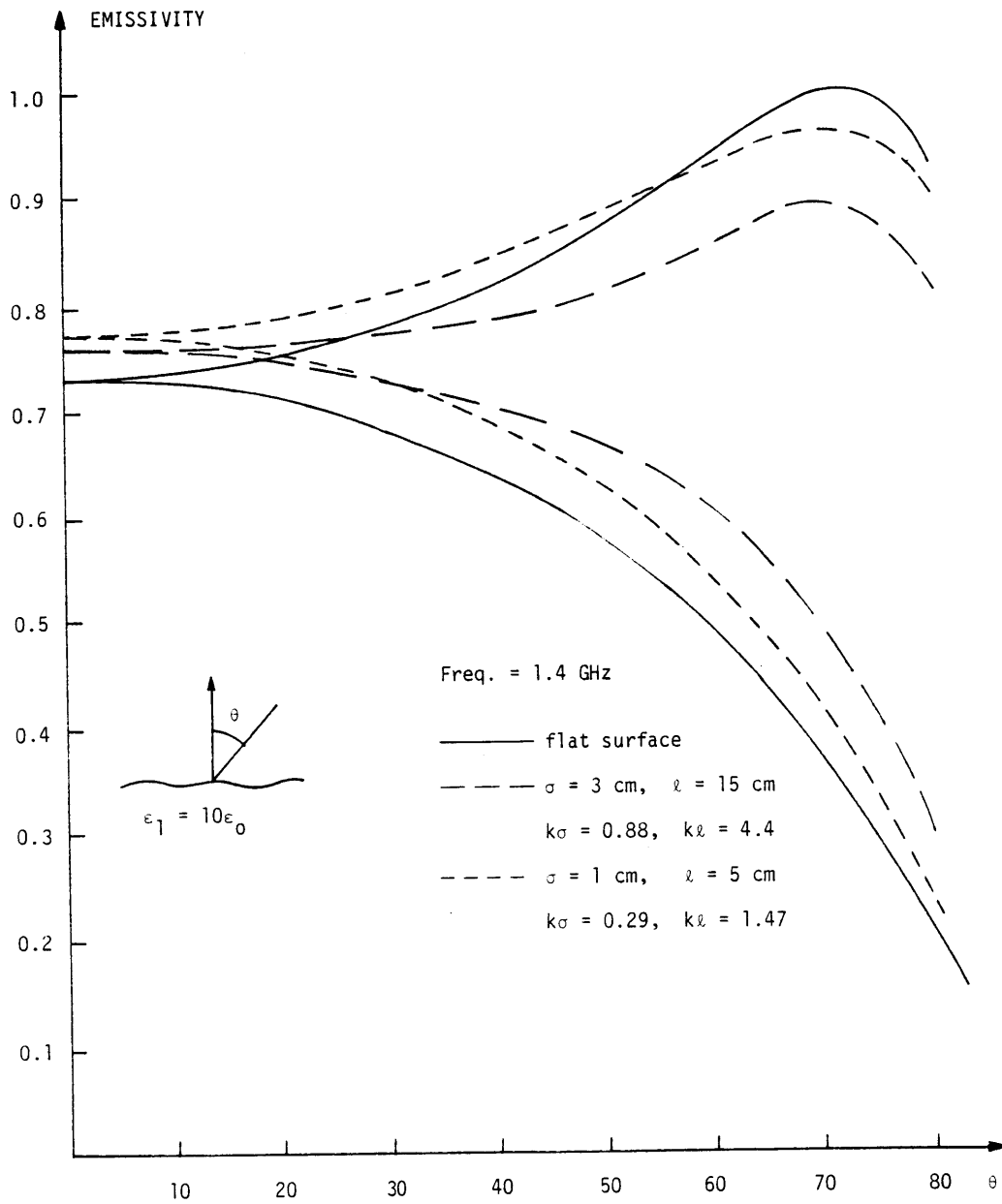


Figure 4.5 Emissivities as a function of observation angle – Modified Small Perturbation Method.

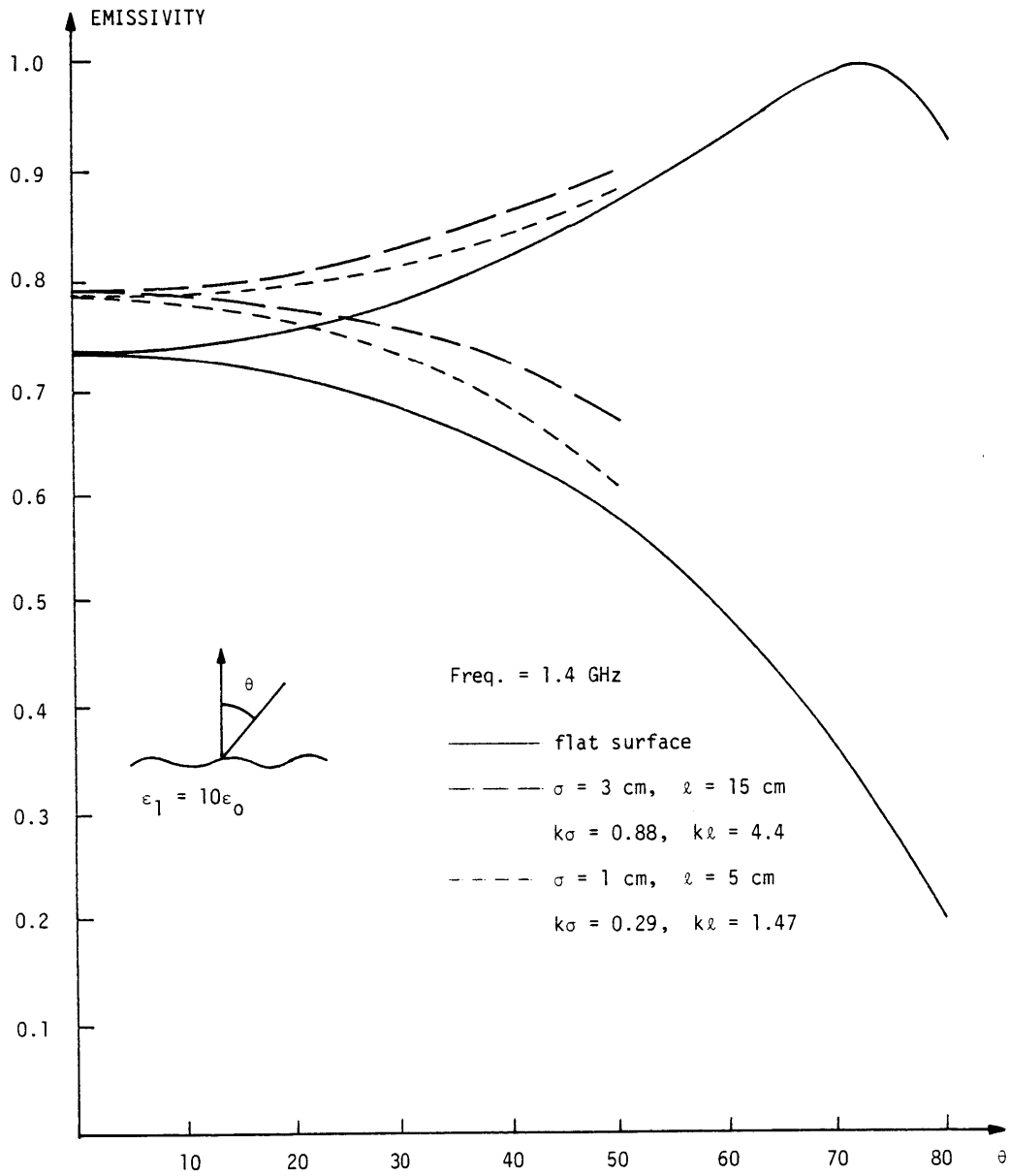


Figure 4.6 Emissivities as a function of observation angle – Kirchhoff Approximation.

CHAPTER 5

Scattering of Electromagnetic Waves from a Randomly Perturbed Quasiperiodic Surface

Scattering of electromagnetic waves from a randomly perturbed quasiperiodic surface is studied for active remote sensing of plowed fields. Kirchhoff approximation is used. Narrow-band Gaussian random variation around the spatial frequency of the sinusoidal variation is used to introduce the quasiperiodicity. The physical optics integral is evaluated to obtain closed-form solutions for coherent and incoherent bistatic scattering coefficients. In the geometrical optics limit, it is shown that the bistatic scattering coefficients are proportional to the probability of the occurrence of the slopes which will specularly reflect the incident wave into the observation direction. The theoretical results are illustrated for the various cases by plotting backscattering cross sections as a function of the angle of incidence. It is shown that there is a large difference between cases where the incident wave vector is parallel or perpendicular to the row direction. When the incident wave vector is perpendicular to the row direction, the maximum value of the backscattering cross section does not necessarily occur at normal incidence. The scattering coefficients can be interpreted as a convolution of the scattering patterns for the sinusoidal and the random rough surfaces. For the backscattering cross sections we observe occurrence of peaks whose relative magnitudes and locations are explained in terms of the scattering patterns for sinusoidal surfaces.

5.1 Introduction

Scattering of electromagnetic waves from a randomly perturbed sinusoidal surface is of interest in the active remote sensing of plowed fields. The variations of the radar scattering coefficients due to the change in the look direction relative to the row direction have been well documented [Batlivala and Ulaby, 1976; Ulaby and Bare, 1979; Fenner *et al.*, 1980]. In the past, the problem of electromagnetic wave scattering from periodic [Waterman, 1975; Jordan and Lang, 1979; Chuang and Kong, 1982] or random [Rice, 1951; Beckmann and Spizzichino, 1963; Stogryn, 1967; Valenzuela, 1967; Sancer, 1969; Leader, 1971; Tsang and Kong, 1980a] rough surfaces has been extensively studied. The problem of scattering by randomly perturbed surface has been studied by assuming that the periodic surface causes a tilting effect [Ulaby *et al.*, 1982]. In this approach the scattering coefficients of the random rough surfaces obtained using the Kirchhoff approximation or small perturbation method is averaged over the change in local incidence angle due to the periodic surface. This approach has also been used to solve the scattering from a composite random rough surface with small and large variations [Semenov, 1966; Wu and Fung, 1972].

In this chapter we use the Kirchhoff approximation to study the scattering of electromagnetic waves from a randomly perturbed quasiperiodic surface. In order to more realistically model the plowed fields we characterize the rough surface as a composite surface with a Gaussian random variation, a sinusoidal variation and a narrow-band Gaussian random variation around the same spatial frequency. In the plowed fields there are some random variations on the period and amplitude of the sinusoidal variation as we move from one row to the next. This variation can be modelled by introducing the narrow-band Gaussian random process on top of the basic

sinusoidal variation, which will cause the surface to be quasiperiodic. The physical optics integral obtained with the Kirchhoff approximation is evaluated to obtain the coherent and incoherent bistatic scattering coefficients. In the geometrical optics limit, the stationary phase method is used to further simplify the results. In this limit it can be shown that the bistatic scattering coefficients are proportional to the probability of the occurrence of the slopes which will specularly reflect the incident wave into the observation direction. The theoretical results are illustrated for the various cases by plotting the backscattering cross sections as a function of the angle of incidence with the incident wave vector either parallel or perpendicular to the row direction. The appearances of peaks will be explained in terms of the scattering patterns for sinusoidal surfaces.

5.2 Formulation

Consider a plane wave incident on a randomly perturbed quasiperiodic surface [Fig. 5.1]. The electric field of the incident wave is given by

$$\bar{E}_i(\bar{r}) = \hat{e}_i E_0 \exp(i\bar{k}_i \cdot \bar{r}) \quad (1)$$

where \bar{k}_i denotes the incident wave vector and \hat{e}_i the polarization of the incident electric field vector. The rough surface is characterized by a height distribution $Z = f(x, y)$, which is given by

$$f(x, y) = \xi(x, y) + A(x) \cos\left(\frac{2\pi}{P}x + \psi(x)\right) + B \cos\left(\frac{2\pi}{P}x + \phi\right) \quad (2)$$

where $\xi(x, y)$ is a Gaussian random variable with zero mean

$$\langle \xi(x, y) \rangle = 0 \quad (3)$$

$A(x) \cos[(2\pi/P)x + \psi(x)]$ is described by a narrow-band Gaussian random process [Dav-
enport and Root, 1958; Appendix A] centered around the spatial frequency of $2\pi/P$
where the variations of the envelope $A(x)$ and the phase $\psi(x)$ are slow compared to
those of $\cos(2\pi/P)x$, and B and ϕ are assumed to be constants. Using the vector Kirch-
hoff approach, the scattered electric field $\bar{E}_s(\bar{r})$ can be expressed in the following form
[Stogryn, 1967; Sancer, 1969; Leader, 1971; Tsang and Kong, 1980a]:

$$\bar{E}_s(\bar{r}) = \frac{ik \exp(ikr)}{4\pi r} E_0 (\bar{I} - \hat{k}_s \hat{k}_i) \int_{A_s} \bar{F}(\alpha, \beta) \exp(i\bar{k}_s \cdot \bar{r}') d\bar{r}'_{\perp} \quad (4)$$

where A_r is the area of the rough surface projected onto the $x - y$ plane, \hat{k}_r is the unit vector in the observation direction, and

$$\bar{k}_d = \bar{k}_i - \bar{k}_r \quad (5)$$

$$\begin{aligned} \bar{F}(\alpha, \beta) = (1 + \alpha^2 + \beta^2)^{1/2} \left\{ -(1 - R_h)(\hat{n} \cdot \hat{k}_i)(\hat{\epsilon}_i \cdot \hat{q}_i)\hat{q}_i + (\hat{\epsilon}_i \cdot \hat{p}_i)(\hat{n} \times \hat{q}_i)(1 + R_v) \right. \\ \left. + (\hat{\epsilon}_i \cdot \hat{q}_i)[\hat{k}_r \times (\hat{n} \times \hat{q}_i)](1 + R_h) + (\hat{\epsilon}_i \cdot \hat{p}_i)(\hat{n}_i \cdot \hat{k}_i)(\hat{k}_r \times \hat{q}_i)(1 - R_v) \right\} \end{aligned} \quad (6)$$

In (6), α and β are the local slopes in the x and y directions,

$$\alpha = \frac{\partial f(x', y')}{\partial x'} \quad (7a)$$

$$\beta = \frac{\partial f(x', y')}{\partial y'} \quad (7b)$$

\hat{n} is the local normal to the rough surface,

$$\hat{n} = \frac{-\hat{x}\alpha - \hat{y}\beta + \hat{z}}{(1 + \alpha^2 + \beta^2)^{1/2}} \quad (8)$$

\hat{p}_i and \hat{q}_i are respectively, the unit vectors in the directions of the local parallel and perpendicular polarizations of the incident wave,

$$\hat{q}_i = \frac{\hat{k}_i \times \hat{n}}{|\hat{k}_i \times \hat{n}|} \quad (9a)$$

$$\hat{p}_i = \hat{q}_i \times \hat{k}_i \quad (9b)$$

R_v and R_h are the Fresnel reflection coefficients for TM and TE waves with local incidence angle:

$$R_h = \frac{-(\hat{n} \cdot \hat{k}_i) - [n_1^2 - 1 + (\hat{n} \cdot \hat{k}_i)^2]^{1/2}}{-(\hat{n} \cdot \hat{k}_i) + [n_1^2 - 1 + (\hat{n} \cdot \hat{k}_i)^2]^{1/2}} \quad (10a)$$

$$R_v = \frac{-n_1^2(\hat{n} \cdot \hat{k}_i) - [n_1^2 - 1 + (\hat{n} \cdot \hat{k}_i)^2]^{1/2}}{-n_1^2(\hat{n} \cdot \hat{k}_i) + [n_1^2 - 1 + (\hat{n} \cdot \hat{k}_i)^2]^{1/2}} \quad (10b)$$

with

$$n_1 = k_1/k$$

$$k_1 = \omega\sqrt{\mu_1\epsilon_1}$$

$$k = \omega\sqrt{\mu_0\epsilon_0}$$

and the orthonormal system for the incident and scattered fields are given by

$$\hat{k}_i = \hat{x} \sin \theta_i \cos \phi_i + \hat{y} \sin \theta_i \sin \phi_i - \hat{z} \cos \theta_i, \quad (12a)$$

$$\hat{h}_i = -\hat{x} \sin \phi_i + \hat{y} \cos \phi_i, \quad (12b)$$

$$\hat{v}_i = -\hat{x} \cos \theta_i \cos \phi_i - \hat{y} \cos \theta_i \sin \phi_i - \hat{z} \sin \theta_i, \quad (12c)$$

$$\hat{k}_s = \hat{x} \sin \theta_s \cos \phi_s + \hat{y} \sin \theta_s \sin \phi_s + \hat{z} \cos \theta_s, \quad (13a)$$

$$\hat{h}_s = -\hat{x} \sin \phi_s + \hat{y} \cos \phi_s, \quad (13b)$$

$$\hat{v}_s = \hat{x} \cos \theta_s \cos \phi_s + \hat{y} \cos \theta_s \sin \phi_s - \hat{z} \sin \theta_s. \quad (13c)$$

The Kirchhoff approximated diffraction integral in its present form is still difficult to evaluate and further approximation is necessary. One commonly used approximation is to expand $\bar{F}(\alpha, \beta)$ in the power series of slope terms about the zero slope and to keep only the first few terms [Leader, 1971; Tsang and Newton, 1982]. However, in this chapter we shall expand $\bar{F}(\alpha, \beta)$ about the slopes at the stationary phase point $\alpha_{s,}$ and $\beta_{s,}$

$$\alpha_{s,} = -\frac{k_{t,r}}{k_{t,z}} \quad (14a)$$

$$\beta_{..} = -\frac{k_{.ly}}{k_{.lz}} \quad (14b)$$

where

$$k_{.lx} = k(\sin \theta_i \cos \phi_i - \sin \theta_s \cos \phi_s) \quad (15a)$$

$$k_{.ly} = k(\sin \theta_i \sin \phi_i - \sin \theta_s \sin \phi_s) \quad (15b)$$

$$k_{.lz} = -k(\cos \theta_i + \cos \theta_s) \quad (15c)$$

Therefore, we expand $\bar{F}(\alpha, \beta)$ as follows:

$$\bar{F}(\alpha, \beta) = \bar{F}(\alpha_{..}, \beta_{..}) + \frac{\partial \bar{F}}{\partial \alpha} \Big|_{\alpha_{..}, \beta_{..}} (\alpha - \alpha_{..}) + \frac{\partial \bar{F}}{\partial \beta} \Big|_{\alpha_{..}, \beta_{..}} (\beta - \beta_{..}) + \dots \quad (16)$$

Keeping only the first term in the above equation, we obtain from (4),

$$\bar{E}_s(\bar{r}) = \frac{ik \exp(ikr)}{4\pi r} E_{..}(\bar{I} - \hat{k}_s \hat{k}_s) \bar{F}(\alpha_{..}, \beta_{..}) I \quad (17)$$

where the integral I is given by

$$I = \int_A \exp(i\bar{k}_{.l} \cdot \bar{r}') d\bar{r}' \quad (18)$$

Then the scattered fields $\bar{E}_s(\bar{r})$ is separated into a mean field $\bar{E}_m(\bar{r})$ and a fluctuating part of the field $\bar{\mathcal{E}}(\bar{r})$

$$\bar{E}_s(\bar{r}) = \bar{E}_m(\bar{r}) + \bar{\mathcal{E}}(\bar{r}) \quad (19)$$

with

$$\langle \bar{\mathcal{E}}(\bar{r}) \rangle = 0 \quad (20)$$

and

$$\langle \bar{E}_s(\bar{r}) \rangle = \bar{E}_m(\bar{r}) \quad (21)$$

so that the total scattered intensity is a sum of coherent and incoherent scattered intensities.

$$\langle |\bar{E}_s|^2 \rangle = |\bar{E}_m(\bar{r})|^2 + \langle |\bar{\mathcal{E}}(\bar{r})|^2 \rangle \quad (22)$$

From (17) and (18), we have

$$\langle |\bar{E}_m(\bar{r})|^2 \rangle = \frac{k^2 |E_0|^2}{16\pi^2 r^2} \left[|\hat{v}_s \cdot \bar{F}(\alpha_s, \beta_s)|^2 + |\hat{h}_s \cdot \bar{F}(\alpha_s, \beta_s)|^2 \right] \langle |I|^2 \rangle \quad (23)$$

and

$$\langle |\bar{\mathcal{E}}(\bar{r})|^2 \rangle = \frac{k^2 |E_0|^2}{16\pi^2 r^2} \left[|\hat{v}_s \cdot \bar{F}(\alpha_s, \beta_s)|^2 + |\hat{h}_s \cdot \bar{F}(\alpha_s, \beta_s)|^2 \right] D_I \quad (24)$$

where

$$D_I = \langle |I|^2 \rangle - \langle |I| \rangle^2 \quad (25)$$

The explicit expressions for $\langle |I|^2 \rangle$ and D_I for the randomly perturbed quasiperiodic surface are derived and expressed in terms of the statistical moments of the height distribution [Appendix B]. The advantage of expanding $\bar{F}(\alpha, \beta)$ around the stationary phase point (α_s, β_s) is that the bistatic scattering coefficients derived from (24) and (25) satisfy the principle of reciprocity and at high frequency limit the geometrical optics solutions can be obtained from (25) without making any modifications [Stogryn, 1967]. Also, since $\bar{F}(\alpha, \beta)$ is evaluated at the stationary phase point the same solution is obtained using total or reflected field on the surface [Holzer and Sung, 1978].

5.3 Coherent and Incoherent Scattering Coefficients

The bistatic scattering coefficients are defined as [Peake, 1959]

$$\gamma_{ab}(\hat{k}_s, \hat{k}_i) = \frac{4\pi r^2 I_{sa}}{A_{ii} \cos \theta_i I_{ib}} \quad (a, b = v, h) \quad (26)$$

where I_{sa} and I_{ib} are, respectively, the intensity of the scattered wave in polarization a and the intensity of the incident wave in polarization b . From (23) and (24) we first calculate the vertically and horizontally polarized coherent and incoherent scattered intensities for the cases of vertically and horizontally polarized incident fields. For an incident field with polarization b_i , the scattered intensities with polarization a_s is given by [Stogryn, 1967]

$$|E_m(\bar{r})|^2 = \frac{k^2 |E_{oi}|^2}{16\pi^2 r^2} |\hat{a}_s \cdot \bar{F}_b(\alpha_{oi}, \beta_{oi})|^2 |I|^2 \quad (27)$$

$$|\mathcal{E}(\bar{r})|^2 = \frac{k^2 |E_{oi}|^2}{16\pi^2 r^2} |\hat{a}_s \cdot \bar{F}_b(\alpha_{oi}, \beta_{oi})|^2 D_I \quad (28)$$

where

$$\bar{F}_b(\alpha_{oi}, \beta_{oi}) = \bar{F}(\alpha_{oi}, \beta_{oi}) \Big|_{i_s = b_i} \quad (29)$$

and

$$|\hat{a}_s \cdot \bar{F}_b(\alpha_{oi}, \beta_{oi})|^2 = \frac{|\bar{k}_{id}|^4}{k^2 |\hat{k}_i \times \hat{k}_s|^4 k_{dz}^2} f_{lm} \quad (30)$$

with

$$f_{vv} = \left| (\hat{h}_s \cdot \hat{k}_i)(\hat{h}_i \cdot \hat{k}_s)R_h + (\hat{v}_s \cdot \hat{k}_i)(\hat{v}_i \cdot \hat{k}_s)R_v \right|^2 \quad (31a)$$

$$f_{vh} = \left| (\hat{h}_s \cdot \hat{k}_i)(\hat{v}_i \cdot \hat{k}_s)R_h - (\hat{v}_s \cdot \hat{k}_i)(\hat{h}_i \cdot \hat{k}_s)R_v \right|^2 \quad (31b)$$

$$f_{hv} = \left| (\hat{v}_s \cdot \hat{k}_i)(\hat{h}_i \cdot \hat{k}_s)R_h - (\hat{h}_s \cdot \hat{k}_i)(\hat{v}_i \cdot \hat{k}_s)R_v \right|^2 \quad (31c)$$

$$f_{hh} = \left| (\hat{v}_s \cdot \hat{k}_i)(\hat{v}_i \cdot \hat{k}_s)R_h + (\hat{h}_s \cdot \hat{k}_i)(\hat{h}_i \cdot \hat{k}_s)R_v \right|^2 \quad (31d)$$

and R_v and R_h , which are given by (10), are evaluated at

$$\hat{n} = \frac{\hat{x}k_{dx}/k_{dz} - \hat{y}k_{dy}/k_{dz} + \hat{z}}{(k_{dx}^2/k_{dz}^2 + k_{dy}^2/k_{dz}^2 + 1)^{1/2}} \quad (32)$$

In view of (27) and (28), the bistatic scattering coefficients can be decomposed into a coherent part γ_{ab}^c and an incoherent part γ_{ab}^i . Substituting in the expressions for $|\langle I \rangle|^2$ and D_I , (B10) and (B18), into (27) and (28), we have

$$\gamma_{ab}(\hat{k}_s, \hat{k}_i) = \gamma_{ab}^c(\hat{k}_s, \hat{k}_i) + \gamma_{ab}^i(\hat{k}_s, \hat{k}_i) \quad (33)$$

where

$$\gamma_{ab}^c(\hat{k}_s, \hat{k}_i) = \frac{\pi |\bar{k}_d|^4}{\cos \theta_i \left| \hat{k}_i \times \hat{k}_s \right|^4 k_{dz}^2} f_{lav} \exp[-k_{dz}^2(\sigma^2 + \sigma_x^2)] \sum_{n=-\infty}^{\infty} |J_n(k_{dz}B)|^2 \delta \left(k_{dx} + n \frac{2\pi}{P} \right) \delta(k_{dy}) \quad (34)$$

$$\gamma_{ab}^i(\hat{k}_s, \hat{k}_i) = \frac{|\bar{k}_d|^4}{\cos \theta_i k^2 \left| \hat{k}_i \times \hat{k}_s \right|^4 k_{dz}^2} f_{lav} (D_{I_1} + D_{I_2}) \quad (35)$$

In (34), J_n is the n th-order Bessel function and δ is the Dirac delta function. It can easily be shown that the bistatic scattering coefficients satisfy the principle of reciprocity,

$$\cos \theta_i \gamma_{ab}(\hat{k}_s, \hat{k}_i) = \cos \theta_s \gamma_{lav}(\hat{k}_i, \hat{k}_s) \quad (36)$$

When the incident wave vector is not perpendicular to the row direction of the periodic surface ($k_{yi} \neq 0$), the coherent scattering coefficient, (34), gives rise to scattered

intensities along the directions of Floquet modes, forming a cone. This conical diffraction is a characteristic of scattering from a periodic surface [Chuang and Kong, 1982]. A part of incoherent scattering coefficient will also give rise to conical diffraction. The second term on the right-hand side of (35) has $\delta(k_{iy})$ dependence and this will give rise to scattered intensities only in the direction $k_{yx} = k_{yi}$ forming a cone shape. However, unlike the coherent term, which only scatters into a set of discrete directions, this term will scatter intensities in all k_{rx} directions.

In the backscattering direction $\theta_s = \theta_i$ and $\phi_s = \phi_i + \pi$. The backscattering cross sections per unit area are defined to be

$$\sigma_{ab}(\hat{k}_i) = \cos \theta_i \gamma_{ab}(-\hat{k}_i, \hat{k}_i) \quad (37)$$

From (33)-(35), we obtain

$$\sigma_{vv}(\hat{k}_i) = \sigma_{hh}(\hat{k}_i) = \sigma^r(\hat{k}_i) + \sigma_1^i(\hat{k}_i) + \sigma_2^i(\hat{k}_i) \quad (38)$$

$$\sigma_{hv}(\hat{k}_i) = \sigma_{vh}(\hat{k}_i) = 0 \quad (39)$$

where

$$\sigma^r(\hat{k}_i) = \frac{4\pi k^2 |R|^2}{\cos^2 \theta_i} \exp[-4k_{zi}^2(\sigma^2 + \sigma_r^2)] \sum_{n=-\infty}^{\infty} |J_n(2k_{zi}B)|^2 \delta\left(2k_{xi} + n\frac{2\pi}{P}\right) \delta(2k_{yi}) \quad (40)$$

$$\begin{aligned} \sigma_1^i(\hat{k}_i) = & \frac{k^2 |R|^2}{\cos^2 \theta_i} \sum_{\mu=-\infty}^{\infty} |J_\mu(2k_{zi}B)|^2 \exp[-4k_{zi}^2(\sigma^2 + \sigma_r^2)] \sum_{m=1}^{\infty} \frac{(4k_{zi}^2 \sigma^2)^m}{m!} \frac{l^2}{m} \\ & \times \left[\exp\left(-\left[\left(\frac{k_{xi} + \mu\pi}{P}\right)^2 + k_{yi}^2\right] \frac{l^2}{m}\right) + \sum_{m'=1}^{\infty} \sum_{n=0}^{m'} \frac{1}{2^{m'}} \binom{m'}{n} \frac{(4k_{zi}^2 \sigma_r^2)^{m'}}{m'} \frac{1}{q} \right. \\ & \left. \times \exp\left(-\left[\frac{k_{xi} + (\mu + m' - 2n)\pi}{P}\right]^2 \frac{l^2}{mq} - k_{yi}^2 \frac{l^2}{m}\right) \right] \quad (41) \end{aligned}$$

with

$$g = \sqrt{1 + \frac{l_z^2 m'}{l_x^2 m}}$$

$$\begin{aligned} \sigma_2^i(\hat{k}_i) &= \frac{2k^2 |R_i|^2}{\cos^2 \theta_i} \delta(2k_{yi}) \sum_{\mu=-\infty}^{\infty} |J_\mu(2k_{zi} B)|^2 \exp[-4k_{zi}^2 (\sigma^2 + \sigma_r^2)] \\ &\times \sum_{m=1}^{\infty} \sum_{n=0}^m \frac{1}{2^m} \binom{m}{n} \sqrt{\frac{\pi}{m}} l_x \frac{(4k_{zi}^2 \sigma_r^2)^m}{m!} \exp\left(-\left[\frac{k_{xi} + (\mu + m - 2n)\pi}{P}\right]^2 \frac{l_x^2}{m}\right) \end{aligned} \quad (42)$$

and R is the Fresnel reflection coefficient at normal incidence. We note that there is no depolarization in the backscattering direction, and because of the $\delta(2k_{yi})$ dependence, $\sigma^i(\hat{k}_i)$ terms contribute only when the incident wave vector is perpendicular to the row direction of the periodic surface.

5.4 Geometrical Optics Solution

Under the geometrical optics limit as $k \rightarrow \infty$, further simplifications can be made for the expressions of $| \langle I \rangle |^2$ and D_I . Since $k_{dz}\sigma, k_{dz}\sigma_s \gg 1$, the coherent component of the scattered fields are negligible and only the incoherent scattering coefficients will remain. Under the stationary phase approximation the bistatic scattering coefficients simplify to

$$\gamma_{ub}(\hat{k}_s, \hat{k}_i) = \frac{|\bar{k}_d|^4}{\cos \theta_s |\hat{k}_i \times \hat{k}_s|^4 k_{dz}^4} f_{bu} \frac{1}{2\pi} \int_{-2\pi}^{2\pi} d\phi' \frac{1}{2s_x s_y} \exp \left(- \frac{\left(\frac{k_{dy}}{k_{dz}} - 2\pi \frac{P}{F} \sin \phi' \right)^2}{2s_x^2} - \frac{\left(\frac{k_{dx}}{k_{dz}} \right)^2}{2s_y^2} \right) \quad (43)$$

where s_x^2 and s_y^2 are, respectively, the mean square surface slopes in the x and y directions

$$s_x^2 = \sigma^2 |C''(0)| + \sigma_x^2 [(2\pi/P)^2 + |C''_x(0)|] \quad (44a)$$

$$s_y^2 = \sigma^2 |C''(0)| \quad (44b)$$

In the above equations, C'' and C''_x are the second derivatives of the correlation functions and for Gaussian correlation functions assumed

$$|C''(0)| = 2/l^2 \quad (45a)$$

$$|C''_x(0)| = 2/l_x^2 \quad (45b)$$

The probability of finding slopes (α, β) at point \bar{r}_\perp on the surface can be calculated to be

$$P[\alpha(\bar{r}_\perp), \beta(\bar{r}_\perp)] = \frac{1}{2\pi s_x s_y} \exp \left(- \frac{[\alpha + 2\pi \frac{P}{F} \sin(\frac{2\pi}{F} x + \phi)]^2}{2s_x^2} - \frac{\beta^2}{2s_y^2} \right) \quad (46)$$

Averaging the above expression over one period we obtain the averaged PDF for α, β

$$P(\alpha, \beta) = \frac{1}{P} \int_0^P dx \frac{1}{2\pi\epsilon_r\epsilon_u} \exp\left(-\frac{[\alpha - 2\pi\frac{\beta}{P} \sin(\frac{2\pi}{P}x + \phi)]^2}{2\epsilon_r^2} - \frac{\beta^2}{2\epsilon_u^2}\right) \quad (47)$$

which is proportional to the geometrical optics solution. Therefore, the geometrical optics result states that the scattered intensity is proportional to the probability of the occurrence of the slopes which will specularly reflect the incident wave into the direction of the scattered wave [Barrick, 1968]. We also note that in the geometrical optics limit there is no difference between the above solution and the solution obtained using the incoherent model [Ulaby *et al.*, 1982] except for the factors due to quasiperiodicity.

5.5 Results and Discussion

The backscattering cross sections per unit area $\sigma_1^i(\hat{k}_i)$ are calculated and illustrated for various cases. The conically diffracted coherent and incoherent components, $\sigma^c(\hat{k}_i)$ and $\sigma_2^i(\hat{k}_i)$, which only contribute when the incident wave is perpendicular to the row direction of the periodic surface, are not included in the calculations. In order to correctly incorporate the contributions from these components, the characteristics of the antenna used to make the measurements must be taken into account.

The results of randomly perturbed sinusoidal surface cases, $\sigma_r = 0$, are first illustrated in Figs. 5.2-5.9. In Fig. 5.2, the backscattering cross sections per unit area $\sigma(\hat{k}_i)$ are plotted as a function of incidence angle for different frequencies. As the frequency is increased, the solution approaches the geometrical optics result as expected. The difference between the cases where the incident wave vector is parallel, $\phi_i = 90^\circ$, or perpendicular, $\phi_i = 0^\circ$, to the row direction is seen to be large. For the $\phi_i = 0^\circ$ case the maximum value of $\sigma(\hat{k}_i)$ is shown to be not at normal incidence. In Fig. 5.3 the effect of change in the amplitude of sinusoidal variation B is illustrated for 5.0 GHz. As B is decreased the results of $\phi_i = 0^\circ$ and $\phi_i = 90^\circ$ cases approach each other and when $B = 0$ we reproduce the random rough surface result which is independent of azimuthal incident angle ϕ_i .

In Fig. 5.4 the effect of the correlation length l at 1.4 GHz is illustrated. As l is increased, the $\sigma(\hat{k}_i)$ falls off faster as a function of θ_i for $\phi_i = 90^\circ$ and there is an appearance of peaks for $\phi_i = 0^\circ$. The change in $\sigma(\hat{k}_r)$ as ϕ_i is varied is shown in Fig. 5.5. The appearance of the peaks for $\phi_i = 0^\circ$ can be explained as follows.

The result for a randomly perturbed sinusoidal surface is related to the convolution of the results for the sinusoidal surface with those of the random rough surface.

For a sinusoidal surface, we have contribution in the backscattering direction only when it coincides with one of the Floquet modes direction.

$$2k_{x,i} = n \frac{2\pi}{P} \quad (48)$$

As l is increased the scattering pattern from a random rough surface is sharply peaked around the specular direction. Therefore, by making l sufficiently large, we obtain the result which is sharply peaked at the mode directions given by (48). This is illustrated in Fig. 5.6(a). The locations and amplitudes of the Floquet modes are plotted in Fig. 5.6(a). Notice that for the cases of $l = 100$ cm, we see from Fig. 5.6(a) that the peaks are visibly illustrated. When l is smaller the scattering pattern of the random rough surface becomes broader and we do not reproduce all the peaks. However, the peaks around the two dominant modes, $n = 1$ and $n = 4$, are still reproduced for $l = 50$ cm. When l is further decreased none of the peaks are reproduced and we have a fairly flat behavior.

In Fig. 5.7(a), the effect of change in B at 1.4 GHz is illustrated. Note that as B is decreased, there seems to be a shifting of the peaks. Since the period P is not changed, the locations of the modes do not change. However, as we can see from Fig. 5.7(b), the amplitude of each mode is changed as B is changed. The location of the mode with the maximum amplitude is shifted as B is varied and the results in Fig. 5.7(a) reflect this effect. When $B = 0$ only the amplitude of the $n = 0$ mode is nonzero and the random rough surface result is reproduced.

The effect of change in the period P is illustrated in Fig. 5.8. The locations of the modes will change as P changes while the amplitude of each mode will not change since B is the same. As can be seen from Fig. 5.8, when P is increased the modes are spaced closer together and when P is decreased the modes become further apart.

The effect of change in σ is shown in Fig. 5.9(a). Initially, as σ is increased the backscattering cross section $\sigma(\hat{k}_i)$ is increased. Then as σ is further increased there is a decrease near normal incidence and a disappearance of one of the peaks. This is due to the change in the scattering characteristics of the random rough surface in the absence of sinusoidal variation. In Fig. 5.9(b) the backscattering cross section for the random rough surface is plotted. Note that for $\sigma = 5$ cm there is a decrease near normal incidence and a broadening of the scattering pattern which explains the trends in Fig. 5.9(a).

In Fig. 5.10(a) and 5.10(b) we illustrate the results for randomly perturbed quasiperiodic surfaces, $B = 0$ and $\sigma_x \neq 0$. In Fig. 5.10(a) the backscattering cross sections are plotted for different correlation lengths l . Again, as l is increased there is an appearance of peaks. But unlike the sinusoidal case, the values of the peaks are monotonically decreasing with increasing angle of incidence. It is interesting to look at the solution in the limit $l_x \rightarrow \infty$ since we obtain a much simpler analytical solution. From (B14) we obtain, for $B = 0$,

$$\begin{aligned} \langle II' \rangle &= \int_{-2L_x}^{2L_x} dx \int_{-2L_y}^{2L_y} dy e^{i\bar{k}_{d\perp} \cdot \bar{r}_\perp} |2L_x - |x|| |2L_y - |y|| \exp[-k_{dz}^2 \sigma^2 + k_{dz}^2 \sigma^2 C(\bar{r}_\perp)] \\ &\quad \times \exp[-k_{dz}^2 \sigma_x^2 + k_{dz}^2 \sigma_x^2 C_x(x)] \end{aligned} \quad (49)$$

In the limit $l_x \rightarrow \infty$, we obtain

$$\begin{aligned} \langle II' \rangle &= \int_{-2L_x}^{2L_x} dx \int_{-2L_y}^{2L_y} dy \sum_{n=-\infty}^{\infty} \exp[-k_{dz}^2 \sigma_x^2] I_n(k_{dz}^2 \sigma_x^2) \exp \left[i \left(\bar{k}_{d\perp} + \hat{x} n \frac{2\pi}{P} \right) \cdot \bar{r}_\perp \right] \\ &\quad \times |2L_x - |x|| |2L_y - |y|| \exp[-k_{dz}^2 \sigma^2 + k_{dz}^2 \sigma^2 C(\bar{r}_\perp)] \end{aligned} \quad (50)$$

where I_n is the n -th order modified Bessel function. This is similar to the randomly perturbed sinusoidal surface result. In this case the amplitudes of the modes are given

by the modified Bessel functions whereas before they were given in terms of the Bessel functions. The amplitudes of the modes are plotted in Fig. 5.10(b) and we can see that they are monotonically decreasing as n is increased, which explains the results in Fig. 5.10(a). Also note that as σ_x is decreased only the first few modes have larger amplitudes and as n is increased they decay much faster. When $\sigma_x = 0$, only the $n = 0$ mode remains and we reproduce the random rough surface results.

The above result in the limit $\sigma_x \rightarrow \infty$, (50), can also be related to the randomly perturbed sinusoidal surface case. When $\sigma_x = 0$, we obtain

$$\begin{aligned} \langle II^* \rangle &= \int_{-2L_x}^{2L_x} dx \int_{-2L_y}^{2L_y} dy \sum_n J_n^2(k_{iz} B) \exp \left[i \left(\bar{k}_{i\perp} + \hat{x} n \frac{2\pi}{P} \right) \cdot \bar{r}_\perp \right] \\ &\quad \times [2L_x - |x|][2L_y - |y|] \exp \left[-k_{iz}^2 \sigma^2 + k_{iz}^2 \sigma^2 C(\bar{r}_\perp) \right] \end{aligned} \quad (51)$$

For a narrow-band Gaussian random process, $A(x) \cos[(2\pi/P)x + \psi(x)]$, the PDF for $A(x)$ and $\psi(x)$ is given by

$$P(A, \psi) = \begin{cases} \frac{A}{2\pi\sigma_x^2} \exp\left(-\frac{A^2}{2\sigma_x^2}\right) & \text{for } A > 0, \quad 0 \leq \psi \leq 2\pi \\ 0 & \text{otherwise} \end{cases} \quad (52)$$

Therefore, if we treat the amplitude B and the phase ψ of sinusoidal variation as random variables with PDF given by (52), and take the average of (51) with respect to B and ψ , we obtain the randomly perturbed quasiperiodic surface result, given by (50), by making use of

$$\int_0^\infty dB J_n^2(k_{iz} B) \frac{B}{\sigma_x^2} \exp\left(-\frac{B^2}{2\sigma_x^2}\right) = \exp(-k_{iz}^2 \sigma_x^2) I_n(-k_{iz}^2 \sigma_x^2) \quad (53)$$

In Figs. 5.11 and 5.12 we illustrate the combined effect of the previous cases. In Fig. 5.11 the backscattering cross sections are plotted for different l for the case

$B = 10$ cm and $\sigma_r = 5$ cm. The $\phi_i = 0^\circ$ results are seen to be much more flatter as a function of incident angle than the corresponding cases in Fig. 5.10(a). The effect of varying σ_r is illustrated in Fig. 5.12. Therefore, by varying σ_r and B we can obtain different combinations of the previous two cases when $\sigma_r = 0$ or $B = 0$.

Appendix A: Narrow-Band Gaussian Random Process

The narrow-band Gaussian random process can be expressed as [Davenport and Root, 1958]

$$A(x) \cos \left[\frac{2\pi}{P} x + \psi(x) \right] = \xi_r(x) \cos \frac{2\pi}{P} x - \xi_s(x) \sin \frac{2\pi}{P} x \quad (A1)$$

where $\xi_r(x)$ and $\xi_s(x)$ are independent Gaussian random variables with zero means

$$\langle \xi_r(x) \rangle = \langle \xi_s(x) \rangle = 0 \quad (A2)$$

and

$$\langle \xi_r(x_1) \xi_r(x_2) \rangle = \langle \xi_s(x_1) \xi_s(x_2) \rangle = \sigma_r^2 C_r(|x_1 - x_2|) \quad (A3)$$

$$\langle \xi_r(x_1) \xi_s(x_2) \rangle = 0 \quad (A4)$$

where σ_r is the standard deviations of $\xi_r(x)$ and $\xi_s(x)$ and $C_r(|x_1 - x_2|)$ is the normalized correlation function. The covariance of narrow-band Gaussian random processes at x_1 and x_2 is given by

$$\langle A(x_1) \cos \left[\frac{2\pi}{P} x_1 + \psi(x_1) \right] A(x_2) \cos \left[\frac{2\pi}{P} x_2 + \psi(x_2) \right] \rangle = \sigma_r^2 C_r(|x_1 - x_2|) \cos \frac{2\pi}{P} (x_1 - x_2) \quad (A5)$$

The probability density function in terms of A and ψ is given by

$$P(A, \psi) = \begin{cases} \frac{A}{2\pi\sigma_r^2} \exp \left(-\frac{A^2}{2\sigma_r^2} \right) & \text{for } A > 0, \quad 0 \leq \psi \leq 2\pi \\ 0 & \text{otherwise} \end{cases} \quad (A6)$$

Appendix B: Calculations of $\langle |I|^2 \rangle$ and D_I

The integral I is given by

$$I = \int_A \exp(i\bar{k}_{d1} \cdot \bar{r}') d\bar{r}' \quad (B1)$$

The ensemble average of I is given by

$$\langle I \rangle = \int_{A..} dx' dy' \exp(ik_{dx}x' + ik_{dy}y') \langle \exp[ik_{dz}f(x', y')] \rangle \quad (B2)$$

with

$$\langle \exp[ik_{dz}f(x', y')] \rangle = \exp \left[-\frac{1}{2}k_{dz}^2(\sigma^2 + \sigma_x^2) \right] \exp \left[ik_{dz}B \cos \left(\frac{2\pi}{P}x' + \phi \right) \right] \quad (B3)$$

where

$$\sigma^2 = \langle \xi^2 \rangle \quad (B4)$$

$$\sigma_x^2 = \langle \xi_x^2 \rangle = \langle \xi_y^2 \rangle \quad (B5)$$

Therefore,

$$\langle I \rangle = 4L_x L_y \exp \left[-\frac{1}{2}k_{dz}^2(\sigma^2 + \sigma_x^2) \right] \sum_{n=-\infty}^{\infty} a_n \operatorname{sinc} \left[\left(k_{dz} + n \frac{2\pi}{P} \right) L_x \right] \operatorname{sinc} [k_{dy}L_y] \quad (B6)$$

where

$$a_n = (-1)^n J_n(-k_{dz}B) \exp \left[in \left(\frac{\pi}{2} + \phi \right) \right] \quad (B7)$$

J_n is the n th-order Bessel function, $2L_x$ and $2L_y$ are the lengths of the rough surface in the x and y directions, respectively, so that

$$A_{\perp} = 4L_x L_y \quad (B8)$$

Assuming that the area illuminated contains many periods ($L_x, L_y \gg P$), we have

$$|\langle I \rangle|^2 \simeq 16L_x^2 L_y^2 \exp[-k_{dz}^2(\sigma^2 + \sigma_x^2)] \sum_{n=-\infty}^{\infty} |a_n|^2 \text{sinc}^2 \left[\left(k_{dz} + n \frac{2\pi}{P} \right) L_x \right] \text{sinc}^2 [k_{dy} L_y] \quad (B9)$$

By allowing L_x and L_y to approach infinity in the above equation, we obtain

$$|\langle I \rangle|^2 = 4\pi^2 A_{\perp} \exp[-k_{dz}^2(\sigma^2 + \sigma_x^2)] \sum_{n=-\infty}^{\infty} |a_n|^2 \delta \left(k_{dz} + n \frac{2\pi}{P} \right) \delta(k_{dy}) \quad (B10)$$

where δ is the Dirac delta function.

The integral for $\langle II' \rangle$ is given by

$$\langle II' \rangle = \int_{A_{\perp}} d\bar{r}_{\perp} \int_{A_{\perp}} d\bar{r}'_{\perp} \exp[i\bar{k}_{dz} \cdot (\bar{r}_{\perp} - \bar{r}'_{\perp})] \langle \exp(i\bar{k}_{dz} [f(x, y) - f(x', y')]) \rangle \quad (B11)$$

With the change of variables we have

$$\begin{aligned} \langle II' \rangle &= \frac{1}{4} \int_{-2L_x+|x|}^{2L_x-|x|} dx' \int_{-2L_y+|y|}^{2L_y-|y|} dy' \int_{-2L_x}^{2L_x} dx \int_{-2L_y}^{2L_y} dy \exp[i\bar{k}_{dz} \cdot \bar{r}_{\perp}] \sum_{n=-\infty}^{\infty} a_n(x) \exp \left[i \frac{n}{2} \frac{2\pi}{P} x' \right] \\ &\times \exp[-k_{dz}^2 \sigma^2 + k_{dz}^2 \sigma^2 C(\bar{r}_{\perp})] \exp \left[-k_{dz}^2 \sigma_x^2 + k_{dz}^2 \sigma_x^2 \cos \frac{2\pi}{P} x C_x(x) \right] \end{aligned} \quad (B12)$$

where

$$a_n(x) = J_n \left[2k_{dz} B \sin \left(\frac{\pi}{P} x \right) \right]$$

Expanding $a_n(x)$ and carrying out the dx' and dy' integrations, we obtain

$$\begin{aligned}
\langle II' \rangle &= \frac{1}{2} \int_{-2L_x}^{2L_x} dx \int_{-2L_y}^{2L_y} dy \sum_{n=-\infty}^{\infty} \sum_{\mu=-\infty}^{\infty} \beta_{n\mu} \exp \left[i \left(\bar{k}_{d\perp} + \hat{x}\mu \frac{2\pi}{P} \right) \cdot \bar{r}_{\perp} \right] [2L_y - |y|] \\
&\times \frac{1}{in \frac{2\pi}{P}} \left\{ \exp \left[in \frac{2\pi}{P} (2L_x - |x|) \right] - \exp \left[-in \frac{2\pi}{P} (2L_x - |x|) \right] \right\} \\
&\times \exp \left[-k_{dz}^2 \sigma^2 + k_{dz}^2 \sigma^2 C(\bar{r}_{\perp}) \right] \exp \left[-k_{dz}^2 \sigma_r^2 + k_{dz}^2 \sigma_r^2 \cos \frac{2\pi}{P} x C_r(x) \right] \quad (B13)
\end{aligned}$$

where

$$\beta_{n\mu} = (-1)^{\mu} J_{n-\mu}(k_{dz}B) J_{n+\mu}(k_{dz}B)$$

It is clear from the above equation that the $n = 0$ term is proportional to L_x while the $n \neq 0$ term is proportional to P . The argument of the Bessel function $k_{dz}B$ will dictate the number of terms that needs to be summed up. However, if $L_x \gg P$ (we eventually take the limit $L_x \rightarrow \infty$ later on), then the $n = 0$ term will make dominant contributions and other terms will be negligible. Therefore, keeping only the $n = 0$ term, we obtain

$$\begin{aligned}
\langle II^* \rangle &= \int_{-2L_x}^{2L_x} dx \int_{-2L_y}^{2L_y} dy \sum_{\mu=-\infty}^{\infty} b_{\mu} \exp \left[i \left(\bar{k}_{d\perp} + \hat{x}\mu \frac{2\pi}{P} \right) \cdot \bar{r}_{\perp} \right] [2L_x - |x|] [2L_y - |y|] \\
&\times \exp \left[-k_{dz}^2 \sigma^2 + k_{dz}^2 \sigma^2 C(\bar{r}_{\perp}) \right] \exp \left[-k_{dz}^2 \sigma_r^2 + k_{dz}^2 \sigma_r^2 \cos \frac{2\pi}{P} x C_r(x) \right] \quad (B14)
\end{aligned}$$

where

$$b_{\mu} = J_{\mu}^2(k_{dz}B) \quad (B15)$$

We assume the correlation functions $C(\bar{r}_{\perp})$ and $C_r(x)$ to have a Gaussian form

$$C(\bar{r}_{\perp}) = \exp \left[-(x^2 + y^2)/l^2 \right] \quad (B16)$$

$$C_r(x) = \exp \left[-x^2/l_r^2 \right] \quad (B17)$$

where l is the correlation length for the random variable $\xi(\bar{r} \perp)$ in the transverse plane and l_x is the correlation length for the random variables $\xi_r(x)$ and $\xi_s(x)$ in the x direction.

The expressions for the standard deviation of the integral I can now be evaluated in a closed form. Assuming $L_x, L_y \gg l, l_x, P$, we obtain from (B10), (B14), (B16), and (B17),

$$D_I = \langle II^* \rangle - \langle I \rangle \langle I^* \rangle = \frac{4\pi A_{11}}{k^2} (D_{I_1} + D_{I_2}) \quad (\text{B18})$$

with

$$\begin{aligned} D_{I_1} = & \frac{k^2}{4} \sum_{\mu=-\infty}^{\infty} b_{\mu} \exp[-k_{dz}^2(\sigma^2 + \sigma_x^2)] \sum_{m=1}^{\infty} \frac{(k_{dz}^2 \sigma^2)^m}{m!} \frac{l^2}{m} \left(\exp \left\{ - \left[\left(k_{dx} + \mu \frac{2\pi}{P} \right)^2 + k_{dy}^2 \right] \frac{l^2}{4m} \right\} \right. \\ & \left. + \sum_{m'=1}^{\infty} \sum_{n=0}^{m'} \frac{1}{2^{m'}} \binom{m'}{n} \frac{(k_{dz}^2 \sigma_x^2)^{m'}}{m'!} \frac{1}{q} \exp \left\{ -k_{dy}^2 \frac{l^2}{4m} - \left[k_{dx} + (\mu + m' - 2n) \frac{2\pi}{P} \right]^2 \frac{l^2}{4mq} \right\} \right) \quad (\text{B19}) \end{aligned}$$

where

$$q = \sqrt{1 + \frac{l^2 m'}{l_x^2 m}}$$

and

$$\begin{aligned} D_{I_2} = & \frac{k^2}{2} \delta(k_{dy}) \sum_{\mu=-\infty}^{\infty} b_{\mu} \sum_{m=1}^{\infty} \sum_{n=0}^m \frac{1}{2^m} \binom{m}{n} \exp[-k_{dz}^2(\sigma^2 + \sigma_x^2)] \sqrt{\frac{\pi}{m}} l_x \frac{(k_{dz}^2 \sigma_x^2)^m}{m!} \\ & \times \exp \left\{ - \left[k_{dx} + (\mu + m - 2n) \frac{2\pi}{P} \right]^2 \frac{l_x^2}{4m} \right\} \quad (\text{B20}) \end{aligned}$$

where we made use of

$$\lim_{L_y \rightarrow \infty} \frac{L_y}{\pi} \text{sinc}^2(k_{dy} L_y) = \delta(k_{dy}) \quad (\text{B21})$$

We note that when $l \gg l_x, P$, the expressions for D_{I_1} , (B19), can be simplified to

$$D_{I_1} \simeq \frac{k^2}{4} \sum_{\mu=-\infty}^{\infty} b_{\mu} \exp[-k_{dz}^2(\sigma^2 + \sigma_x^2)] \sum_{m=1}^{\infty} \frac{(k_{dz}^2 \sigma^2)^m}{m!} \frac{l^2}{m} \exp \left\{ - \left[\left(k_{dx} + \mu \frac{2\pi}{P} \right)^2 + k_{dy}^2 \right] \frac{l^2}{4m} \right\} \quad (\text{B22})$$

After some manipulations, the above expression further simplifies to

$$D_{l_1} \simeq \frac{1}{P} \int_0^P dx \frac{k^2}{4} \exp \left[-k_{dz}^2 (\sigma^2 + \sigma_r^2) \right] \sum_{m=1}^{\infty} \frac{(k_{dz}^2 \sigma^2)^m}{m!} \frac{l^2}{m} \\ \times \exp \left\{ - \left[\left(k_{dx} + k_{dz} 2\pi \frac{B}{P} \sin \frac{2\pi}{P} x \right)^2 - k_{du}^2 \right] \frac{l^2}{4m} \right\} \quad (B23)$$

The above result is consistent with the result obtained using the incoherent model [Ulaby *et al.*, 1982] where the physical optics solutions is averaged over the local slopes. This is due to the fact that when the period P is much larger than the correlation length l then within the correlation length the periodic component will appear to be planar with the local slope.

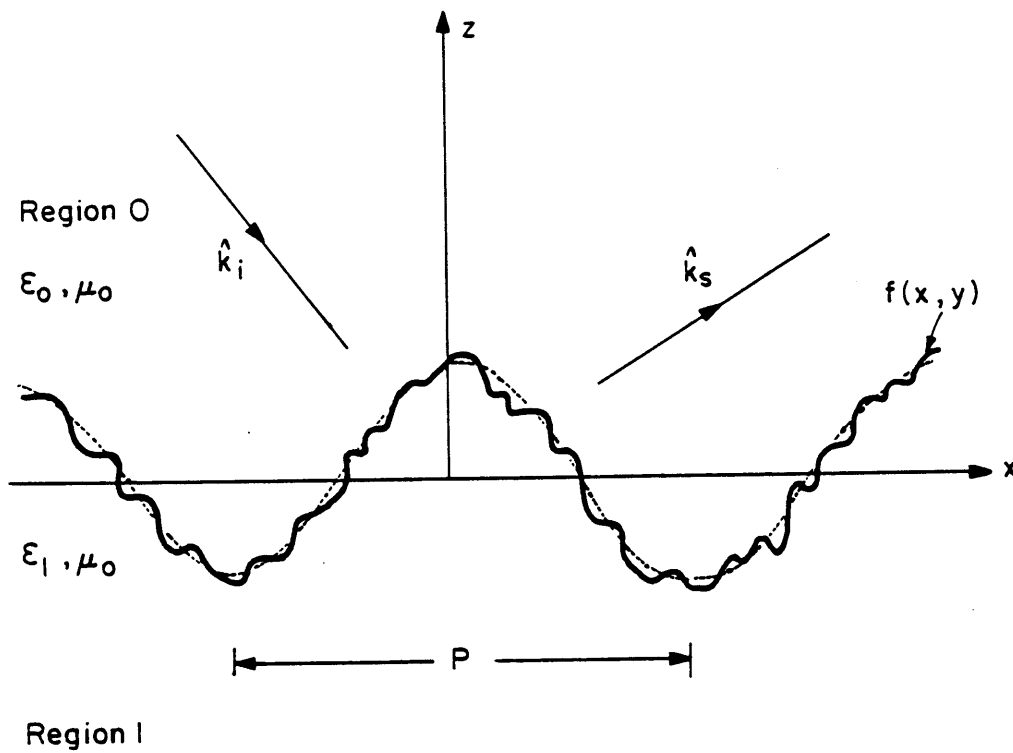


Figure 5.1 Geometrical configuration of the problem.

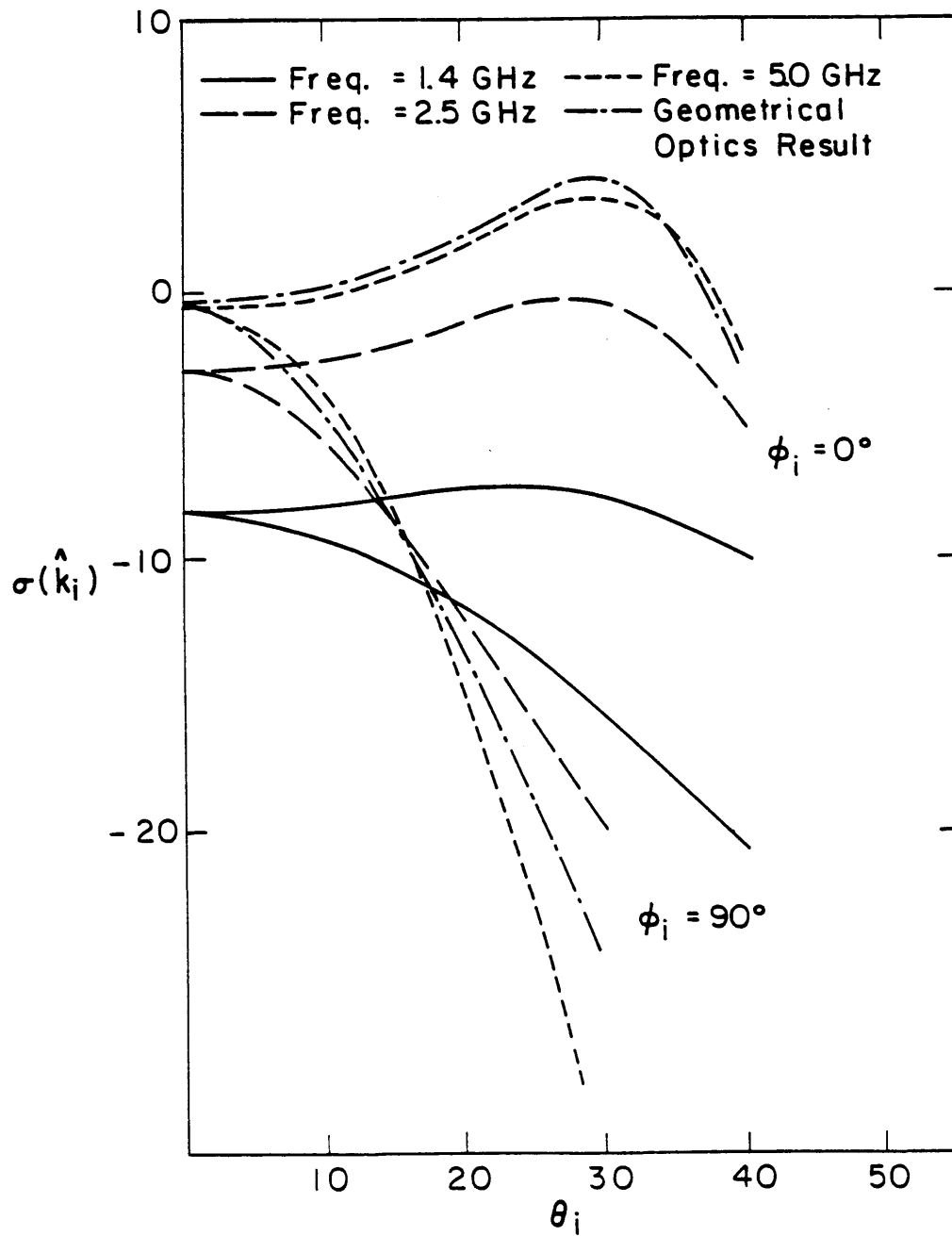


Figure 5.2 $\sigma(\hat{k}_i)$ as a function of θ_i for different frequencies with $\sigma = 1$ cm, $l = 10$ cm, $B = 10$ cm, $P = 100$ cm, $\sigma_s = 0$, and $\epsilon_1 = (6.0 + i0.6)\epsilon_0$.

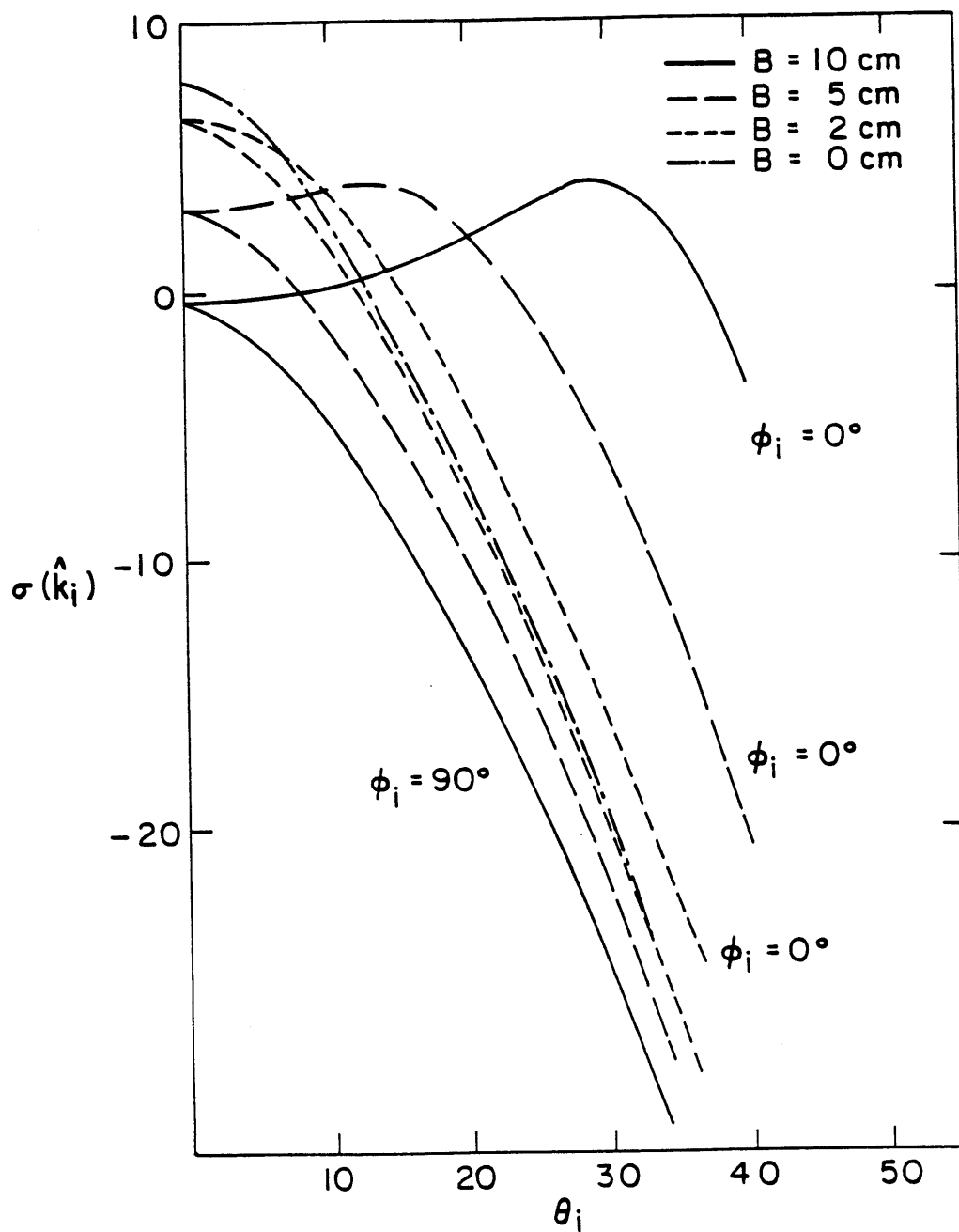


Figure 5.3 $\sigma(\hat{k}_i)$ as a function of θ_i for different values of B at 5.0 GHz with $P = 100$ cm, $\sigma = 1$ cm, $l = 10$ cm, $\sigma_x = 0$, and $\epsilon_1 = (6.0 + i0.6)\epsilon_0$.

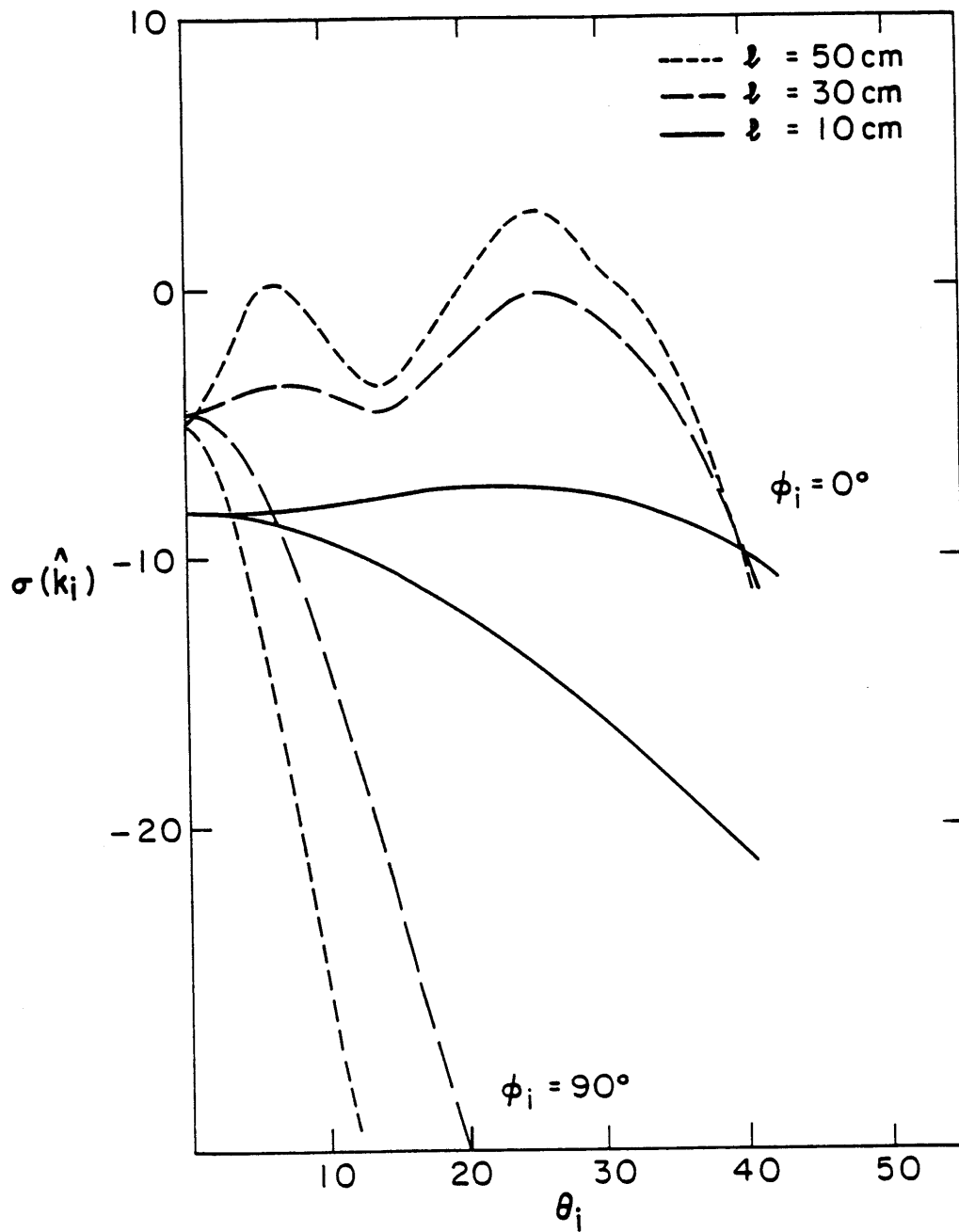


Figure 5.4 $\sigma(\hat{k}_i)$ as a function of θ_i for different values of l at 1.4 GHz with $\sigma = 1$ cm, $B = 10$ cm, $P = 100$ cm, $\sigma_r = 0$, and $\epsilon_1 = (6.0 + i0.6)\epsilon_0$.

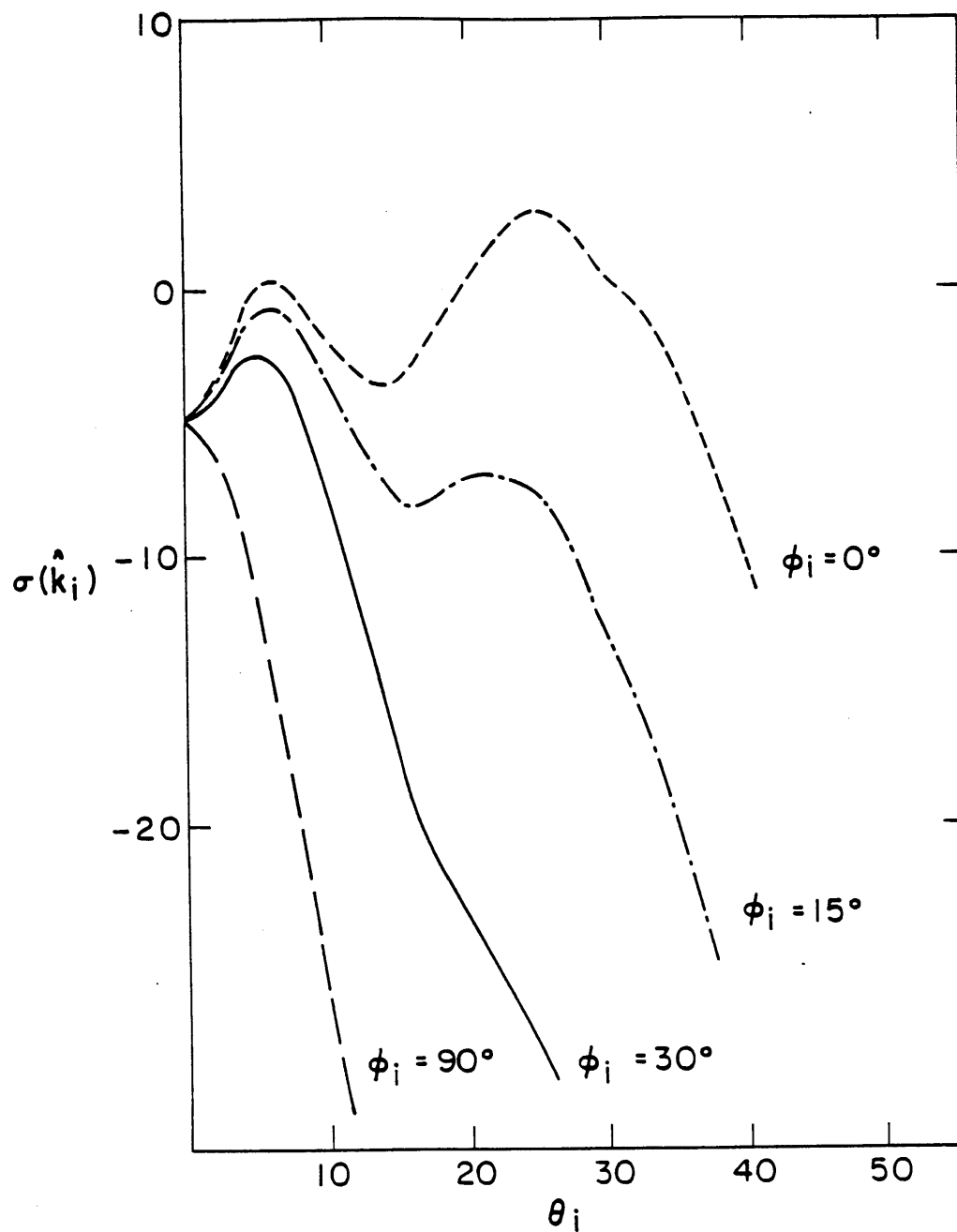


Figure 5.5 $\sigma(\hat{k}_i)$ as a function of θ_i for different azimuthal angle of incidence ϕ_i at 1.4 GHz with $\sigma = 1$ cm, $l = 50$ cm, $B = 10$ cm, $P = 100$ cm, $\sigma_x = 0$, and $\epsilon_1 = (6.0 + i0.6)\epsilon_0$.

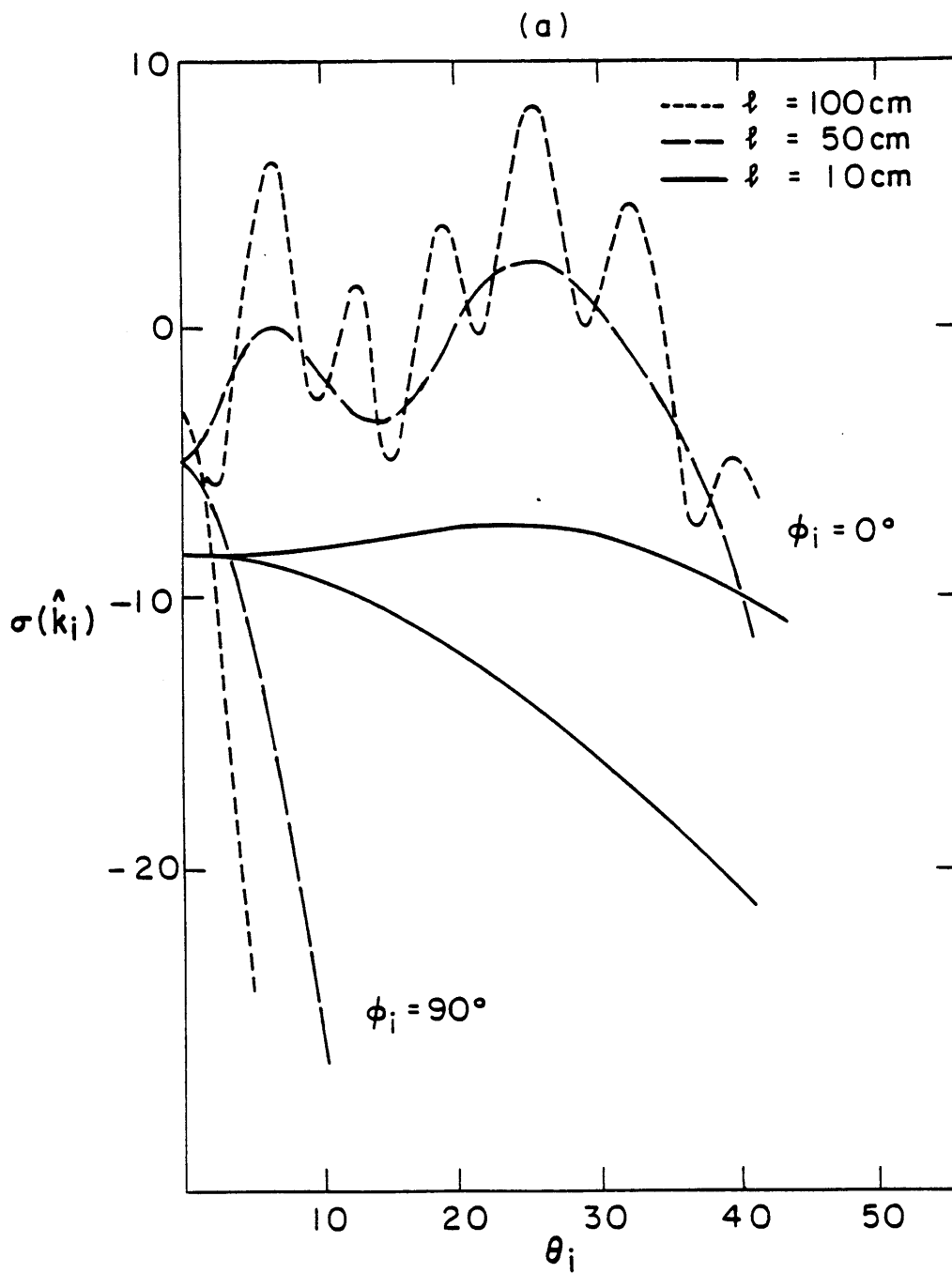


Figure 5.6 (a) $\sigma(\hat{k}_i)$ as a function of θ_i for different values of l at 1.4 GHz with $\sigma = 1$ cm, $B = 10$ cm, $P = 100$ cm, $\sigma_r = 0$, and $\epsilon_1 = (6.0 + i0.6)\epsilon_0$.

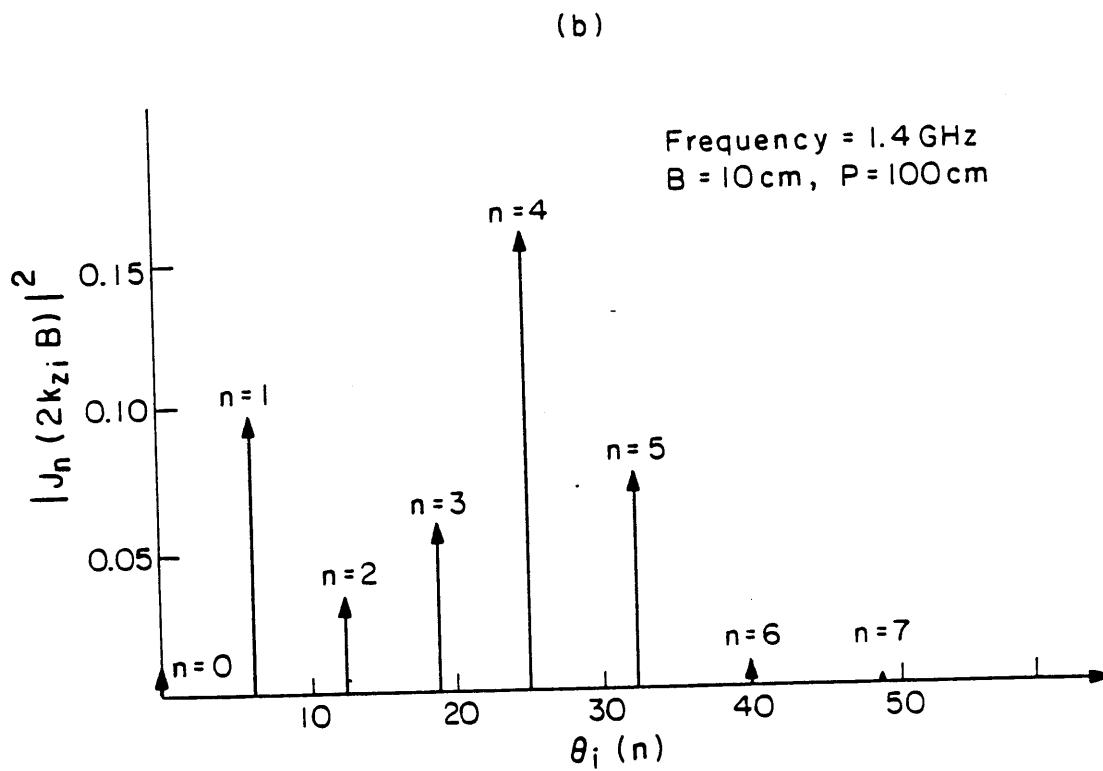


Figure 5.6 (b) Locations and amplitudes of the modes for $B = 10\text{ cm}$.

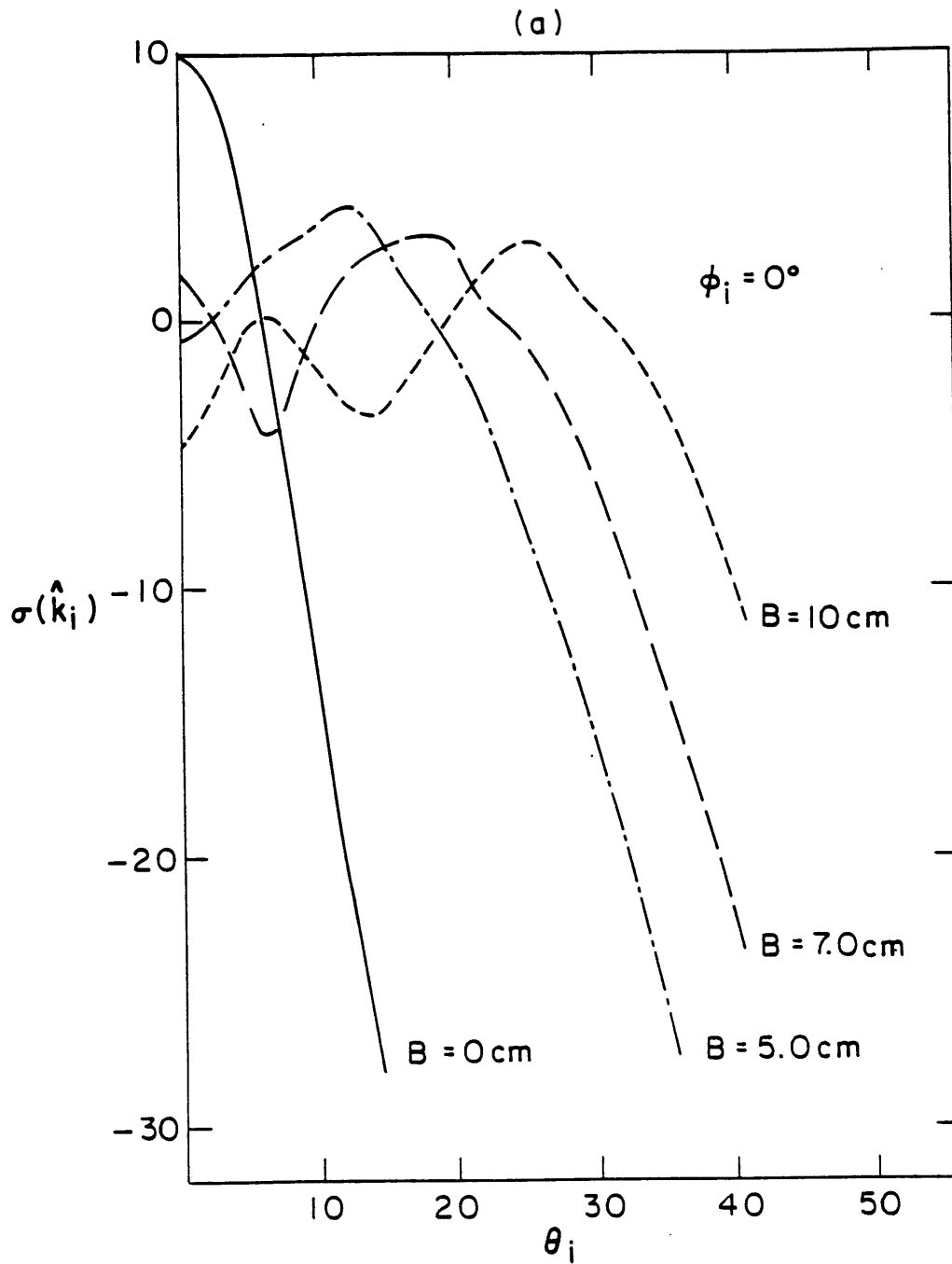


Figure 5.7 (a) $\sigma(\hat{k}_i)$ as a function of θ_i for different values of B at 1.4 GHz with $\sigma = 1$ cm, $l = 50$ cm, $P = 100$ cm, $\sigma_s = 0$, and $\epsilon_1 = (6.0 + i0.6)\epsilon_0$.

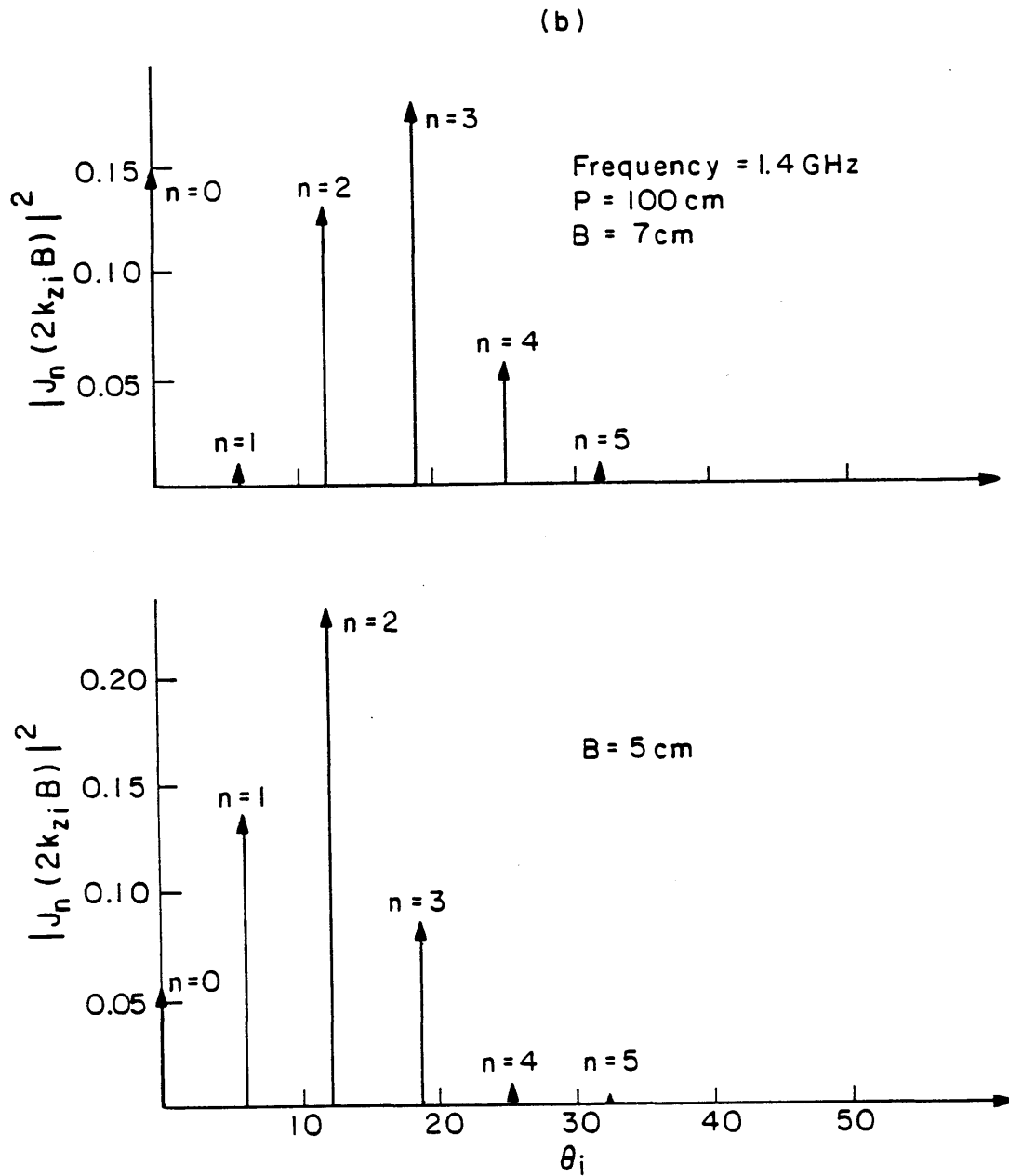


Figure 5.7 (b) Locations and amplitudes of the modes for $B = 7$ cm and $B = 5$ cm.

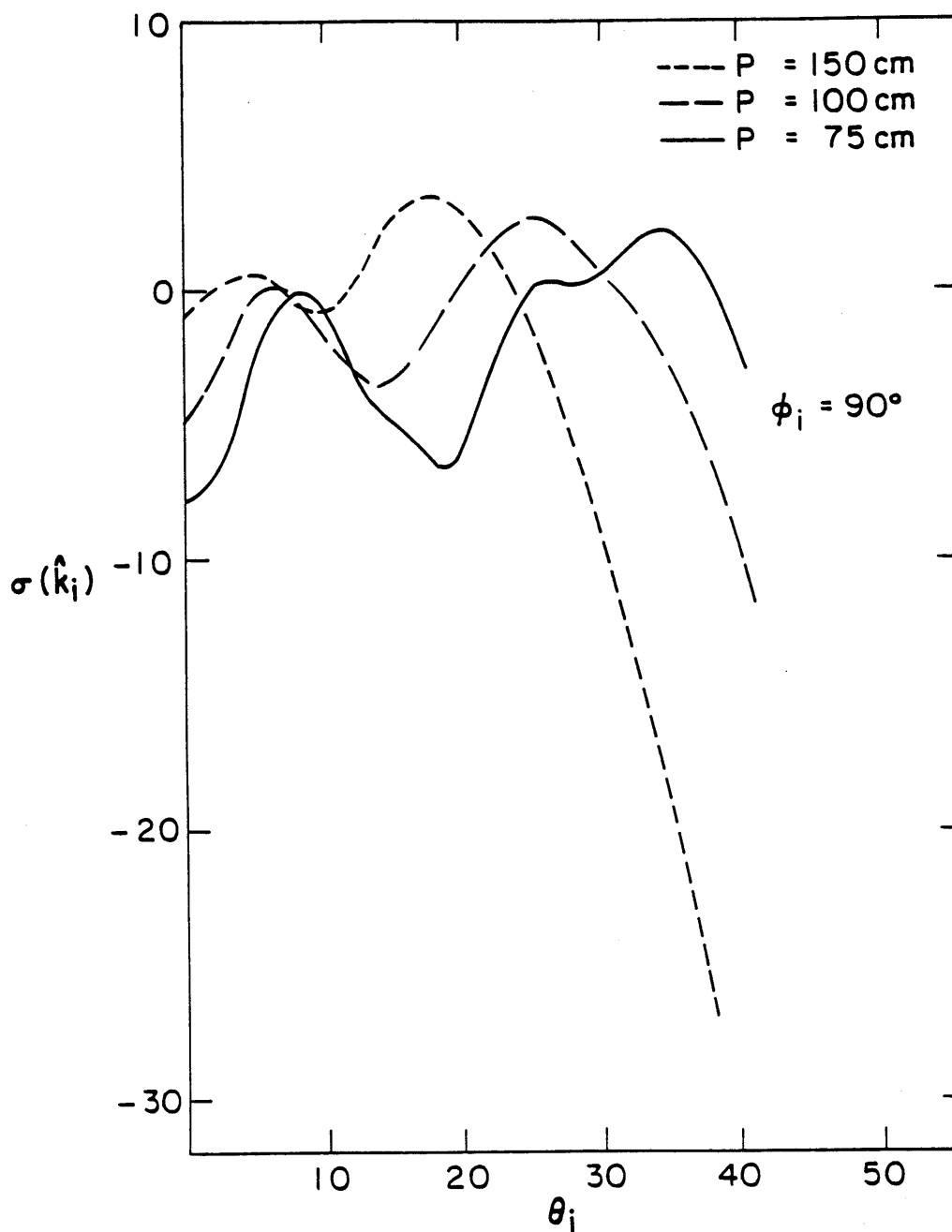


Figure 5.8 $\sigma(\hat{k}_i)$ as a function of θ_i for different values of P at 1.4 GHz with $\sigma = 1$ cm.

$l = 50$ cm, $B = 10$ cm, $P = 100$ cm, $\sigma_r = 0$, and $\epsilon_1 = (6.0 + i0.6)\epsilon_0$.

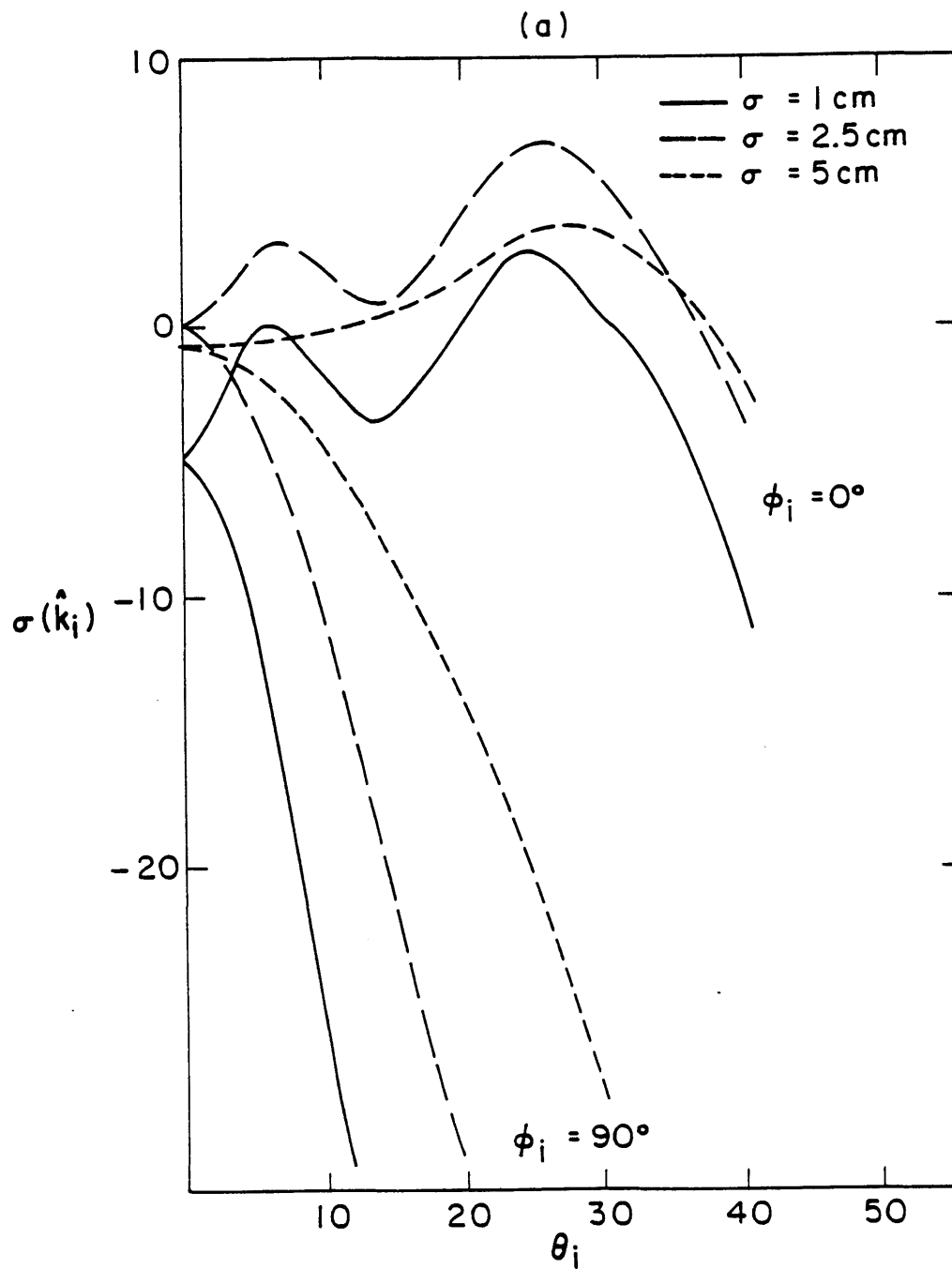


Figure 5.9 (a) $\sigma(\hat{k}_i)$ as a function of θ_i for different values of σ at 1.4 GHz with $l = 50$ cm, $B = 10$ cm, $P = 100$ cm, $\sigma_s = 0$, and $\epsilon_1 = (6.0 + i0.6)\epsilon_0$.

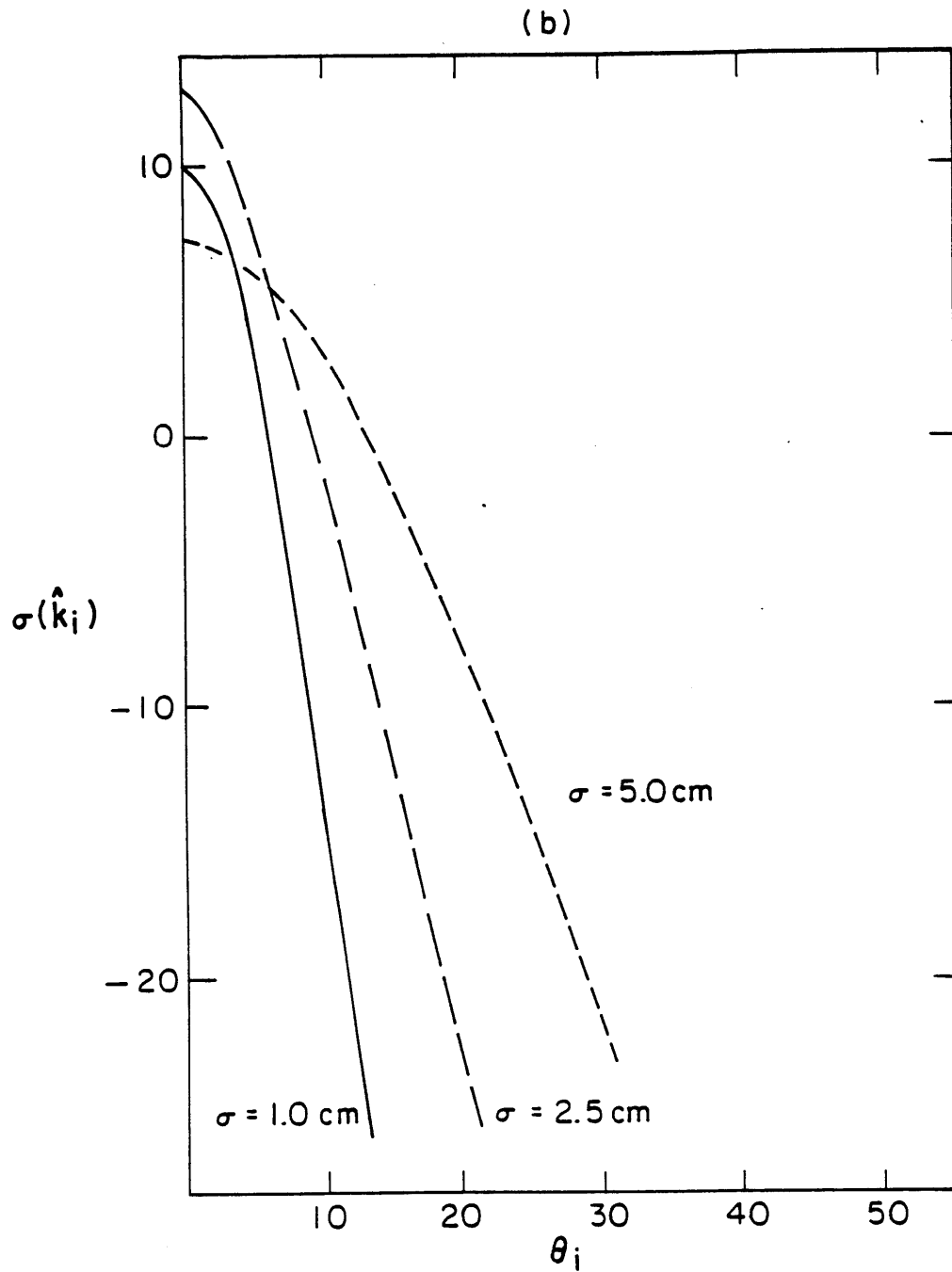


Figure 5.9 (b) $\sigma(\hat{k}_i)$ as a function of θ_i for different values of σ at 1.4 GHz with $l = 50 \text{ cm}$, $B = 0$, $\sigma_r = 0$, and $\epsilon_1 = (6.0 + i0.6)\epsilon_{r,0}$.

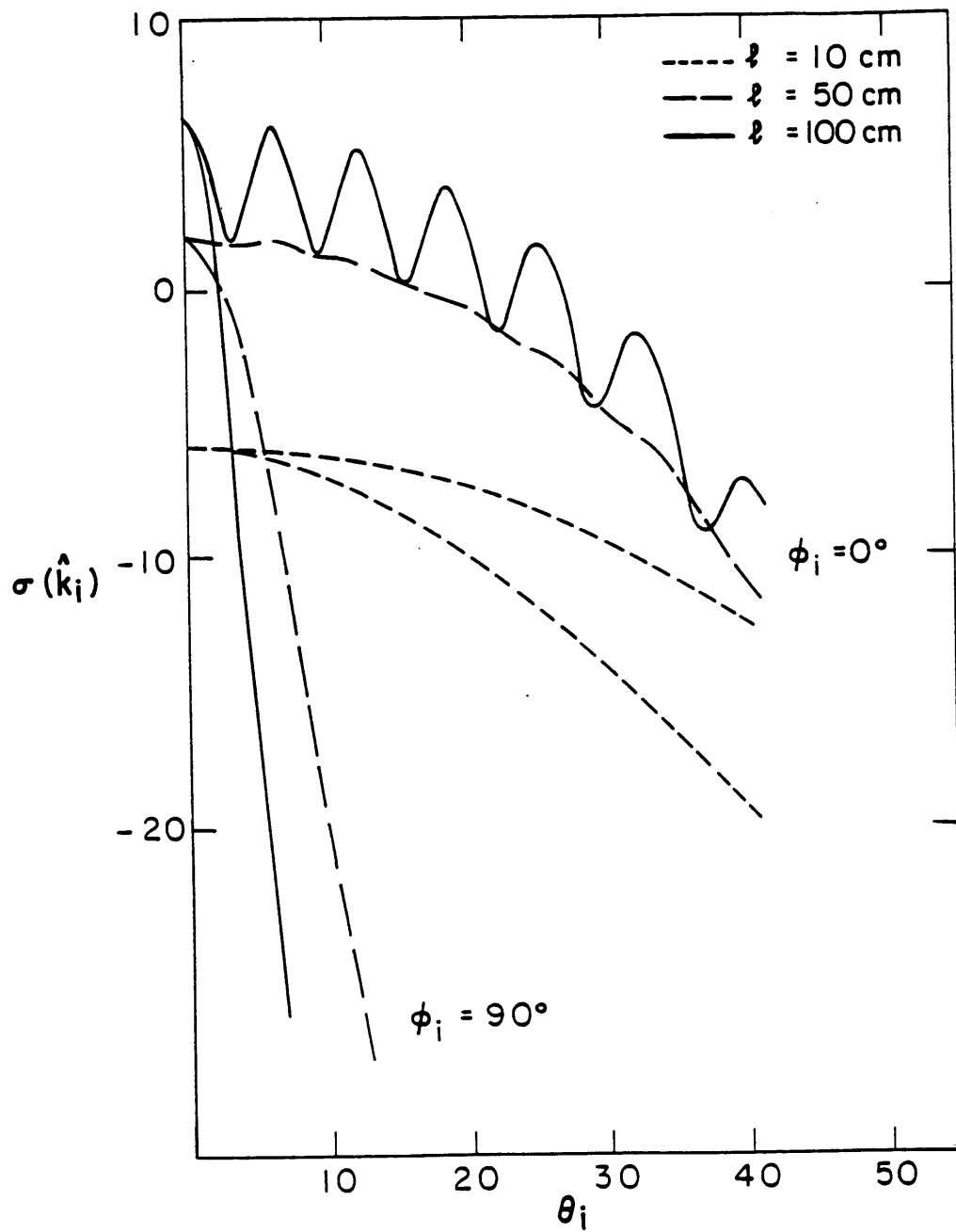


Figure 5.10 (a) $\sigma(\hat{k}_i)$ as a function of θ_i , for different values of l at 1.4 GHz with $\sigma = 1$ cm, $B = 0$, $P = 100$ cm, $\sigma_r = 5$ cm, $l_r = 300$ cm, and $\epsilon_1 = (6.0 + i0.6)\epsilon_0$.

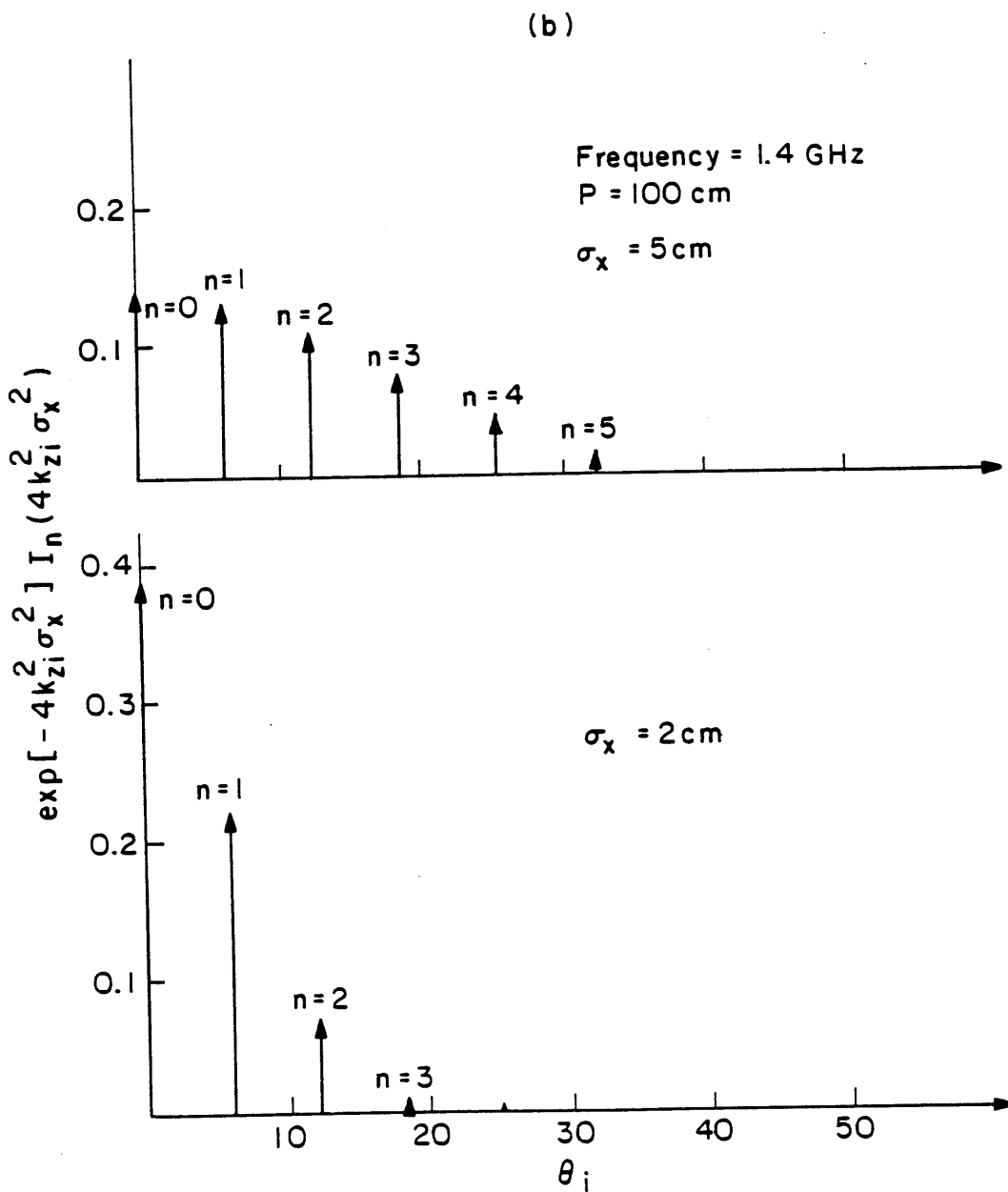


Figure 5.10 (b) Locations and amplitudes of the modes for $\sigma_r = 5$ cm and $\sigma_r = 2$ cm.

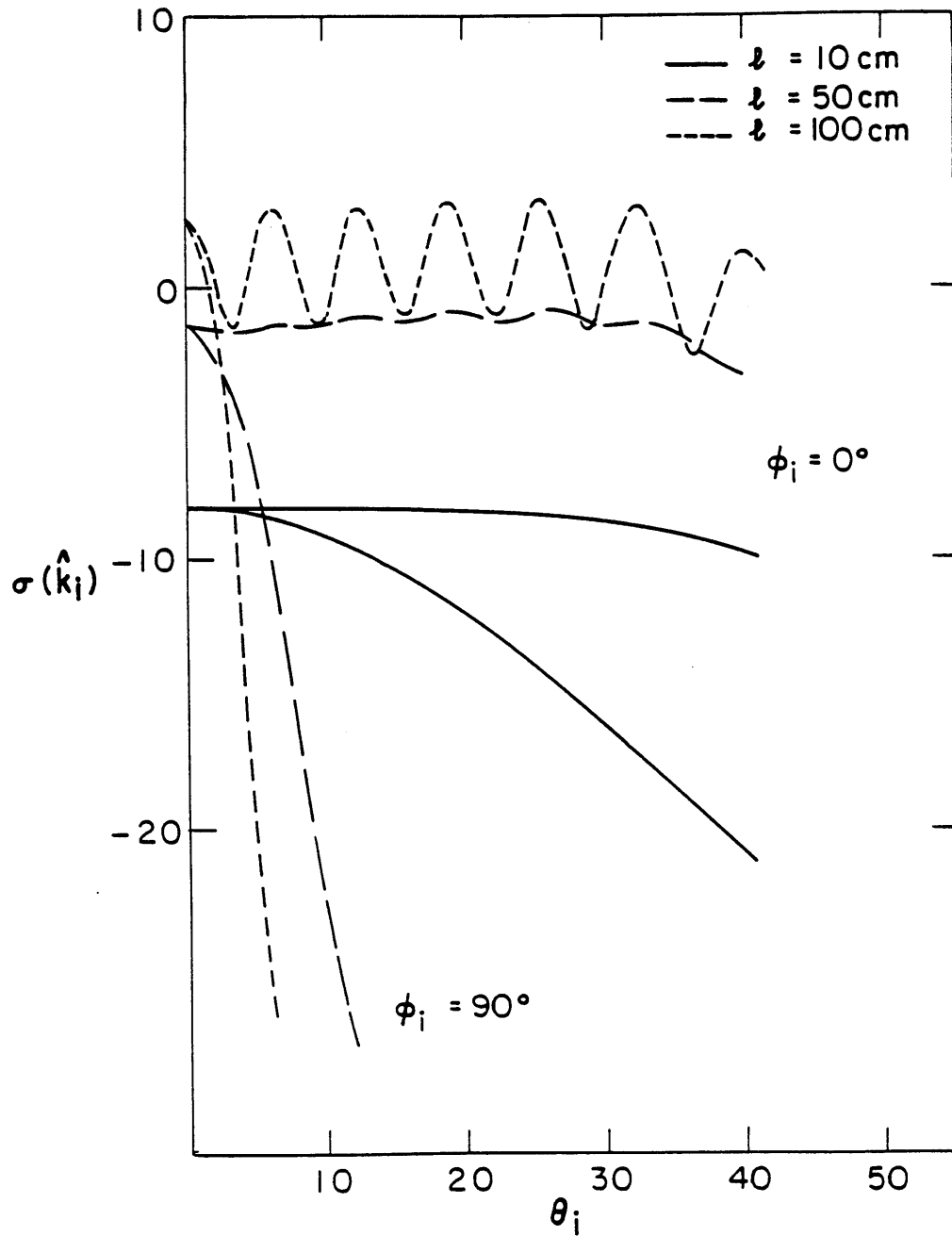


Figure 5.11 $\sigma(\hat{k}_i)$ as a function of θ_i for different values of l at 1.4 GHz with $\sigma = 1$ cm, $B = 10$ cm, $P = 100$ cm, $\sigma_r = 5$ cm, $l_r = 300$ cm, and $\epsilon_1 = (6.0 + i0.6)\epsilon_0$.

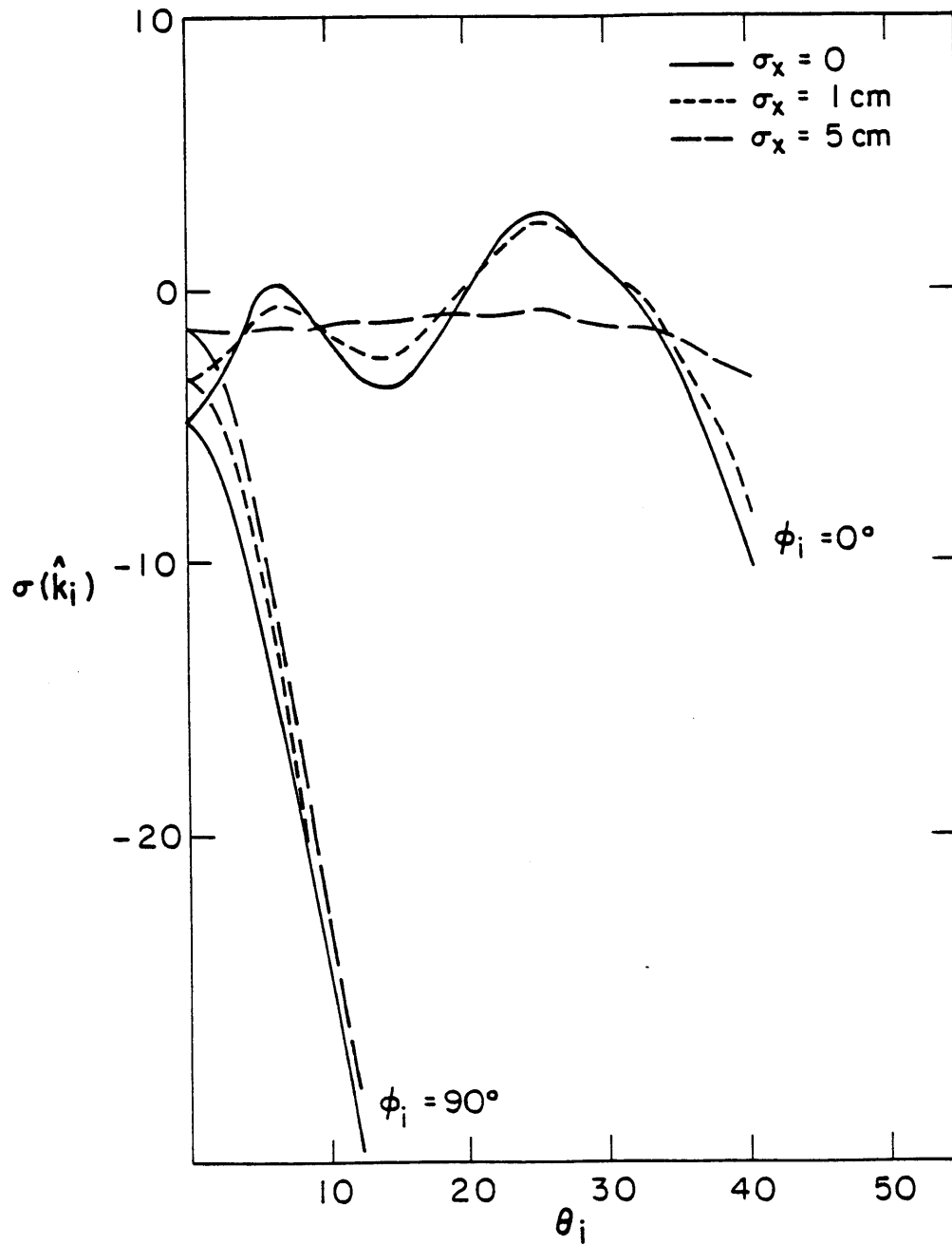


Figure 5.12 $\sigma(\hat{k}_i)$ as a function of θ_i for different values of σ_x at 1.4 GHz with $\sigma = 1$ cm, $l = 50$ cm, $B = 10$ cm, $P = 100$ cm, $l_x = 300$ cm, and $\epsilon_1 = (6.0 + i0.6)\epsilon_0$.

CHAPTER 6

Radiative Transfer Theory for Passive Remote Sensing of Multi-Layered Random Medium

Microwave thermal emission from the multi-layered random medium is studied using the radiative transfer theory. The brightness temperature is obtained by solving the radiative transfer equations numerically using the quadrature method. The effective boundary conditions are derived which reduce the complexity of the problem to that of a two-layer case. The theoretical results are illustrated for the various cases by plotting brightness temperatures as functions of frequency and observation angle.

6.1 Introduction

In the microwave remote sensing of earth terrain, the multi-layered random medium or discrete scatterer models have been applied to account for the volume scattering effects. The multi-layered models have shown to be more realistic in interpreting the remote sensing data [Njoku and Kong, 1977; Tsang *et al.*, 1975, 1977, Tsang and Kong, 1979]. In the active remote sensing, the scattering from a multi-layered random medium has been solved using the Born approximation and the propagation matrix formalism [Zuniga *et al.*, 1979]. The radiative transfer theory also has been applied to scattering from a multi-layer of Rayleigh scatterers with rough boundaries where the iterative approach is used to obtain solutions to first-order [Shin, 1980; Karam and Fung, 1982]. In the passive remote sensing the radiative transfer theory has been used to study thermal microwave emission from a multi-layered random medium with laminar structures [Djermakoye and Kong, 1979]. The propagation matrix formalism [Kong, 1975] is applied to obtain closed form solutions. For the inhomogeneous slab random medium with nonuniform scattering, absorption and temperature profiles in the vertical direction, the method of invariant imbedding has been used [Tsang and Kong, 1977b]. The boundary value problem of the radiative transfer equations is converted to an initial value problem starting at zero slab thickness. Thermal microwave emission from a three-layer random medium with three-dimensional variations has also been studied using the radiative transfer theory [Tsang and Kong, 1980b]. The quadrature method [Tsang and Kong, 1976b, 1977a] is used and the results are found to be useful in the interpretation of snow data exhibiting diurnal changes [Hofer and Schanda, 1978; Stiles and Ulaby, 1980].

In this chapter we solve the problem of thermal microwave emission from a multi-

layered random medium on top of homogeneous halfspace using the radiative transfer theory. The brightness temperatures are calculated using a numerical approach. The quadrature method where the integrals in the radiative transfer equations are replaced by the summation over the discrete quadrature angles is used. The resulting system of first-order differential equations is solved by obtaining eigenvalues and eigenvectors and matching the boundary conditions. The effective boundary conditions are derived in terms of the effective reflection matrices and the effective source vectors to reduce the complexity of the problem to that of a two-layer problem. The effective reflection matrices and the effective source vectors can be solved recursively by considering only one layer at a time. The numerical results are illustrated by plotting brightness temperatures as functions of frequency and observation angle.

6.2 Formulation

Consider N -layered random medium on top of a homogeneous halfspace with permittivity ϵ_{N-1} and physical temperature T_{N-1} [Fig. 6.1]. The l -th layer is characterized by the permittivity $\epsilon_l + \epsilon_{fl}$, where ϵ_{fl} stands for the randomly fluctuating part whose amplitude is very small and whose ensemble average is zero, and the temperature T_l . The radiative transfer equations which govern the propagation of intensities inside the l -th random layer are, for $0 < \theta_l < \pi$,

$$\cos \theta_l \frac{d}{dz} \bar{I}_l(\theta_l, z) = -K_{al} \bar{I}_l(\theta_l, z) - \bar{K}_{sl}(\theta_l) \cdot \bar{I}_l(\theta_l, z) + K_{al} C_l T_l + \int_0^\pi d\theta'_l \sin \theta'_l \bar{P}_l(\theta_l, \theta'_l) \cdot \bar{I}_l(\theta'_l, z) \quad (1)$$

where

$$\bar{I}_l(\theta_l, z) = \begin{bmatrix} I_{vl}(\theta_l, z) \\ I_{hl}(\theta_l, z) \end{bmatrix} \quad (2)$$

I_{vl} is the vertically polarized intensity, I_{hl} is the horizontally polarized intensity, K_{al} denotes the absorption loss, $\bar{K}_{sl}(\theta_l)$ denotes the scattering loss, $C_l = K \epsilon'_l / \epsilon_{\infty} \lambda^2$ with K denoting the Boltzmann constant, and $\bar{P}_l(\theta_l, \theta'_l)$ is the scattering function matrix which relates scattered intensities into the direction θ_l to the incident intensities in the direction θ'_l . The random permittivity fluctuation is characterized by the variance of the fluctuation δ_l and the correlation function with lateral correlation length l_{pl} and vertical correlation length l_{zl} . The correlation function is assumed to have gaussian dependence laterally and exponential dependence vertically. The scattering function matrix and the scattering coefficient have been derived by applying Born approximation with the far-field solution and are well known [Appendix].

The boundary conditions are, for $0 < \theta_l < \pi/2$, at $z = d_l$ where $l = 1, 2, \dots, N$

$$\bar{I}_{l+1}(\pi - \theta_{l+1}, z = -d_l) = \bar{R}_{(l+1)l}(\theta_{l+1}) \cdot \bar{I}_{l+1}(\theta_{l+1}, z = -d_l) + \bar{T}_{l(l+1)} \cdot \bar{I}_l(\pi - \theta_l, z = -d_l) \quad (3)$$

$$\bar{I}_l(\theta_l, z = -d_l) = \bar{\bar{R}}_{l(l+1)}(\theta_l) \cdot \bar{I}_l(\pi - \theta_l, z = -d_l) - \bar{\bar{T}}_{(l+1)l}(\theta_{l+1}) \cdot \bar{I}_{l+1}(\theta_{l+1}, z = -d_l) \quad (4)$$

and at $z = 0$

$$\bar{I}_l(\pi - \theta_l, z = 0) = \bar{\bar{R}}_{10}(\theta_1) \cdot \bar{I}_1(\theta_1, z = 0) - \bar{\bar{T}}_{01}(\theta_{..}) \cdot \bar{I}_{sky}(\theta_{..}) \quad (5)$$

where we have broken up intensities into upward going intensities $\bar{I}_l(\theta_l, z)$ and downward going intensities $\bar{I}_l(\pi - \theta_l, z)$. In the above equations $\bar{\bar{T}}_{l(l+1)}(\theta_l)$ represents the coupling from region l to region $l + 1$ and $\bar{\bar{R}}_{l(l+1)}(\theta_l)$ represents the coupling from upward going intensities into downward going intensities at the boundary of region l and region $l + 1$, [Chapter 7, Appendix B]. The sky radiation $\bar{I}_{sky}(\theta_{..})$ is taken to be

$$\bar{I}_{sky}(\theta_{..}) = C_{..} T_{air} [1 - e^{-K_{..} t \sec \theta_{..}}] \quad (6)$$

where T_{air} denotes the air temperature, $K_{..}$ denotes the absorption coefficient of the air, t is the thickness of the atmosphere, and $C_{..} = K/\lambda^2$.

Once the radiative transfer equations are solved subject to the boundary conditions (3) and (4), the brightness temperature as measured by a radiometer is obtained from

$$\bar{T}_E(\theta_{..}) = \frac{1}{C_{..}} \bar{\bar{T}}_{10}(\theta_1) \cdot \bar{I}_1(\theta_1, z = 0) + \frac{1}{C_{..}} \bar{\bar{R}}_{01}(\theta_{..}) \cdot \bar{I}_{sky}(\theta_{..}) \quad (7)$$

where

$$\bar{T}_E(\theta_{..}) = \begin{bmatrix} T_{Ev}(\theta_{..}) \\ T_{Eh}(\theta_{..}) \end{bmatrix} \quad (8)$$

6.3 Quadrature Method

The radiative transfer equations for the l -th random layer will be solved numerically using the quadrature method. First, the particular solution is given by

$$\bar{I}_l'(\theta_l, z) = C_l T_l \quad (9)$$

The homogeneous solutions are obtained by applying the quadrature method where the integrals in the radiative transfer equations are replaced by the summation over the discrete quadrature angles. The resulting system of first-order differential equations with constant coefficients are solved by obtaining eigenvalues and eigenvectors and matching the boundary conditions. In obtaining eigenvalues and eigenvectors the order of system of equations can be reduced by factor of two by making use of the symmetry properties of the scattering function matrix and noting that the eigenvalues occur in pairs such that if ξ is an eigenvalue so is $-\xi$.

Breaking up the intensities into upward and downward propagating intensities, denoted by superscripts $+$ and $-$ respectively, we apply the quadrature method over the n_l quadrature angles. In the absence of the source term, the following set of equations are obtained by making use of the symmetry properties of the scattering function matrix:

$$\bar{\mu}_l \cdot \frac{d}{dz} \bar{I}_l^+ = -\bar{K}_{.l} \cdot \bar{I}_l^+ + \bar{F}_l \cdot \bar{I}_l^+ + \bar{B}_l \cdot \bar{I}_l^- \quad (10a)$$

$$-\bar{\mu}_l \cdot \frac{d}{dz} \bar{I}_l^- = -\bar{K}_{.l} \cdot \bar{I}_l^- + \bar{B}_l \cdot \bar{I}_l^+ + \bar{F}_l \cdot \bar{I}_l^- \quad (10b)$$

where I_l^+ and I_l^- are $2n_l \times 1$ matrices

$$\bar{I}_l^+ = \begin{bmatrix} I_{vl}(\mu_{l1}, z) \\ \vdots \\ I_{vl}(\mu_{ln}, z) \\ I_{hl}(\mu_{l1}, z) \\ \vdots \\ I_{hl}(\mu_{ln}, z) \end{bmatrix} \quad \bar{I}_l^- = \begin{bmatrix} I_{vl}(-\mu_{l1}, z) \\ \vdots \\ I_{vl}(-\mu_{ln}, z) \\ I_{hl}(-\mu_{l1}, z) \\ \vdots \\ I_{hl}(-\mu_{ln}, z) \end{bmatrix} \quad (11)$$

\bar{F}_l and \bar{B}_l are $2n_l \times 2n_l$ matrices

$$\bar{F}_l = \begin{bmatrix} P_{11_l}(\mu_{l1}, \mu_{l1}) & \cdots & P_{11_l}(\mu_{l1}, \mu_{ln}) & P_{12_l}(\mu_{l1}, \mu_{l1}) & \cdots & P_{12_l}(\mu_{l1}, \mu_{ln}) \\ \vdots & \vdots & \vdots & \vdots & \vdots & \vdots \\ P_{11_l}(\mu_{ln}, \mu_{l1}) & \cdots & P_{11_l}(\mu_{ln}, \mu_{ln}) & P_{12_l}(\mu_{ln}, \mu_{l1}) & \cdots & P_{12_l}(\mu_{ln}, \mu_{ln}) \\ P_{21_l}(\mu_{l1}, \mu_{l1}) & \cdots & P_{21_l}(\mu_{l1}, \mu_{ln}) & P_{22_l}(\mu_{l1}, \mu_{l1}) & \cdots & P_{22_l}(\mu_{l1}, \mu_{ln}) \\ \vdots & \vdots & \vdots & \vdots & \vdots & \vdots \\ P_{21_l}(\mu_{ln}, \mu_{l1}) & \cdots & P_{21_l}(\mu_{ln}, \mu_{ln}) & P_{22_l}(\mu_{ln}, \mu_{l1}) & \cdots & P_{22_l}(\mu_{ln}, \mu_{ln}) \end{bmatrix} \quad (12)$$

$$\bar{B}_l = \begin{bmatrix} P_{11_l}(\mu_{l1}, -\mu_{l1}) & \cdots & P_{11_l}(\mu_{l1}, -\mu_{ln}) & P_{12_l}(\mu_{l1}, -\mu_{l1}) & \cdots & P_{12_l}(\mu_{l1}, -\mu_{ln}) \\ \vdots & \vdots & \vdots & \vdots & \vdots & \vdots \\ P_{11_l}(\mu_{ln}, -\mu_{l1}) & \cdots & P_{11_l}(\mu_{ln}, -\mu_{ln}) & P_{12_l}(\mu_{ln}, -\mu_{l1}) & \cdots & P_{12_l}(\mu_{ln}, -\mu_{ln}) \\ P_{21_l}(\mu_{l1}, -\mu_{l1}) & \cdots & P_{21_l}(\mu_{l1}, -\mu_{ln}) & P_{22_l}(\mu_{l1}, -\mu_{l1}) & \cdots & P_{22_l}(\mu_{l1}, -\mu_{ln}) \\ \vdots & \vdots & \vdots & \vdots & \vdots & \vdots \\ P_{21_l}(\mu_{ln}, -\mu_{l1}) & \cdots & P_{21_l}(\mu_{ln}, -\mu_{ln}) & P_{22_l}(\mu_{ln}, -\mu_{l1}) & \cdots & P_{22_l}(\mu_{ln}, -\mu_{ln}) \end{bmatrix} \quad (13)$$

and \bar{K}_{cl} , $\bar{\mu}_l$ and \bar{a}_l are the $2n_l \times 2n_l$ diagonal matrices

$$\bar{K}_{cl} = \text{diag}[K_{cvt_1}, \dots, K_{cvt_{n_l}}, K_{cht_1}, \dots, K_{cht_{n_l}}] \quad (14)$$

$$\bar{\mu}_l = \text{diag}[\mu_{l1}, \dots, \mu_{ln}, \mu_{l1}, \dots, \mu_{ln}] \quad (15)$$

$$\bar{a}_l = \text{diag}[a_{l1}, \dots, a_{ln}, a_{l1}, \dots, a_{ln}] \quad (16)$$

In the above equation $\pm\mu_{li}$ and a_{li} are discrete quadrature angles and the corresponding weighting functions and they obey the relations $a_{li} = a_{-li}$ and $\mu_{li} = -\mu_{-li}$. The extinction coefficients K_{cl} can be calculated as follows:

$$K_{cl} = K_{al} + \sum_{j=1}^{2n_l} (F_{l,j} a_{lj} + B_{l,j} a_{lj}) \quad i = 1, \dots, 2n_l \quad (17)$$

The quadrature angles in the different layers are related by the Snell's law. Since ϵ'_l are not the same the number of quadrature angles will vary from one layer to the next. In order to have θ_{li} scan the whole range of angles in the region l , we first apply the Gaussian quadrature method to the layer l' where $\epsilon_{l'}$ is the largest. Then, $\pm\mu_{l'}$ are the zeroes of the Legendre polynomial $P_{2n}(\mu'_{l'})$ and $a_{l'i}$ are the corresponding Christoffel weighting functions. We have $n_{l'} = n$ where n denotes the largest quadrature points. Once the quadrature angles in region l' are fixed, the quadrature angles in the other regions l are related to the angles in region l' by the Snell's law.

$$\theta_{li} = \sin^{-1}[\sqrt{\epsilon'_{l'}/\epsilon'_l} \sin \theta_{l'i}] \quad (18)$$

Since $\epsilon'_l \leq \epsilon'_{l'}$, we have, in general, $n_l \leq n_{l'}$.

For the layers where $\epsilon'_l \neq \epsilon'_{l'}$, the trapezoidal rule of integration is used. We have

$$\int_{-1}^1 d\mu_l f(\mu_l) = \sum_{j=-n_l}^{n_l} a_{lj} f(\mu_{lj}) = \sum_{j=1}^{n_l} a_{lj} [f(\mu_{lj}) + f(-\mu_{lj})] \quad (19)$$

where

$$a_{l1} = 1 - \frac{1}{2}(\mu_{l1} + \mu_{l2}) \quad (20a)$$

$$a_{lj} = \frac{1}{2}(\mu_{l(j-1)} - \mu_{l(j+1)}) \quad j = 2, \dots, n_l - 1 \quad (20b)$$

$$a_{ln_l} = \frac{1}{2}(\mu_{ln_l} + \mu_{l(n_l-1)}) \quad (20c)$$

When $\epsilon'_l = \epsilon'_{l'}$, the Gaussian-Legendre quadrature method is used for layer l .

The number of eigen-equations in the quadrature method can be reduced by the factor of two by defining

$$\bar{I}_{al} = \bar{I}_l^+ + \bar{I}_l^- \quad (21a)$$

$$\bar{I}_{sl} = \bar{I}_l^+ - \bar{I}_l^- \quad (21b)$$

Then, from (10), we obtain

$$\bar{\mu}_l \cdot \frac{d}{dz} \bar{I}_{ul} = \bar{W}_l \cdot \bar{I}_{sl} \quad (22a)$$

$$\bar{\mu}_l \cdot \frac{d}{dz} \bar{I}_{sl} = \bar{A}_l \cdot \bar{I}_{ul} \quad (22b)$$

where \bar{W}_l and \bar{A}_l are the $4n_l \times 4n_l$ matrices

$$\bar{W}_l = -\bar{K}_{cl} + (\bar{F}_l - \bar{B}_l) \cdot \bar{a}_l \quad (23a)$$

$$\bar{A}_l = -\bar{K}_{cl} + (\bar{F}_l + \bar{B}_l) \cdot \bar{a}_l \quad (23b)$$

The homogeneous solution can be obtained in the form

$$\bar{I}_{ul} = \bar{I}_{ul} \cdot e^{\alpha_l z} \quad (24a)$$

$$\bar{I}_{sl} = \bar{I}_{sl} \cdot e^{\alpha_l z} \quad (24b)$$

Substituting the above equations into (22a) and (22b), we now have $2n_l$ eigenvalue equations.

$$(\bar{\mu}_l^{-1} \cdot \bar{W}_l \cdot \bar{\mu}_l^{-1} \cdot \bar{A}_l - \alpha_l^2 \bar{I}_l) \cdot \bar{I}_{ul} = 0 \quad (25)$$

$$\bar{I}_{sl} = \alpha_l^{-1} \bar{\mu}_l^{-1} \cdot \bar{A}_l \cdot \bar{I}_{ul} \quad (26)$$

where \bar{I}_l is an $n_l \times n_l$ identity matrix. Thus, if α_l is an eigenvalue, so is $-\alpha_l$. Once the eigenvalues α_{li} and the corresponding eigenvectors \bar{I}_{ul} are obtained, we let $\bar{E}_l = (\bar{I}_{ul_1}, \bar{I}_{ul_2}, \dots, \bar{I}_{ul_{2n_l}})$ be the $2n_l \times 2n_l$ eigenmatrix. Then the total solution for the upward and downward propagating intensities are given by

$$\bar{I}_l^+ = C_l \left[\bar{T}_l + (\bar{E}_l + \bar{Q}_l) \cdot \bar{D}_l(z + d_{l-1}) \cdot \bar{x}_l + (\bar{E}_l - \bar{Q}_l) \cdot \bar{U}_l(z + d_l) \cdot \bar{y}_l \right] \quad (27a)$$

$$\bar{I}_l^- = C_l \left[\bar{T}_l + (\bar{E}_l - \bar{Q}_l) \cdot \bar{D}_l(z + d_{l-1}) \cdot \bar{x}_l + (\bar{E}_l + \bar{Q}_l) \cdot \bar{U}_l(z + d_l) \cdot \bar{y}_l \right] \quad (27b)$$

where

$$\bar{Q}_l = \bar{\mu}_l^{-1} \cdot \bar{A}_l \cdot \bar{E}_l \cdot \bar{\alpha}_l^{-1} \quad (28)$$

$$\bar{\alpha}_l = \text{diag}[\alpha_{l1}, \alpha_{l2}, \dots, \alpha_{l2n_l}] \quad (29)$$

$$\bar{D}_l(z) = \text{diag}[e^{\alpha_{l1}z}, e^{\alpha_{l2}z}, \dots, e^{\alpha_{l2n_l}z}] \quad (30)$$

$$\bar{U}_l(z) = \text{diag}[e^{-\alpha_{l1}z}, e^{-\alpha_{l2}z}, \dots, e^{-\alpha_{l2n_l}z}] \quad (31)$$

\bar{T}_l is the $2n_l \times 1$ matrix

$$\bar{T}_l = \begin{bmatrix} T_l \\ T_l \\ \vdots \\ T_l \end{bmatrix} \quad (32)$$

and \bar{x}_l and \bar{y}_l are the $2n_l \times 1$ matrices which represent $4n_l$ unknowns to be determined by the boundary conditions.

The boundary conditions, which are to be used to determine the constants \bar{x}_l and \bar{y}_l , can be obtained by discretizing the boundary conditions for the radiative transfer equations given by (3)–(5). They are, at $z = -d_l$, $l = 1, 2, \dots, N$

$$\bar{I}_{l+1}^-(z = -d_l) = \bar{R}_{l(l+1)} \cdot \bar{I}_{l+1}^+(z = -d_l) + \bar{T}_{l(l+1)} \cdot \bar{I}_l^-(z = -d_l) \quad (33)$$

$$\bar{I}_l^+(z = -d_l) = \bar{R}_{l(l+1)} \cdot \bar{I}_l^-(z = -d_l) + \bar{T}_{(l+1)l} \cdot \bar{I}_{l+1}(z = -d_l) \quad (34)$$

and at $z = 0$

$$\bar{I}_1^-(z = 0) = \bar{R}_{10} \cdot \bar{I}_1^-(z = 0) - \bar{T}_{01} \cdot \bar{I}_{s,ky} \quad (35)$$

where $\bar{R}_{l(l+1)}$ is the $2n_l \times 2n_l$ matrix which is obtained by evaluating the coupling matrix $\bar{R}_{l(l+1)}(\theta_l)$ at n_l discrete angles, and $\bar{T}_{l(l+1)}$ is the $2n_l \times 2n_{l+1}$ matrix which is obtained by evaluating the coupling matrix $\bar{T}_{l(l+1)}(\theta_l)$ at the quadrature angles.

6.4 Effective Boundary Conditions

The problem of determining the unknown constants \bar{x}_l and \bar{y}_l by matching the boundary conditions at $N - 1$ boundaries can be simplified greatly by using the effective boundary conditions. The idea is to come up with the effective boundary condition at $z = -d_l$ in terms of the properties of the region l and the effective boundary condition at $z = -d_l$. Thus, only a two-layer problem needs to be solved at a time. The effective boundary conditions can be derived in terms of the effective reflection matrices and the effective source vectors which can be solved recursively. Therefore, the size of the matrices need not be increased compared to the two-layer case and the complexity of the problem is not increased. In this way the brightness temperature can be computed very efficiently.

Consider l -th random layer for $l = 1, 2, \dots, N$. First, we assume that the effective boundary conditions at $z = -d_l$ can be expressed as follows:

$$\bar{I}_l^+(z = -d_l) = \bar{\bar{R}}_{l(l+1)}^{eff} \cdot \bar{I}_l^-(z = -d_l) + \bar{\bar{T}}_{(l+1)l} \cdot \bar{I}_{l+1}^{eff} \quad (36)$$

where the effective reflection matrix $\bar{\bar{R}}_{l(l+1)}^{eff}$ and the effective source vector \bar{I}_{l+1}^{eff} contain all the information regarding l' -th layer where $l' < l$. Our goal is to come up with an effective boundary condition at $z = -d_l$ which relates the downward propagating intensity to the upward propagating intensity in region $l - 1$. Thus, the effective reflection matrix and the effective source vector at $z = -d_{l-1}$, $\bar{\bar{R}}_{(l-1)l}^{eff}$ and \bar{I}_l^{eff} , should be expressed in terms of the properties of the l -th layer and the effective reflection matrix and source vector at $z = -d_l$. The boundary conditions at $z = -d_{l-1}$ is given by

$$\bar{I}_l^-(z = -d_{l-1}) = \bar{\bar{R}}_{l(l+1)} \cdot \bar{I}_l^+(z = -d_{l-1}) - \bar{\bar{T}}_{(l-1)l} \cdot \bar{I}_{l-1}^-(z = -d_{l-1}) \quad (37)$$

and

$$\bar{I}_{l-1}^+(z = -d_{l-1}) = \bar{R}_{l(l-1)} \cdot \bar{I}_{l-1}^-(z = -d_{l-1}) + \bar{T}_{l(l-1)} \cdot \bar{I}_l^+(z = -d_{l-1}) \quad (38)$$

Substituting in the solutions for the upward and downward propagating intensities, given by (27), into the boundary conditions (36) and (37), we obtain

$$\begin{aligned} & \left[(\bar{E}_l - \bar{Q}_l) - \bar{R}_{l(l-1)} \cdot (\bar{E}_l + \bar{Q}_l) \right] \cdot \bar{x}_l + \left[(\bar{E}_l + \bar{Q}_l) - \bar{R}_{l(l-1)} \cdot (\bar{E}_l - \bar{Q}_l) \right] \cdot \bar{D}_l(-d_l - d_{l-1}) \cdot \bar{y}_l \\ & = - \left[\bar{I}_l - \bar{R}_{l(l-1)} \right] \cdot \bar{T}_l + \frac{1}{C_l} \bar{T}_{l(l-1)} \cdot \bar{I}_{l-1}^-(z = -d_{l-1}) \end{aligned} \quad (39)$$

$$\begin{aligned} & \left[(\bar{E}_l + \bar{Q}_l) - \bar{R}_{l(l+1)}^{eff} \cdot (\bar{E}_l - \bar{Q}_l) \right] \cdot \bar{D}_l(-d_l - d_{l-1}) \cdot \bar{x}_l + \left[(\bar{E}_l - \bar{Q}_l) - \bar{R}_{l(l+1)}^{eff} \cdot (\bar{E}_l + \bar{Q}_l) \right] \cdot \bar{y}_l \\ & = - \left[\bar{I}_l - \bar{R}_{l(l+1)}^{eff} \right] \cdot \bar{T}_l + \frac{1}{C_l} \bar{T}_{l(l+1)} \cdot \bar{I}_{l+1}^{eff} \end{aligned} \quad (40)$$

The above equations can be solved for the constants \bar{x}_l and \bar{y}_l . We let

$$\bar{f}_l = \begin{bmatrix} \bar{x}_l \\ \bar{y}_l \end{bmatrix} \quad (41)$$

$$\bar{M}_l = \begin{bmatrix} \bar{M}_{11l} & \bar{M}_{12l} \\ \bar{M}_{21l} & \bar{M}_{22l} \end{bmatrix} \quad (42)$$

$$\bar{N}_l = \begin{bmatrix} \bar{I}_l \\ 0 \end{bmatrix} \quad \bar{N}'_l = \begin{bmatrix} 0 \\ \bar{I}_l \end{bmatrix} \quad (43)$$

$$\bar{O}_l = \begin{bmatrix} -\bar{I}_l + \bar{R}_{l(l-1)} \\ -\bar{I}_l + \bar{R}_{l(l+1)}^{eff} \end{bmatrix} \quad (44)$$

where

$$\bar{M}_{11} = (\bar{E}_l - \bar{Q}_l) - \bar{R}_{l(l-1)} \cdot (\bar{E}_l - \bar{Q}_l) \quad (45a)$$

$$\bar{M}_{12} = [(\bar{E}_l + \bar{Q}_l) - \bar{R}_{l(l-1)} \cdot (\bar{E}_l - \bar{Q}_l)] \cdot \bar{D}_l(-(d_l - d_{l-1})) \quad (45b)$$

$$\bar{M}_{21} = [(\bar{E}_l + \bar{Q}_l) - \bar{R}_{l(l-1)}^{eff} \cdot (\bar{E}_l - \bar{Q}_l)] \cdot \bar{D}_l(-(d_l - d_{l-1})) \quad (45c)$$

$$\bar{M}_{22} = (\bar{E}_l - \bar{Q}_l) - \bar{R}_{l(l-1)}^{eff} \cdot (\bar{E}_l - \bar{Q}_l) \quad (45d)$$

Then, (39) and (40) can be written into a compact form as

$$\bar{M}_l \cdot \bar{f}_l = \frac{1}{C_l} \bar{N}_l \cdot \bar{T}_{(l-1)l} \cdot \bar{I}_{l-1}^-(z = -d_{l-1}) + \bar{O}_l \cdot \bar{T}_l + \frac{1}{C_l} \bar{N}'_l \cdot \bar{T}_{(l+1)l} \cdot \bar{I}_{l+1}^{eff} \quad (46)$$

The boundary condition (38) can now be used to derive the effective boundary condition at $z = -d_l$. We have, from (27),

$$\bar{I}_l^+(z = -d_{l-1}) = C_l \left[\bar{T}_l + (\bar{E}_l + \bar{Q}_l) \cdot \bar{x}_l + (\bar{E}_l - \bar{Q}_l) \cdot \bar{D}_l(-(d_l - d_{l-1})) \cdot \bar{y}_l \right] \quad (47)$$

We let

$$\bar{L}_l = \left[\bar{L}_{1l} \quad \bar{L}_{2l} \right] \quad (48)$$

where

$$\bar{L}_{1l} = (\bar{E}_l + \bar{Q}_l) \quad (49a)$$

$$\bar{L}_{2l} = (\bar{E}_l - \bar{Q}_l) \cdot \bar{D}_l(-(d_l - d_{l-1})) \quad (49b)$$

Then, making use of (46), we obtain

$$\bar{I}_l^+(z = -d_{l-1}) = C_l \bar{T}_l + \bar{L}_l \cdot \bar{M}_l^{-1} \cdot \left[\bar{N}_l \cdot \bar{T}_{(l-1)l} \cdot \bar{I}_{l-1}^-(z = -d_{l-1}) - C_l \bar{O}_l \cdot \bar{T}_l + \bar{N}_l' \cdot \bar{T}_{(l+1)l} \cdot \bar{I}_{l+1}^{eff} \right] \quad (50)$$

Substituting the above equation into (38) we obtain the following effective boundary conditions at $z = -d_{l-1}$,

$$\bar{I}_{l-1}^-(z = -d_{l-1}) = \bar{R}_{(l-1)l}^{eff} \cdot \bar{I}_{l-1}^-(z = -d_{l-1}) + \bar{T}_{l(l-1)} \cdot \bar{I}_l^{eff} \quad (51)$$

where

$$\bar{R}_{(l-1)l}^{eff} = \bar{R}_{(l-1)l} + \bar{T}_{l(l-1)} \cdot \bar{L}_l \cdot \bar{M}_l^{-1} \cdot \bar{N}_l \cdot \bar{T}_{(l-1)l} \quad (52)$$

and

$$\bar{I}_l^{eff} = C_l \bar{T}_l + C_l \bar{L}_l \cdot \bar{M}_l^{-1} \cdot \bar{O}_l \cdot \bar{T}_l + \bar{L}_l \cdot \bar{M}_l^{-1} \cdot \bar{N}_l' \cdot \bar{T}_{(l+1)l} \cdot \bar{I}_{l+1}^{eff} \quad (53)$$

The above effective boundary condition at $z = -d_{l-1}$ is defined in terms of the properties of the l -th layer and the effective boundary condition at $z = -d_l$. Therefore, the effective reflection matrix and the effective source vector can be calculated recursively, and we only need to consider a two-layer problem at a time. Note that at $z = -d_N$, we have

$$\bar{R}_{N(N+1)}^{eff} = \bar{R}_{N(N+1)} \quad (54)$$

and

$$\bar{I}_{N+1}^{eff} = \bar{I}_{N+1}^+ = C_{N+1} \bar{T}_{N+1} \quad (55)$$

We start the calculation at the N -th layer where $\bar{R}_{N(N+1)}$ and \bar{I}_{N+1}^+ are known and obtain the effective boundary condition at $z = -d_{N-1}$. Once the effective boundary at

$z = -d_{N-1}$ is obtained we start over and calculate the effective boundary conditions at $z = -d_{N-2}$. This is repeated until we have calculated \bar{R}_{01}^{eff} and \bar{I}_1^{eff} . Then, the brightness temperature is obtained from

$$\bar{T}_B = \frac{1}{C_{\nu}} \bar{R}_{01}^{eff} \bar{I}_{skd} + \frac{1}{C_{\nu}} \bar{T}_{10} \bar{I}_1^{eff} \quad (56)$$

6.5 Results and Discussion

In this section we illustrate the numerical results of the brightness temperatures for layered random medium. In our calculations $n = 16$ is used. In Figures 6.2–6.6 we show the result of data matching of the brightness temperature measurements from a snow field [Shiue *et al.*, 1978]. Experiments have been conducted by NASA Goddard Space Flight Center in cooperation with the National Bureau of Standards in the Rocky Mountains of Colorado during the winter season of 1977-1978. A set of four microwave radiometers at frequencies 5, 10.7, 18, and 37 GHz were used to measure the brightness temperature of a snowpack. In Fig. 6.2, the brightness temperatures are plotted as a function of frequency for viewing angle of 33° , and matched with a two-layer model. Ground truth measurements of depth gives $d = 66$ cm. The angular dependence of the brightness temperatures at four different frequencies are matched with the same theoretical parameters in Figs. 6.3, 6.4, 6.5 and 6.6.

In Fig. 6.7, the brightness temperatures is plotted as a function of frequency for a three-layer random medium and compared with the two-layer case. In a three-layer case we introduced a thin lossy layer at the top to model the melting of snowpack in the afternoon due to sun-light illumination. This model can be used to explain the diurnal change in the snowfield [Hofer and Schanda, 1978; Stiles and Ulaby, 1980] where brightness temperature decreases as a function of frequency in the morning and increases in the afternoon.

Appendix: Scattering Function Matrix, Scattering Coefficient, and Absorption Coefficient for the Random Medium

The scattering function matrix have been derived for the random medium whose fluctuating permittivity is characterized by the correlation function

$$\langle \epsilon_{jl}(\bar{r}') \epsilon_{jl}^*(\bar{r}'') \rangle = \delta_l \epsilon_l^2 b_l(\bar{r}' - \bar{r}'') \quad (A1)$$

where δ_l is the variance of the fluctuation and the function $b_l(\bar{r}' - \bar{r}'')$ is the normalized correlation function. For the correlation function we assume gaussian dependence laterally and exponential dependence vertically

$$b_l(\bar{r}' - \bar{r}'') = \exp \left[-\frac{(x' - x'')^2 + (y' - y'')^2}{l_{\rho l}^2} - \frac{|z' - z''|}{l_{z l}} \right] \quad (A2)$$

The spectral density for the above correlation function is given by

$$\begin{aligned} \Phi_l(\theta_l, \phi_l; \theta'_l, \phi'_l) &= \frac{l_{z l} l_{\rho l}^2}{4\pi^2 [1 + k_l^2 l_{z l}^2 (\cos \theta'_l - \cos \theta_l)^2]} \\ &\times \exp \left[-\frac{k_l^2 l_{\rho l}^2}{4} [\sin^2 \theta'_l + \sin^2 \theta_l - 2 \sin \theta'_l \sin \theta_l \cos(\phi'_l - \phi_l)] \right] \end{aligned} \quad (A2)$$

The scattering function matrix is given by [Tsang and Kong, 1976b]

$$\bar{\bar{P}}_l(\theta_l, \theta'_l) = \begin{bmatrix} P_{11l} & P_{12l} \\ P_{21l} & P_{22l} \end{bmatrix} \quad (A3)$$

where

$$\begin{aligned} P_{11l} &= q_l(\theta_l, \theta'_l) e^{-\eta_l} \left[\sin^2 \theta_l \sin^2 \theta'_l I_0(x_l) + 2 \sin \theta_l \sin \theta'_l \cos \theta_l \cos \theta'_l I_1(x_l) \right. \\ &\quad \left. + \frac{1}{2} \cos^2 \theta_l \cos^2 \theta'_l (I_0(x_l) + I_2(x_l)) \right] \end{aligned} \quad (A4)$$

$$P_{12i} = q_i(\theta_i, \theta'_i) \epsilon^{-y_i} \frac{1}{2} \cos^2 \theta_i (I_0(x_i) - I_2(x_i)) \quad (A5)$$

$$P_{21i} = q_i(\theta_i, \theta'_i) \epsilon^{-y_i} \frac{1}{2} \cos^2 \theta'_i (I_0(x_i) - I_2(x_i)) \quad (A6)$$

$$P_{22i} = q_i(\theta_i, \theta'_i) \epsilon^{-y_i} \frac{1}{2} (I_0(x_i) - I_2(x_i)) \quad (A7)$$

with

$$q_i(\theta_i, \theta'_i) = \frac{\delta_i k_i'^4}{4} \frac{l_{\rho i}^2 l_{z i}}{1 + k_i'^2 l_{z i}^2 (\cos \theta_i - \cos \theta'_i)^2} \quad (A8)$$

$$y_i = \frac{1}{4} k_i'^2 l_{\rho i}^2 (\sin^2 \theta_i + \sin^2 \theta'_i) \quad (A9)$$

$$x_i = \frac{1}{2} k_i'^2 l_{\rho i}^2 \sin \theta_i \sin \theta'_i \quad (A10)$$

and I_m is the m -th order modified Bessel function.

The scattering coefficient $\overline{\overline{K}}_{sl}(\theta_l)$ is given by

$$\overline{\overline{K}}_{sl}(\theta_l) = \begin{bmatrix} K_{sl} & 0 \\ 0 & K_{hl} \end{bmatrix} \quad (A11)$$

where

$$K_{sl}(\theta'_l) = \int_0^\pi d\theta_l \sin \theta_l [P_{11i}(\theta_l, \theta'_l) + P_{21i}(\theta_l, \theta'_l)] \quad (A12)$$

$$K_{hl}(\theta'_l) = \int_0^\pi d\theta_l \sin \theta_l [P_{12i}(\theta_l, \theta'_l) + P_{22i}(\theta_l, \theta'_l)] \quad (A13)$$

The absorption coefficient K_{al} is given by

$$K_{al} = 2k_i'' \quad (A14)$$

where k_i'' is the imaginary part of the wave number in region l .

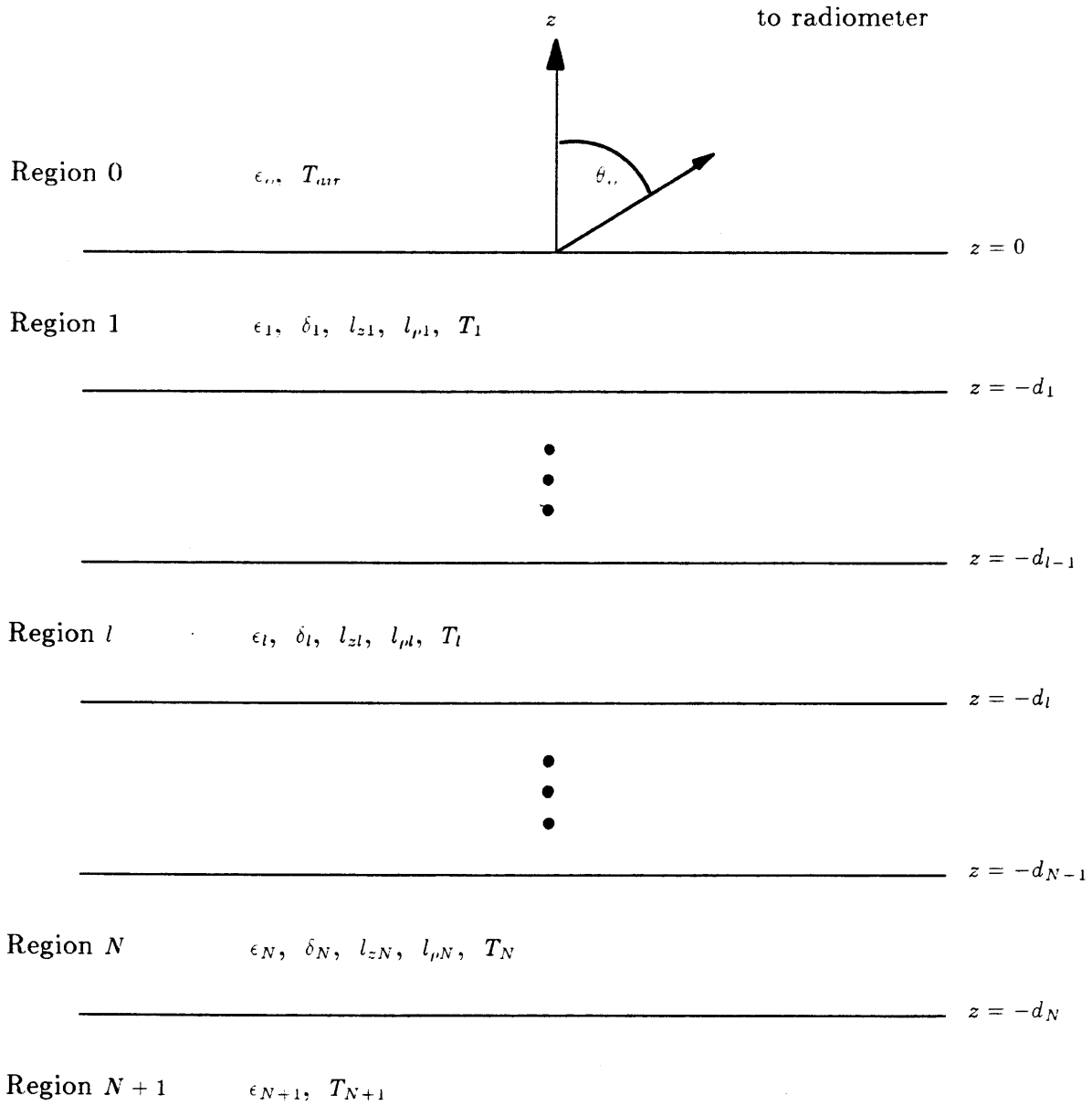


Figure 6.1 Geometrical configuration of the problem.

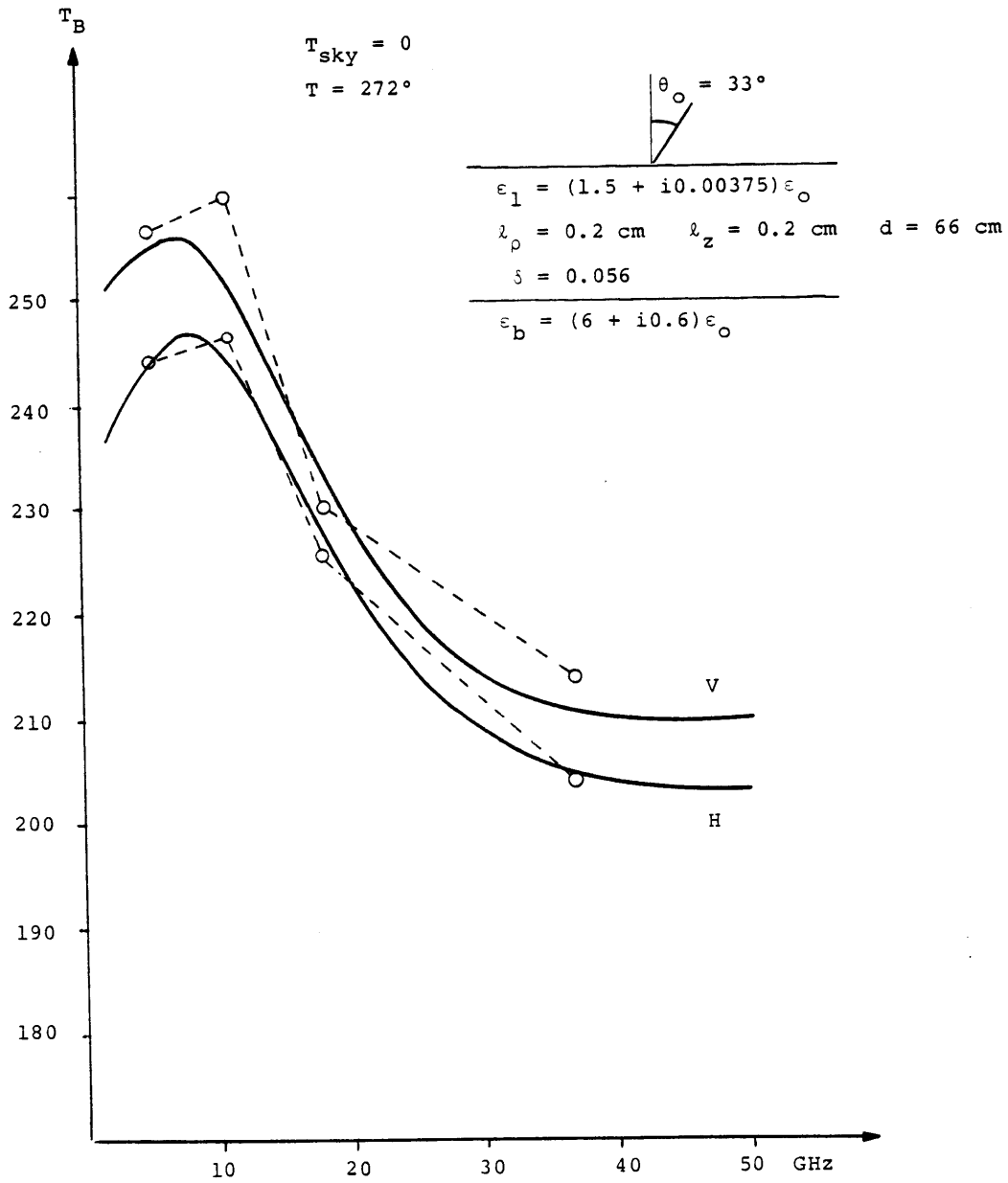


Figure 6.2 Brightness temperature as a function of frequency.

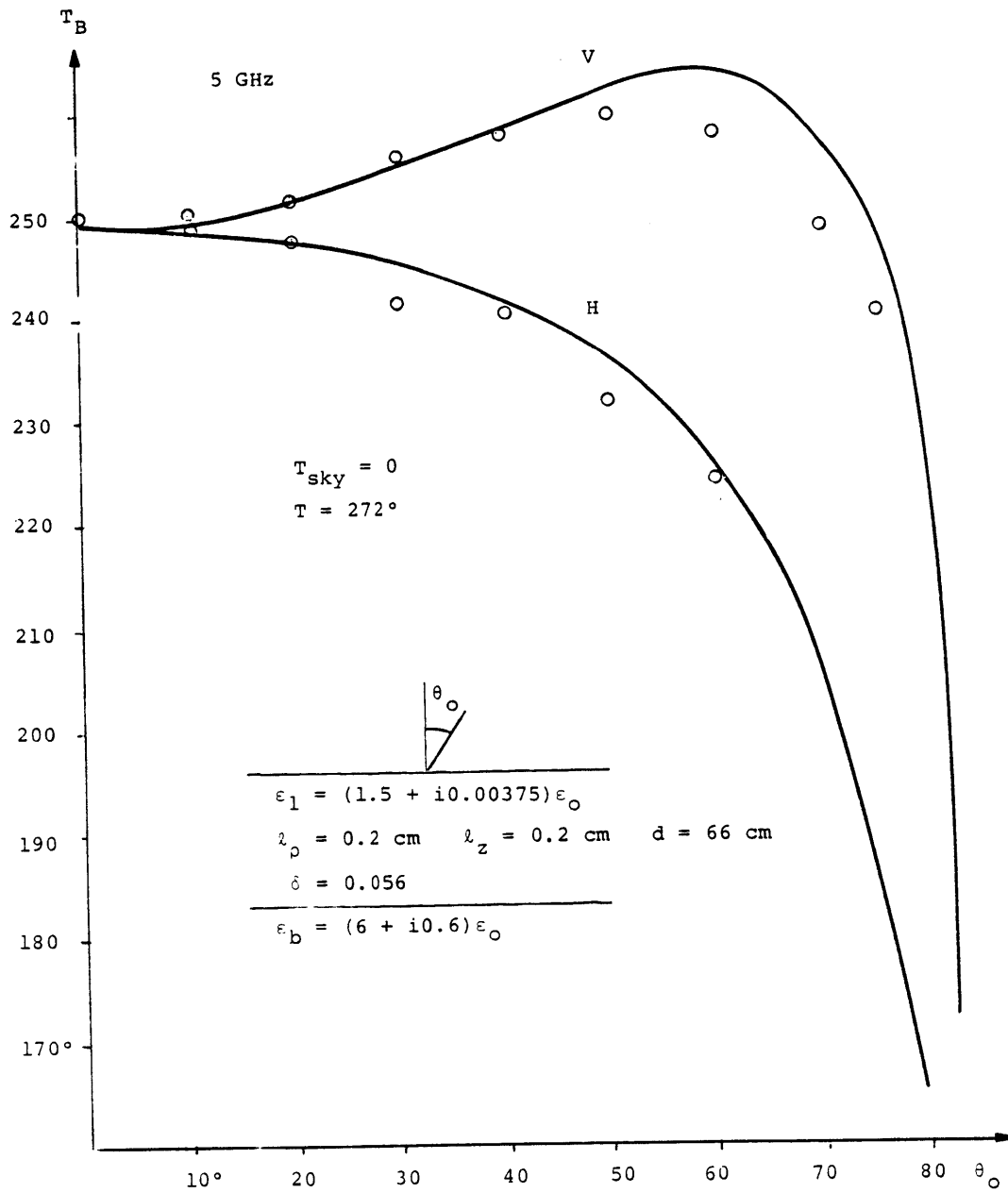


Figure 6.3 Brightness temperature as a function of observation angle at 5 GHz.

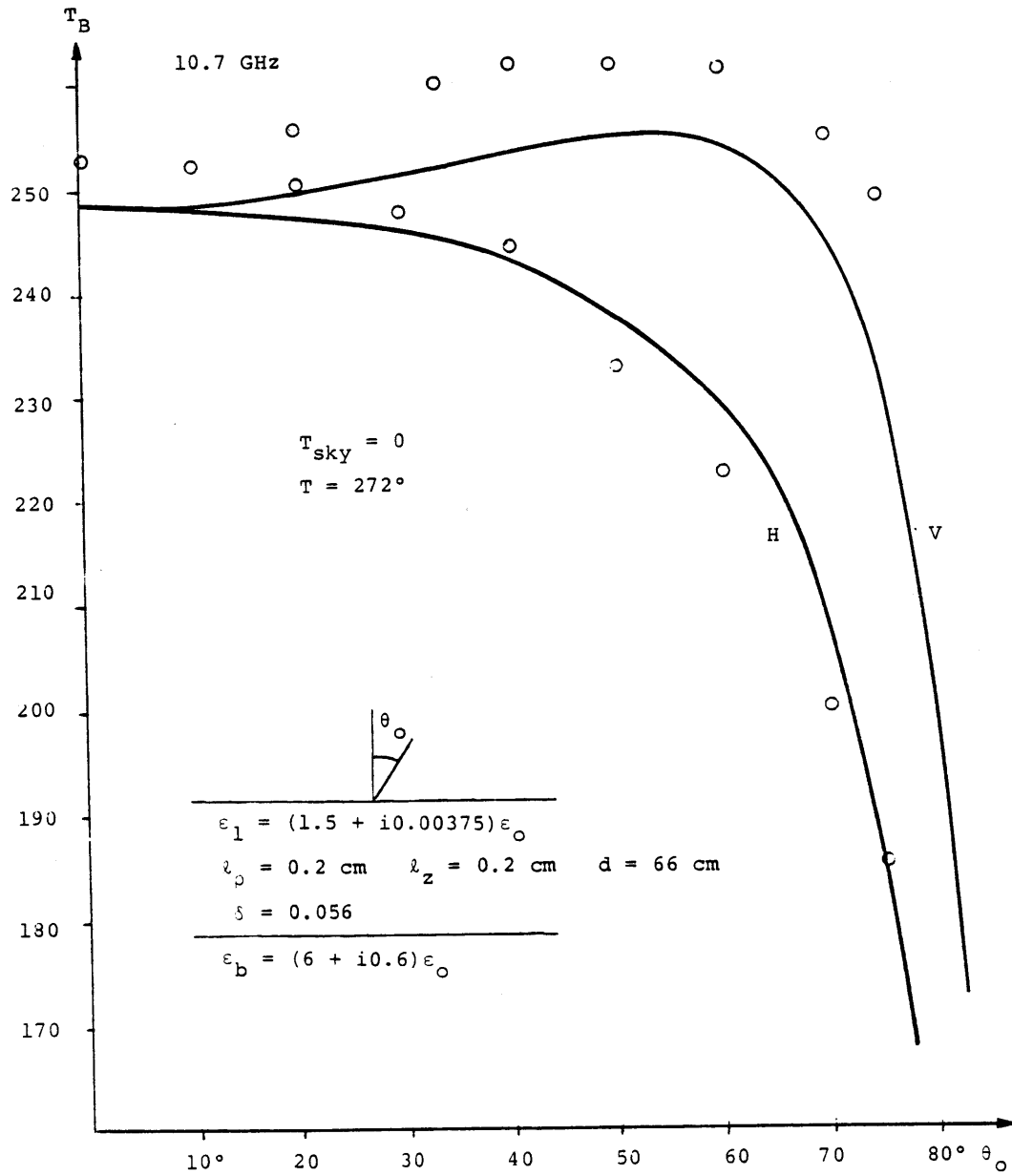


Figure 6.4 Brightness temperature as a function of observation angle at 10.7 GHz.

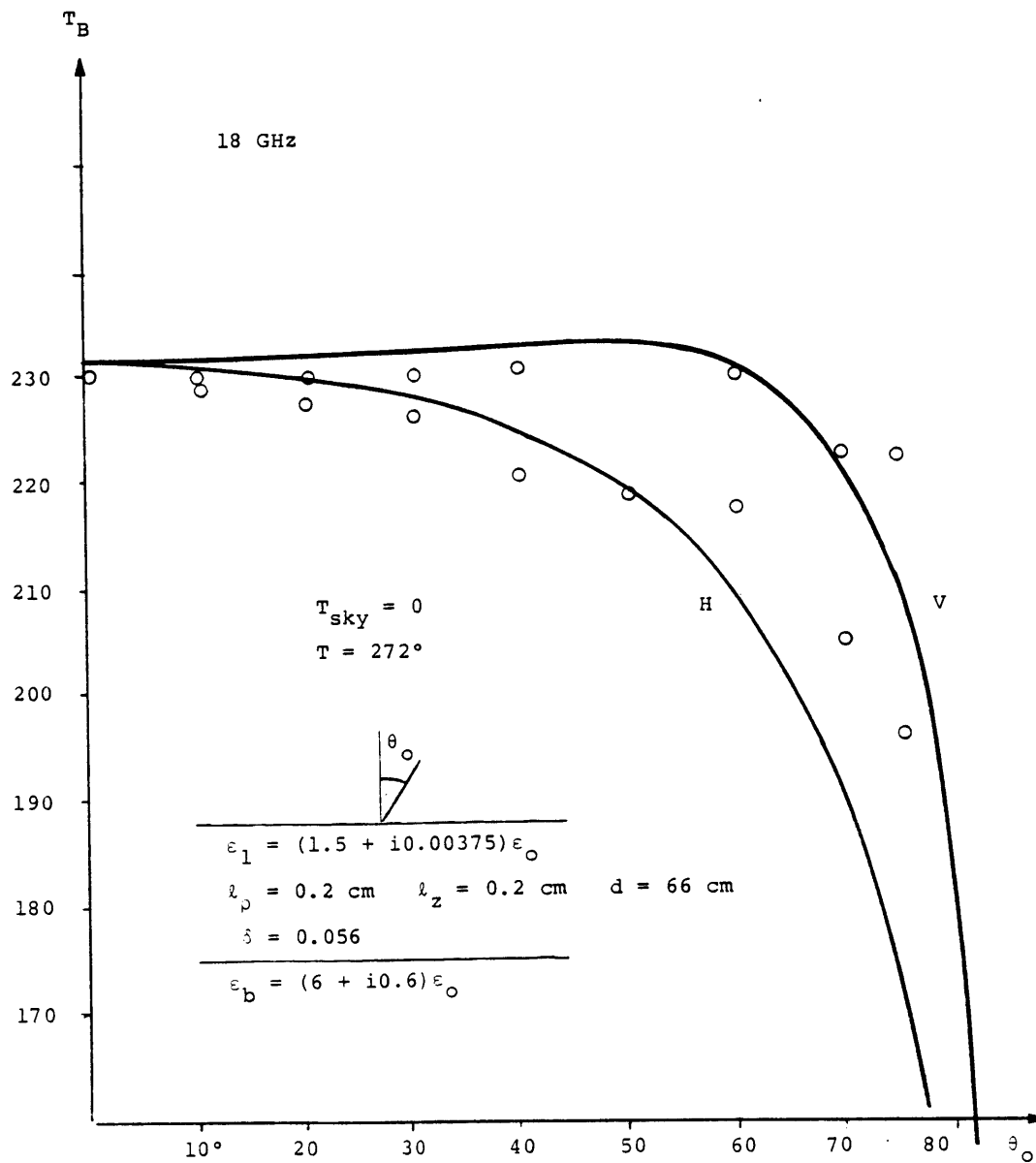


Figure 6.5 Brightness temperature as a function of observation angle at 18 GHz.

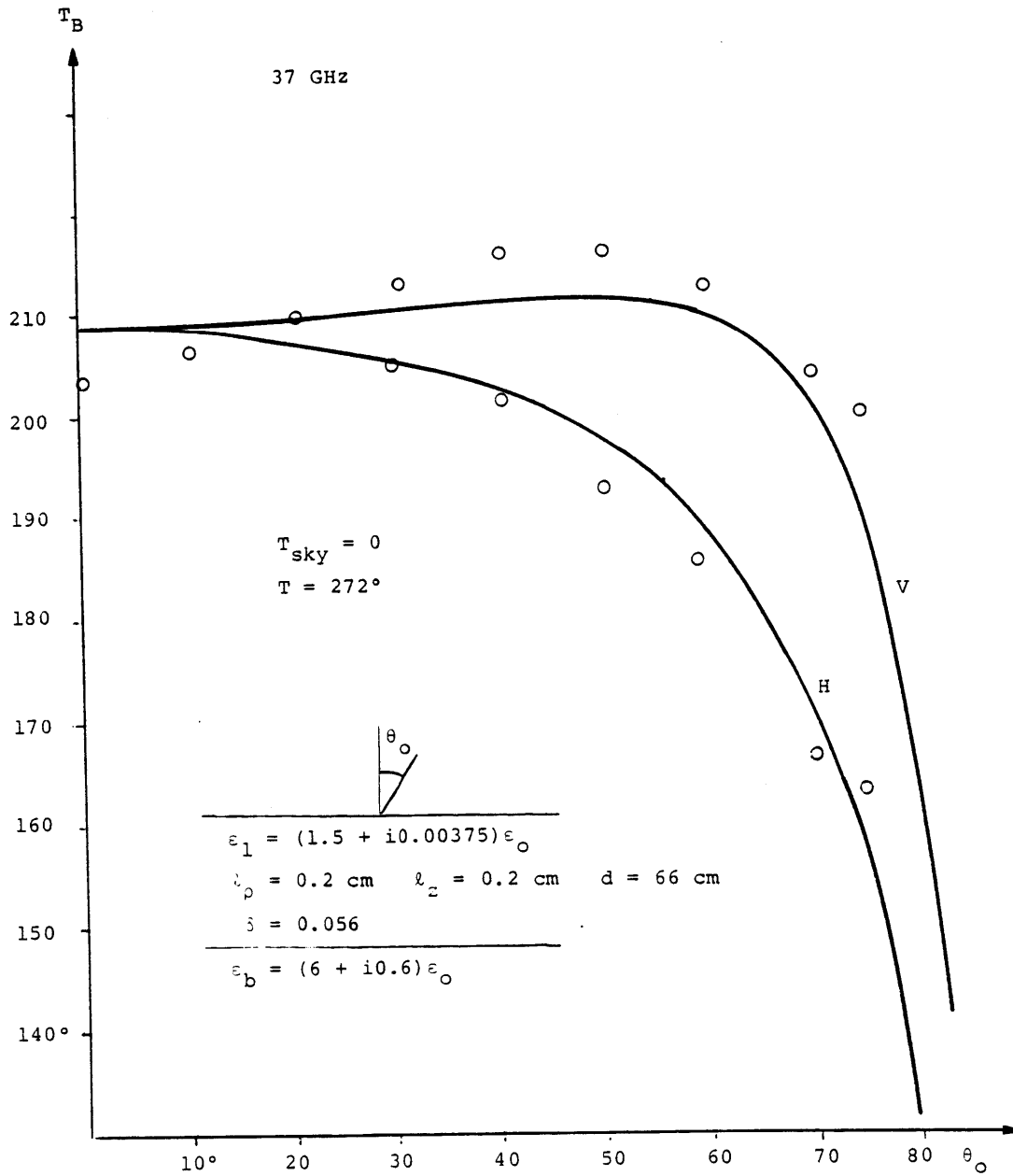


Figure 6.6 Brightness temperature as a function of observation angle at 37 GHz.

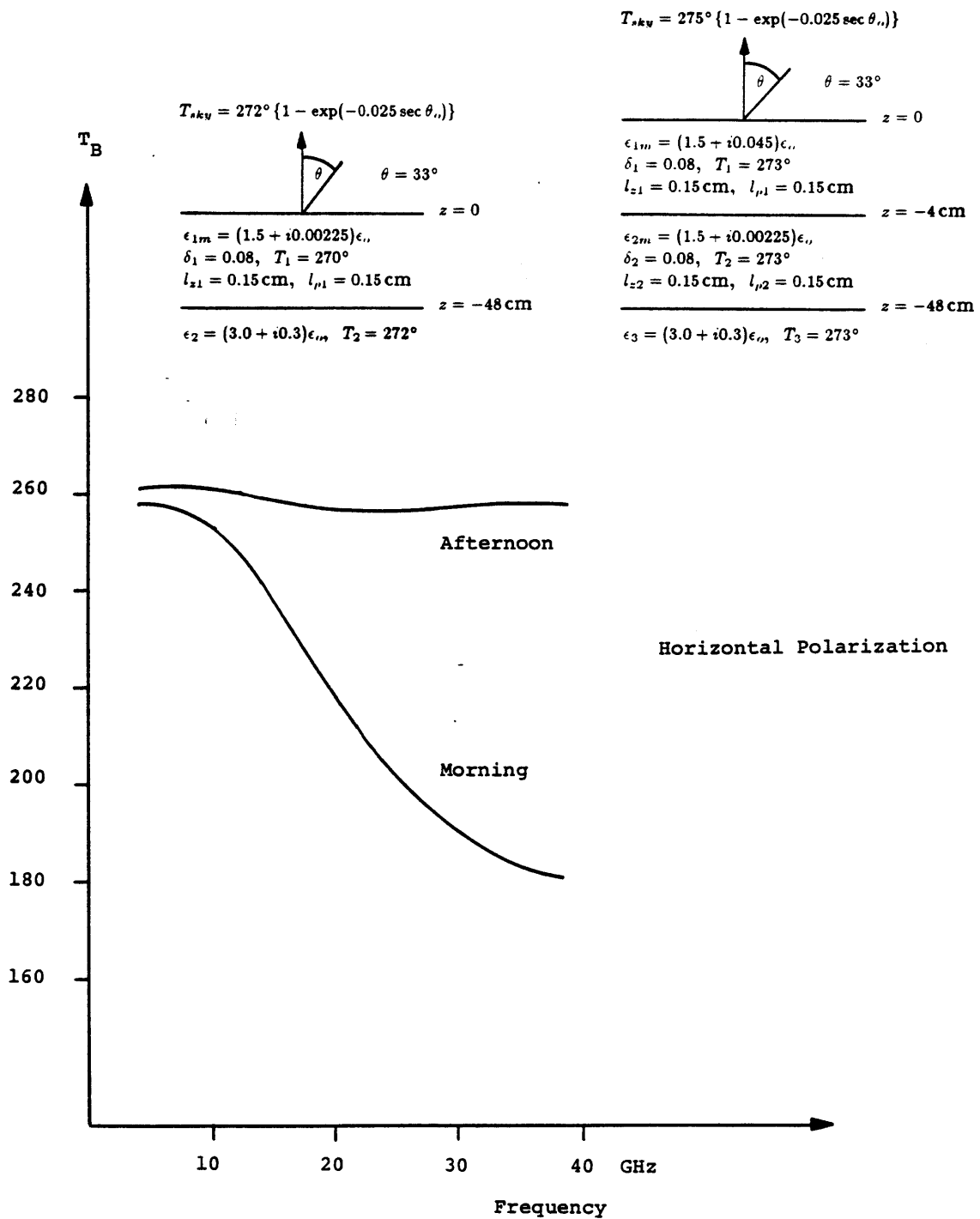


Figure 6.7 Brightness temperature as a function of frequency for a three-layer random medium.

CHAPTER 7**Radiative Transfer Theory for Active Remote Sensing
of Two-Layer Random Medium**

The radiative transfer theory with a two-layer random medium model is used to study the effect of volume scattering for active remote sensing of low-loss and scattering dominant areas. Bistatic scattering coefficients are obtained by solving the radiative transfer equations numerically using the Fourier-series expansion in the azimuthal direction and the Gaussian quadrature method. Depolarization effect in the backscattering direction is exhibited. Theoretical results are compared and illustrated for the various cases.

7.1 Introduction

In microwave remote sensing of earth terrain, the effects of volume scattering have been treated with random medium and discrete scatterer models for terrain media. The discrete scatterer model with the radiative transfer theory has been used to study passive and active microwave remote sensing. In passive remote sensing, Rayleigh and Mie scattering functions have been used to study the thermal microwave emission from layered medium with planar and rough interfaces [England, 1975; Chang *et al.*, 1976; Tsang and Kong, 1977a, 1979; Kong *et al.*, 1979; Fung and Chen, 1981a; Shin and Kong, 1982]. In active remote sensing, the Rayleigh scattering model has been used extensively [Shin and Kong, 1981; Fung and Eom, 1981; Fung and Chen, 1981b; Karam and Fung, 1982]. The random medium model with the radiative transfer theory has been used to study passive remote sensing from layered earth terrain [Gurvich *et al.*, 1973; Tsang and Kong, 1975, 1976b, 1980b; Djermakoye and Kong, 1979; Chuang and Kong, 1980]. In active remote sensing, wave approaches with iterative solutions have been used widely with the random medium model to calculate the scattering coefficients [Tsang and Kong, 1976a; Zuniga and Kong, 1980; Zuniga *et al.*, 1979, 1980]. The depolarization effect in the backscattering direction has been shown to be the second-order effect [Zuniga *et al.*, 1980]. The radiative transfer theory with the random medium model has been applied to active remote sensing by Tsang and Kong [1978] where the iterative approach is applied to second order in albedo to calculate the bistatic scattering coefficients from a halfspace random medium.

In this chapter we solve the problem of scattering from a layer of random medium on top of a homogeneous halfspace using the radiative transfer theory. Using all four Stokes parameters the bistatic scattering coefficients are calculated using a numeri-

cal approach which provides a valid solution for both small and large albedos. A Fourier-series expansion in the azimuthal direction is used to eliminate the azimuthal ϕ dependence from the radiative transfer equations. Then the set of equations without the ϕ dependence is solved using the method of Gaussian quadrature. The integrals in the radiative transfer equations are replaced by a Gaussian quadrature and the resulting system of first-order differential equations is solved by obtaining eigenvalues and eigenvectors and matching the boundary conditions. The order of system of eigen-equations is reduced for more efficient computation by making use of the symmetry properties of the scattering function matrix. The numerical results are illustrated by plotting backscattering cross sections and the bistatic scattering coefficients as functions of frequency, incident angle, and the scattering angles.

7.2 Formulation

Consider a layer of random medium characterized by the permittivity $\epsilon_1 + \epsilon_f$, where ϵ_f stands for the randomly fluctuating part whose amplitude is very small and whose ensemble average is zero, on top of a homogeneous medium with permittivity ϵ_2 [Fig. 7.1]. The radiative transfer equations which govern the propagation of intensities inside the scattering medium are, for $0 < \theta < \pi$,

$$\cos \theta \frac{d}{dz} \bar{I}(\theta, \phi, z) = -K_a \bar{I}(\theta, \phi, z) - \bar{K}_s(\theta) \cdot \bar{I}(\theta, \phi, z) + \int_0^\pi d\theta' \sin \theta' \int_0^{2\pi} d\phi' \bar{P}(\theta, \phi; \theta', \phi') \cdot \bar{I}(\theta', \phi', z) \quad (1)$$

where

$$\bar{I}(\theta, \phi, z) = \begin{bmatrix} I_v(\theta, \phi, z) \\ I_h(\theta, \phi, z) \\ U(\theta, \phi, z) \\ V(\theta, \phi, z) \end{bmatrix} \quad (2)$$

I_v is the vertically polarized specific intensity, I_h is the horizontally polarized specific intensity, and U and V represent the correlation between two polarizations [Tsang and Kong, 1978; Shin and Kong, 1981], $\bar{P}(\theta, \phi; \theta', \phi')$ is a 4×4 scattering function matrix, which relates scattered intensities into the direction (θ, ϕ) from the incident intensities in the direction (θ', ϕ') , K_a is the loss per unit length due to absorption, and $\bar{K}_s(\theta)$ is the loss per unit length due to scattering. The random permittivity fluctuation is characterized by the variance of the fluctuation δ and the correlation function with lateral correlation length l_r and vertical correlation length l_z . The scattering function matrix and the scattering coefficient have been derived by applying Born approximation with the far-field solution and the explicit expressions for the correlation function with gaussian dependence laterally and exponential dependence vertically are given in Appendix A [Tsang and Kong, 1978].

Consider an incident wave with specific intensity $\bar{I}_{oi}(\pi - \theta_o, \phi_o)$ impinging from region 0, which is assumed to be free space, upon the scattering layer. The incident beam in region 0 assumes the form

$$\bar{I}_{oi}(\pi - \theta_o, \phi_o) = \bar{I}_{oi} \delta(\cos \theta_o - \cos \theta_{oi}) \delta(\phi_o - \phi_{oi}) \quad (3)$$

where the use of Dirac delta function is made.

The boundary conditions for the four Stokes parameters at a planar dielectric interface have been derived [Tsang and Kong, 1975] from the continuity of tangential electric and magnetic fields. The results are, for $0 < \theta < \pi/2$, at $z = 0$,

$$\bar{I}(\pi - \theta, \phi, z = 0) = \bar{\bar{T}}_{01}(\theta_o) \cdot \bar{I}_{oi}(\pi - \theta_o, \phi_o) + \bar{\bar{R}}_{10}(\theta) \cdot \bar{I}(\theta, \phi, z = 0) \quad (4)$$

and, at $z = -d$,

$$\bar{I}(\theta, \phi, z = -d) = \bar{\bar{R}}_{12}(\theta) \cdot \bar{I}(\pi - \theta, \phi, z = -d) \quad (5)$$

where we have broken up intensities in the scattering layer into upward going intensities $\bar{I}(\theta, \phi, z)$ and downward going intensities $\bar{I}(\pi - \theta, \phi, z)$. In the above equations, $\bar{\bar{T}}_{01}(\theta_o)$ represents the coupling from region 0 to region 1, $\bar{\bar{R}}_{10}(\theta)$ represents the coupling from upward going intensities into downward going intensities at the boundary of region 1 and region 0, and $\bar{\bar{R}}_{12}(\theta)$ represents similar coupling at the boundary of region 1 and region 2 [Appendix B].

Once the radiative transfer equations are solved subject to the boundary conditions (4) and (5), the intensity in the direction (θ_{os}, ϕ_{os}) in region 0 is

$$\bar{I}_o(\theta_{os}, \phi_{os}) = \bar{\bar{T}}_{10}(\theta_s) \cdot \bar{I}(\theta_s, \phi_s, z = 0) + \bar{\bar{R}}_{01}(\theta_o) \cdot \bar{I}_{oi}(\pi - \theta_o, \phi_o) \quad (6)$$

where $\bar{T}_{10}(\theta)$ represents the coupling from region 1 to region 0. The bistatic scattering coefficients $\gamma_{\beta\alpha}(\theta_{os}, \phi_{os}; \theta_{oi}, \phi_{oi})$ are defined as the ratio of the scattered power of polarization β per unit solid angle in the direction (θ_{os}, ϕ_{os}) and the intercepted incident power of polarization α in the direction (θ_{oi}, ϕ_{oi}) averaged over 4π radians [Peake, 1959].

$$\gamma_{\beta\alpha}(\theta_{os}, \phi_{os}; \theta_{oi}, \phi_{oi}) = 4\pi \frac{\cos \theta_{os} I_{\beta\alpha}(\theta_{os}, \phi_{os})}{\cos \theta_{oi} I_{\alpha\alpha}} \quad (7)$$

where $\alpha, \beta = v$ or h with v denoting vertical polarization and h denoting horizontal polarization. In the backscattering direction $\theta_{os} = \theta_{oi}$ and $\phi_{os} = \pi - \phi_{oi}$. The backscattering cross sections per unit area are defined to be

$$\sigma_{\beta\alpha}(\theta_{oi}) = \cos \theta_{oi} \gamma_{\beta\alpha}(\theta_{oi}, \pi + \phi_{oi}; \theta_{oi}, \phi_{oi}) \quad (8)$$

7.3 Fourier Series Expansion

The radiative transfer equations can be solved using an iterative approach which gives closed form solutions [Tsang and Kong, 1978; Shin and Kong, 1981] when the effect of scattering is small (small albedo). The radiative transfer equations and the boundary conditions are cast into the integral equation form, then an iterative process is applied to solve the integral equation to both the first and second order in albedo. The depolarization of the backscattered intensities has been shown to be the second-order effect. However, for the general cases when the effect of scattering is not small, we must resort to the numerical approach to solve the radiative transfer equations. We first use a Fourier-series expansion in the azimuthal direction to eliminate the ϕ -dependence from the radiative transfer equations. We let

$$\bar{I}(\theta, \phi, z) = \sum_{m=0}^{\infty} \left[\bar{I}^{m_c}(\theta, z) \cos m(\phi - \phi_i) + \bar{I}^{m_s}(\theta, z) \sin m(\phi - \phi_i) \right] \quad (8)$$

$$\bar{\bar{P}}(\theta, \phi; \theta', \phi') = \sum_{m=0}^{\infty} \frac{1}{(1 + \delta_m)\pi} \left[\bar{\bar{P}}^{m_c}(\theta, \theta') \cos m(\phi - \phi') + \bar{\bar{P}}^{m_s}(\theta, \theta') \sin m(\phi - \phi') \right] \quad (9)$$

where superscript m indicates the order of harmonic in the azimuthal direction, superscripts c and s indicate the cosine and sine dependence, and Neumann number $\delta_m = 0$ for $m \neq 0$ and $\delta_0 = 1$. Also note that the zeroth-order sine dependence terms are zero.

$$\bar{I}''^s(\theta, z) = 0 \quad (10a)$$

$$\bar{\bar{P}}''^s(\theta, \theta') = 0 \quad (10b)$$

Substituting (8) and (9) into the radiative transfer equations, the ϕ' -integration can be carried out. Then, by collecting terms with the same sine or cosine dependence, we

obtain a set of equations without the ϕ dependence. For $m = 0, 1, 2, \dots$

$$\begin{aligned} \cos \theta \frac{d}{dz} \bar{I}^{mc}(\theta, z) &= -K_a \bar{I}^{mc}(\theta, z) - \bar{K}_s(\theta) \cdot \bar{I}^{mc}(\theta, z) \\ &+ \int_0^\pi d\theta' \sin \theta' \left[\bar{P}^{mc}(\theta, \theta') \cdot \bar{I}^{ms}(\theta', z) - \bar{P}^{ms}(\theta, \theta') \cdot \bar{I}^{mc}(\theta', z) \right] \end{aligned} \quad (11)$$

$$\begin{aligned} \cos \theta \frac{d}{dz} \bar{I}^{ms}(\theta, z) &= -K_a \bar{I}^{ms}(\theta, z) - \bar{K}_s(\theta) \cdot \bar{I}^{ms}(\theta, z) \\ &+ \int_0^\pi d\theta' \sin \theta' \left[\bar{P}^{ms}(\theta, \theta') \cdot \bar{I}^{mc}(\theta', z) + \bar{P}^{mc}(\theta, \theta') \cdot \bar{I}^{ms}(\theta', z) \right] \end{aligned} \quad (12)$$

The closed form expressions for the Fourier-series expanded scattering function matrices $\bar{P}^{mc}(\theta, \theta')$ and $\bar{P}^{ms}(\theta, \theta')$ are obtained [Appendix C]. We note that for azimuthally isotropic media the scattering function matrix can be expanded as

$$\bar{P}^{mc}(\theta, \theta') = \begin{bmatrix} P_{11}^{mc} & P_{12}^{mc} & 0 & 0 \\ P_{21}^{mc} & P_{22}^{mc} & 0 & 0 \\ 0 & 0 & P_{33}^{mc} & P_{34}^{mc} \\ 0 & 0 & P_{43}^{mc} & P_{44}^{mc} \end{bmatrix} \quad (13a)$$

$$\bar{P}^{ms}(\theta, \theta') = \begin{bmatrix} 0 & 0 & P_{13}^{ms} & P_{14}^{ms} \\ 0 & 0 & P_{23}^{ms} & P_{24}^{ms} \\ P_{31}^{ms} & P_{32}^{ms} & 0 & 0 \\ P_{41}^{ms} & P_{42}^{ms} & 0 & 0 \end{bmatrix} \quad (13b)$$

Thus, the coupled equations (11) and (12) can be changed into two decoupled equations by defining

$$\bar{I}^{mc}(\theta, z) = \begin{bmatrix} I_v^{mc}(\theta, z) \\ I_h^{mc}(\theta, z) \\ U^{ms}(\theta, z) \\ V^{ms}(\theta, z) \end{bmatrix} \quad (14a)$$

$$\bar{I}^{ms}(\theta, z) = \begin{bmatrix} I_v^{ms}(\theta, z) \\ I_h^{ms}(\theta, z) \\ U^{mc}(\theta, z) \\ V^{mc}(\theta, z) \end{bmatrix} \quad (14b)$$

where superscripts e and o stands for even or odd dependence in the first two Stokes parameters. Decoupled equations are given by, for $m = 0, 1, 2, \dots$

$$\cos \theta \frac{d}{dz} \bar{I}^{m_e}(\theta, z) = -K_a \bar{I}^{m_e}(\theta, z) - \bar{K}_s(\theta) \cdot \bar{I}^{m_e}(\theta, z) + \int_0^\pi d\theta' \sin \theta' \bar{P}^{m_e}(\theta, \theta') \cdot \bar{I}^{m_e}(\theta', z) \quad (15a)$$

$$\cos \theta \frac{d}{dz} \bar{I}^{m_o}(\theta, z) = -K_a \bar{I}^{m_o}(\theta, z) - \bar{K}_s(\theta) \cdot \bar{I}^{m_o}(\theta, z) + \int_0^\pi d\theta' \sin \theta' \bar{P}^{m_o}(\theta, \theta') \cdot \bar{I}^{m_o}(\theta', z) \quad (15b)$$

where

$$\bar{P}^{m_e}(\theta, \theta') = \begin{bmatrix} P_{11}^{m_e} & P_{12}^{m_e} & -P_{13}^{m_e} & -P_{14}^{m_e} \\ P_{21}^{m_e} & P_{22}^{m_e} & -P_{23}^{m_e} & -P_{24}^{m_e} \\ P_{31}^{m_e} & P_{32}^{m_e} & P_{33}^{m_e} & P_{34}^{m_e} \\ P_{41}^{m_e} & P_{42}^{m_e} & P_{43}^{m_e} & P_{44}^{m_e} \end{bmatrix} \quad (16a)$$

$$\bar{P}^{m_o}(\theta, \theta') = \begin{bmatrix} P_{11}^{m_o} & P_{12}^{m_o} & P_{13}^{m_o} & P_{14}^{m_o} \\ P_{21}^{m_o} & P_{22}^{m_o} & P_{23}^{m_o} & P_{24}^{m_o} \\ P_{31}^{m_o} & P_{32}^{m_o} & P_{33}^{m_o} & P_{34}^{m_o} \\ P_{41}^{m_o} & P_{42}^{m_o} & P_{43}^{m_o} & P_{44}^{m_o} \end{bmatrix} \quad (16b)$$

In order to derive the boundary conditions for the Fourier-series expanded intensities, we first expand the incident intensity $\bar{I}_{oi}(\pi - \theta_o, \phi_o)$ into the Fourier series:

$$\begin{aligned} \bar{I}_{oi}(\pi - \theta_o, \phi_o) &= \bar{I}_{oi} \delta(\cos \theta_o - \cos \theta_{oi}) \delta(\phi_o - \phi_{oi}) \\ &= \bar{I}_{oi} \delta(\cos \theta_o - \cos \theta_{oi}) \sum_{m=0}^{\infty} \frac{1}{(\delta_m + 1)\pi} \cos m(\phi_o - \phi_{oi}) \end{aligned} \quad (17)$$

Substituting the above equation along with the Fourier-series expanded intensities into the boundary conditions in (4) and (5) and collecting terms with the same azimuthal dependence, the boundary conditions for each harmonic can be obtained. The results are, for $\alpha = e$ or o , and $0 < \theta < \pi/2$, at $z = 0$

$$\bar{I}^{m_\alpha}(\pi - \theta, z = 0) = \bar{T}_{01}(\theta_o) \cdot \bar{I}_{oi}^{m_\alpha}(\pi - \theta_o) + \bar{R}_{10}(\theta) \cdot \bar{I}^{m_\alpha}(\theta, z = 0) \quad (18)$$

and at $z = -d$

$$\bar{I}^{m\alpha}(\theta, z = -d) = \bar{R}_{12}(\theta) \cdot \bar{I}^{m\alpha}(\pi - \theta, z = -d) \quad (19)$$

where

$$\bar{I}_{oi}^{m\alpha}(\pi - \theta_o) = \bar{I}_{oi}^{m\alpha} \frac{1}{(\delta_m + 1)\pi} \delta(\cos \theta_o - \cos \theta_{oi}) \quad (20)$$

with

$$\bar{I}_{oi}^{mc} = \begin{bmatrix} I_{vi} \\ I_{hi} \\ 0 \\ 0 \end{bmatrix} \quad (21a)$$

$$\bar{I}_{oi}^{m\alpha} = \begin{bmatrix} 0 \\ 0 \\ U_i \\ V_i \end{bmatrix} \quad (21b)$$

We define m_{max} to be the number of harmonics that has to be kept in the expansion of the scattering function matrix such that

$$\bar{P}^{mc}(\theta, \theta') \simeq \bar{P}^{m\alpha}(\theta, \theta') \simeq 0 \quad \text{for } m > m_{max} \quad (22)$$

Then, for $m > m_{max}$ the radiative transfer equations simplify to

$$\cos \theta \frac{d}{dz} \bar{I}^{mc}(\theta, z) = -K_a \bar{I}^{m\alpha} - \bar{K}_s(\theta) \cdot \bar{I}^{mc}(\theta, z) \quad (23a)$$

$$\cos \theta \frac{d}{dz} \bar{I}^{m\alpha}(\theta, z) = -K_a \bar{I}^{m\alpha} - \bar{K}_s(\theta) \cdot \bar{I}^{m\alpha}(\theta, z) \quad (23b)$$

and the solutions to these equations can be obtained analytically, without resorting to the numerical approach.

7.4 Gaussian Quadrature Method

The set of decoupled radiative transfer equations without the azimuthal dependence for each harmonic can be solved numerically using the Gaussian quadrature method. The integrals in the radiative transfer equations are replaced by a Gaussian quadrature, an appropriately weighted sum over $2n$ intervals between $2n$ zeroes of the even-order Legendre polynomial $P_{2n}(\theta)$. The resulting system of $8n$ first-order differential equations are solved by obtaining eigenvalues and eigenvectors and matching the boundary conditions. In obtaining the eigenvalues and eigenvectors, the order of system of equations can be reduced by factor two to $4n$ equations by making use of the symmetry properties of the scattering function matrix and noting that the eigenvalues occur in pairs such that if ξ is an eigenvalue, so is $-\xi$. We first break up the radiative transfer equations into two set of equations by defining, for $\alpha = e, \beta = o$ or $\alpha = o, \beta = e$, and $m = 0, 1, 2, \dots$

$$\bar{I}_1(\theta, z) \equiv \begin{bmatrix} I_{1_1}(\theta, z) \\ I_{1_2}(\theta, z) \end{bmatrix} = \begin{bmatrix} I_v^{m\alpha}(\theta, z) \\ I_h^{m\alpha}(\theta, z) \end{bmatrix} \quad (24a)$$

$$\bar{I}_2(\theta, z) \equiv \begin{bmatrix} I_{2_1}(\theta, z) \\ I_{2_2}(\theta, z) \end{bmatrix} = \begin{bmatrix} U^{m\beta}(\theta, z) \\ V^{m\beta}(\theta, z) \end{bmatrix} \quad (24b)$$

$$\bar{\bar{P}}_{11}(\theta, \theta') \equiv \begin{bmatrix} P_{11_{11}} & P_{11_{12}} \\ P_{11_{21}} & P_{11_{22}} \end{bmatrix} = \begin{bmatrix} P_{11}^{m\alpha} & P_{12}^{m\alpha} \\ P_{21}^{m\alpha} & P_{22}^{m\alpha} \end{bmatrix} \quad (25a)$$

$$\bar{\bar{P}}_{12}(\theta, \theta') \equiv \begin{bmatrix} P_{12_{11}} & P_{12_{12}} \\ P_{12_{21}} & P_{12_{22}} \end{bmatrix} = \begin{bmatrix} P_{13}^{m\alpha} & P_{14}^{m\alpha} \\ P_{23}^{m\alpha} & P_{24}^{m\alpha} \end{bmatrix} \quad (25b)$$

$$\bar{\bar{P}}_{21}(\theta, \theta') \equiv \begin{bmatrix} P_{21_{11}} & P_{21_{12}} \\ P_{21_{21}} & P_{21_{22}} \end{bmatrix} = \begin{bmatrix} P_{31}^{m\alpha} & P_{32}^{m\alpha} \\ P_{41}^{m\alpha} & P_{42}^{m\alpha} \end{bmatrix} \quad (25c)$$

$$\bar{\bar{P}}_{22}(\theta, \theta') \equiv \begin{bmatrix} P_{22_{11}} & P_{22_{12}} \\ P_{22_{21}} & P_{22_{22}} \end{bmatrix} = \begin{bmatrix} P_{33}^{m\alpha} & P_{34}^{m\alpha} \\ P_{43}^{m\alpha} & P_{44}^{m\alpha} \end{bmatrix} \quad (25d)$$

We then have

$$\cos \theta \frac{d}{dz} \bar{I}_1(\theta, z) = -\bar{K}_{c1}(\theta) + \int_0^\pi d\theta' \sin \theta' \left[\bar{P}_{11}(\theta, \theta') \cdot \bar{I}_1(\theta', z) + \bar{P}_{12}(\theta, \theta') \cdot \bar{I}_2(\theta', z) \right] \quad (26a)$$

$$\cos \theta \frac{d}{dz} \bar{I}_2(\theta, z) = -\bar{K}_{c2}(\theta) + \int_0^\pi d\theta' \sin \theta' \left[\bar{P}_{21}(\theta, \theta') \cdot \bar{I}_1(\theta', z) + \bar{P}_{22}(\theta, \theta') \cdot \bar{I}_2(\theta', z) \right] \quad (26b)$$

where

$$\bar{K}_{c1}(\theta) = K_a + \bar{K}_{s1} \quad (27a)$$

$$\bar{K}_{c2}(\theta) = K_a + \bar{K}_{s2} \quad (27b)$$

with

$$\bar{K}_{s1} = \begin{bmatrix} K_v & 0 \\ 0 & K_h \end{bmatrix} \quad (28a)$$

$$\bar{K}_{s2} = \begin{bmatrix} \frac{K_v + K_h}{2} & 0 \\ 0 & \frac{K_v + K_h}{2} \end{bmatrix} \quad (28b)$$

The scattering function matrix can be shown to satisfy the following properties. For $\alpha, \beta = 1$ or 2 ,

$$\bar{P}_{\alpha\alpha}(\theta, \theta') = \bar{P}_{\alpha\alpha}(\pi - \theta, \pi - \theta') \quad (29a)$$

$$\bar{P}_{\alpha\alpha}(\pi - \theta, \theta') = \bar{P}_{\alpha\alpha}(\theta, \pi - \theta') \quad (29b)$$

and for $\alpha \neq \beta$

$$\bar{P}_{\alpha\beta}(\theta, \theta') = -\bar{P}_{\alpha\beta}(\pi - \theta, \pi - \theta') \quad (30a)$$

$$\bar{P}_{\alpha\beta}(\pi - \theta, \theta') = -\bar{P}_{\alpha\beta}(\theta, \pi - \theta') \quad (30b)$$

Further breaking up the intensities into upward and downward propagating intensities, denoted by superscripts + and - respectively, and applying the Gaussian quadrature method, we obtain the following set of equations by making use of the symmetry properties of the scattering function matrix:

$$\bar{\mu} \cdot \frac{d}{dz} \bar{I}_1^+ = -\bar{K}_{e1} \cdot \bar{I}_1^+ + \bar{F}_{11} \cdot \bar{I}_1^+ + \bar{B}_{11} \cdot \bar{I}_1^- + \bar{F}_{12} \cdot \bar{I}_2^+ + \bar{B}_{12} \cdot \bar{I}_2^- \quad (31a)$$

$$-\bar{\mu} \cdot \frac{d}{dz} \bar{I}_1^- = -\bar{K}_{e1} \cdot \bar{I}_1^- + \bar{B}_{11} \cdot \bar{I}_1^+ + \bar{F}_{11} \cdot \bar{I}_1^- - \bar{B}_{12} \cdot \bar{I}_2^+ - \bar{F}_{12} \cdot \bar{I}_2^- \quad (31b)$$

$$\bar{\mu} \cdot \frac{d}{dz} \bar{I}_2^+ = -\bar{K}_{e2} \cdot \bar{I}_2^+ + \bar{F}_{21} \cdot \bar{I}_1^+ + \bar{B}_{21} \cdot \bar{I}_1^- + \bar{F}_{22} \cdot \bar{I}_2^+ + \bar{B}_{22} \cdot \bar{I}_2^- \quad (32a)$$

$$-\bar{\mu} \cdot \frac{d}{dz} \bar{I}_2^- = -\bar{K}_{e2} \cdot \bar{I}_2^- - \bar{B}_{21} \cdot \bar{I}_1^+ - \bar{F}_{21} \cdot \bar{I}_1^- + \bar{B}_{22} \cdot \bar{I}_2^+ + \bar{F}_{22} \cdot \bar{I}_2^- \quad (31b)$$

where, for $\alpha, \beta = 1, 2$, I_α^+ and I_α^- are $2n \times 1$ matrices

$$\bar{I}_\alpha^+ = \begin{bmatrix} I_{\alpha 1}(\mu_1, z) \\ \vdots \\ I_{\alpha 1}(\mu_n, z) \\ I_{\alpha 2}(\mu_1, z) \\ \vdots \\ I_{\alpha 2}(\mu_n, z) \end{bmatrix} \quad \bar{I}_\alpha^- = \begin{bmatrix} I_{\alpha 1}(-\mu_1, z) \\ \vdots \\ I_{\alpha 1}(-\mu_n, z) \\ I_{\alpha 2}(-\mu_1, z) \\ \vdots \\ I_{\alpha 2}(-\mu_n, z) \end{bmatrix} \quad (33)$$

and $\bar{F}_{\alpha\beta}$ and $\bar{B}_{\alpha\beta}$ are $2n \times 2n$ matrices

$$\bar{F}_{\alpha\beta} = \begin{bmatrix} P_{\alpha\beta 11}(\mu_1, \mu_1) & \cdots & P_{\alpha\beta 11}(\mu_1, \mu_n) & P_{\alpha\beta 12}(\mu_1, \mu_1) & \cdots & P_{\alpha\beta 12}(\mu_1, \mu_n) \\ \vdots & \vdots & \vdots & \vdots & \vdots & \vdots \\ P_{\alpha\beta 11}(\mu_n, \mu_1) & \cdots & P_{\alpha\beta 11}(\mu_n, \mu_n) & P_{\alpha\beta 12}(\mu_n, \mu_1) & \cdots & P_{\alpha\beta 12}(\mu_n, \mu_n) \\ P_{\alpha\beta 21}(\mu_1, \mu_1) & \cdots & P_{\alpha\beta 21}(\mu_1, \mu_n) & P_{\alpha\beta 22}(\mu_1, \mu_1) & \cdots & P_{\alpha\beta 22}(\mu_1, \mu_n) \\ \vdots & \vdots & \vdots & \vdots & \vdots & \vdots \\ P_{\alpha\beta 21}(\mu_n, \mu_1) & \cdots & P_{\alpha\beta 21}(\mu_n, \mu_n) & P_{\alpha\beta 22}(\mu_n, \mu_1) & \cdots & P_{\alpha\beta 22}(\mu_n, \mu_n) \end{bmatrix} \quad (34)$$

$$\bar{B}_{\alpha\beta} = \begin{bmatrix} P_{\alpha\beta 11}(\mu_1, -\mu_1) & \cdots & P_{\alpha\beta 11}(\mu_1, -\mu_n) & P_{\alpha\beta 12}(\mu_1, -\mu_1) & \cdots & P_{\alpha\beta 12}(\mu_1, -\mu_n) \\ \vdots & \vdots & \vdots & \vdots & \vdots & \vdots \\ P_{\alpha\beta 11}(\mu_n, -\mu_1) & \cdots & P_{\alpha\beta 11}(\mu_n, -\mu_n) & P_{\alpha\beta 12}(\mu_n, -\mu_1) & \cdots & P_{\alpha\beta 12}(\mu_n, -\mu_n) \\ P_{\alpha\beta 21}(\mu_1, -\mu_1) & \cdots & P_{\alpha\beta 21}(\mu_1, -\mu_n) & P_{\alpha\beta 22}(\mu_1, -\mu_1) & \cdots & P_{\alpha\beta 22}(\mu_1, -\mu_n) \\ \vdots & \vdots & \vdots & \vdots & \vdots & \vdots \\ P_{\alpha\beta 21}(\mu_n, -\mu_1) & \cdots & P_{\alpha\beta 21}(\mu_n, -\mu_n) & P_{\alpha\beta 22}(\mu_n, -\mu_1) & \cdots & P_{\alpha\beta 22}(\mu_n, -\mu_n) \end{bmatrix} \quad (35)$$

and $\bar{\mu}$ and \bar{a} are the $2n \times 2n$ diagonal matrices

$$\bar{\mu} = \text{diag}[\mu_1, \dots, \mu_n, \mu_1, \dots, \mu_n] \quad (36)$$

$$\bar{a} = \text{diag}[a_1, \dots, a_n, a_1, \dots, a_n] \quad (37)$$

In the above equation $\pm\mu_i$ are the zeroes of the Legendre polynomial $P_{2n}(\mu)$ and a_i are the corresponding Christoffel weighting functions and we made use of the relations $a_i = a_{-i}$ and $\mu_i = -\mu_{-i}$.

The system of $8n$ first-order differential equations, (31) and (32), can be cast into more compact form by defining $4n \times 1$ matrices \bar{I}_a and \bar{I}_s

$$\bar{I}_a = \begin{bmatrix} \bar{I}_{a1} \\ \bar{I}_{s2} \end{bmatrix} \quad \bar{I}_s = \begin{bmatrix} \bar{I}_{s1} \\ \bar{I}_{a2} \end{bmatrix} \quad (38)$$

such that upward propagating intensity \bar{I}^+ is given by

$$\bar{I}^+ \equiv \begin{bmatrix} \bar{I}_1^+ \\ \bar{I}_2^+ \end{bmatrix} = \frac{1}{2}[\bar{I}_a + \bar{I}_s] \quad (39)$$

and where, for $l = 1, 2$, $\bar{I}_{al} = \bar{I}_l^+ + \bar{I}_l^-$ and $\bar{I}_{sl} = \bar{I}_l^+ - \bar{I}_l^-$. Then, from (31) and (32), we obtain

$$\bar{\mu} \cdot \frac{d}{dz} \bar{I}_a = \bar{W} \cdot \bar{I}_s \quad (40a)$$

$$\bar{\mu} \cdot \frac{d}{dz} \bar{I}_s = \bar{A} \cdot \bar{I}_a \quad (40b)$$

where \bar{W} and \bar{A} are the $4n \times 4n$ matrices

$$\bar{W} = - \begin{bmatrix} \bar{K}_{c1} & 0 \\ 0 & \bar{K}_{c2} \end{bmatrix} + \begin{bmatrix} (\bar{F}_{11} - \bar{B}_{11}) & (\bar{F}_{12} + \bar{B}_{12}) \\ (\bar{F}_{21} - \bar{B}_{21}) & (\bar{F}_{22} + \bar{B}_{22}) \end{bmatrix} \cdot \bar{a} \quad (41a)$$

$$\bar{A} = - \begin{bmatrix} \bar{K}_{c1} & 0 \\ 0 & \bar{K}_{c2} \end{bmatrix} + \begin{bmatrix} (\bar{F}_{11} + \bar{B}_{11}) & (\bar{F}_{12} - \bar{B}_{12}) \\ (\bar{F}_{21} + \bar{B}_{21}) & (\bar{F}_{22} - \bar{B}_{22}) \end{bmatrix} \cdot \bar{a} \quad (42b)$$

and the $\bar{\mu}$ and \bar{a} are $4n \times 4n$ diagonal matrices

$$\bar{\mu} = \text{diag}[\mu_1, \dots, \mu_n, \mu_1, \dots, \mu_n, \mu_1, \dots, \mu_n, \mu_1, \dots, \mu_n] \quad (41a)$$

$$\bar{a} = \text{diag}[a_1, \dots, a_n, a_1, \dots, a_n, a_1, \dots, a_n, a_1, \dots, a_n] \quad (42b)$$

The homogeneous solution can be obtained in the form

$$\bar{I}_u = \bar{I}_{u0} e^{\alpha z} \quad (43a)$$

$$\bar{I}_s = \bar{I}_{s0} e^{\alpha z} \quad (43b)$$

Substituting the above equations into (40a) and (40b), we now have $4n$ eigenvalue equations.

$$(\bar{\mu}^{-1} \cdot \bar{W} \cdot \bar{\mu}^{-1} \cdot \bar{A} - \alpha^2 \bar{I}) \cdot \bar{I}_{u0} = 0 \quad (44)$$

$$\bar{I}_{s0} = \alpha^{-1} \bar{\mu}^{-1} \cdot \bar{A} \cdot \bar{I}_{u0} \quad (45)$$

where \bar{I} is an identity matrix. Thus, if α is an eigenvalue, so is $-\alpha$. Once the eigenvalues α_i and the corresponding eigenvectors \bar{I}_{ui} are obtained, we let $\bar{E} = (\bar{I}_{u1}, \bar{I}_{u2}, \dots, \bar{I}_{u4n})$ be the $4n \times 4n$ eigenmatrix. Then the total solution for the upward propagating intensity is given by

$$\bar{I}^+ = (\bar{E} + \bar{Q}) \cdot \bar{D}(z) \cdot \bar{x} + (\bar{E} - \bar{Q}) \cdot \bar{U}(z+d) \cdot \bar{y} \quad (46)$$

where

$$\bar{Q} = \bar{\mu}^{-1} \cdot \bar{A} \cdot \bar{E} \cdot \bar{\alpha}^{-1} \quad (47)$$

$$\bar{\alpha} = \text{diag}[\alpha_1, \alpha_2, \dots, \alpha_{4n}] \quad (48)$$

$$\bar{D}(z) = \text{diag}[e^{\mu_1 z}, e^{\mu_2 z}, \dots, e^{\mu_{4n} z}] \quad (49)$$

$$\bar{U}(z) = \text{diag}[e^{-\mu_1 z}, e^{-\mu_2 z}, \dots, e^{-\mu_{4n} z}] \quad (50)$$

and \bar{x} and \bar{y} are the $4n \times 1$ matrices which represent $8n$ unknowns to be determined by the boundary conditions.

In a similar manner, the downward propagating intensity \bar{I}^- can be calculated. We obtain,

$$\bar{I}^- = (\bar{E}' + \bar{Q}') \cdot \bar{D}(z) \cdot \bar{x} + (\bar{E}' - \bar{Q}') \cdot \bar{U}(z+d) \cdot \bar{y} \quad (51)$$

where

$$\bar{E}' = \bar{\mu}^{-1} \cdot \bar{W}' \cdot \bar{Q} \cdot \bar{\alpha}^{-1} \quad (52a)$$

$$\bar{Q}' = \bar{\mu}^{-1} \cdot \bar{A}' \cdot \bar{E} \cdot \bar{\alpha}^{-1} \quad (52b)$$

and

$$\bar{W}' = - \begin{bmatrix} \bar{K}_{,1} & 0 \\ 0 & -\bar{K}_{,2} \end{bmatrix} + \begin{bmatrix} (\bar{F}_{11} - \bar{B}_{11}) & (\bar{F}_{12} + \bar{B}_{12}) \\ -(\bar{F}_{21} - \bar{B}_{21}) & -(\bar{F}_{22} + \bar{B}_{22}) \end{bmatrix} \cdot \bar{a} \quad (53a)$$

$$\bar{A}' = - \begin{bmatrix} -\bar{K}_{,1} & 0 \\ 0 & \bar{K}_{,2} \end{bmatrix} + \begin{bmatrix} -(\bar{F}_{11} + \bar{B}_{11}) & -(\bar{F}_{12} - \bar{B}_{12}) \\ (\bar{F}_{21} - \bar{B}_{21}) & (\bar{F}_{22} - \bar{B}_{22}) \end{bmatrix} \cdot \bar{a} \quad (53b)$$

In the random medium model, the eigenvalue equations can be simplified further since there is no coupling between the first three Stokes parameters, I_v , I_h , and U , and the last Stokes parameter V in the scattering function matrix. However, the Stokes parameters U and V are coupled together in the boundary conditions and, in general, we have to keep all four Stokes parameters.

The boundary conditions, which are to be used to determine the constants \bar{x} and \bar{y} of the upward and downward propagating intensities given by (46) and (51), are, at $z = -d$,

$$\bar{I}^+(z = -d) = \bar{\bar{R}}_{12} \cdot \bar{I}^-(z = -d) \quad (54)$$

and at $z = 0$

$$\bar{I}^-(z = 0) = \bar{\bar{R}}_{10} \cdot \bar{I}^+(z = 0) - \bar{\bar{T}}_{01} \cdot \bar{I}_n^- \quad (55)$$

where $\bar{\bar{R}}_{12}$ and $\bar{\bar{R}}_{10}$ are the $4n \times 4n$ matrices which are obtained by evaluating the 4×4 coupling matrices $\bar{\bar{R}}_{12}(\theta)$ and $\bar{\bar{R}}_{10}(\theta)$ at n discrete quadrature angles, and $\bar{\bar{T}}_{01}$ is the $4n \times 4n_f$ matrix which is obtained by evaluating the coupling matrix $\bar{\bar{T}}_{01}$ at the quadrature angles. The n_f is the number of quadrature angles in region 0 and the quadrature angles are related by the Snell's law. Since $\epsilon'_1 \geq \epsilon_0$, we have $n_f \leq n$. Thus, for the quadrature angles in region 1 which are greater than the critical angle between regions 1 and 0, θ_i , where $i > n_f$, there is no incident intensity. In the above equation (55), the incident intensity \bar{I}_n^- is obtained by discretizing the incident intensity given by (20), which is given in terms of the delta function. One way to bypass the problem of discretizing the delta function is to change the source term at the boundary into the source term in the volume by calculating the zeroth-order solution explicitly and using the radiative transfer equations for the higher order terms with the zeroth-order solution acting as the volume source [Fung and Chen, 1981b]. In this section we discretize the delta function in a consistent manner and keep the source term at the boundary. This approach gives the same solution as the other approach and also the formulation does not have to be changed when the boundary conditions are changed to incorporate the rough surface scattering [Fung and Chen, 1981b].

Consider an integral given by

$$I = \int_0^\pi d\theta' \sin \theta' f(\theta, \theta') g(\theta') \quad (56)$$

Using the Gaussian quadrature method the integral I is approximated as

$$I \simeq \sum_{j=-n}^n a_j f(\theta, \theta_j) g_j \quad (57)$$

If we now let $g(\theta') = \delta(\cos \theta'_n - \cos \theta_{in})$ where θ_{in} is one of the quadrature angles in region 0, then the integral I can be evaluated exactly to give

$$I = f(\theta, \theta_i) \frac{\epsilon_n \cos \theta_{in}}{\epsilon'_1 \cos \theta_i} \quad (58)$$

where θ_i is the corresponding incident angle in region 1 which is related to θ_{in} by Snell's law, and we made use of [Tsang and Kong, 1978]

$$d\theta' \sin \theta' d\phi' = d\theta'_n \sin \theta'_n \frac{\epsilon_n \cos \theta_{in}}{\epsilon'_1 \cos \theta_i} d\phi'_n \quad (59)$$

Therefore, comparing (58) with (57), we obtain the discrete form for the delta function:

$$g_j = \delta_{ji} \frac{1}{a_j} \frac{\epsilon_n \cos \theta_{in}}{\epsilon'_1 \cos \theta_i} \quad (60)$$

where

$$\delta_{ji} = \begin{cases} 1 & \text{if } j = i \\ 0 & \text{otherwise} \end{cases} \quad (61)$$

The incident intensities for even and odd terms in each harmonics, given by (20), can now be cast into the quadrature form by making use of the above relations.

Substituting in the expressions for the upward and downward propagating intensities into the boundary conditions (54) and (55), we obtain the following $8n$ equations for $8n$ unknowns \bar{x} and \bar{y} :

$$\left[(\bar{E}' + \bar{Q}') - \bar{R}_{10} \cdot (\bar{E} + \bar{Q}) \right] \cdot \bar{x} + \left[(\bar{E}' - \bar{Q}') - \bar{R}_{10} \cdot (\bar{E} - \bar{Q}) \right] \cdot \bar{D}(-d) \cdot \bar{y} = \bar{T}_{01} \cdot \bar{I}_{..i} \quad (62a)$$

$$\left[(\bar{E} + \bar{Q}) - \bar{R}_{12} \cdot (\bar{E}' + \bar{Q}') \right] \cdot \bar{D}(-d) \cdot \bar{x} - \left[(\bar{E} - \bar{Q}) - \bar{R}_{12} \cdot (\bar{E}' - \bar{Q}') \right] \cdot \bar{y} = 0 \quad (62b)$$

The above equations can be solved for the constants \bar{x} and \bar{y} for each case when the incident intensity is at one of the quadrature angles. Note that in the halfspace random medium case when $d \rightarrow \infty$, $\bar{D} \rightarrow 0$ and the equations for \bar{x} and \bar{y} become decoupled and the matrix equation does not become singular [Fung and Chen, 1981b]. This is due to the form of the solution assumed in (46) and (51).

Once the constants \bar{x} and \bar{y} are determined, the scattered intensities from region 1 to region 0, represented by the first term on the right-hand-side of (6), can be determined. We have

$$\begin{aligned} \bar{I}_{..s} &= \bar{T}_{10} \cdot \bar{I}^+(z=0) \\ &= \bar{T}_{10} \cdot \left[(\bar{E} + \bar{Q}) \cdot \bar{x} + (\bar{E} - \bar{Q}) \cdot \bar{D}(-d) \cdot \bar{y} \right] \end{aligned} \quad (63)$$

Thus, the complete solution can be obtained by solving the radiative transfer equations using the Gaussian quadrature method for each harmonic as outlined above and reintroducing the azimuthal dependence. The total scattered intensities in region 0 is given by

$$\bar{I}_{..s}(\phi_{..}) = \left\{ \bar{R}_{01} + \bar{T}_{10} \cdot \left[\bar{I} - \bar{R}_{10} \cdot \bar{R}_{12} \cdot \exp[-\bar{\mu}^{-1} \cdot \bar{K} \cdot d] \right]^{-1} \cdot \bar{T}_{01} \right\} \cdot \bar{I}_{..i} \delta(\phi_{..} - \phi_{..i})$$

$$\begin{aligned}
& - \sum_{m=0}^{m_{max}} \left\{ \bar{T}_{10} \cdot \left[\bar{I}^{m,s+}(z=0) - \left[\bar{I} - \bar{R}_{10} \cdot \bar{R}_{12} \cdot \exp\{-\mu^{-1} \cdot \bar{K} \cdot d\} \right]^{-1} \cdot \bar{T}_{01} \cdot \bar{I}_{oi}^{m,c} \right] \cos m(\phi_o - \phi_{oi}) \right. \\
& \quad \left. + \bar{T}_{10} \cdot \bar{I}^{m,s+}(z=0) \sin m(\phi_o - \phi_{oi}) \right\} \tag{64}
\end{aligned}$$

where we have summed up the zeroth-order solution and $\bar{I}^{m,c-}(z=0)$ and $\bar{I}^{m,s+}(z=0)$ are the upward propagating m th cosine and sine harmonics evaluated at $z=0$. Once the scattered intensities in region 0 are obtained, the bistatic scattering coefficients and the backscattering cross sections can be obtained from (7) and (8). We note that if we are only interested in calculating the scattering intensities for vertically or horizontally polarized intensities only, then we only need to calculate the even series. This is because the odd series, represented by (14b), are zero due to the fact the incident intensity for the odd series as given by (21b) is zero.

7.5 Results and Discussion

The backscattering cross sections and the bistatic scattering coefficients are calculated and illustrated for the various cases. In our calculations $n = 16$ is used. The backscattering cross sections are illustrated as functions of frequency and incident angle. The bistatic scattering coefficients are plotted as functions of scattering angles θ_s and ϕ_s .

In Fig. 7.2 the horizontally polarized and depolarized backscattering cross sections are plotted as a function of frequency for a 48cm thick random medium. Backscattering cross sections increase as frequency is increased. This is due to the fact that as frequency increases the albedo $[K_s/(K_a + K_s)]$ increases and the scattering becomes dominant over the absorption. Also, the difference between the like-like polarized return and the depolarized return decreases. In Fig. 7.3 the backscattering cross sections are plotted as a function of incident angle at 10 GHz.

In Fig. 7.4, the bistatic scattering coefficients γ_{hh} and γ_{vh} are plotted as a function of scattering angle θ_s . The positive θ_s corresponds to the forward scattering case where $\phi_s = 0$ whereas negative θ_s corresponds to the backward scattering case with $\phi_s = 180^\circ$. We note that there is symmetry about the $\theta_s = 0$ axis which is the typical of Rayleigh scatterers. For correlation lengths small compared to the wavelength, the scattering pattern of the random medium is that of the Rayleigh scatterers [Tsang and Kong, 1976b]. The number of harmonics needed in this case was three which is the same as the case involving Rayleigh scatterers [Shin and Kong, 1981]. In Fig. 7.5 we show the bistatic scattering coefficients for larger correlation length l_c . Unlike the previous case there is no symmetry. The number of harmonics needed in the computation is also larger than the previous case.

In Figs. 7.6–7.9, the bistatic scattering coefficients are plotted as a function of azimuthal scattering angle ϕ_s for $\theta_i = \theta_s = 33^\circ$. We only plot from $\phi_s = 0^\circ$ to $\phi_s = 180^\circ$ because the bistatic scattering coefficients are symmetrical. In Fig. 7.6, the bistatic scattering coefficients γ_{hh} and γ_{vh} are plotted for the case of small correlation length l_p . There is a symmetry in the bistatic scattering coefficients about $\phi_s = 90^\circ$. In Fig. 7.7, γ_{hh} and γ_{vv} are compared. We note there is no symmetry for the bistatic scattering coefficient γ_{vv} . In Figs. 7.8 and 7.9, the bistatic scattering coefficients are plotted for the case of large correlation length l_p . We note that the scattering coefficients are more peaked toward the forward scattering direction and that there is no symmetry about the $\phi_s = 90^\circ$ axis.

Appendix A: Scattering Function Matrix, Scattering Coefficient, and Absorption Coefficient for the Random Medium

The scattering function matrix have been derived for the random medium whose fluctuating permittivity is characterized by the correlation function

$$\langle \epsilon_f(\bar{r}') \epsilon_f^*(\bar{r}'') \rangle = \delta \epsilon_1'^2 b(\bar{r}' - \bar{r}'') \quad (A1)$$

where δ is the variance of the fluctuation and the function $b(\bar{r}' - \bar{r}'')$ is the normalized correlation function. The scattering function matrix is given by [Tsang and Kong, 1978]

$$\bar{\bar{P}}(\theta, \phi; \theta', \phi') = \frac{\pi k_1'^4 \delta}{2} \Phi(\theta, \phi; \theta', \phi') \begin{bmatrix} p_{11} & p_{12} & p_{13} & 0 \\ p_{21} & p_{22} & p_{23} & 0 \\ p_{31} & p_{32} & p_{33} & 0 \\ 0 & 0 & 0 & p_{44} \end{bmatrix} \quad (A2)$$

where $\Phi(\theta, \phi; \theta', \phi')$ is the spectral density of the fluctuation which is given by the Fourier transform of the correlation function and

$$p_{11} = \sin^2 \theta \sin^2 \theta' + 2 \sin \theta \sin \theta' \cos \theta \cos \theta' \cos(\phi - \phi') + \cos^2 \theta \cos^2 \theta' \cos^2(\phi - \phi') \quad (A3)$$

$$p_{12} = \cos^2 \theta \sin^2(\phi - \phi') \quad (A4)$$

$$p_{13} = \cos \theta \sin \theta \sin \theta' \sin(\phi - \phi') + \cos^2 \theta \cos \theta' \sin(\phi - \phi') \cos(\phi - \phi') \quad (A5)$$

$$p_{21} = \cos^2 \theta' \sin^2(\phi - \phi') \quad (A6)$$

$$p_{22} = \cos^2(\phi - \phi') \quad (A7)$$

$$p_{23} = -\cos \theta' \sin(\phi - \phi') \cos(\phi - \phi') \quad (A8)$$

$$p_{31} = -2 \sin \theta \sin \theta' \cos \theta' \sin(\phi - \phi') - 2 \cos \theta \cos^2 \theta' \cos(\phi - \phi') \sin(\phi - \phi') \quad (\text{A9})$$

$$p_{32} = 2 \cos \theta \sin(\phi - \phi') \cos(\phi - \phi') \quad (\text{A10})$$

$$p_{33} = \sin \theta \sin \theta' \cos(\phi - \phi') + \cos \theta \cos \theta' [\cos^2(\phi - \phi') - \sin^2(\phi - \phi')] \quad (\text{A11})$$

$$p_{44} = \sin \theta \sin \theta' \cos(\phi - \phi') + \cos \theta \cos \theta' \quad (\text{A12})$$

For the correlation function we assume gaussian dependence laterally and exponential dependence vertically

$$b(\bar{r}' - \bar{r}'') = \exp \left[-\frac{(x' - x'')^2 + (y' - y'')^2}{l_\rho^2} - \frac{|z' - z''|}{l_z} \right] \quad (\text{A13})$$

Then the spectral density is given by

$$\Phi(\theta, \phi; \theta', \phi') = \frac{l_z l_\rho^2}{4\pi^2 [1 + k_1'^2 l_z^2 (\cos \theta' - \cos \theta)^2]} \exp \left[-\frac{k_1'^2 l_\rho^2}{4} |\sin^2 \theta' + \sin^2 \theta - 2 \sin \theta' \sin \theta \cos(\phi' - \phi)| \right] \quad (\text{A14})$$

The scattering coefficient $\bar{K}_s(\theta)$ is given by

$$\bar{K}_s(\theta) = \begin{bmatrix} K_v & 0 & 0 & 0 \\ 0 & K_h & 0 & 0 \\ 0 & 0 & \frac{K_v + K_h}{2} & 0 \\ 0 & 0 & 0 & \frac{K_v + K_h}{2} \end{bmatrix} \quad (\text{A15})$$

where

$$K_v(\theta') = \int_{4\pi} d\Omega \frac{\pi k_1'^4 \delta}{2} \Phi(\theta, \phi; \theta', \phi') [p_{11}(\theta, \phi; \theta', \phi') + p_{21}(\theta, \phi; \theta', \phi')] \quad (\text{A16})$$

$$K_h(\theta') = \int_{4\pi} d\Omega \frac{\pi k_1'^4 \delta}{2} \Phi(\theta, \phi; \theta', \phi') [p_{12}(\theta, \phi; \theta', \phi') + p_{22}(\theta, \phi; \theta', \phi')] \quad (\text{A17})$$

and the $d\Omega$ integration is carried over a 4π solid angle. The absorption coefficient K_a is given by

$$K_a = 2k_1'' \quad (\text{A18})$$

where k_1'' is the imaginary part of the wave number in region 1.

Appendix B: Coupling Matrices for Stokes Parameters at Planar Dielectric Interface

The coupling matrices in the boundary conditions take the form [Tsang and Kong, 1978; Shin and Kong, 1981], for $\alpha, \beta = 0, 1, 2$,

$$\bar{\bar{T}}_{\alpha\beta}(\theta_\alpha) = \frac{\epsilon'_\beta}{\epsilon'_\alpha} \begin{bmatrix} t_{v\alpha\beta}(\theta_\alpha) & 0 & 0 & 0 \\ 0 & t_{h\alpha\beta}(\theta_\alpha) & 0 & 0 \\ 0 & 0 & g_{\alpha\beta}(\theta_\alpha) & -h_{\alpha\beta}(\theta_\alpha) \\ 0 & 0 & h_{\alpha\beta}(\theta_\alpha) & g_{\alpha\beta}(\theta_\alpha) \end{bmatrix} \quad (B1)$$

and

$$\bar{\bar{R}}_{\alpha\beta}(\theta_\alpha) = \begin{bmatrix} r_{v\alpha\beta}(\theta_\alpha) & 0 & 0 & 0 \\ 0 & r_{h\alpha\beta}(\theta_\alpha) & 0 & 0 \\ 0 & 0 & W_{\alpha\beta}(\theta_\alpha) & -Z_{\alpha\beta}(\theta_\alpha) \\ 0 & 0 & Z_{\alpha\beta}(\theta_\alpha) & W_{\alpha\beta}(\theta_\alpha) \end{bmatrix} \quad (B2)$$

where

$$t_{v\alpha\beta}(\theta_\alpha) = 1 - r_{v\alpha\beta}(\theta_\alpha) \quad (B3)$$

$$t_{h\alpha\beta}(\theta_\alpha) = 1 - r_{h\alpha\beta}(\theta_\alpha) \quad (B4)$$

$$g_{\alpha\beta}(\theta_\alpha) = (\cos \theta_\beta / \cos \theta_\alpha) \operatorname{Re}(Y_{\alpha\beta} X_{\alpha\beta}^*) \quad (B5)$$

$$h_{\alpha\beta}(\theta_\alpha) = (\cos \theta_\beta / \cos \theta_\alpha) \operatorname{Im}(Y_{\alpha\beta} X_{\alpha\beta}^*) \quad (B6)$$

for θ_α , less than the critical angle, otherwise

$$g_{\alpha\beta}(\theta_\alpha) = h_{\alpha\beta}(\theta_\alpha) = 0 \quad (B7)$$

and

$$X_{\alpha\beta}(\theta_\alpha) = 1 + R_{\alpha\beta}(\theta_\alpha) \quad (B8)$$

$$Y_{\alpha\beta}(\theta_\alpha) = 1 + S_{\alpha\beta}(\theta_\alpha) \quad (B9)$$

where $R_{\alpha\beta}(\theta_\alpha)$ and $S_{\alpha\beta}(\theta_\alpha)$ are the TE and TM Fresnel reflection coefficients, and

$$\tau_{v\alpha\beta}(\theta_\alpha) = |S_{\alpha\beta}(\theta_\alpha)|^2 \quad (B10)$$

$$\tau_{h\alpha\beta}(\theta_\alpha) = |R_{\alpha\beta}(\theta_\alpha)|^2 \quad (B11)$$

$$W_{\alpha\beta}(\theta_\alpha) = \text{Re}(S_{\alpha\beta}R_{\alpha\beta}^*) \quad (B12)$$

$$Z_{\alpha\beta}(\theta_\alpha) = \text{Im}(S_{\alpha\beta}R_{\alpha\beta}^*) \quad (B13)$$

Appendix C: Fourier Series Expansion of the Scattering Function Matrix

The scattering function matrix given in Appendix A can be expanded into the cosine and sine series as follows:

$$\bar{P}(\theta, \phi : \theta' \phi') = \sum_{m=0}^{\infty} \frac{1}{(\delta_m + 1)\pi} \left[\bar{P}^{m,c}(\theta, \theta') \cos m(\phi - \phi') + \bar{P}^{m,s}(\theta, \theta') \sin m(\phi - \phi') \right] \quad (C1)$$

where

$$\bar{P}^{m,c}(\theta, \theta') = q(\theta, \theta') \begin{bmatrix} P_{11}^{m,c} & P_{12}^{m,c} & 0 & 0 \\ P_{21}^{m,c} & P_{22}^{m,c} & 0 & 0 \\ 0 & 0 & P_{33}^{m,c} & P_{34}^{m,c} \\ 0 & 0 & P_{43}^{m,c} & P_{44}^{m,c} \end{bmatrix} \quad (C2)$$

$$\bar{P}^{m,s}(\theta, \theta') = q(\theta, \theta') \begin{bmatrix} 0 & 0 & P_{13}^{m,s} & P_{14}^{m,s} \\ 0 & 0 & P_{23}^{m,s} & P_{24}^{m,s} \\ P_{31}^{m,s} & P_{32}^{m,s} & 0 & 0 \\ P_{41}^{m,s} & P_{42}^{m,s} & 0 & 0 \end{bmatrix} \quad (C3)$$

with

$$q(\theta, \theta') = \frac{\delta k_1^4}{4} \frac{l_\mu^2 l_z}{1 + k_1^2 l_\mu^2 (\cos \theta - \cos \theta')^2} \quad (C4)$$

$$P_{11}^{m,c} = e^{-y} \left[\sin^2 \theta \sin^2 \theta' I_m(x) + \sin \theta \sin \theta' \cos \theta \cos \theta' (I_{m-1}(x) + I_{m+1}(x)) \right. \\ \left. + \cos^2 \theta \cos^2 \theta' \left(\frac{1}{2} I_m(x) + \frac{1}{4} I_{m-2}(x) + \frac{1}{4} I_{m+2}(x) \right) \right] \quad (C5)$$

$$P_{12}^{m,c} = e^{-y} \cos^2 \theta \frac{1}{2} \left[I_m(x) - \frac{1}{2} (I_{m-2}(x) + I_{m+2}(x)) \right] \quad (C6)$$

$$P_{21}^{m,c} = e^{-y} \cos^2 \theta' \frac{1}{2} \left[I_m(x) - \frac{1}{2} (I_{m-2}(x) + I_{m+2}(x)) \right] \quad (C7)$$

$$P_{22}^{m,c} = e^{-y} \frac{1}{2} \left[I_m(x) + \frac{1}{2} (I_{m-2}(x) + I_{m+2}(x)) \right] \quad (C8)$$

$$p_{33}^{m,c} = e^{-y} \frac{1}{2} \left[\sin \theta \sin \theta' (I_{m-1}(x) + I_{m+1}(x)) + \cos \theta \cos \theta' (I_{m-2}(x) + I_{m+2}(x)) \right] \quad (C9)$$

$$p_{44}^{m,c} = e^{-y} \left[\cos \theta \cos \theta' I_m(x) + \sin \theta \sin \theta' \frac{1}{2} (I_{m-1}(x) + I_{m+1}(x)) \right] \quad (C10)$$

$$p_{34}^{m,c} = p_{43}^{m,c} = 0 \quad (C11)$$

$$p_{13}^{m,s} = e^{-y} \cos \theta \frac{1}{2} \left[\sin \theta \sin \theta' (I_{m-1}(x) - I_{m+1}(x)) + \frac{1}{2} \cos \theta \cos \theta' (I_{m-2}(x) - I_{m+2}(x)) \right] \quad (C12)$$

$$p_{23}^{m,s} = -e^{-y} \cos \theta' \frac{1}{4} (I_{m-2}(x) - I_{m+2}(x)) \quad (C13)$$

$$p_{31}^{m,s} = -e^{-y} \cos \theta' \left[\sin \theta \sin \theta' (I_{m-1}(x) - I_{m+1}(x)) + \frac{1}{2} \cos \theta \cos \theta' (I_{m-2}(x) - I_{m+2}(x)) \right] \quad (C14)$$

$$p_{32}^{m,s} = e^{-y} \cos \theta \frac{1}{2} (I_{m-2}(x) - I_{m+2}(x)) \quad (C15)$$

$$p_{14}^{m,s} = p_{24}^{m,s} = p_{41}^{m,s} = p_{42}^{m,s} = 0 \quad (C16)$$

$$y = \frac{1}{4} k_1'^2 l_\rho'^2 (\sin^2 \theta + \sin^2 \theta') \quad (C17)$$

$$x = \frac{1}{2} k_1'^2 l_\rho'^2 \sin \theta \sin \theta' \quad (C18)$$

and I_m is the m -th order modified Bessel function.

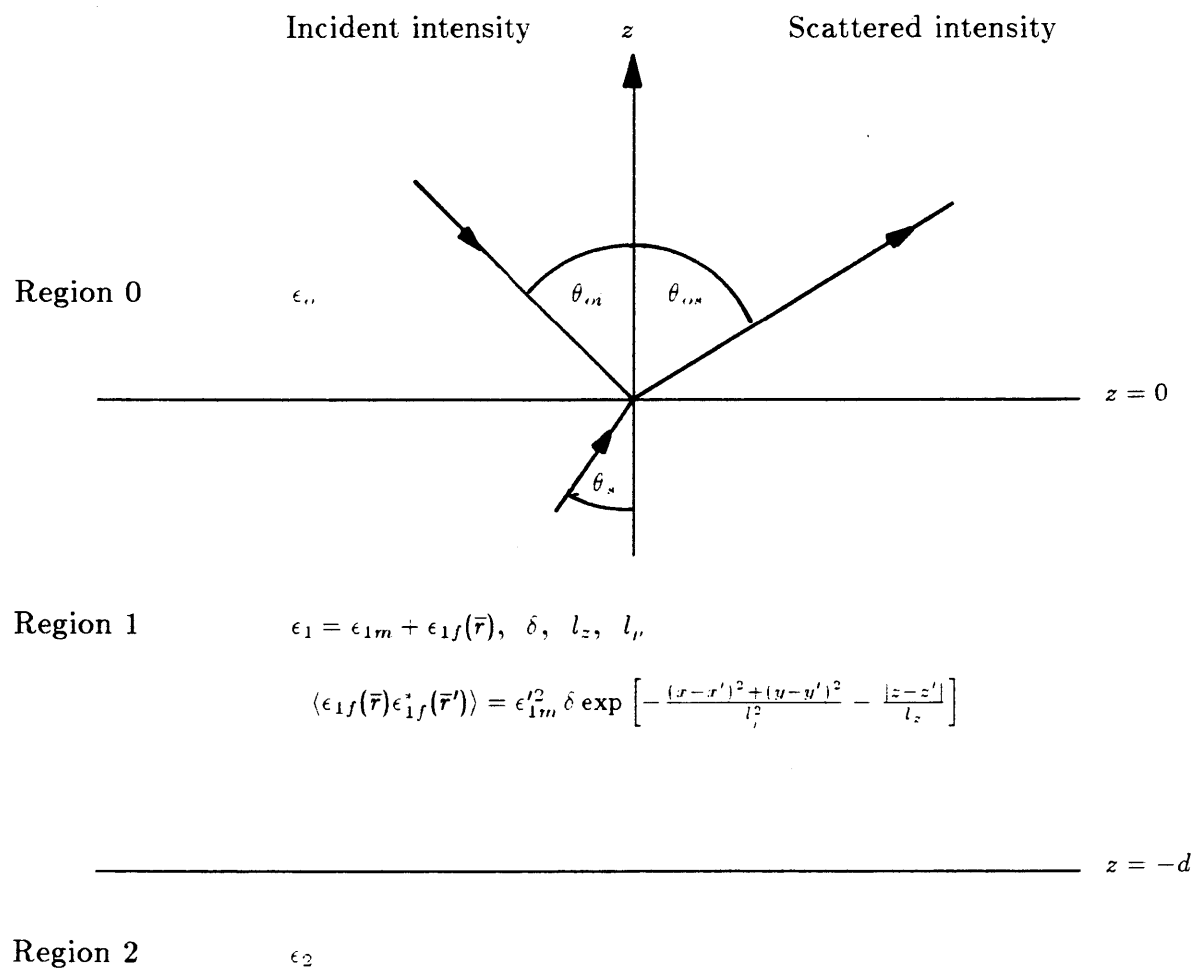


Figure 7.1 Geometrical configuration of the problem.

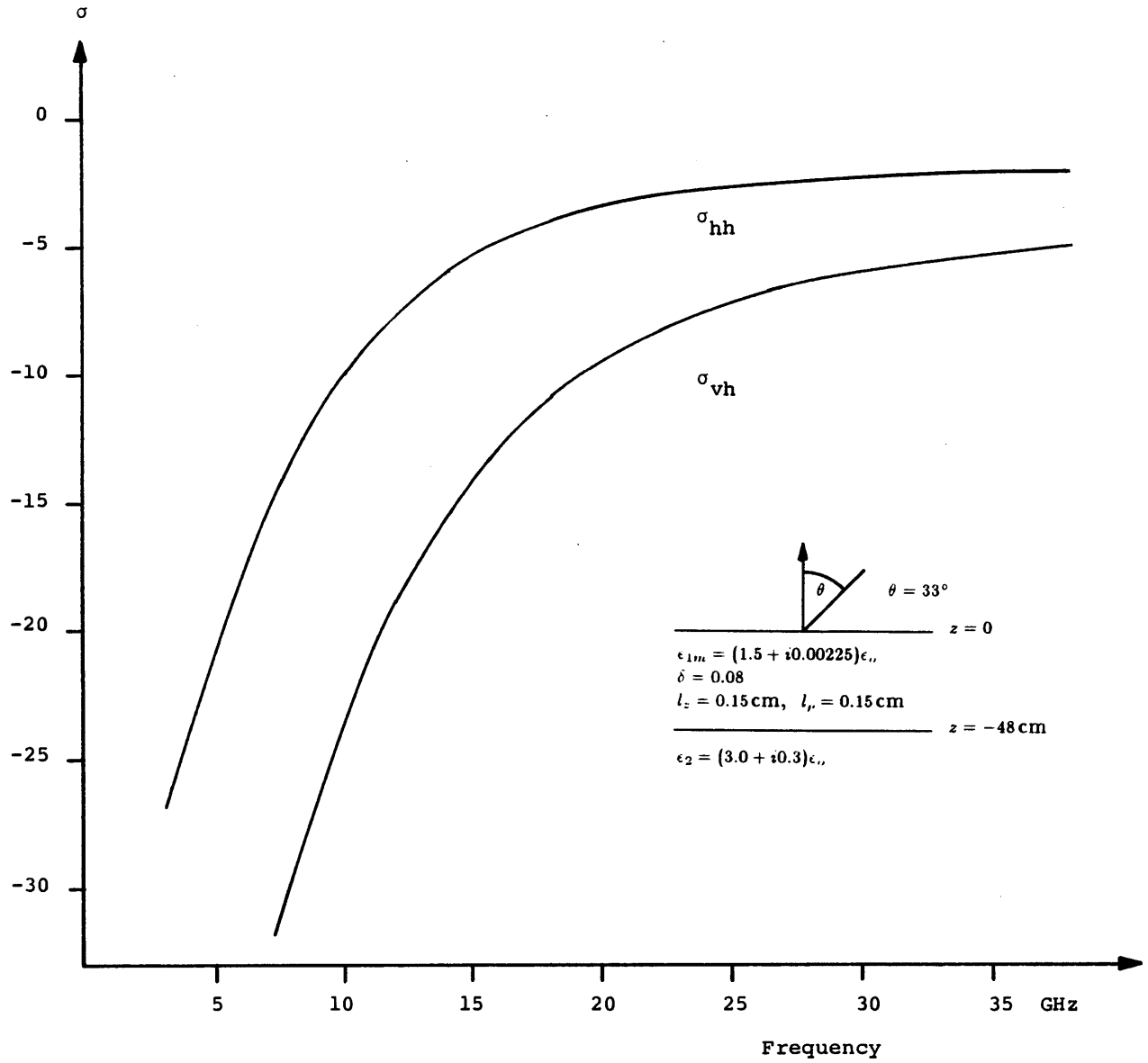


Figure 7.2 Backscattering cross sections as a function of frequency.

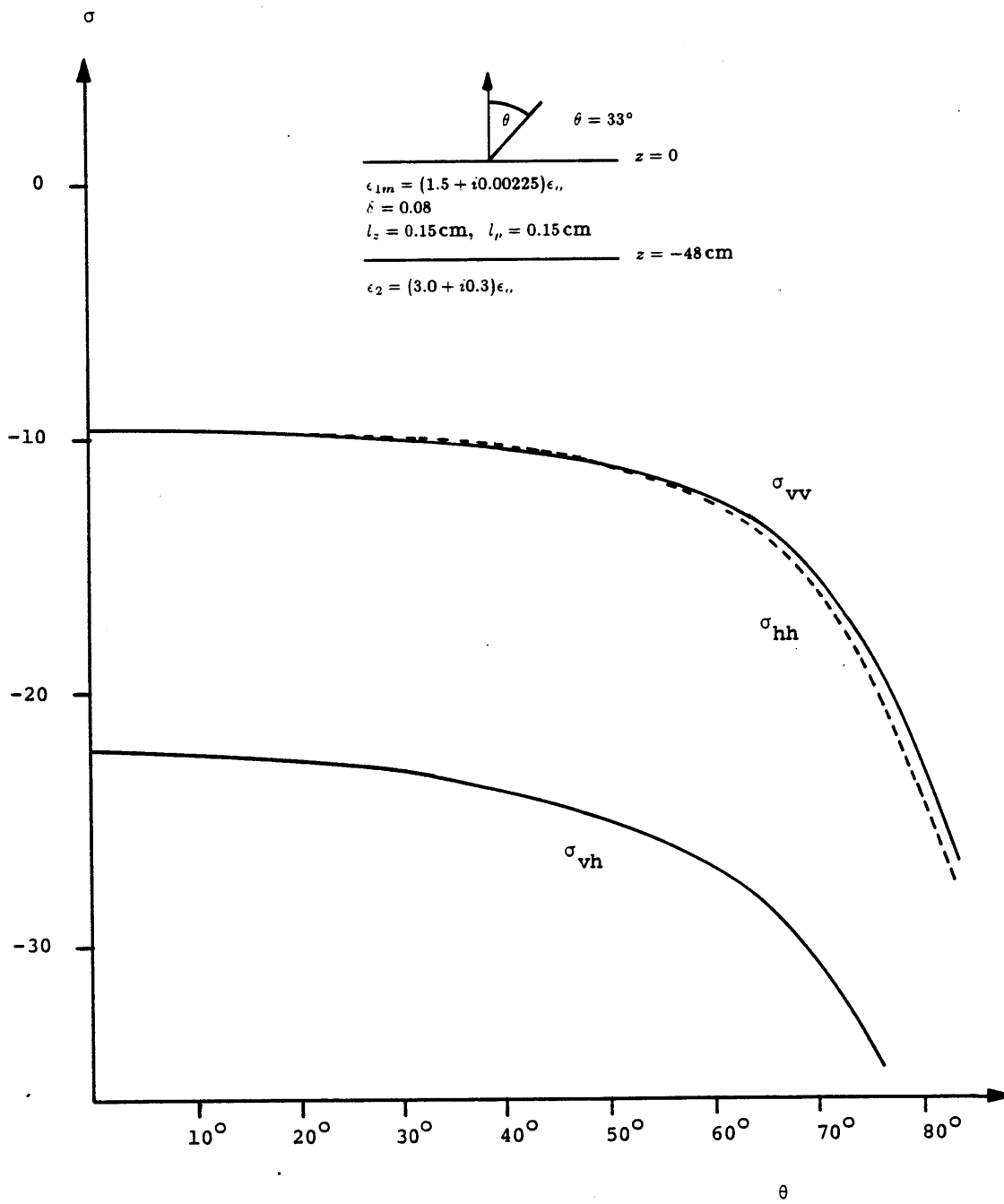


Figure 7.3 Backscattering cross sections as a function of incident angle at 10 GHz.

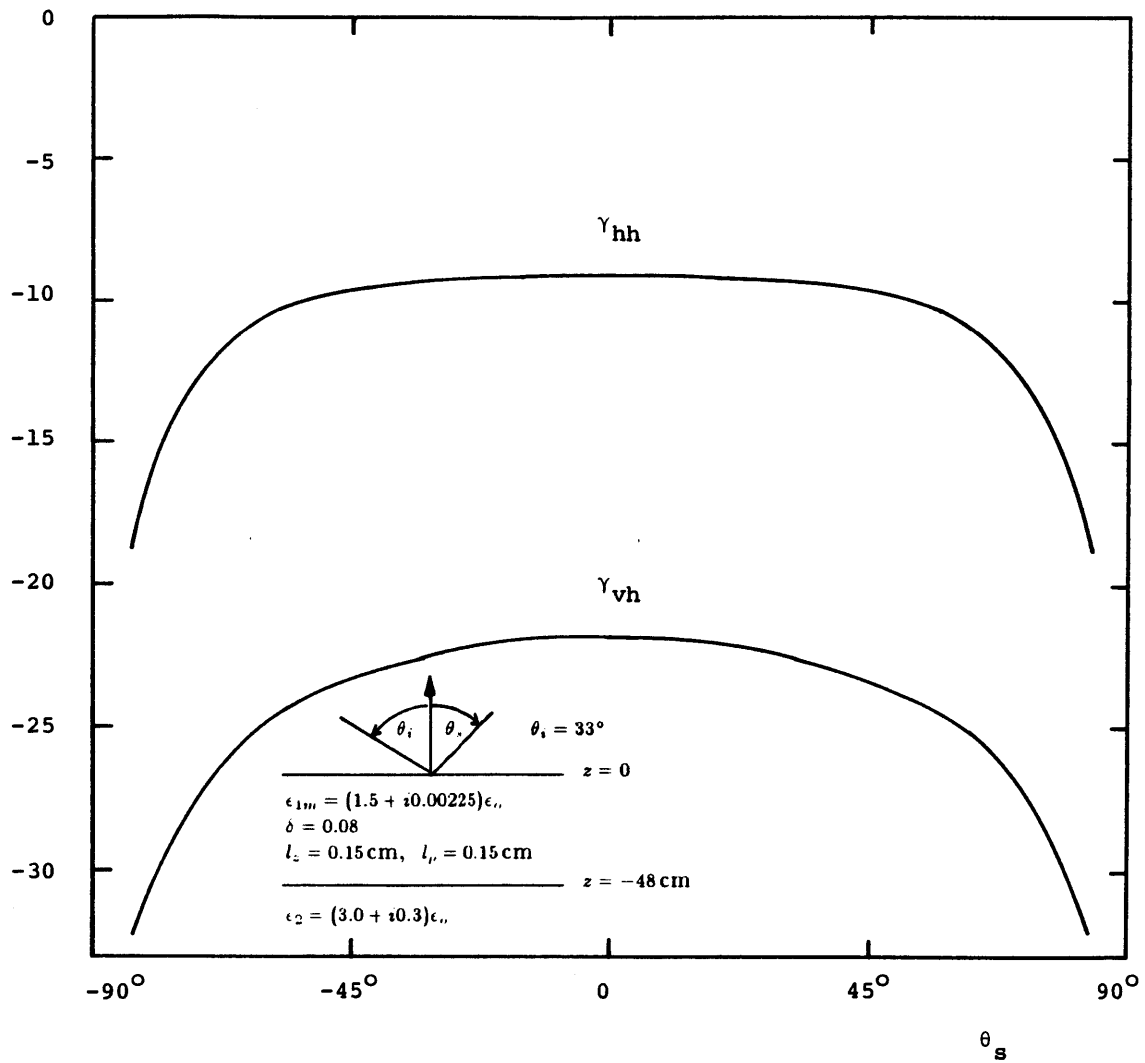


Figure 7.4 Bistatic scattering coefficients γ_{hh} and γ_{vh} as a function of scattering angle θ_s at 10 GHz.

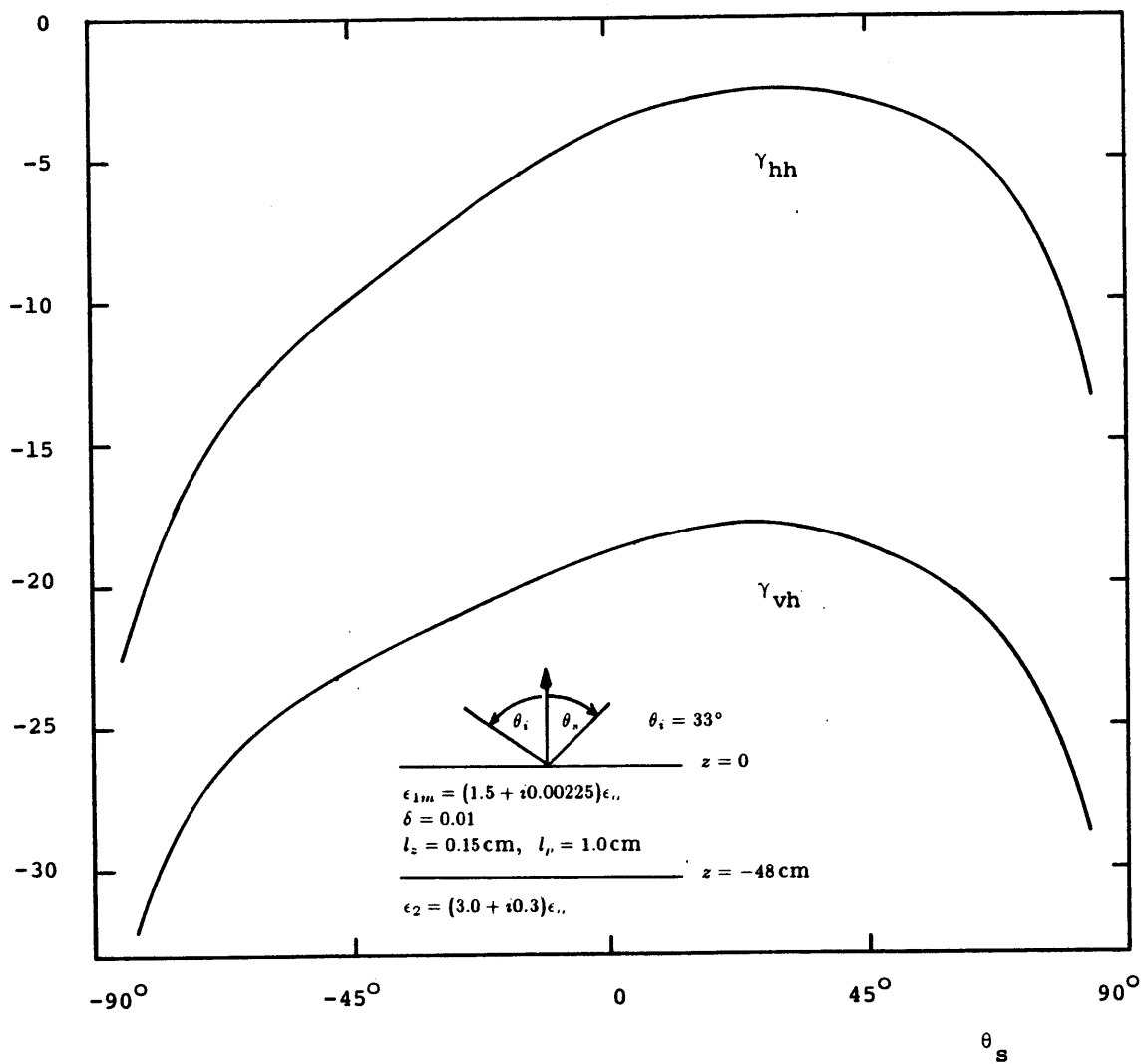


Figure 7.5 Bistatic scattering coefficients γ_{hh} and γ_{vh} as a function of scattering angle θ_s at 10 GHz.

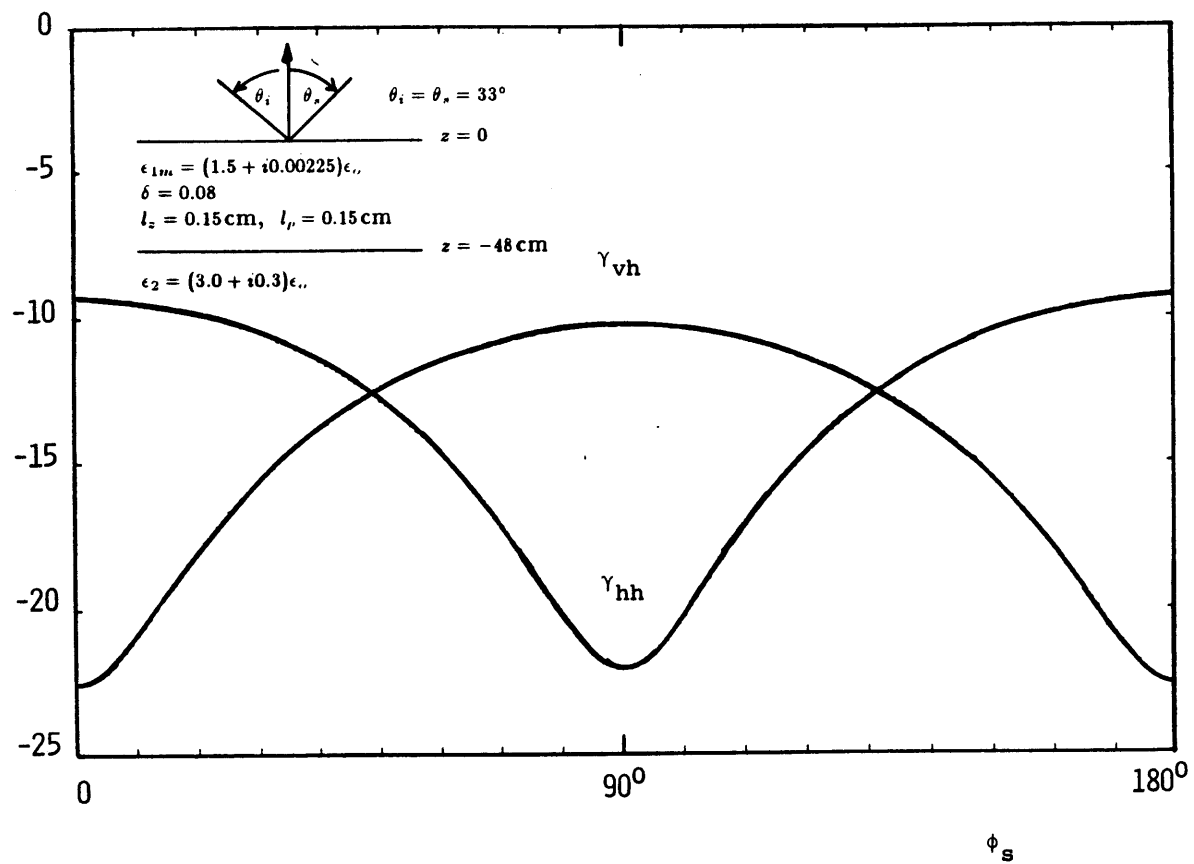


Figure 7.6 Bistatic scattering coefficients γ_{hh} and γ_{vh} as a function of azimuthal scattering angle ϕ_s at 10 GHz.

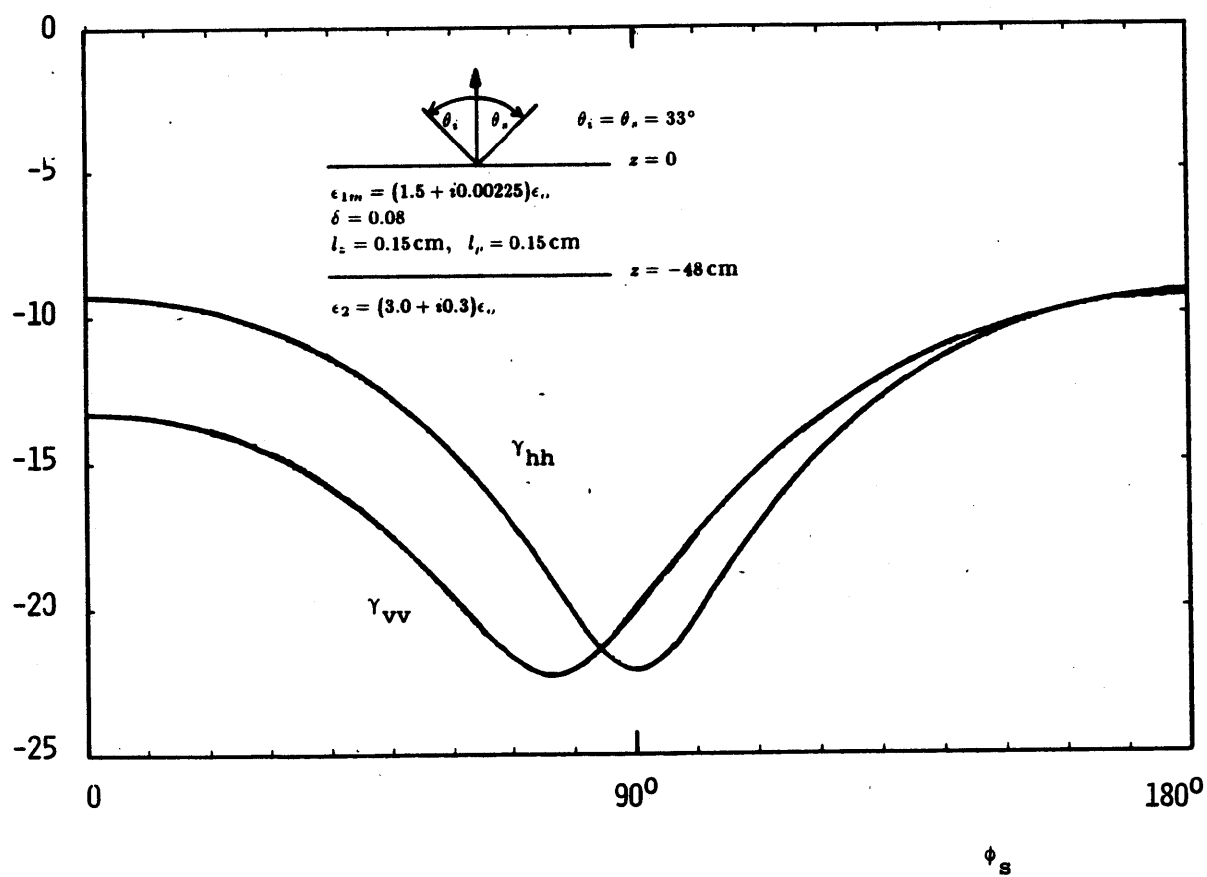


Figure 7.7 Bistatic scattering coefficients γ_{hh} and γ_{vv} as a function of azimuthal scattering angle ϕ_s at 10 GHz.

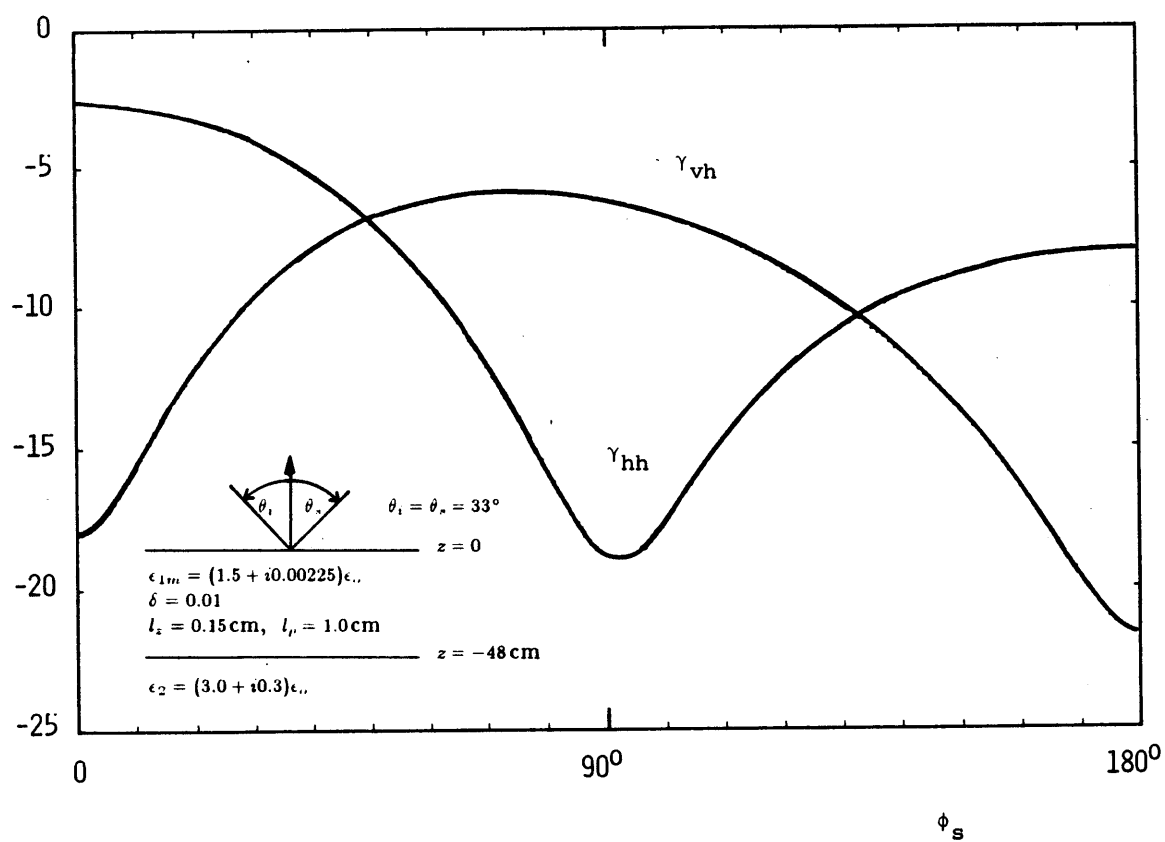


Figure 7.8 Bistatic scattering coefficients γ_{hh} and γ_{vh} as a function of azimuthal scattering angle ϕ_s at 10 GHz.

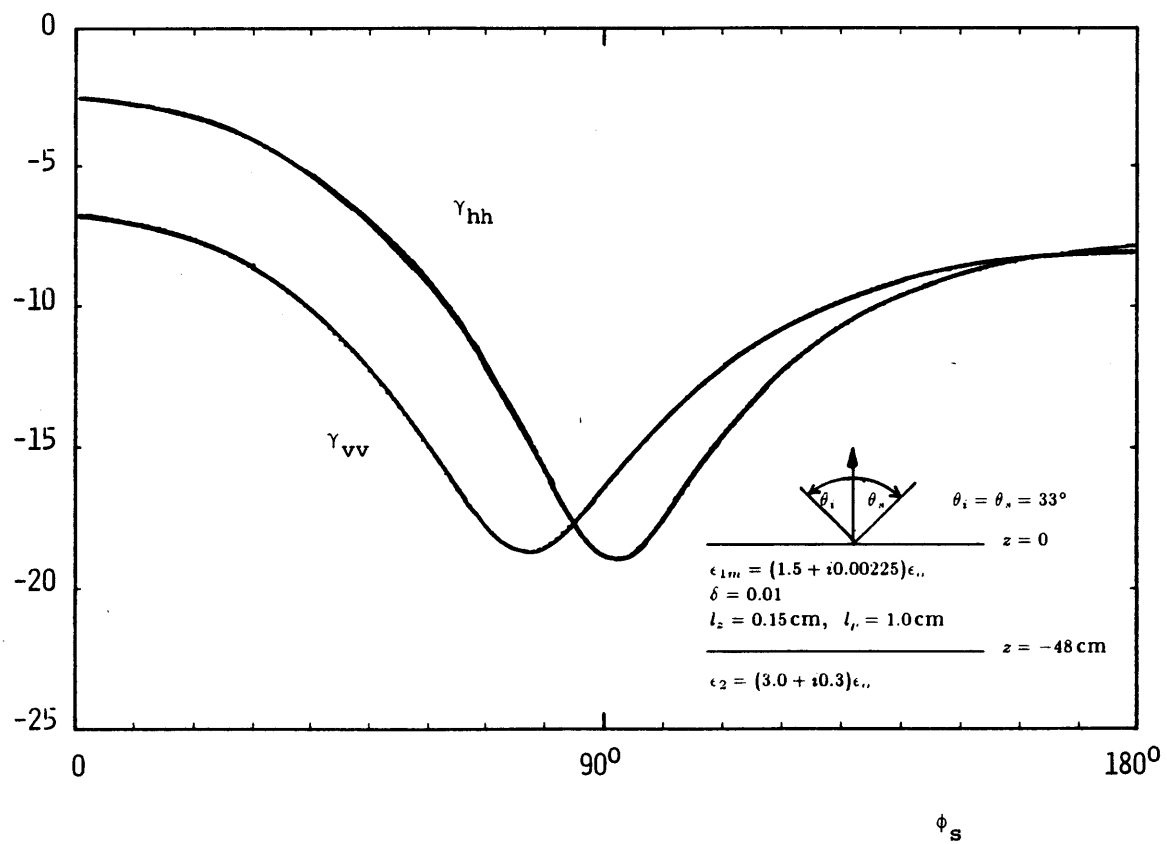


Figure 7.9 Bistatic scattering coefficients γ_{hh} and γ_{vv} as a function of azimuthal scattering angle ϕ_s at 10 GHz.

CHAPTER 8

Radiative Transfer Theory for Active Remote Sensing of Multi-Layered Random Medium

The scattering from multi-layered random medium is studied using the radiative transfer theory. Bistatic scattering coefficients are obtained by numerically solving the radiative transfer equations using Fourier-series expansion in the azimuthal direction and the Gaussian quadrature method. The effective boundary conditions are derived which reduce the complexity of the problem to that of a two-layer case. Theoretical results are compared and illustrated for the various cases.

8.1 Introduction

In the microwave remote sensing of earth terrain, multi-layered random medium or discrete scatterer models have been applied to account for the volume scattering effects. The multi-layered models have shown to be more realistic in interpreting the remote sensing data [Tsang *et al.*, 1975, 1977; Njoku and Kong, 1977; Tsang and Kong, 1979]. In the passive remote sensing the radiative transfer theory has been used to study thermal microwave emission from a multi-layered random medium with laminar structures [Djermakoye and Kong, 1979]. The propagation matrix formulism is applied to obtain closed form solutions. For the inhomogeneous slab random medium with nonuniform scattering, absorption and temperature profiles in the vertical direction, the method of invariant imbedding has been used [Tsang and Kong, 1977b]. The boundary value problem of the radiative transfer equations is converted to an initial value problem starting at zero slab thickness. In the active remote sensing, the scattering from multi-layered random medium has been solved using the Born approximation and the propagation matrix formulism [Zuniga *et al.*, 1979]. The radiative transfer theory also has been applied to scattering from multi-layer of Rayleigh scatterers with rough boundaries where the iterative approach is used to obtain solutions to first-order [Shin, 1980; Karam and Fung, 1982].

In this chapter we solve the problem of scattering from a multi-layered random medium on top of homogeneous halfspace using the radiative transfer theory. The bistatic scattering coefficients are calculated using a numerical approach. A Fourier-series expansion in the azimuthal direction is used to eliminate the azimuthal ϕ dependence from the radiative transfer equations. Then, the set of equations without the ϕ -dependence is solved using the Gaussian quadrature method where the integrals

in the radiative transfer equations are replaced by the Gaussian quadrature and the resulting system of first-order differential equations is solve by obtaining eigenvalues and eigenvectors and matching the boundary conditions. The effective boundary conditions are derived in terms of the effective reflection matrices to reduce the complexity of the problem to that of a two-layer problem. The effective reflection matrices can be solved recursively by considering only one layer at a time. The numerical results are illustrated by plotting backscattering cross sections as a function of frequency for multi-layered cases.

8.2 Formulation

Consider a N -layered random medium on top of a homogeneous halfspace with permittivity ϵ_{N+1} [Fig. 8.1]. The l -th layer is characterized by the permittivity $\epsilon_l - \epsilon_{fl}$, where ϵ_{fl} stands for the randomly fluctuating part whose amplitude is very small and whose ensemble average is zero, and the mean permittivity has small imaginary part, $\epsilon_l = \epsilon'_l + i\epsilon''_l$ where $\epsilon''_l \ll \epsilon'_l$. We further assume that the real part of the mean permittivities of the random layers are the same. $\epsilon'_l = \epsilon'_1$ for $l = 2, 3, \dots, N$. The radiative transfer equations which govern the propagation of intensities inside the l -th random medium are, for $0 < \theta < \pi$,

$$\cos \theta \frac{d}{dz} \bar{I}_l(\theta, \phi, z) = -K_{ul} \bar{I}_l(\theta, \phi, z) - \bar{K}_{sl}(\theta) \cdot \bar{I}_l(\theta, \phi, z) + \int_0^\pi d\theta' \sin \theta' \int_0^{2\pi} d\phi' \bar{P}_l(\theta, \phi; \theta', \phi') \cdot \bar{I}_l(\theta', \phi', z) \quad (1)$$

where

$$\bar{I}_l(\theta, \phi, z) = \begin{bmatrix} I_{vl}(\theta, \phi, z) \\ I_{hl}(\theta, \phi, z) \\ U_l(\theta, \phi, z) \\ V_l(\theta, \phi, z) \end{bmatrix} \quad (2)$$

I_{vl} is the vertically polarized specific intensity, I_{hl} is the horizontally polarized specific intensity, and U_l and V_l represent the correlation between two polarizations [Tsang and Kong, 1978; Shin and Kong, 1981], $\bar{P}_l(\theta, \phi; \theta', \phi')$ is a 4×4 scattering function matrix, which relates scattered intensities into the direction (θ, ϕ) to the incident intensities in the direction (θ', ϕ') , K_{ul} is the loss per unit length due to absorption, and $\bar{K}_{sl}(\theta)$ is the loss per unit length due to scattering. The random permittivity fluctuation is characterized by the variance of the fluctuation ϵ''_l and the correlation function with lateral correlation length l_{pl} and vertical correlation length l_{zl} . The correlation function

is assumed to have gaussian dependence laterally and exponential dependence vertically. The scattering function matrix and the scattering coefficient have been derived by applying Born approximation with the far-field solution and are well known [Tsang and Kong, 1978].

Consider an incident wave with specific intensity $\bar{I}_{i,n}(\pi - \theta_{i,n}, \phi_{i,n})$ impinging from region 0, which is assumed to be free space, upon the layered random medium. The incident beam in region 0 assumes the form

$$\bar{I}_{i,n}(\pi - \theta_{i,n}, \phi_{i,n}) = \bar{I}_{i,n} \delta(\cos \theta_{i,n} - \cos \theta_{i,n}) \delta(\phi_{i,n} - \phi_{i,n}) \quad (3)$$

where the use of Dirac delta function is made.

The boundary conditions for the specific intensities are [Tsang and Kong, 1978] for $0 < \theta < \pi/2$, at $z = d_l$ where $l = 1, 2, \dots, N - 1$

$$\bar{I}_{l+1}(\pi - \theta, \phi, z = -d_l) = \bar{I}_l(\pi - \theta, \phi, z = -d_l) \quad (4)$$

$$\bar{I}_l(\theta, \phi, z = -d_l) = \bar{I}_{l+1}(\theta, \phi, z = -d_l) \quad (5)$$

at $z = -d_N$

$$\bar{I}_N(\theta, \phi, z = -d_N) = \bar{\bar{R}}_{N(N+1)}(\theta) \cdot \bar{I}_N(\pi - \theta, \phi, z = -d_N) \quad (6)$$

and, at $z = 0$

$$\bar{I}_1(\pi - \theta, \phi, z = 0) = \bar{\bar{T}}_{01}(\theta_{i,n}) \cdot \bar{I}_{i,n}(\pi - \theta_{i,n}, \phi_{i,n}) + \bar{\bar{R}}_{10} \cdot \bar{I}_1(\theta, \phi, z = 0) \quad (7)$$

where we have broken up intensities in the scattering layer into upward going intensities $\bar{I}_l(\theta, \phi, z)$ and downward going intensities $\bar{I}_l(\pi - \theta, \phi, z)$. In the above equations $\bar{\bar{T}}_{01}(\theta_{i,n})$

represents the coupling from region 0 to region 1, $\bar{\bar{R}}_{10}(\theta)$ represents the coupling from upward going intensities into downward going intensities at the boundary of region 1 and region 0, and $\bar{\bar{R}}_{N(N+1)}(\theta)$ represents similar coupling at the boundary of region N and region $N + 1$ [Chapter 7, Appendix B].

Once the radiative transfer equations are solved subject to the boundary conditions (4) and (5), the scattered intensity in the direction $(\theta_{oss}, \phi_{oss})$ in region 0 is

$$\bar{I}_0(\theta_{oss}, \phi_{oss}) = \bar{\bar{T}}_{10}(\theta_s) \cdot \bar{I}_1(\theta_s, \phi_s, z = 0) + \bar{\bar{R}}_{01}(\theta_{oi}) \cdot \bar{I}_{oi}(\pi - \theta_{oi}, \phi_{oi}) \quad (8)$$

where $\bar{\bar{T}}_{10}(\theta)$ represents the coupling from region 1 to region 0. The bistatic scattering coefficients $\gamma_{\beta\alpha}(\theta_{oss}, \phi_{oss}; \theta_{oi}, \phi_{oi})$ are defined as the ratio of the scattered power of polarization β per unit solid angle in the direction $(\theta_{oss}, \phi_{oss})$ and the intercepted incident power of polarization α in the direction (θ_{oi}, ϕ_{oi}) averaged over 4π radians [Tsang and Kong, 1978; Peake, 1959].

$$\gamma_{\beta\alpha}(\theta_{oss}, \phi_{oss}; \theta_{oi}, \phi_{oi}) = 4\pi \frac{\cos \theta_{oss} I_{oi\beta s}(\theta_{oss}, \phi_{oss})}{\cos \theta_{oi} I_{oi\alpha i}} \quad (9)$$

where $\alpha, \beta = v$ or h with v denoting vertical polarization and h denoting horizontal polarization. In the backscattering direction $\theta_{oss} = \theta_{oi}$ and $\phi_{oss} = \pi + \phi_{oi}$. The backscattering cross sections per unit area are defined to be

$$\sigma_{\beta\alpha}(\theta_{oi}) = \cos \theta_{oi} \gamma_{\beta\alpha}(\theta_{oi}, \pi + \phi_{oi}; \theta_{oi}, \phi_{oi}) \quad (10)$$

8.3 Numerical Solution

The radiative transfer equations can be solved using a numerical approach. First, the azimuthal dependence from the radiative transfer equations are eliminated using the Fourier series expansion. Then, the resulting set of equations without the azimuthal dependence is solved numerically using the Gaussian quadrature method. The integrals in the radiative transfer theory are replaced by Gaussian quadratures and the resulting system of first-order differential equation with constant coefficients are solved by obtaining eigenvalues and eigenvectors and matching the boundary conditions.

The numerical solution for the specific intensities inside the l -th layer is given by [Chapter 7], for each harmonic and for even or odd series,

$$\bar{I}_l^+ = (\bar{E}_l + \bar{Q}_l) \cdot \bar{D}_l(z + d_{l-1}) \cdot \bar{x}_l + (\bar{E}_l - \bar{Q}_l) \cdot \bar{U}_l(z + d_l) \cdot \bar{y}_l \quad (11a)$$

$$\bar{I}_l^- = (\bar{E}'_l + \bar{Q}'_l) \cdot \bar{D}_l(z + d_{l-1}) \cdot \bar{x}_l + (\bar{E}'_l - \bar{Q}'_l) \cdot \bar{U}_l(z + d_l) \cdot \bar{y}_l \quad (11b)$$

where \bar{I}_l^+ and \bar{I}_l^- represent the upward and downward propagating intensities and \bar{x}_l and \bar{y}_l are the unknown constants.

The boundary conditions, which are to be used to determine the constants \bar{x}_l and \bar{y}_l of the upward and downward propagating intensities given by (11), can be obtained by discretizing the boundary conditions for the radiative transfer equations given by (4)–(7). They are, at $z = -d_l$, $l = 1, 2, \dots, N - 1$

$$\bar{I}_l^+(z = -d_l) = \bar{I}_{l-1}^+(z = -d_l) \quad (12)$$

$$\bar{I}_{l-1}^-(z = -d_l) = \bar{I}_l^-(z = -d_l) \quad (13)$$

at $z = -d_N$

$$\bar{I}_N^+(z = -d_N) = \bar{R}_{N(N+1)} \cdot \bar{I}_N^-(z = -d_N) \quad (14)$$

and at $z = 0$

$$\bar{I}_1^-(z = 0) = \bar{R}_{10} \cdot \bar{I}_1^+(z = 0) + \bar{T}_{01} \cdot \bar{I}_{0s}^- \quad (15)$$

Once the constants \bar{x}_l and \bar{y}_l are determined, the scattered intensities in region 0 from the random medium, represented by the first term on the right-hand-side of (8), can be determined. We have

$$\begin{aligned} \bar{I}_{0s}^- &= \bar{T}_{10} \cdot \bar{I}_1^+(z = 0) \\ &= \bar{T}_{10} \cdot \left[(\bar{E}_1 + \bar{Q}_1) \cdot \bar{x}_1 + (\bar{E}_1 - \bar{Q}_1) \cdot \bar{D}_1(-d_1) \cdot \bar{y}_1 \right] \end{aligned} \quad (16)$$

The complete solution is obtained by solving the radiative transfer equations using the Gaussian quadrature method for each harmonic and reintroducing the azimuthal dependence. The total scattered intensities in region 0 is given by

$$\begin{aligned} \bar{I}_{0s}(\phi_s) &= \left\{ \bar{R}_{01} + \bar{T}_{10} \cdot \left[\bar{I} - \bar{R}_{10} \cdot \bar{R}_{N(N+1)} \cdot \exp\{-\bar{\mu}^{-1} \cdot \bar{K} \cdot d\} \right]^{-1} \cdot \bar{T}_{01} \right\} \cdot \bar{I}_{0s}^- \delta(\phi_s - \phi_{0s}) \\ &+ \sum_{m=0}^{m_{max}} \left\{ \bar{T}_{10} \cdot \left[\bar{I}_1^{m,+}(z = 0) - \left[\bar{I} - \bar{R}_{10} \cdot \bar{R}_{N(N+1)} \cdot \exp\{-\bar{\mu}^{-1} \cdot \bar{K} \cdot d\} \right]^{-1} \cdot \bar{T}_{01} \cdot \bar{I}_{0s}^{m,-} \right] \right. \\ &\quad \left. + \bar{T}_{10} \cdot \bar{I}_1^{m,+}(z = 0) \sin m(\phi_s - \phi_{0s}) \right\} \end{aligned} \quad (17)$$

where

$$\bar{K} \cdot d = \sum_{l=1}^N \bar{K}_{,l} (d_l - d_{l-1}) \quad (18)$$

and $\bar{I}_1^{m,+}(z = 0)$ and $\bar{I}_1^{m,-}(z = 0)$ are the upward propagating m th cosine and sine harmonics evaluated at $z = 0$. In (17) the zeroth-order solution has been summed up. Once the scattered intensities in region 0 are obtained, the bistatic scattering coefficients and the backscattering cross sections can be obtained from (9) and (10).

8.4 Effective Boundary Conditions

The problem of determining the unknown constants \bar{x}_l and \bar{y}_l by matching the boundary conditions at $N+1$ boundaries can be simplified greatly by using the effective boundary conditions. The idea is to come up with the effective boundary condition at $z = -d_l$ in terms of the properties of the region l and the effective boundary condition at $z = -d_l$. Thus, only a two-layer problem needs to be solved at a time. The effective boundary conditions can be derived in terms of the effective reflection matrices which can be solved recursively. Therefore, the sizes of the matrices need not be increased compared to the two-layer case and the complexity of the problem is not increased. In this way the scattered intensity can be computed very efficiently.

Consider l -th random layer for $l = 2, 3, \dots, N$. First, we assume that the effective boundary conditions at $z = -d_l$ can be expressed as follows:

$$\bar{I}_l^+(z = -d_l) = \bar{\bar{R}}_{l(l+1)}^{eff} \cdot \bar{I}_l^-(z = -d_l) \quad (19)$$

where the effective reflection matrix contains all the information regarding l' -th layer where $l' < l$. Our goal is to come up with an effective boundary condition at $z = -d_l$ which relates the downward propagating intensity to the upward propagating intensity in region $l-1$. Thus, the effective reflection matrix at $z = -d_{l-1}$, $\bar{\bar{R}}_{(l-1)l}^{eff}$, should be expressed in terms of the properties of the l -th layer and the effective reflection matrix at $z = -d_l$. The boundary conditions at $z = -d_{l-1}$ are given by

$$\bar{I}_l^-(z = -d_{l-1}) = \bar{I}_{l-1}^-(z = -d_{l-1}) \quad (20)$$

and

$$\bar{I}_{l-1}^+(z = -d_{l-1}) = \bar{I}_l^+(z = -d_{l-1}) \quad (21)$$

Substituting in the solutions for the upward and downward propagating intensities, given by (11), into the boundary conditions (19) and (20), we obtain

$$(\bar{E}'_l + \bar{Q}'_l) \cdot \bar{x}_l + (\bar{E}'_l - \bar{Q}'_l) \cdot \bar{D}(-(d_l - d_{l-1})) \cdot \bar{y}_l = \bar{I}_{l-1}^-(z = -d_{l-1}) \quad (22)$$

$$\left[(\bar{E}_l + \bar{Q}_l) - \bar{R}_{l(l+1)}^{eff} \cdot (\bar{E}'_l + \bar{Q}'_l) \right] \cdot \bar{D}(-(d_l - d_{l-1})) \bar{x}_l + \left[(\bar{E}_l - \bar{Q}_l) - \bar{R}_{l(l+1)}^{eff} \cdot (\bar{E}'_l - \bar{Q}'_l) \right] \cdot \bar{y}_l = 0 \quad (23)$$

The above equations can be solved for the constants \bar{x}_l and \bar{y}_l . We let

$$\bar{c}_l = \begin{bmatrix} \bar{x}_l \\ \bar{y}_l \end{bmatrix} \quad (24)$$

$$\bar{M}_l = \begin{bmatrix} \bar{M}_{11; l} & \bar{M}_{12; l} \\ \bar{M}_{21; l} & \bar{M}_{22; l} \end{bmatrix} \quad (25)$$

$$\bar{N}_l = \begin{bmatrix} \bar{I}_l \\ 0 \end{bmatrix} \quad (26)$$

where

$$\bar{M}_{11; l} = (\bar{E}'_l + \bar{Q}'_l) \quad (27a)$$

$$\bar{M}_{12; l} = (\bar{E}'_l - \bar{Q}'_l) \cdot \bar{D}_l(-(d_l - d_{l-1})) \quad (27b)$$

$$\bar{M}_{21; l} = \left[(\bar{E}_l + \bar{Q}_l) - \bar{R}_{l(l-1)}^{eff} \cdot (\bar{E}'_l + \bar{Q}'_l) \right] \cdot \bar{D}_l(-(d_l - d_{l-1})) \quad (27c)$$

$$\bar{M}_{22; l} = (\bar{E}_l - \bar{Q}_l) - \bar{R}_{l(l+1)}^{eff} \cdot (\bar{E}'_l - \bar{Q}'_l) \quad (27d)$$

Then, (22) and (23) can be written in compact form as

$$\bar{M}_l \cdot \bar{c}_l = \bar{N}_l \cdot \bar{I}_{l-1}^-(z = -d_{l-1}) \quad (28)$$

Therefore, the constants \bar{x}_l and \bar{y}_l are given in terms of $\bar{I}_{l-1}^-(z = -d_{l-1})$.

$$\bar{c}_l = \bar{M}_l^{-1} \cdot \bar{N}_l \cdot \bar{I}_{l-1}^-(z = -d_{l-1}) \quad (29)$$

The boundary condition (21) can now be used to relate \bar{I}_{l-1}^- to \bar{I}_{l-1}^+ . Substituting (11) into (21), we have

$$\bar{I}_{l-1}^+(z = -d_{l-1}) = (\bar{E}_l + \bar{Q}_l) \cdot \bar{x}_l + (\bar{E}_l - \bar{Q}_l) \cdot \bar{D}(-(d_l - d_{l-1})) \cdot \bar{y}_l \quad (30)$$

We let

$$\bar{L}_l = \begin{bmatrix} \bar{L}_{1l} & \bar{L}_{2l} \end{bmatrix} \quad (31)$$

where

$$\bar{L}_{1l} = (\bar{E}_l + \bar{Q}_l) \quad (32a)$$

$$\bar{L}_{2l} = (\bar{E}_l - \bar{Q}_l) \cdot \bar{D}_l(-(d_l - d_{l-1})) \quad (32b)$$

Then, substituting (29) into (30) we obtain the following effective boundary condition at $z = -d_{l-1}$:

$$\bar{I}_{l-1}^+(z = -d_{l-1}) = \bar{R}_{(l-1)l}^{eff} \cdot \bar{I}_{l-1}^-(z = -d_{l-1}) \quad (33)$$

where

$$\bar{R}_{(l-1)l}^{eff} = \bar{L}_l \cdot \bar{M}_l^{-1} \cdot \bar{N}_l \quad (34)$$

The above effective reflection matrix at $z = -d_{l-1}$ is defined in terms of the properties of the l -th layer and the effective reflection matrix at $z = -d_l$. Therefore, the effective

reflection matrix can be calculated recursively and we only need to consider a two-layer problem at a time. Note that at $z = -d_N$, we have

$$\bar{\bar{R}}_{N(N+1)}^{eff} = \bar{\bar{R}}_{N(N+1)} \quad (35)$$

We start the calculation at the N -th layer where $\bar{\bar{R}}_{N(N+1)}$ is known and obtain the effective reflection matrix at $z = -d_{N-1}$. Once $\bar{\bar{R}}_{(N-1)N}^{eff}$ is obtained we start over and calculate the effective reflection matrix at $z = -d_{N-2}$. This is repeated until we have calculated $\bar{\bar{R}}_{12}^{eff}$, the effective reflection matrix at $z = -d_1$. In region 1, we obtain the following equations for the constants \bar{x}_1 and \bar{y}_1 upon matching the boundary conditions:

$$\left[(\bar{E}'_1 + \bar{Q}'_1) - \bar{R}_{10} \cdot (\bar{E}_1 + \bar{Q}_1) \right] \cdot \bar{x}_1 + \left[(\bar{E}'_1 - \bar{Q}'_1) - \bar{R}_{10} \cdot (\bar{E}_1 - \bar{Q}_1) \right] \cdot \bar{D}_1(-d_1) \cdot \bar{y}_1 = \bar{T}_{01} \cdot \bar{I}_{oi}^- \quad (36)$$

$$\left[(\bar{E}_1 + \bar{Q}_1) - \bar{R}_{12}^{eff} \cdot (\bar{E}'_1 + \bar{Q}'_1) \right] \cdot \bar{D}_1(-d_1) \bar{x}_1 + \left[(\bar{E}_1 - \bar{Q}_1) - \bar{R}_{12}^{eff} \cdot (\bar{E}'_1 - \bar{Q}'_1) \right] \cdot \bar{y}_1 = 0 \quad (37)$$

The above equations can be solved for the constants \bar{x}_1 and \bar{y}_1 . Then, the scattered intensity in region 0 is obtained from (16) and (17).

8.5 Results and Discussion

In this section we illustrate the numerical results of the backscattering cross sections for layered random medium. In our calculations $n = 16$ is used. In Figs. 8.2 and 8.3, the backscattering cross sections for like-like polarized return σ_{hh} and for depolarized return σ_{vh} are plotted as a function of frequency. The results for three-layer random medium are compared with the two-layer case. In the three-layer case we introduced a thin lossy layer at the top, which can be used to model the melting of snowpack in the afternoon due to sun-light illumination [Hofer and Schanda, 1978; Stiles and Ulaby, 1980]. The parameters used were the same as the ones used in Chapter 6 to illustrate the diurnal change in the brightness temperature measurements from snowpacks. We note that in the afternoon, compared with the morning case, there is a slight decrease in the backscattered power at low frequencies while the decrease may be substantial at higher frequencies.

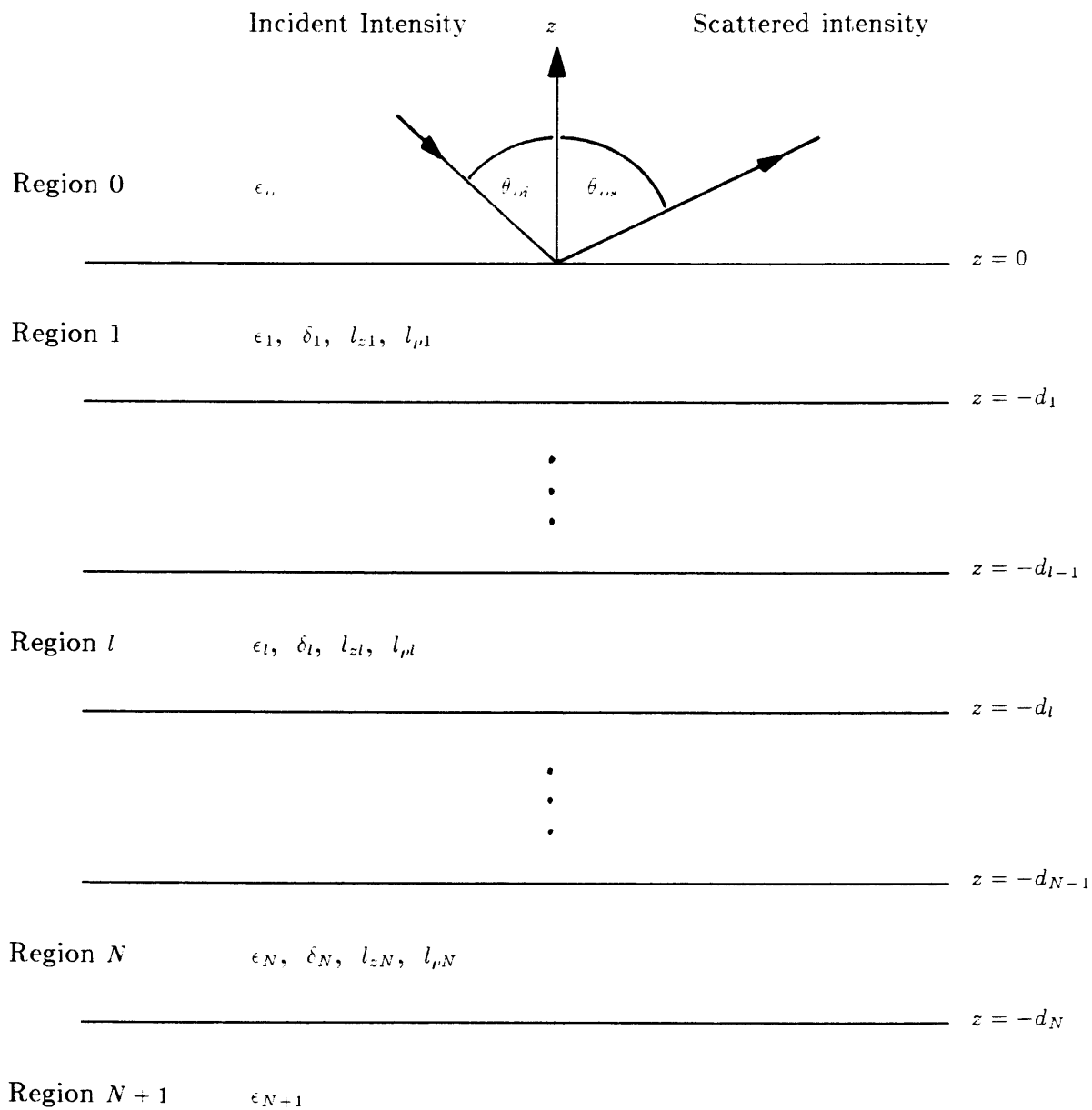


Figure 8.1 Geometrical configuration of the problem.

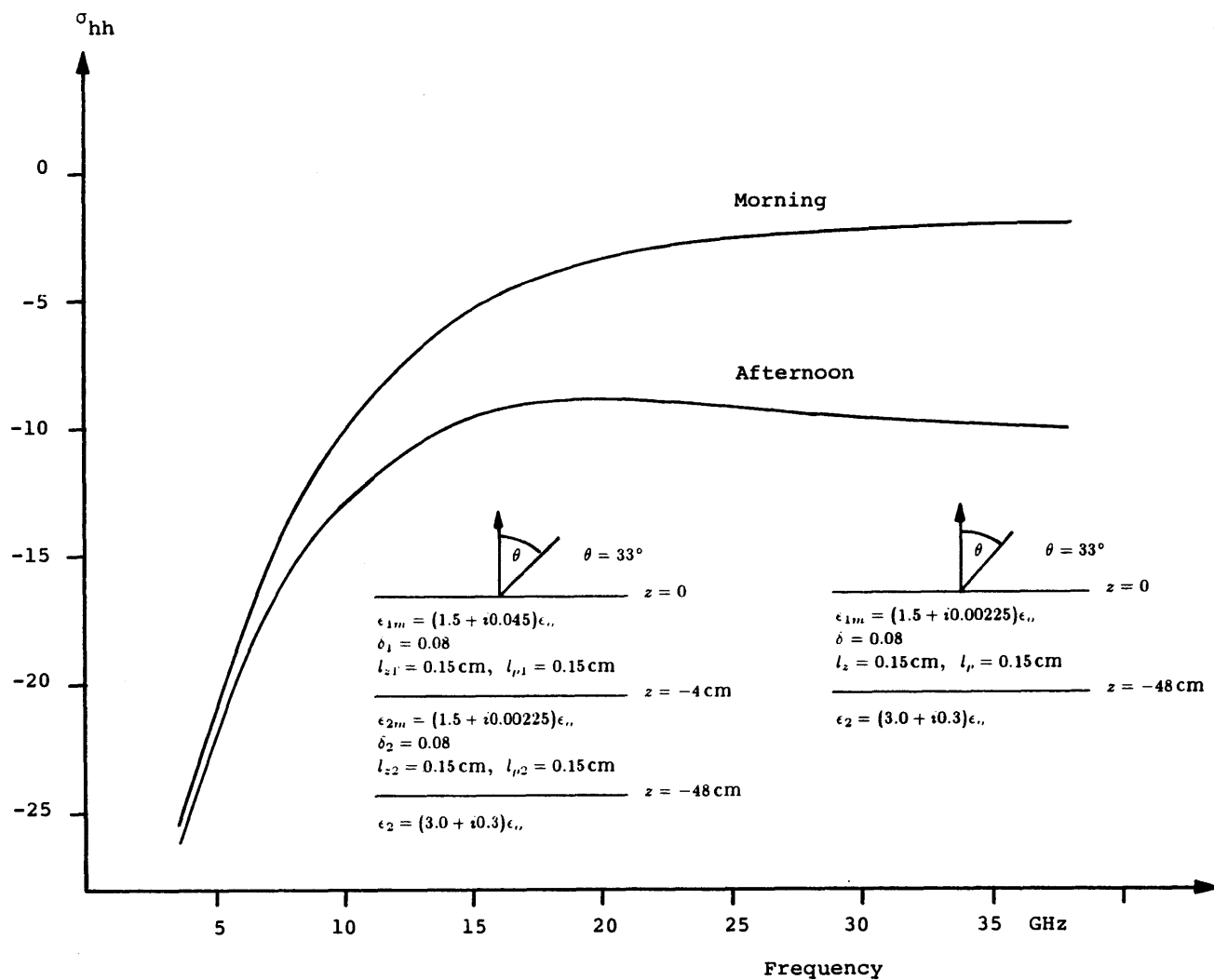


Figure 8.2 Backscattering cross section for horizontally polarized like-like return σ_{hh} as a function of frequency for a three-layer random medium.

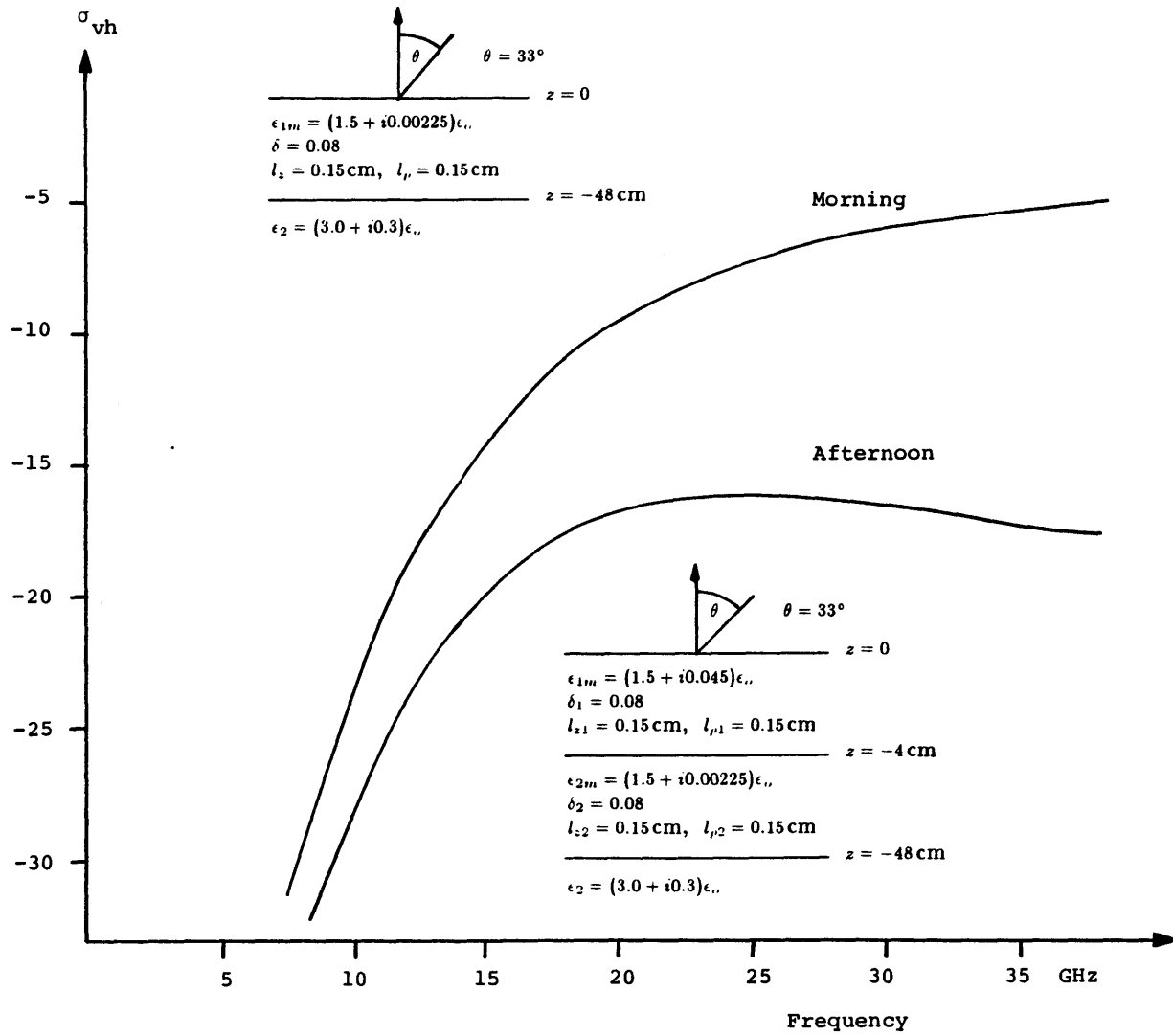


Figure 8.3 Backscattering cross section for depolarized return σ_{vh} as a function of frequency for a three-layer random medium.

CHAPTER 9

Theory for Thermal Microwave Emission from a Homogeneous Layer with Rough Surfaces Containing Spherical Scatterers

The radiative transfer theory is used to solve the problem of thermal microwave emission from a homogeneous layer containing spherical scatterers. To model volume scattering effects, we use the Mie phase functions. To model rough top and bottom interfaces, we use the bistatic coefficients for a randomly rough surface obtained using a combination of Kirchhoff theory and geometrical optics approach. Because the bistatic coefficients violate energy conservation, there is ambiguity in the emissivity. However, using two alternate formulations, the upper and lower limits of the emissivity are calculated. The effect of a rough surface is incorporated into the radiative transfer theory by modifying the boundary conditions for the intensities. The radiative transfer equations are then solved numerically by using a Gaussian quadrature method, and the results are illustrated by plotting the brightness temperatures as a function of observation angle for different polarizations. It is shown that the presence of a bottom rough surface increases the brightness temperature except at high angles for vertical polarization. The rough surface at the top boundary makes the angular behavior flatter and displays smaller differences between horizontal and vertical polarizations.

9.1 Introduction

In the passive microwave remote sensing of earth terrain the scattering effects due to medium inhomogeneities and rough interfaces play a dominant role in the determination of brightness temperatures. The effects of volume scattering have been treated with two theoretical models for the terrain media: (1) the random medium model where scattering effects can be accounted for by introducing a randomly fluctuating part in the permittivities, and (2) the discrete scatterer model where discrete scatterers are imbedded in a homogeneous background medium. The random medium model has been used extensively to study the thermal microwave emission from earth terrain [Tsang and Kong, 1975, 1976a,b,c, 1980b; Djermakoye and Kong, 1979]. Using the discrete scatterer model, England [1975] first examined emission darkening of a medium containing Rayleigh scatterers with the radiative transfer theory. More generalized results have been obtained [Chang *et al.*, 1976; Tsang and Kong, 1977a, 1979; Kong *et al.*, 1979] by making use of Mie scattering phase functions. These previous works on volume scattering all assumed planar boundaries, and the effect of rough surface scattering was neglected. However, in order to understand in a more meaningful way the problem of thermal microwave emission from natural terrains, we must study a composite model that can account for both the volume and surface scattering effects.

In this chapter we use radiative transfer theory to solve the problem of thermal microwave emission from a scattering layer overlaying a homogeneous half space with rough interfaces at the top and bottom boundaries. Mie scattering phase functions are used for volume scattering, and the bistatic scattering coefficients of a Gaussian random surface, obtained using a combination of the Kirchhoff approximation and a geometrical optics approach, are used for rough surface scattering. The rough surface

effects are incorporated into the radiative transfer equations by modifying the boundary conditions satisfied by the intensities at the top and bottom interfaces. The radiative transfer equations are solved numerically, using the Gaussian quadrature method. We use two alternate formulations to calculate the emissivity of the scattering layer. By calculating the bistatic coefficients of a scattering layer with rough top and bottom interfaces and integrating over the scattered angles in the upper hemisphere we obtain an upper limit for the emissivity by invoking the principle of reciprocity. A lower limit for the emissivity is obtained by directly calculating thermal microwave emission and assuming that the same medium is at a uniform temperature. The theoretical results are illustrated by plotting the brightness temperatures as functions of observation angle and polarization.

9.2 Formulation

Consider a slab of a homogeneous medium with permittivity $\epsilon_1 = \epsilon'_1 + i\epsilon''_1$ and physical temperature T_1 , containing randomly distributed spherical scatterers with radius a and permittivity $\epsilon_s = \epsilon'_s + i\epsilon''_s$, on top of a homogeneous medium with a permittivity $\epsilon_2 = \epsilon'_2 + i\epsilon''_2$ and temperature T_2 [Fig. 9.1]. The radiative transfer equations that govern the propagation of intensities inside the scattering layer are, for $0 < \theta < \pi$,

$$\cos \theta \frac{d}{dz} \bar{I}(\theta, z) = -K_a \bar{I}(\theta, z) - K_s \bar{I}(\theta, z) + K_a C_1 T_1 + \int_0^\pi d\theta' \sin \theta' \bar{P}(\theta, \theta') \cdot \bar{I}(\theta', z) \quad (1)$$

where

$$\bar{I}(\theta, z) = \begin{bmatrix} \bar{I}_v(\theta, z) \\ \bar{I}_h(\theta, z) \end{bmatrix} \quad (2)$$

I_v is the vertically polarized intensity, I_h is the horizontally polarized intensity, K_a denotes the absorption loss, K_s denotes the scattering loss, $C_1 = K\epsilon'_1/\epsilon_0\lambda^2$ with K denoting the Boltzmann constant, and $\bar{P}(\theta, \theta')$ is the scattering function matrix which relates the intensity scattered in the direction θ to the intensity incident in the direction θ' . For spherical scatterers of arbitrary size the Mie scattering phase functions can be used, and the expressions for the absorption and scattering coefficients K_a and K_s and the scattering function matrix $\bar{P}(\theta, \theta')$ are given in Appendix A [Tsang and Kong, 1977a].

The boundary conditions are, for $0 < \theta < \pi/2$ at $z = 0$,

$$\bar{I}(\pi - \theta, z = 0) = \int_0^{\pi/2} d\theta' \sin \theta' \bar{R}_{10}(\theta, \theta') \cdot \bar{I}(\theta', z = 0) \quad (3)$$

and at $z = -d$

$$\begin{aligned} \bar{I}(\theta, z = -d) &= \int_0^{\pi/2} d\theta' \sin \theta' \bar{R}_{12}(\theta, \theta') \cdot \bar{I}(\pi - \theta', z = -d) \\ &+ \int_0^{\pi/2} d\theta'_2 \sin \theta'_2 \bar{T}_{21}(\theta, \theta'_2) \cdot \bar{I}_2(\theta'_2) \end{aligned} \quad (4)$$

where we have broken up intensities into upward going intensities $\bar{I}(\theta, z)$ and downward going intensities $\bar{I}(\pi - \theta, z)$. In the above equations, $\bar{\bar{R}}_{10}(\theta, \theta')$ represents the coupling from upward going intensities in the direction θ' into the downward going intensities in the direction $(\pi - \theta)$ at the boundary of region 1 and region 0, $\bar{\bar{R}}_{12}(\theta, \theta')$ represents similar coupling at the boundary of region 1 and region 2, and $\bar{\bar{T}}_{12}(\theta, \theta')$ represents the coupling from region 2 to region 1. Once the radiative transfer equations are solved subject to the boundary conditions (3) and (4), the brightness temperature as measured by a radiometer is obtained from

$$\bar{T}_B(\theta_{\nu}) = \frac{1}{C_{\nu}} \int_0^{\pi/2} d\theta' \sin \theta' \bar{\bar{T}}_{10}(\theta_{\nu}, \theta') \cdot \bar{I}(\theta', z = 0) \quad (5)$$

where

$$\bar{T}_B(\theta_{\nu}) = \begin{bmatrix} T_{Bv}(\theta_{\nu}) \\ T_{Bh}(\theta_{\nu}) \end{bmatrix} \quad (6)$$

$\bar{\bar{T}}_{10}(\theta_{\nu}, \theta')$ represents coupling from region 1 to region 0 and $C_{\nu} = K/\lambda^2$. When $T_1 = T_2$, the emissivity of the medium can be calculated by

$$\begin{bmatrix} e_v(\theta_{\nu}) \\ e_h(\theta_{\nu}) \end{bmatrix} = \frac{1}{T_1} \begin{bmatrix} T_{Bv}(\theta_{\nu}) \\ T_{Bh}(\theta_{\nu}) \end{bmatrix} \quad (7)$$

9.3 Boundary Conditions

The boundary conditions for the intensities at the planar dielectric interfaces have been derived from the continuity of tangential electric and magnetic fields [Tsang and Kong, 1978]. For a rough interface the coupling matrices can be obtained from bistatic scattering coefficients for a rough interface. We model the interface to be an isotropic Gaussian random surface and assume that the Kirchhoff approximation can be used. The bistatic reflectivity function between the scattered direction \hat{k}_s and the incident direction \hat{k}_i is defined to be

$$P_{lm}(\hat{k}_s, \hat{k}_i) = \frac{r^2(S_r)_l}{(S_o)_a A_o \cos \theta_i} \quad (8)$$

and the bistatic transmissivity function between \hat{k}_t and \hat{k}_i is defined to be

$$Q_{lm}(\hat{k}_t, \hat{k}_i) = \frac{r^2(S_t)_l}{(S_o)_a A_o \cos \theta_i} \quad (9)$$

where subscript a represents the polarization of the incident wave, subscript b the polarization of the scattered wave, S_o , S_r , S_t the Poynting power density of the incident, scattered, and transmitted waves, A_o the area of the rough surface projected onto the xy plane, θ_i the incident angle, and r the distance from the observation point to the surface. The expressions for $P_{lm}(\hat{k}_s, \hat{k}_i)$ and $Q_{lm}(\hat{k}_t, \hat{k}_i)$ have been derived by means of vector diffraction integral and the method of stationary phase and are well known [Stogryn, 1967; Tsang and Kong, 1980a] (also see Appendix B). It has been shown that the solution obtained under the Kirchhoff approximation satisfies reciprocity but violates energy conservation [Lynch and Wagner, 1968,1970; Tsang and Kong, 1980a]. This

is due to the neglect of the effects of multiple scattering and shadowing. There have been many works on incorporating the shadowing effect into the bistatic coefficients [Beckman, 1965; Wagner, 1967; Smith, 1967a,b; Sancer, 1969]. In this chapter we use the shadowing function derived by Sancer [1969] and modify the bistatic reflectivity and transmissivity functions as follows:

$$\bar{P}(\hat{k}_s, \hat{k}_i) = S(\theta_s, \theta_i) \begin{bmatrix} P_{vv}(\hat{k}_s, \hat{k}_i) & P_{vh}(\hat{k}_s, \hat{k}_i) \\ P_{hv}(\hat{k}_s, \hat{k}_i) & P_{hh}(\hat{k}_s, \hat{k}_i) \end{bmatrix} \quad (10)$$

$$\bar{Q}(\hat{k}_t, \hat{k}_i) = S(\theta_t, \theta_i) \begin{bmatrix} Q_{vv}(\hat{k}_s, \hat{k}_i) & Q_{vh}(\hat{k}_s, \hat{k}_i) \\ Q_{hv}(\hat{k}_s, \hat{k}_i) & Q_{hh}(\hat{k}_s, \hat{k}_i) \end{bmatrix} \quad (11)$$

where

$$S(\theta_1, \theta_2) = \frac{1}{1 + \Lambda(\mu_1) + \Lambda(\mu_2)} \quad (12)$$

$$\Lambda(\mu) = \frac{1}{2} \left[\sqrt{2/\pi} \frac{s}{\mu} \exp(-\mu^2/2s^2) - \operatorname{erfc}(\mu/\sqrt{2}s) \right] \quad (13)$$

s^2 is the mean square surface slope, $\mu = \cot \theta$, and erfc is the complementary error function.

Making use of (8) and (9) to relate the reflected and transmitted intensities to the incident intensities, we obtain

$$\bar{I}_s(\theta_s, \phi_s) = \int_0^{\pi/2} d\theta_i \int_0^{2\pi} d\phi_i \frac{\cos \theta_i}{\cos \theta_s} \bar{P}(\hat{k}_s, \hat{k}_i) \cdot \bar{I}_i(\theta_i, \phi_i) \quad (14)$$

$$\bar{I}_t(\theta_t, \phi_t) = \int_0^{\pi/2} d\theta_i \int_0^{2\pi} d\phi_i \frac{\cos \theta_i}{\cos \theta_t} \bar{Q}(\hat{k}_t, \hat{k}_i) \cdot \bar{I}_i(\theta_i, \phi_i) \quad (15)$$

Comparing the above equations with (3) and (4) and noting that the thermal microwave emission is independent of the azimuthal angle ϕ , we obtain the coupling matrices:

$$\bar{T}_{st}(\theta_{st}, \theta_{st}) = \int_0^{2\pi} d\phi_{st} \frac{\cos \theta_{st}}{\cos \theta_{st}} \bar{Q}(\hat{k}_{st}, \hat{k}_{st}) \quad (16)$$

$$\bar{R}_{\alpha\beta}(\hat{\theta}_{\alpha s}, \hat{\theta}_{\alpha i}) = \int_0^{2\pi} d\phi_{\alpha i} \frac{\cos \hat{\theta}_{\alpha i}}{\cos \hat{\theta}_{\alpha s}} \bar{P}(\hat{k}_{\beta s}, \hat{k}_{\alpha i}) \quad (17)$$

The single scattering solution under the Kirchhoff approximation neglects the multiple scattering effect. Therefore, even with the shadowing effects accounted for, the energy conservation is only approximately observed. It can be shown that

$$\sum_{\alpha} \int_0^{2/\pi} d\theta_s \sin \theta_s \int_0^{2\pi} d\phi_s P_{\alpha\beta}(\hat{k}_s, \hat{k}_i) S(\theta_s, \theta_i) - \sum_{\alpha} \int_0^{2/\pi} d\theta_t \sin \theta_t \int_0^{2\pi} d\phi_t Q_{\alpha\beta}(\hat{k}_t, \hat{k}_i) S(\theta_t, \theta_i) \leq 1 \quad (18)$$

Because of this violation of energy conservation there is ambiguity in the emissivity of a rough surface [Tsang and Kong, 1980a]. The emissivity of a medium may also be calculated with a commonly used formula [Peake, 1959],

$$e_{\alpha}(\hat{k}_i) = 1 - \sum_{\beta} \frac{1}{4\pi} \int_{\text{hemisphere}} d\Omega_k \gamma_{\beta\alpha}(\hat{k}_s, \hat{k}_i) \quad (19)$$

where $\gamma_{\alpha\beta}(\hat{k}_s, \hat{k}_i)$ is the bistatic scattering coefficient due to the rough surface and volume scattering. The radiative transfer equations satisfy reciprocity and energy conservation. Therefore, for planar boundaries the above formula and the result of (7) are the same since the transmissivities and the reflectivities for the planar boundaries also satisfy reciprocity and energy conservation. However, for the rough surface case, because of violation of energy conservation, results due to (7) and (19) are not the same, and there is ambiguity in the emissivity.

9.4 Emissivity

The radiative transfer theory can be used to calculate the commonly used emissivity [Equation (19)] of a layer of homogeneous medium containing spherical scatterers with rough interfaces. The radiative transfer equations inside the scattering medium take the form [Shin and Kong, 1981]

$$\cos \theta \frac{d}{dz} \bar{I}(\theta, \phi, z) = -K_s \bar{I}(\theta, \phi, z) - K_r \bar{I}(\theta, \phi, z) + \int_0^{2\pi} d\phi' \int_0^\pi d\theta' \sin \theta' \bar{P}(\theta, \phi; \theta', \phi') \cdot \bar{I}(\theta', \phi', z) \quad (20)$$

where the intensity $\bar{I}(\theta, \phi, z)$ contains all four Stoke's parameters,

$$\bar{I}(\theta, \phi, z) = \begin{bmatrix} I_v(\theta, \phi, z) \\ I_h(\theta, \phi, z) \\ U(\theta, \phi, z) \\ V(\theta, \phi, z) \end{bmatrix} \quad (21)$$

The boundary conditions are, for $0 < \theta < \pi/2$,

$$\begin{aligned} \bar{I}(\pi - \theta, \phi, z = 0) &= \int_0^{2\pi} d\phi_{..} \int_0^{\pi/2} d\theta_{..} \sin \theta_{..} \bar{T}_{01}(\theta, \phi; \theta_{..}, \phi_{..}) \cdot \bar{I}_{..i}(\pi - \theta_{..}, \phi_{..}) \\ &+ \int_0^{2\pi} d\phi' \int_0^{\pi/2} d\theta' \sin \theta' \bar{R}_{10}(\theta, \phi; \theta', \phi') \cdot \bar{I}(\theta', \phi', z = 0) \end{aligned} \quad (22)$$

$$\bar{I}(\theta, \phi, z = -d) = \int_0^{2\pi} d\phi' \int_0^{\pi/2} d\theta' \sin \theta' \bar{R}_{12}(\theta, \phi; \theta', \phi') \cdot \bar{I}(\pi - \theta', \phi', z = -d) \quad (23)$$

The incident beam in region 0, $\bar{I}_{..i}(\pi - \theta_{..}, \phi_{..})$, assumes the form

$$\bar{I}_{..i}(\pi - \theta_{..}, \phi_{..}) = \bar{I}_{..i} \delta(\cos \theta_{..} - \cos \theta_{..i}) \delta(\phi_{..} - \phi_{..i}) \quad (24)$$

where the use of the Dirac delta function is made.

Once the radiative transfer equations are solved subject to the boundary conditions, the scattered intensity in the direction (θ_{os}, ϕ_{os}) in region 0 is determined from

$$\begin{aligned} \bar{I}_{os}(\theta_{os}, \phi_{os}) = & \int_0^{2\pi} d\phi_{oi} \int_0^{\pi/2} d\theta_{oi} \sin \theta_{oi} \bar{\bar{R}}_{01}(\theta_{os}, \phi_{os}; \theta_{oi}, \phi_{oi}) \bar{I}_{oi}(\pi - \theta_{oi}, \phi_{oi}) \\ & + \int_0^{2\pi} d\phi' \int_0^{\pi/2} d\theta' \sin \theta' \bar{\bar{T}}_{10}(\theta_{os}, \phi_{os}; \theta', \phi') \bar{I}(\theta', \phi', z = 0) \end{aligned} \quad (25)$$

The bistatic scattering coefficient $\gamma_{\beta\alpha}(\theta_{os}, \phi_{os}; \theta_{oi}, \phi_{oi})$ is defined as the ratio of scattered power of polarization β per unit solid angle in the direction (θ_{os}, ϕ_{os}) and the intercepted incident power of polarization α in the direction (θ_{oi}, ϕ_{oi}) averaged over 4π radians.

$$\gamma_{\beta\alpha}(\theta_{os}, \phi_{os}; \theta_{oi}, \phi_{oi}) = \frac{4\pi \cos \theta_{os} I_{\beta s}}{\cos \theta_{oi} I_{\alpha i}} \quad (26)$$

with $\alpha, \beta = v$ or h .

The radiative transfer equations can be solved with a numerical approach. A Fourier series expansion is used to eliminate the azimuthal ϕ dependence from the radiative transfer equations. We let

$$\bar{I}(\theta, \phi, z) = \bar{I}'(\theta, z) + \sum_{m=1}^{\infty} \left[\bar{I}^{m'c}(\theta, z) \cos m(\phi - \phi_i) + \bar{I}^{m's}(\theta, z) \sin m(\phi - \phi_i) \right] \quad (27)$$

$$\bar{\bar{P}}(\theta, \phi; \theta', \phi') = \bar{\bar{P}}'(\theta, z) + \sum_{m=1}^{\infty} \left[\bar{\bar{P}}^{m'c}(\theta, \theta') \cos m(\phi - \phi') + \bar{\bar{P}}^{m's}(\theta, \theta') \sin m(\phi - \phi') \right] \quad (28)$$

where the superscript m indicates the order of harmonics in the azimuthal direction and the superscripts c and s indicate the cosine and sine dependence. Substituting (27) and (28) into the radiative transfer equations, the ϕ' integration can be carried

out. Then, by collecting terms with the same cosine or sine dependence, we obtain, for $m = 0$,

$$\cos \theta \frac{d}{dz} \bar{I}''(\theta, z) = -K_n \bar{I}''(\theta, z) - K_s \bar{I}''(\theta, z) + 2\pi \int_0^\pi d\theta' \sin \theta' \bar{P}''(\theta, \theta') \cdot \bar{I}''(\theta', z) \quad (29)$$

and for $m \geq 1$

$$\begin{aligned} \cos \theta \frac{d}{dz} \bar{I}'''(\theta, z) &= -K_n \bar{I}'''(\theta, z) - K_s \bar{I}'''(\theta, z) \\ &+ \pi \int_0^\pi d\theta' \sin \theta' \left\{ \bar{P}'''(\theta, \theta') \cdot \bar{I}'''(\theta', z) - \bar{P}'''(\theta, \theta') \cdot \bar{I}'''(\theta', z) \right\} \end{aligned} \quad (30)$$

$$\begin{aligned} \cos \theta \frac{d}{dz} \bar{I}''''(\theta, z) &= -K_n \bar{I}''''(\theta, z) - K_s \bar{I}''''(\theta, z) \\ &+ \pi \int_0^\pi d\theta' \sin \theta' \left\{ \bar{P}''''(\theta, \theta') \cdot \bar{I}''''(\theta', z) - \bar{P}''''(\theta, \theta') \cdot \bar{I}''''(\theta', z) \right\} \end{aligned} \quad (31)$$

Similarly, by expanding the reflection and transmission matrices and the incident intensity into Fourier series, the boundary conditions for each harmonic can be obtained from (22) and (23). Once the scattered intensities in region 0 are obtained, the bistatic scattering coefficients can be obtained from (26). In terms of its Fourier components,

$$\begin{aligned} \gamma_{\theta_{os}, \phi_{os}; \theta_{oi}, \phi_{oi}} &= 4\pi \cos \theta_{os} \frac{1}{\cos \theta_{oi} I_{oi}} \\ &\times \left\{ I_{\beta_{os}}''(\theta_{os}) + \sum_{m=1}^{\infty} [I_{\beta_{os}}'''(\theta_{os}) \cos m(\phi_{os} - \phi_{oi}) + I_{\beta_{os}}''''(\theta_{os}) \sin m(\phi_{os} - \phi_{oi})] \right\} \end{aligned} \quad (33)$$

Then, the emissivity can be obtained using (19)

$$\begin{aligned} e_{oi}(\theta_{oi}) &= 1 - \sum_{\theta} \frac{1}{4\pi} \int_0^{\pi/2} d\theta_{os} \sin \theta_{os} \int_0^{2\pi} d\phi_{os} \gamma_{\beta_{os}}(\theta_{os}, \phi_{os}; \theta_{oi}, \phi_{oi}) \\ &= 1 - \sum_{\theta} \int_0^{\pi/2} d\theta_{os} \sin \theta_{os} \frac{2\pi \cos \theta_{os} I_{\beta_{os}}''(\theta_{os})}{\cos \theta_{oi} I_{oi}} \end{aligned} \quad (33)$$

We note that in calculating the emissivity only the zeroth-order harmonic is needed because of ϕ_{os} integration, and therefore the complexity of the problem is the same as the formulation in Section 9.2.

9.5 Numerical Results and Discussion

Our task now is to solve the radiative transfer equations subject to the boundary conditions. We solve the equations by a numerical approach using a Gaussian quadrature method. We first replace the boundary conditions by a Gaussian quadrature, an appropriately weighted sum over $2n$ intervals between $2n$ zeroes of the even-order Legendre polynomial $P_{2n}(\theta)$. In our calculations, $n = 16$ is used. The resulting system of first-order differential equations with constant coefficients is then solved by obtaining eigenvalues and eigenvectors and matching the boundary conditions [Tsang and Kong, 1977a, 1980b]. Once the brightness temperatures and the bistatic scattering coefficients are obtained, we can calculate the upper and lower limits of the emissivity using (19) and (7), respectively. The emissivity calculated using (19) represents the upper limit of the correct solution since the bistatic scattering coefficients are obtained using only the single scattering solution for the rough interfaces. If the higher-order scattering effects at the rough surfaces are included, the net reflected power will be higher and the emissivity will always be lower. The emissivity calculated using (6) and (7) with boundary conditions incorporating only single scattering effects represents the lower limit of the correct solution. If the higher-order scattering effects at the rough interfaces are included, the elements of the transmission and reflection matrices in (18) and (17) will both increase. Consequently, more thermal emission from the bottom homogeneous medium and the scattering medium will be transmitted, and the emissivity is always increased. Therefore, the two results represent the upper and lower limits of the correct solution, and the ambiguity is due to the violation of energy conservation. Note that a well-defined emissivity of a medium depends on (1) the satisfaction of reciprocity relations, and (2) the satisfaction of conservation of energy by bistatic

scattering coefficients.

In Fig. 9.2, the effect of the rough bottom boundary is illustrated by plotting the brightness temperatures as a function of observation angle for the vertical and horizontal polarizations (optical depth = $K.d$). The volume scattering effects are not included in order to isolate the rough surface scattering effects on the emissivities. The solid lines represent the upper and lower limits of the correct solution for the rough surface case, and the dotted lines represent the plane boundary case. Compared to the planar bottom boundary case, there is a general increase in the brightness temperature except at the high angles for vertical polarization. This decrease is due to the decrease in the emissivity of the bottom medium for the vertical polarization. The increase in the brightness temperature at nadir is due to the interaction of the rough bottom boundary and the top boundary. If we consider an incident beam at nadir, some of the reflected intensities from the rough bottom boundary will be incident at the first boundary at an angle greater than the critical angle. Therefore, the net reflected intensity in region 0 is smaller, and the emissivity will increase. Also note the larger ambiguity for the horizontal polarization due to worse energy conservation. If we keep all the parameters the same and increase the permittivity ϵ_2 , the overall brightness temperature will decrease due to higher reflectivity at the bottom boundary. Also, the difference between the plane and rough bottom boundaries is greater [Fig. 9.3]. In Fig. 9.4, the mean square surface slope s^2 is increased to 0.1. There is a larger increase in the brightness temperature. However, the ambiguity is also larger due to worse energy conservation. In Fig. 9.5 we increase the permittivity of region 1, $\epsilon_1 = (3.0 + i0.0018)\epsilon_0$, and also increase $\epsilon_2 = 12\epsilon_0$, such that \bar{R}_{12} and \bar{T}_{21} remain the same. We note the larger difference between the results of plane and rough bottom boundaries. This is due to the fact that for larger ϵ_1 the critical angle is smaller.

In Figs. 9.6 and 9.7, the brightness temperature is plotted for the cases of rough top boundary for two different mean square surface slopes. Both polarizations show the flattening of the angular behavior. For larger mean square surface slope, the angular behavior is more flat and also the ambiguity is increased. In Fig. 9.8 the results for the rough top and bottom boundaries are illustrated. We see that the effects of rough top and bottom boundaries are superimposed resulting in increasing of the brightness temperature at nadir and flattening of the angular behavior.

In Figs. 9.9, 9.10, and 9.11, the results of volume scattering (albedo = $K_v/(K_v + K_s)$) combined with the rough surface scattering are shown. There is darkening of the brightness temperature due to volume scattering. Also, there is larger coupling of the intensities propagating in the different directions causing the larger ambiguities at nadir angles. In Figs. 9.12 and 9.13, we compare the theoretical results with an experimental data set obtained during the winter season of 1977-78 in Colorado [Shiue *et al.*, 1978] for vertical and horizontal polarizations at 18 GHz. The combined volume and rough surface scattering model gives a better match with the data set which exhibits a fairly flat angular behavior.

Appendix A: Absorption Coefficient, Scattering Coefficient, and Scattering Function Matrix for a Homogeneous Medium Containing Mie Scatterers

The scattering coefficient K_s is given by

$$K_s = N \frac{2\pi}{k_1'^2} \sum_{n=1}^{\infty} (2n+1) (|A_n|^2 + |B_n|^2) \quad (A1)$$

where N is the number of scattering spheres per unit volume and k_1' is the real part of the wave number in region 1, k_1 . The coefficients A_n and B_n are given by [Deirmendjian, 1969]

$$A_n = -\frac{\text{Re}[q_n(\rho_1)] [k_s/k_1' F_n(\rho_2) + n/\rho_1] - \text{Re}[q_{n-1}(\rho_1)]}{q_n(\rho_1) [k_s/k_1' F_n(\rho_2) + n/\rho_1] - q_{n-1}(\rho_1)} \quad (A2)$$

$$B_n = -\frac{\text{Re}[q_n(\rho_1)] [k_1'/k_s F_n(\rho_2) + n/\rho_1] - \text{Re}[q_{n-1}(\rho_1)]}{q_n(\rho_1) [k_1'/k_s F_n(\rho_2) + n/\rho_1] - q_{n-1}(\rho_1)} \quad (A3)$$

where $k_s = \omega \sqrt{\mu_r \epsilon_s}$, $\rho_1 = k_1' a$, and $\rho_2 = k_s a$. The function $F_n(\rho_2)$ satisfy the recurrence formula

$$F_n(\rho_2) = -\frac{n}{\rho_2} + \left[\frac{n}{\rho_2} - F_{n-1}(\rho_2) \right]^{-1} \quad (A4)$$

and

$$F_0(\rho_2) = \cot \rho_2 \quad (A5)$$

The function $q_n(\rho_1)$ satisfy the recurrence formula

$$q_n(\rho_1) = \frac{2n-1}{\rho_1} q_{n-1}(\rho_1) - q_{n-2}(\rho_1) \quad (A6)$$

and

$$q_0(\rho_1) = -i \exp(i\rho_1) \quad (A7)$$

$$q_1(\rho_1) = -\exp(i\rho_1) \left[1 - \frac{1}{\rho_1} \right] \quad (\text{A8})$$

The absorption coefficient K_a can be divided into two parts, K_{ab} and K_{as} . K_{ab} is the absorption due to the background medium. and K_{as} is the absorption coefficient due to the scatterers.

$$K_a = K_{ab} + K_{as} \quad (\text{A9})$$

$$K_{ab} = 2k_1''(1 - f) \quad (\text{A10})$$

$$K_{as} = K_{ext} - K_s \quad (\text{A11})$$

where f is the fractional volume occupied by the scatterers and K_{ext} is the extinction coefficient due to the scatterers which is given by

$$K_{ext} = -N \frac{2\pi}{k_1'^2} \sum_{n=1}^{\infty} (2n+1) \text{Re}(A_n + B_n) \quad (\text{A12})$$

The scattering function matrix is given by [Tsang and Kong, 1977a]

$$\bar{P}(\theta, \theta') = \begin{bmatrix} P_{11}(\theta, \theta') & P_{12}(\theta, \theta') \\ P_{21}(\theta, \theta') & P_{22}(\theta, \theta') \end{bmatrix} \quad (\text{A13})$$

$$P_{11}(\theta, \theta') = \frac{8\pi N}{k_1'^2} \left| \sum_{n=1}^{\infty} \frac{B_n}{n(n+1)} s_n''(\cos \theta) s_n''(\cos \theta') \right|^2 + \frac{16\pi N}{k_1'^2} \sum_{m=1}^{\infty} \left| \sum_{n=m}^{\infty} \frac{1}{n(n+1)} [A_n m^2 t_n'''(\cos \theta) t_n'''(\cos \theta') + B_n s_n'''(\cos \theta) s_n'''(\cos \theta')] \right|^2 \quad (\text{A14})$$

$$P_{12}(\theta, \theta') = \frac{16\pi N}{k_1'^2} \sum_{m=1}^{\infty} \left| \sum_{n=m}^{\infty} \frac{m}{n(n+1)} [A_n t_n'''(\cos \theta) s_n'''(\cos \theta') + B_n s_n'''(\cos \theta) t_n'''(\cos \theta')] \right|^2 \quad (\text{A15})$$

$$P_{21}(\theta, \theta') = \frac{16\pi N}{k_1'^2} \sum_{m=1}^{\infty} \left| \sum_{n=m}^{\infty} \frac{m}{n(n+1)} [A_n s_n'''(\cos \theta) t_n'''(\cos \theta') + B_n t_n'''(\cos \theta) s_n'''(\cos \theta')] \right|^2 \quad (\text{A16})$$

$$P_{22}(\theta, \theta') = \frac{8\pi N}{k_1'^2} \left| \sum_{n=1}^{\infty} \frac{A_n}{n(n+1)} s_n''(\cos \theta) s_n''(\cos \theta') \right|^2 \\ + \frac{16\pi N}{k_1'^2} \sum_{m=1}^{\infty} \left| \sum_{n=m}^{\infty} \frac{1}{n(n+1)} [A_n s_n'''(\cos \theta) s_n'''(\cos \theta') + B_n m^2 t_n'''(\cos \theta) t_n'''(\cos \theta')] \right|^2 \quad (\text{A17})$$

where

$$t_n'''(\cos \theta) = \frac{P_n'''(\cos \theta)}{\sin \theta} \left(\frac{(2n+1)(n-m)!}{2(n+m)!} \right)^{1/2} \quad (\text{A18})$$

$$s_n'''(\cos \theta) = n \cos \theta t_n'''(\cos \theta) - \left[\frac{2n-1}{2n-1} (n^2 - m^2) \right]^{1/2} t_{n-1}'''(\cos \theta) \quad (\text{A19})$$

and $P_n'''(\cos \theta)$ is the associated Legendre polynomial of degree n and order m . The function $t_n'''(\cos \theta)$ obeys the recurrence relations

$$t_{m+1}'''(\cos \theta) = -\sin \theta \left[\frac{2m+3}{2m+2} \right]^{1/2} t_m'''(\cos \theta) \quad (\text{A20})$$

$$t_{m+1}'''(\cos \theta) = (2m+3)^{1/2} \cos \theta t_m'''(\cos \theta) \quad (\text{A21})$$

$$t_n'''(\cos \theta) = \left[\frac{2n+1}{n^2 - m^2} \right]^{1/2} \left((2n-1)^{1/2} \cos \theta t_{n-1}'''(\cos \theta) - \left[\frac{(n-1)^2 - m^2}{2n-3} \right]^{1/2} t_{n-2}'''(\cos \theta) \right) \quad (\text{A22})$$

Note that $t_1'''(\cos \theta) = -\sqrt{3}/2$ and $s_n'''(\cos \theta) = m \cos \theta t_n'''(\cos \theta)$. The functions $t_n'''(\cos \theta)$ and $s_n'''(\cos \theta)$ are well behaved as n and m become large.

Appendix B: Bistatic Reflectivity and Transmissivity Functions for Gaussian Random Surface

The bistatic reflectivity functions have been determined to be [Stogryn, 1967]

$$P_{lm}(\hat{k}_s, \hat{k}_i) = \frac{|\bar{k}_d|^4}{4 |\hat{k}_i \times \hat{k}_s|^4 k_{dz}^4 \cos \theta_i} \frac{1}{2\pi s^2} \exp \left[-\frac{k_{dz}^2}{2s^2 k_{dz}^2} \right] f_{lm} \quad (B1)$$

where

$$f_{vv} = \left| (\hat{h}_s \cdot \hat{k}_i)(\hat{h}_i \cdot \hat{k}_s)R_h + (\hat{v}_s \cdot \hat{k}_i)(\hat{v}_i \cdot \hat{k}_s)R_v \right|^2$$

$$f_{vh} = \left| (\hat{h}_s \cdot \hat{k}_i)(\hat{v}_i \cdot \hat{k}_s)R_h - (\hat{v}_s \cdot \hat{k}_i)(\hat{h}_i \cdot \hat{k}_s)R_v \right|^2$$

$$f_{hv} = \left| (\hat{v}_s \cdot \hat{k}_i)(\hat{h}_i \cdot \hat{k}_s)R_h - (\hat{h}_s \cdot \hat{k}_i)(\hat{v}_i \cdot \hat{k}_s)R_v \right|^2$$

$$f_{hh} = \left| (\hat{v}_s \cdot \hat{k}_i)(\hat{v}_i \cdot \hat{k}_s)R_h + (\hat{h}_s \cdot \hat{k}_i)(\hat{h}_i \cdot \hat{k}_s)R_v \right|^2$$

$$\hat{k}_i = \hat{x} \sin \theta_i \cos \phi_i + \hat{y} \sin \theta_i \sin \phi_i - \hat{z} \cos \theta_i$$

$$\hat{k}_s = \hat{x} \sin \theta_s \cos \phi_s + \hat{y} \sin \theta_s \sin \phi_s + \hat{z} \cos \theta_s$$

$$\hat{h}_i = -\hat{x} \sin \phi_i + \hat{y} \cos \phi_i = \hat{z} \times \hat{k}_i / |\hat{z} \times \hat{k}_i|$$

$$\hat{h}_s = -\hat{x} \sin \phi_s + \hat{y} \cos \phi_s = \hat{z} \times \hat{k}_s / |\hat{z} \times \hat{k}_s|$$

$$\hat{v}_i = -\hat{x} \cos \theta_i \cos \phi_i - \hat{y} \cos \theta_i \sin \phi_i - \hat{z} \sin \theta_i = \hat{h}_i \times \hat{k}_i$$

$$\hat{v}_s = \hat{x} \cos \theta_s \cos \phi_s + \hat{y} \cos \theta_s \sin \phi_s - \hat{z} \sin \theta_s = \hat{h}_s \times \hat{k}_s$$

$$\bar{k}_d = \bar{k}_i - \bar{k}_s = \hat{x}k_{dx} + \hat{y}k_{dy} + \hat{z}k_{dz}$$

$$k_{dx} = k(\sin \theta_i \cos \phi_i - \sin \theta_s \cos \phi_s)$$

$$k_{dy} = k(\sin \theta_i \sin \phi_i - \sin \theta_s \sin \phi_s)$$

$$k_{dz} = -k(\cos \theta_i + \cos \theta_s)$$

$$k_{dp}^2 = k_{dx}^2 + k_{dy}^2$$

s^2 is the mean square surface slope and the reflection coefficients for the horizontal and vertical polarizations are

$$R_h = \frac{-(\hat{n} \cdot \hat{k}_i) - |n_i^2 - 1 + (\hat{n} \cdot \hat{k}_i)^2|^{1/2}}{-(\hat{n} \cdot \hat{k}_i) + |n_i^2 - 1 + (\hat{n} \cdot \hat{k}_i)^2|^{1/2}}$$

$$R_v = \frac{-n_i^2(\hat{n} \cdot \hat{k}_i) - |n_i^2 - 1 + (\hat{n} \cdot \hat{k}_i)^2|^{1/2}}{-n_i^2(\hat{n} \cdot \hat{k}_i) + |n_i^2 - 1 + (\hat{n} \cdot \hat{k}_i)^2|^{1/2}}$$

with

$$\hat{n} = \frac{\hat{x}k_{dx}/k_{dz} + \hat{y}k_{dy}/k_{dz} + \hat{z}}{(k_{dx}^2/k_{dz}^2 + k_{dy}^2/k_{dz}^2 + 1)^{1/2}}$$

$$n_t = k_t/k$$

$$k = \omega\sqrt{\mu_r\epsilon}$$

$$k_t = \omega\sqrt{\mu_r\epsilon_t}$$

The bistatic transmissivity functions have been determined to be [Tsang and Kong, 1980a]

$$Q_{ba}(\hat{k}_t, \hat{k}_i) = \frac{k_t^2}{|\hat{k}_i \times \hat{k}_t|^4} \frac{\eta}{\eta_t} \frac{|\bar{k}_d|^2 (\hat{n} \cdot \hat{k}_t)^2}{k_{dz}^4 \cos \theta_i} \frac{1}{2\pi s^2} \exp \left[-\frac{k_{dp}^2}{2s^2 k_{dz}^2} \right] W_{ba} \quad (B2)$$

where

$$W_{ba} = \left| (\hat{h}_t \cdot \hat{k}_i)(\hat{h}_i \cdot \hat{k}_t)(1 + R_h) + (\hat{v}_t \cdot \hat{k}_i)(\hat{v}_i \cdot \hat{k}_t) \frac{1 + R_v}{n_t} \right|^2$$

$$W_{h,r} = \left| -(\hat{v}_t \cdot \hat{k}_i)(\hat{h}_i \cdot \hat{k}_t)(1 + R_h) - (\hat{h}_t \cdot \hat{k}_i)(\hat{v}_i \cdot \hat{k}_t) \frac{1 + R_r}{n_t} \right|^2$$

$$W_{v,h} = \left| (\hat{h}_t \cdot \hat{k}_i)(\hat{v}_i \cdot \hat{k}_t)(1 + R_h) - (\hat{v}_t \cdot \hat{k}_i)(\hat{h}_i \cdot \hat{k}_t) \frac{1 + R_r}{n_t} \right|^2$$

$$W_{h,h} = \left| (\hat{v}_t \cdot \hat{k}_i)(\hat{v}_i \cdot \hat{k}_t)(1 + R_h) + (\hat{h}_t \cdot \hat{k}_i)(\hat{h}_i \cdot \hat{k}_t) \frac{1 + R_r}{n_t} \right|^2$$

$$\hat{k}_t = \hat{x} \sin \theta_t \cos \phi_t + \hat{y} \sin \theta_t \sin \phi_t - \hat{z} \cos \theta_t$$

$$\hat{h}_t = -\hat{x} \sin \phi_t + \hat{y} \cos \phi_t$$

$$\hat{v}_t = -\hat{x} \cos \theta_t \cos \phi_t - \hat{y} \cos \theta_t \sin \phi_t - \hat{z} \sin \theta_t$$

$$\bar{k}_{,d} = \bar{k}_i - \bar{k}_t = \hat{x} k_{,dx} + \hat{y} k_{,dy} + \hat{z} k_{,dz}$$

$$k_{,dx} = k \sin \theta_i \cos \phi_i - k_t \sin \theta_t \cos \phi_t$$

$$k_{,dy} = k \sin \theta_i \sin \phi_i - k_t \sin \theta_t \sin \phi_t$$

$$k_{,dz} = -k \cos \theta_i + k_t \cos \theta_t$$

$$R_h = \frac{(\hat{n} \cdot \hat{k}_i) - (\hat{n} \cdot \hat{k}_t) n_t}{(\hat{n} \cdot \hat{k}_i) + (\hat{n} \cdot \hat{k}_t) n_t}$$

$$R_r = \frac{n_t(\hat{n} \cdot \hat{k}_i) - (\hat{n} \cdot \hat{k}_t) n_t}{n_t(\hat{n} \cdot \hat{k}_i) + (\hat{n} \cdot \hat{k}_t) n_t}$$

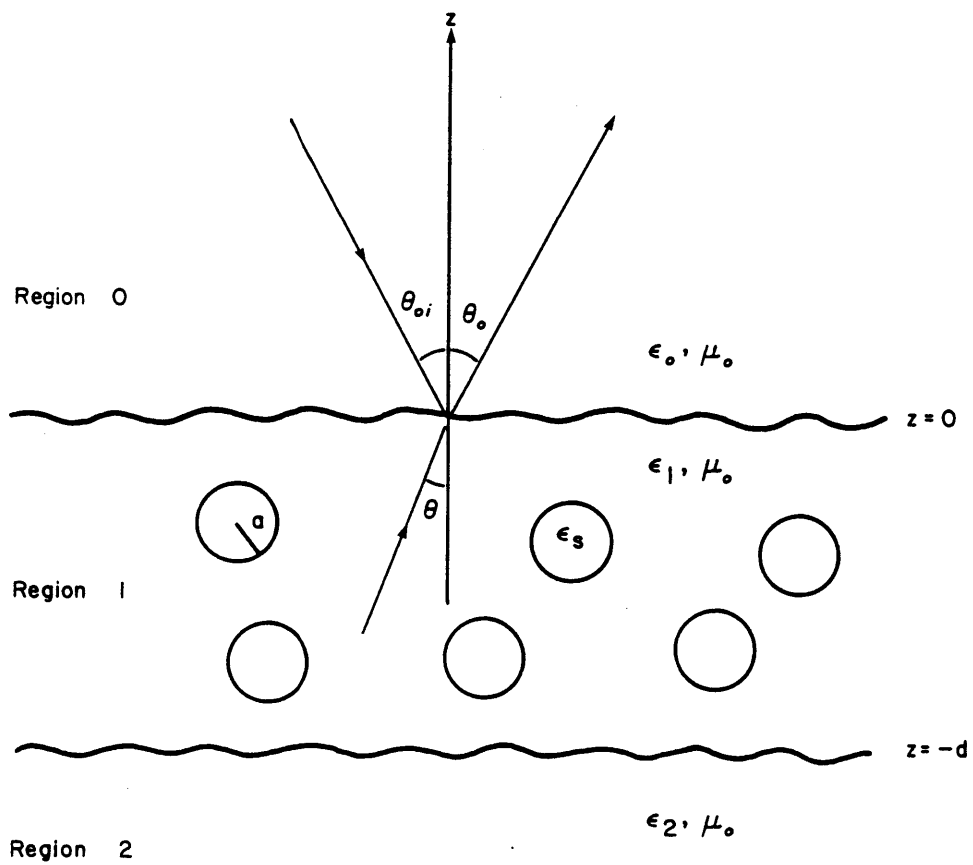


Figure 9.1 Geometrical configuration of the problem.

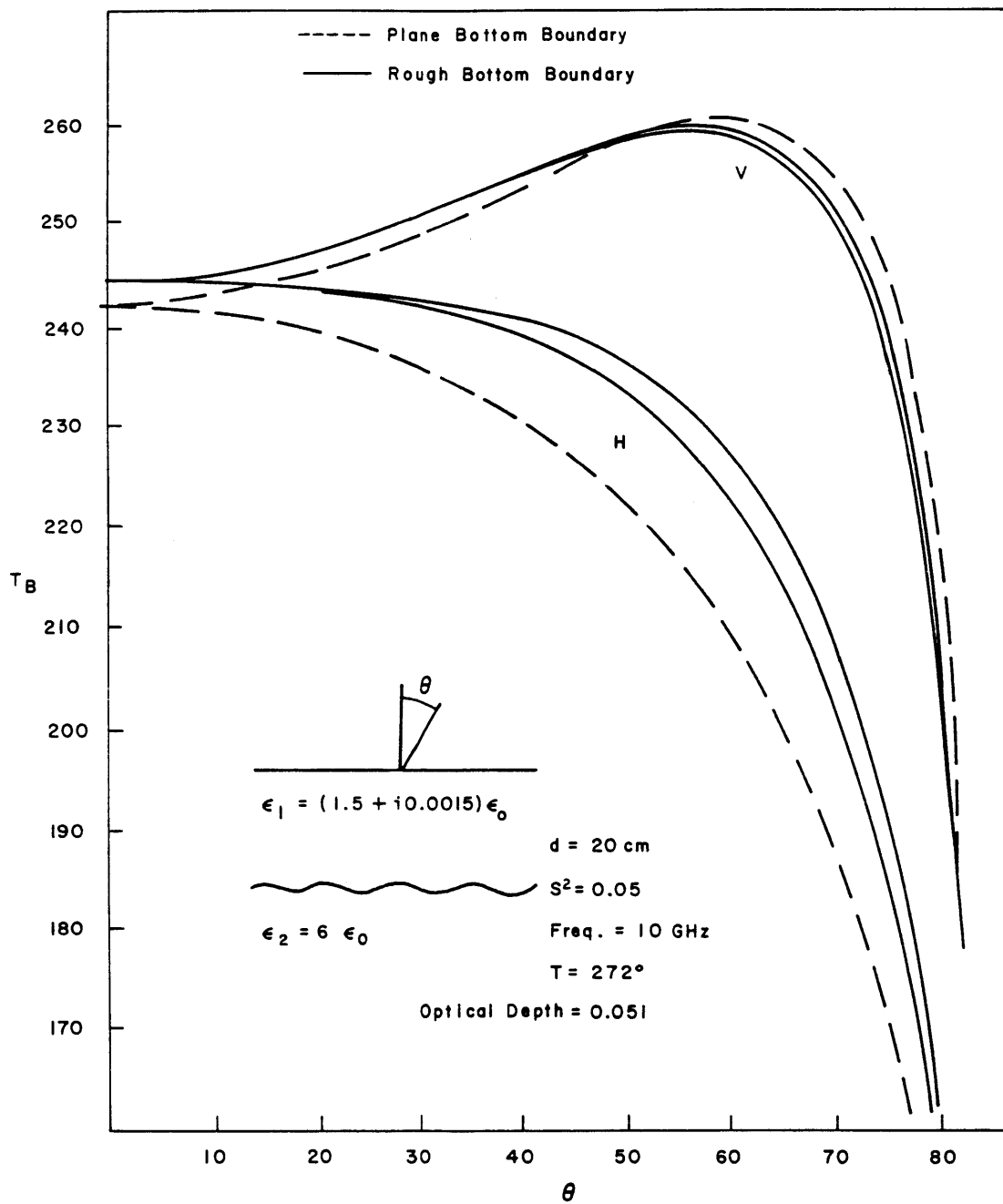


Figure 9.2 Brightness temperature as a function of angle for rough surface at bottom boundary.

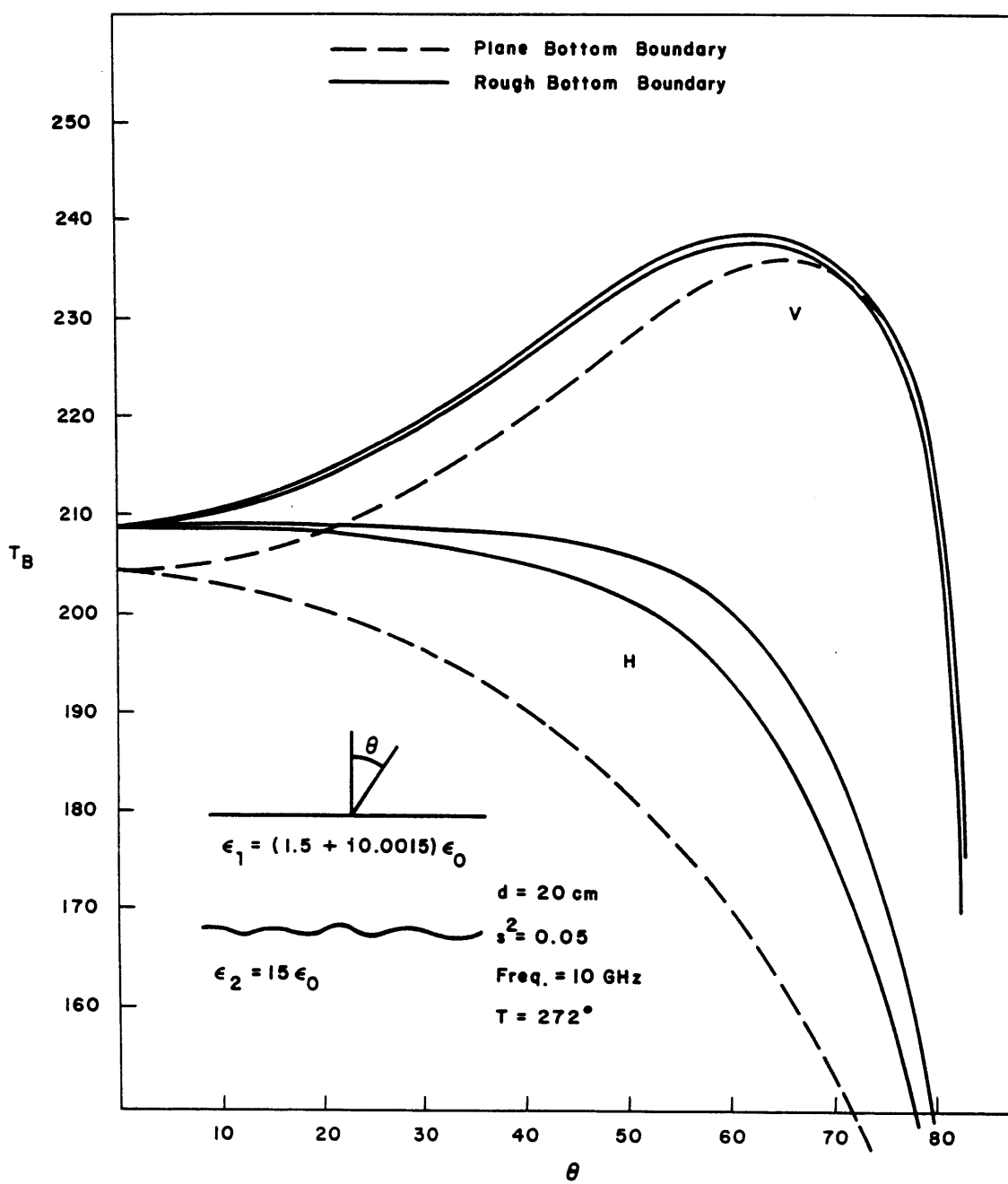


Figure 9.3 Brightness temperature as a function of angle for rough surface at bottom boundary with $\epsilon_2 = 15\epsilon_0$.

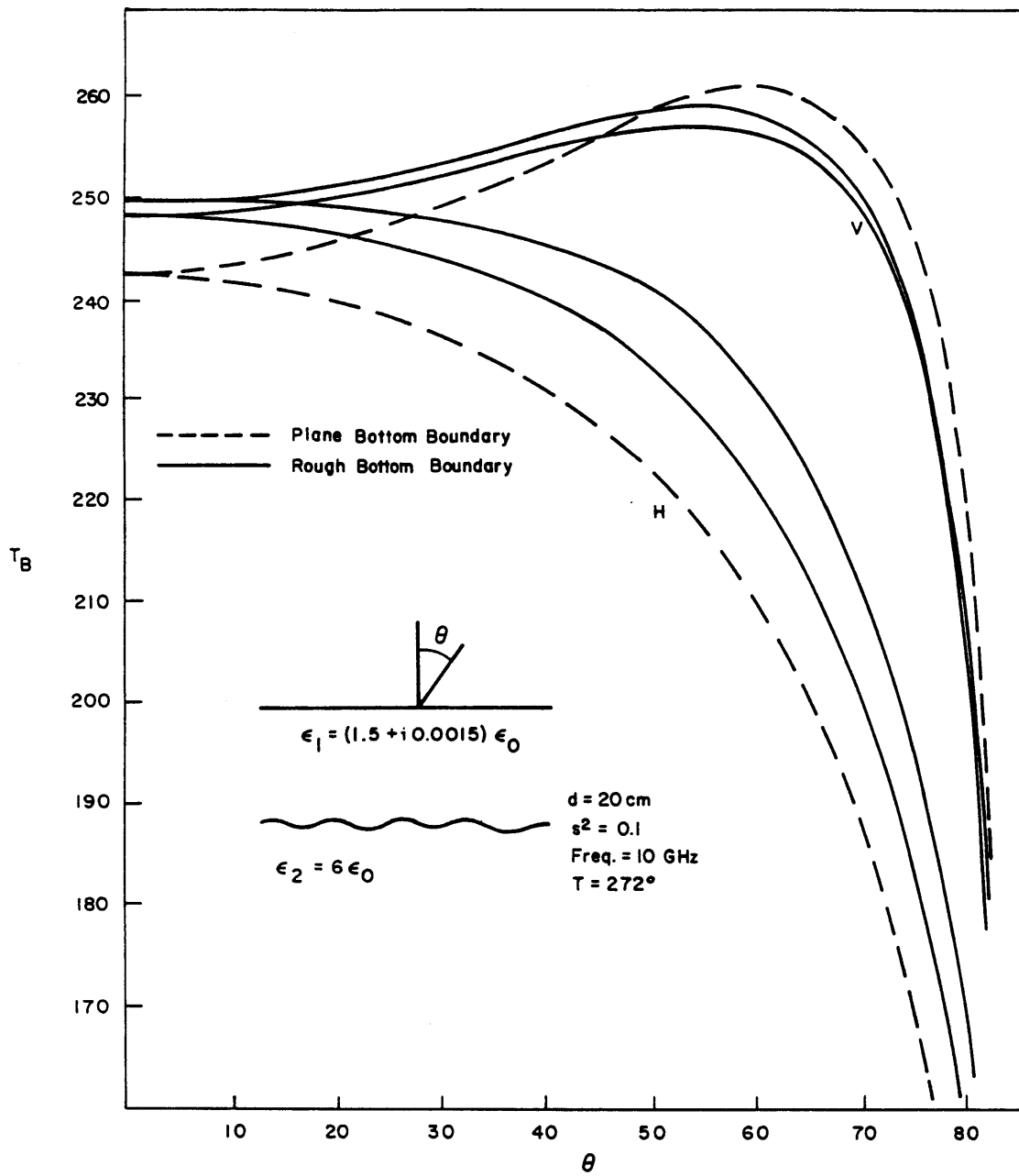


Figure 9.4 Brightness temperature as a function of angle for rough surface at bottom boundary with $s^2 = 0.1$.

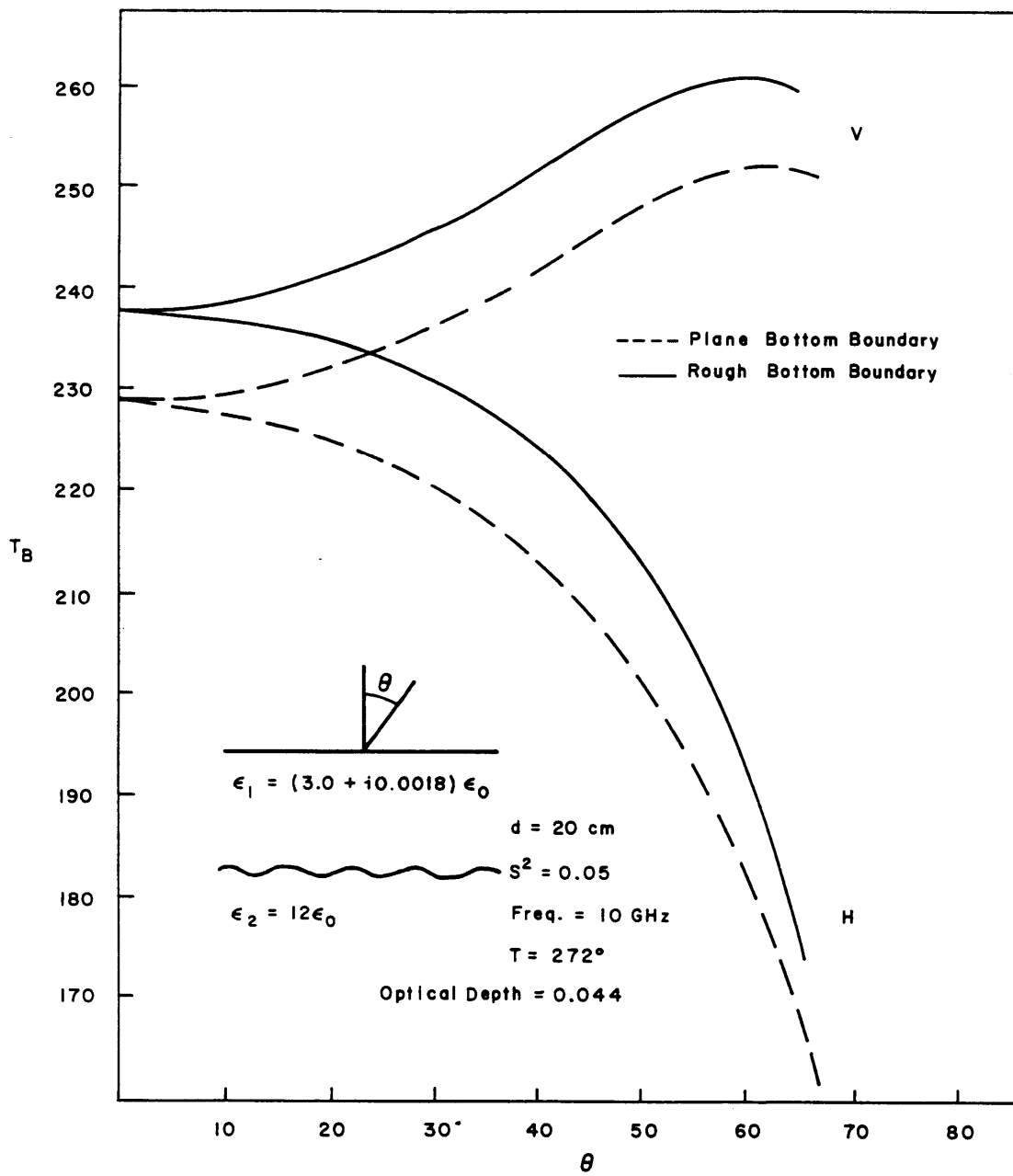


Figure 9.5 Brightness temperature as a function of angle for rough surface at bottom boundary with $\epsilon_1 = (3.0 + i0.0018)\epsilon_0$.

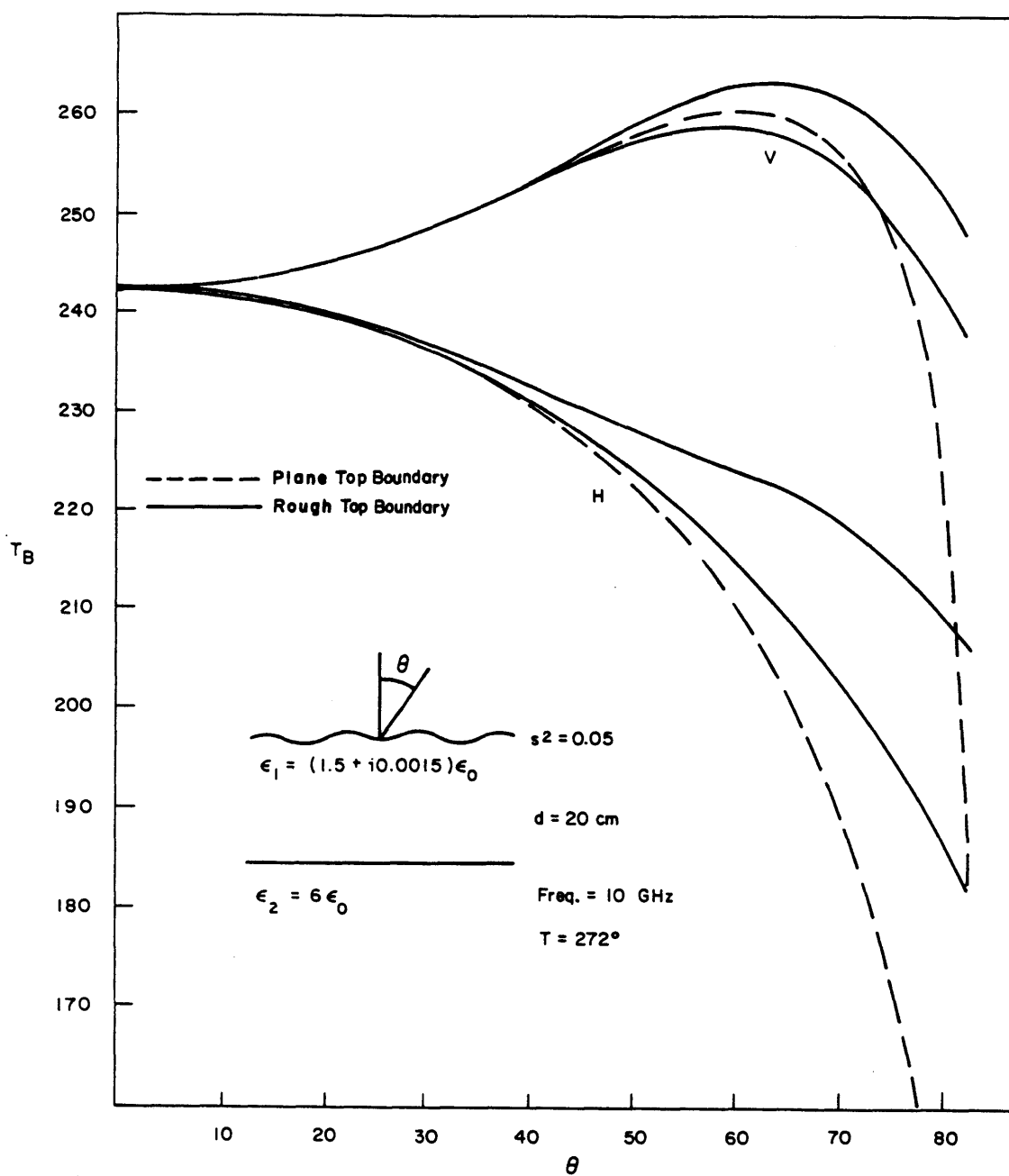


Figure 9.6 Brightness temperature as a function of angle for rough surface at top boundary.

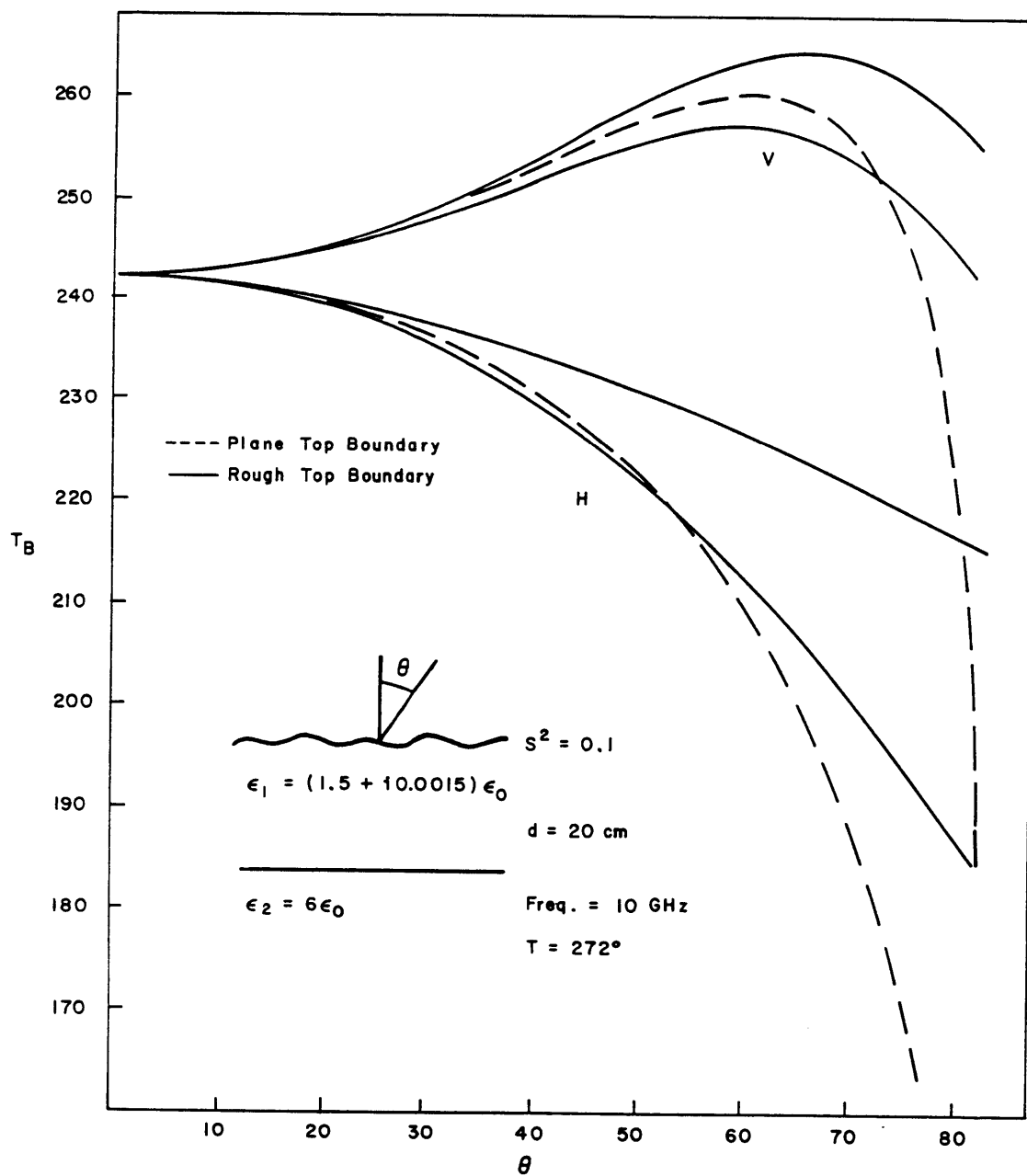


Figure 9.7 Brightness temperature as a function of angle for rough surface at top boundary with $\epsilon^2 = 0.1$.

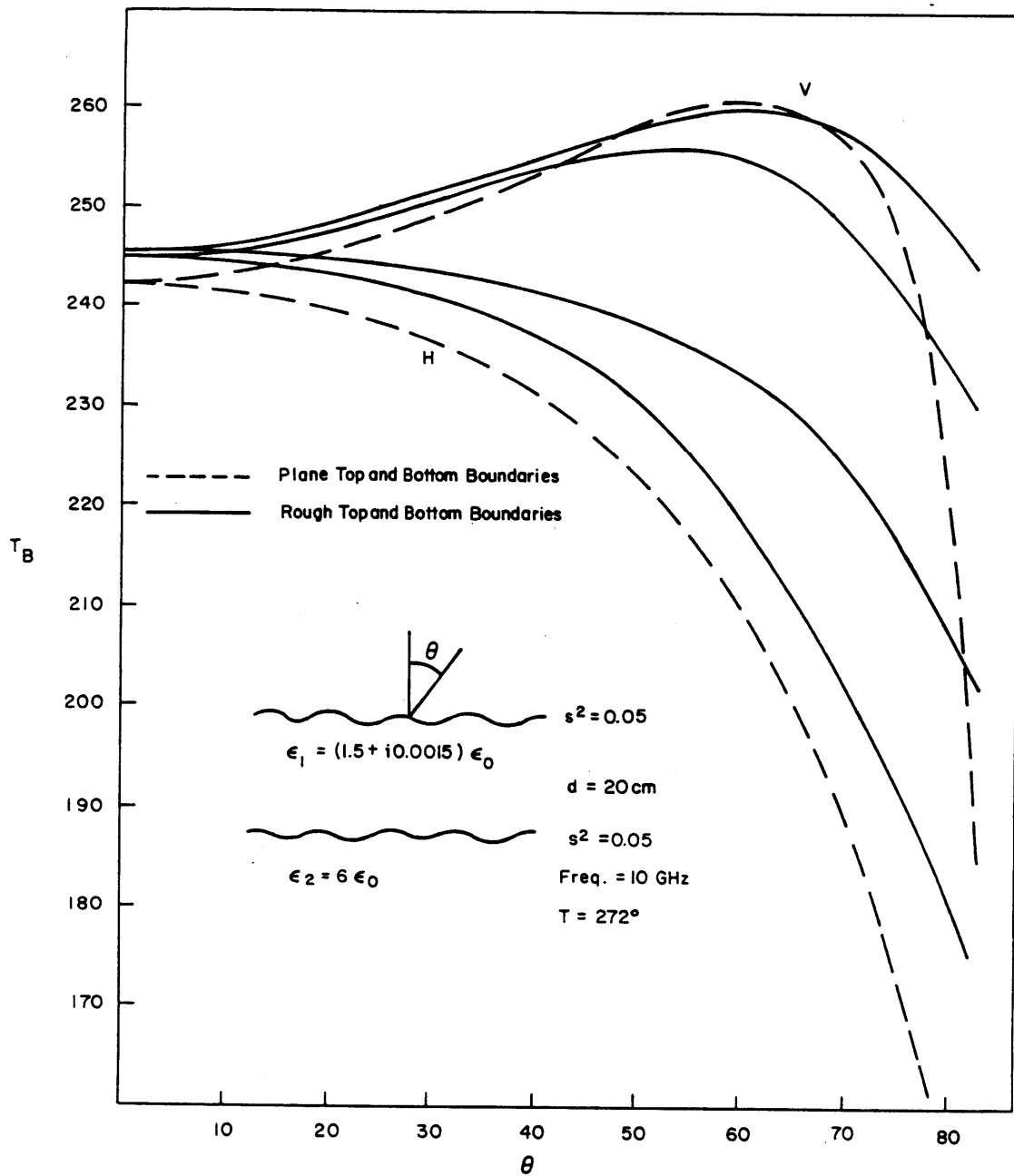


Figure 9.8 Brightness temperature as a function of angle for rough surfaces at top and bottom boundaries.

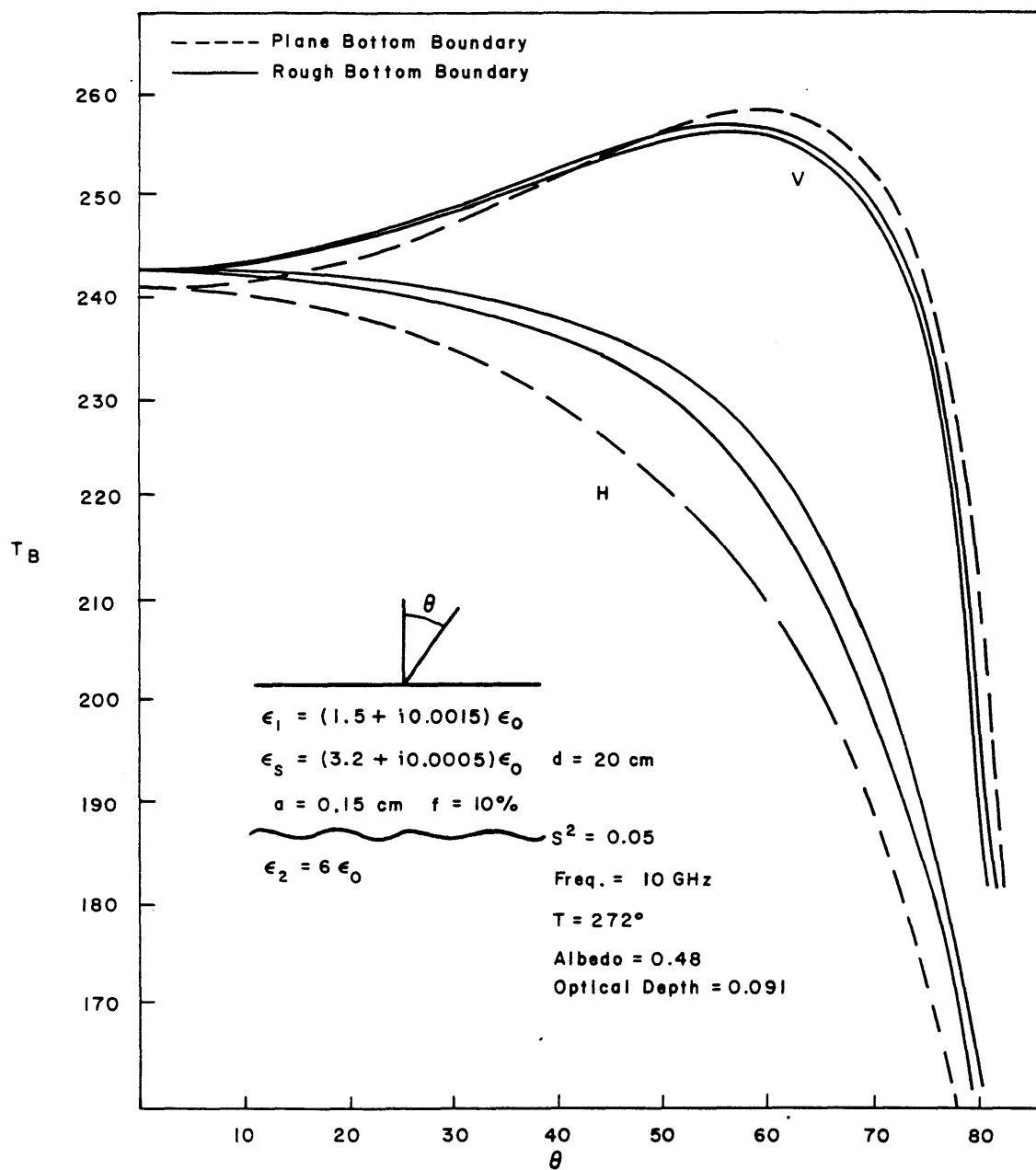


Figure 9.9 Brightness temperature as a function of angle for rough surface at bottom boundary with volume scattering.

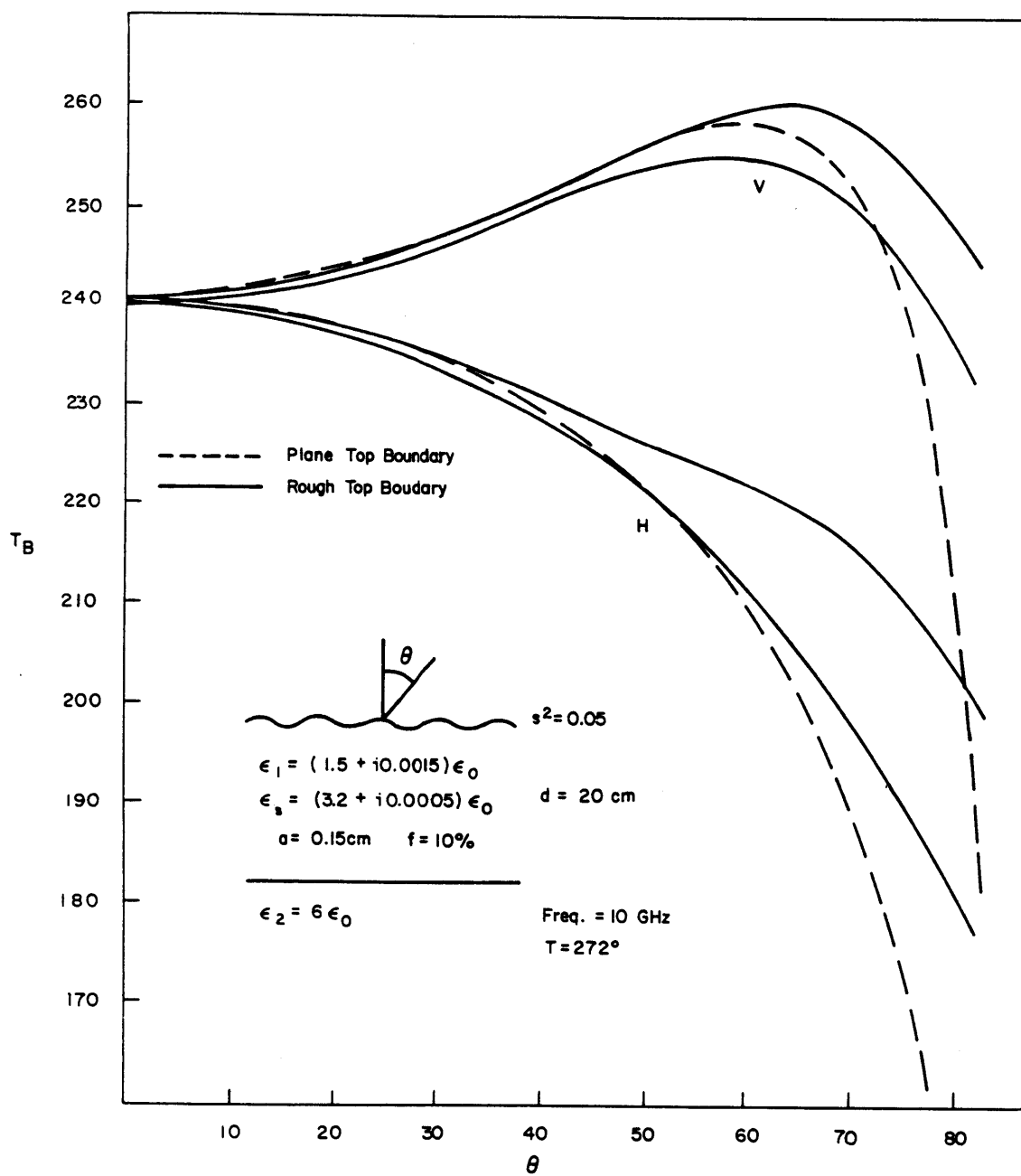


Figure 9.10 Brightness temperature as a function of angle for rough surface at top boundary with volume scattering.

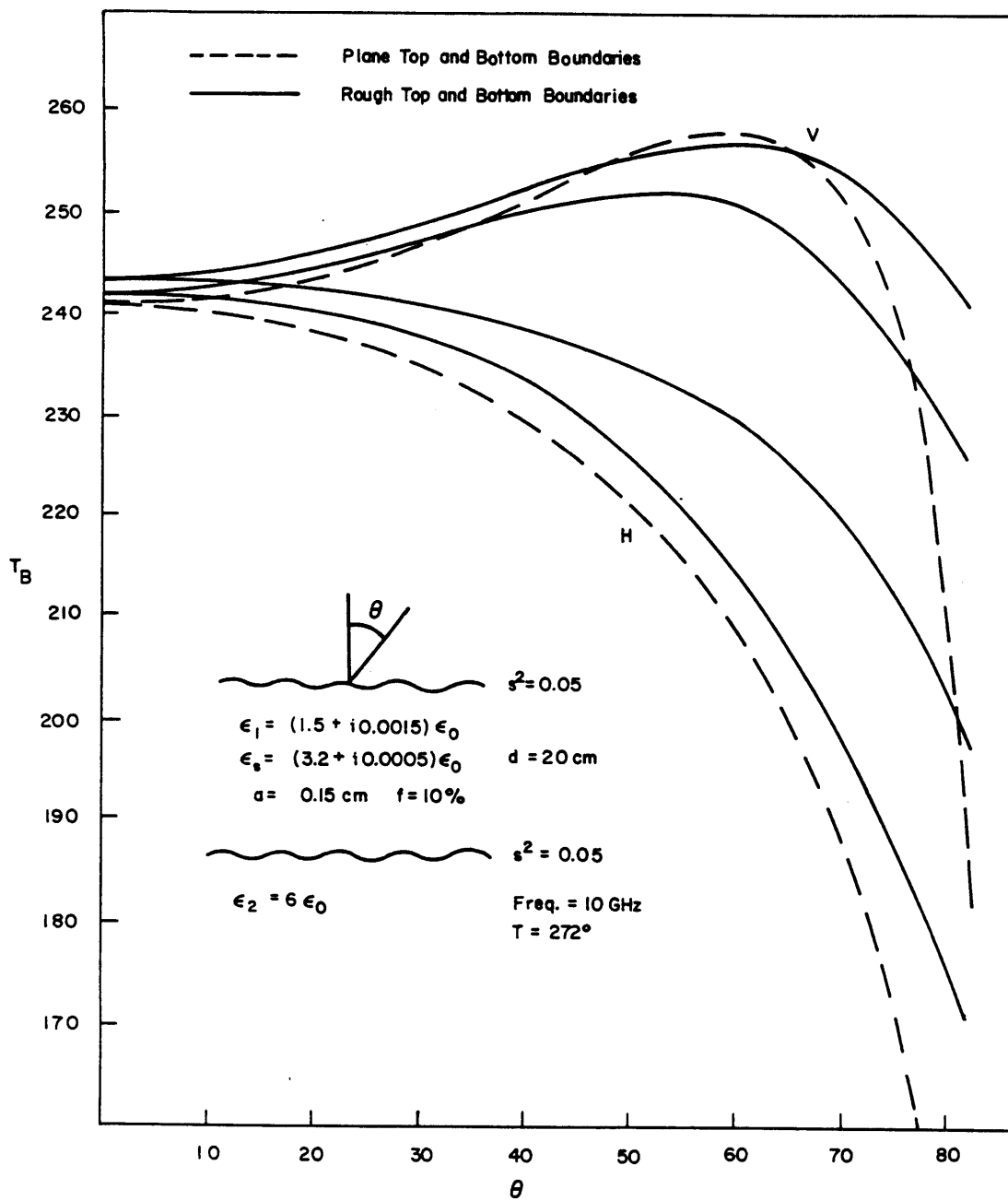


Figure 9.11 Brightness temperature as a function of angle for rough surface at top and bottom boundaries with volume scattering.

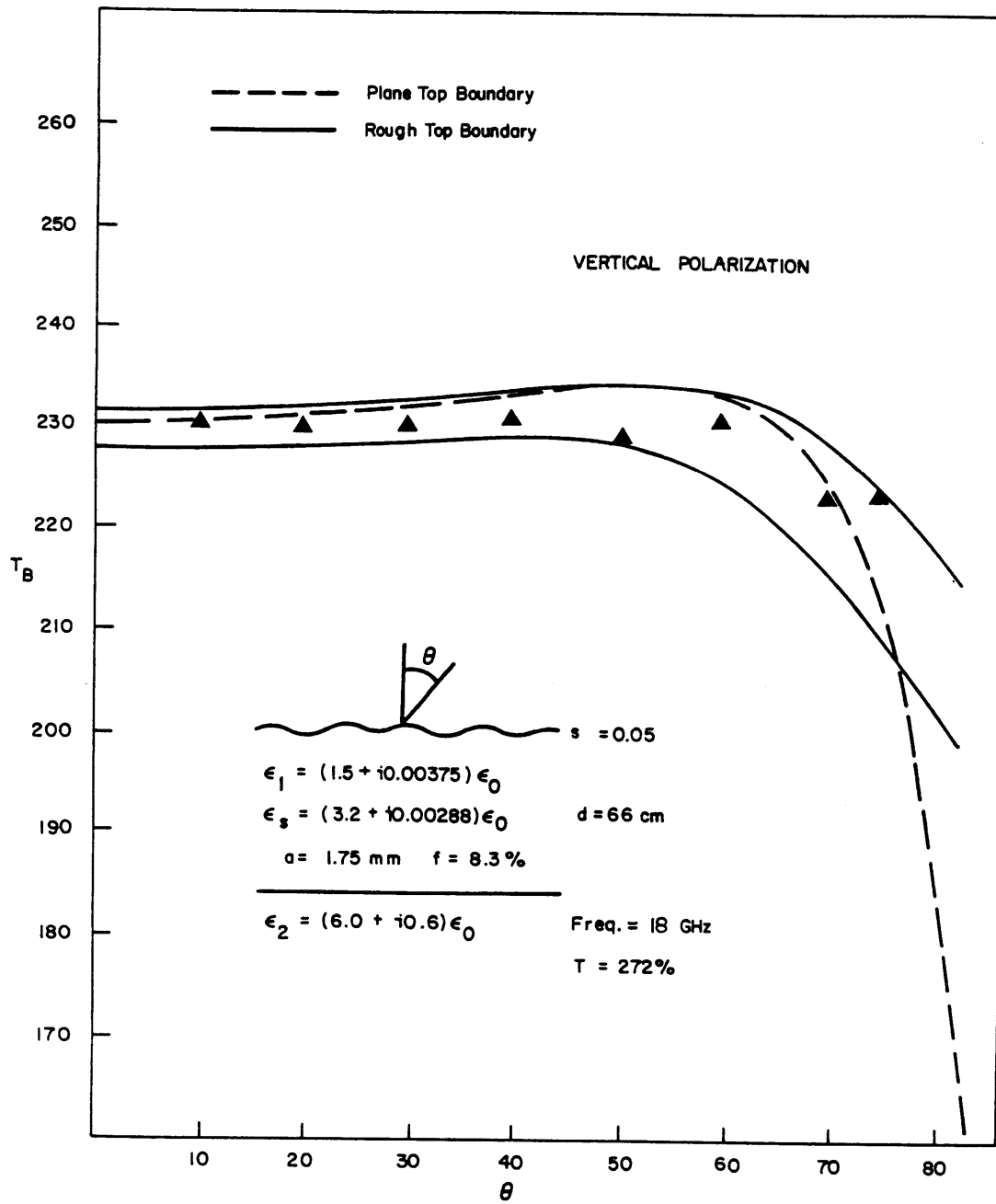


Figure 9.12 Brightness temperature as a function of angle at 18 GHz for vertical polarization.

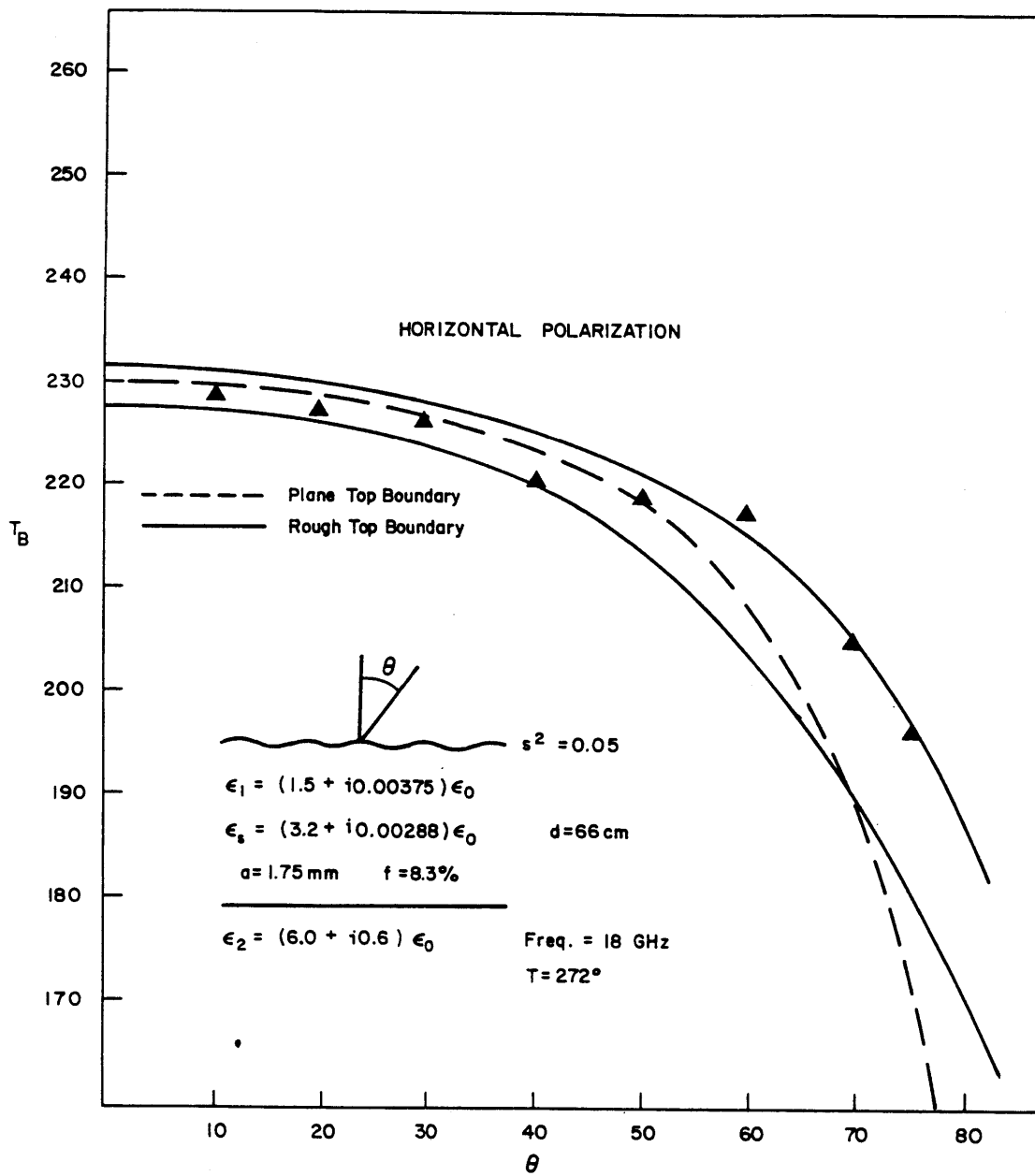


Figure 9.13 Brightness temperature as a function of angle at 18 GHz for horizontal polarization.

CHAPTER 10

Theory for Active Remote Sensing of Two-Layer Random Medium with Rough Surfaces

The radiative transfer theory is used to solve the problem of scattering from a layer of random medium on top of a homogeneous halfspace with rough top and bottom boundaries. The coherent and incoherent bistatic scattering coefficients for the rough surface are used to modify the boundary conditions. The radiative transfer equations are solved numerically using the Fourier-series expansion in the azimuthal direction and the Gaussian quadrature method. The combined volume and rough surface scattering effects are studied by calculating the bistatic scattering coefficients. The theoretical results are compared and illustrated for the various cases.

10.1 Introduction

In microwave remote sensing of earth terrain, the effects of volume scattering have been treated with random medium and discrete scatterer models for terrain media. The discrete scatterer model with the radiative transfer theory has been used to study passive and active microwave remote sensing. In passive remote sensing, Rayleigh and Mie scattering functions have been used to study the thermal microwave emission from layered medium with planar and rough interfaces [England, 1975; Chang *et al.*, 1976; Tsang and Kong, 1977a, 1979; Kong *et al.*, 1979; Fung and Chen, 1981a; Shin and Kong, 1982]. In active remote sensing, the Rayleigh scattering model has been used extensively [Shin and Kong, 1981; Fung and Eom, 1981; Fung and Chen, 1981b; Karam and Fung, 1982]. The random medium model with the radiative transfer theory has been used to study passive remote sensing from layered earth terrain [Gurvich *et al.*, 1973; Tsang and Kong, 1975, 1976b, 1980b; Djermakoye and Kong, 1979; Chuang and Kong, 1980]. In active remote sensing, wave approaches with iterative solutions have been used widely with the random medium model to calculate the scattering coefficients [Tsang and Kong, 1976a; Zuniga and Kong, 1980; Zuniga *et al.*, 1979, 1980]. The radiative transfer theory with the random medium model has been applied to active remote sensing by Tsang and Kong [1978] where the iterative approach is applied to second order in albedo to calculate the bistatic scattering coefficients from a halfspace random medium. In order to more realistically model the natural terrain, a composite model that can account for both the volume and rough surface scattering effects are needed. The Rayleigh scattering model for the volume scattering with the geometrical optics solution for the random rough surface scattering have been used to study the combined effects [Fung and Eom, 1981; Fung and Chen, 1981b; Karam and

Fung, 1982).

In this chapter we use the radiative transfer theory to solve the problem of scattering from a layer of random medium on top of a homogeneous halfspace with rough interfaces at the top and bottom boundaries. Using all four Stokes parameters the bistatic scattering coefficients are calculated using a numerical approach which provides a valid solution for both small and large albedos. The coherent and incoherent bistatic scattering coefficients for the rough surface are used to modify the boundary conditions satisfied by the intensities at the top and bottom interfaces. A Fourier-series expansion in the azimuthal direction is used to eliminate the azimuthal ϕ -dependence from the radiative transfer equations and the boundary conditions. Then the set of equations without the ϕ -dependence is solved using the method of Gaussian quadrature. The integrals in the radiative transfer equations are replaced by a Gaussian quadrature and the resulting system of first-order differential equations is solved by obtaining eigenvalues and eigenvectors and matching the boundary conditions. Legendre quadrature method is used to properly discretize the boundary conditions which contain both the coherent and incoherent bistatic scattering coefficients. The numerical results are illustrated by plotting backscattering cross sections as functions of incident angle and frequency.

10.2 Formulation

Consider a layer of random medium with rough interfaces characterized by the permittivity $\epsilon_1 + \epsilon_f$, where ϵ_f stands for the randomly fluctuating part whose amplitude is very small and whose ensemble average is zero, on top of a homogeneous medium with permittivity ϵ_2 [Fig. 10.1]. The radiative transfer equations which govern the propagation of intensities inside the scattering medium are, for $0 < \theta < \pi$,

$$\cos \theta \frac{d}{dz} \bar{I}(\theta, \phi, z) = -K_a \bar{I}(\theta, \phi, z) - \bar{K}_s(\theta) \cdot \bar{I}(\theta, \phi, z) + \int_0^\pi d\theta' \sin \theta' \int_0^{2\pi} d\phi' \bar{P}(\theta, \phi; \theta', \phi') \cdot \bar{I}(\theta', \phi', z) \quad (1)$$

where

$$\bar{I}(\theta, \phi, z) = \begin{bmatrix} I_v(\theta, \phi, z) \\ I_h(\theta, \phi, z) \\ U(\theta, \phi, z) \\ V(\theta, \phi, z) \end{bmatrix} \quad (2)$$

I_v is the vertically polarized specific intensity, I_h is the horizontally polarized specific intensity, and U and V representing the correlation between two polarizations [Tsang and Kong, 1978; Shin and Kong, 1981], $\bar{P}(\theta, \phi; \theta', \phi')$ is a 4×4 scattering function matrix, which relates scattered intensities into the direction (θ, ϕ) from the incident intensities in the direction (θ', ϕ') , K_a is the loss per unit length due to absorption, and $\bar{K}_s(\theta)$ is the loss per unit length due to scattering. The random permittivity fluctuation is characterized by the variance of the fluctuation δ and the correlation function with lateral correlation length l_r and vertical correlation length l_z . The scattering function matrix and the scattering coefficient have been derived by applying Born approximation with the far-field solution and the explicit expressions for the correlation function with gaussian dependence laterally and exponential dependence vertically are given in Chapter 7 [Tsang and Kong, 1978; Chapter 7, Appendix A].

Consider an incident wave with specific intensity $\bar{I}_{oi}(\pi - \theta_{oi}, \phi_{oi})$ impinging from region 0, which is assumed to be free space, upon the scattering layer. The incident beam in region 0 assumes the form

$$\bar{I}_{oi}(\pi - \theta_{oi}, \phi_{oi}) = \bar{I}_{oi} \delta(\cos \theta_{oi} - \cos \theta_{oi}) \delta(\phi_{oi} - \phi_{oi}) \quad (3)$$

where the use of Dirac delta function is made.

The boundary conditions are, for $0 < \theta < \pi/2$,

$$\begin{aligned} \bar{I}(\pi - \theta, \phi, z = 0) = & \int_0^{2\pi} d\phi' \int_0^{\pi/2} d\theta' \sin \theta' \bar{T}_{01}(\theta, \phi; \theta', \phi') \cdot \bar{I}_{oi}(\pi - \theta', \phi') \\ & + \int_0^{2\pi} d\phi' \int_0^{\pi/2} d\theta' \sin \theta' \bar{R}_{10}(\theta, \phi; \theta', \phi') \cdot \bar{I}(\theta', \phi', z = 0) \end{aligned} \quad (4)$$

$$\bar{I}(\theta, \phi, z = -d) = \int_0^{2\pi} d\phi' \int_0^{\pi/2} d\theta' \sin \theta' \bar{R}_{12}(\theta, \phi; \theta', \phi') \cdot \bar{I}(\pi - \theta', \phi, z = -d) \quad (5)$$

where we have broken up the intensities in the scattering layer into upward going intensities $\bar{I}(\theta, \phi, z)$ and downward going intensities $\bar{I}(\pi - \theta, \phi, z)$. In the above equations $\bar{T}_{01}(\theta, \phi; \theta', \phi')$ represents the coupling from region 0 to region 1, $\bar{R}_{10}(\theta, \phi; \theta', \phi')$ represents the coupling from upward going intensity in the direction (θ', ϕ') into downward going intensity in the direction $(\pi - \theta, \phi)$ at the boundary of region 1 and region 0, and $\bar{R}_{12}(\theta, \phi; \theta', \phi')$ represents similar coupling at the boundary of region 1 and region 2.

Once the radiative transfer equations are solved subject to the boundary conditions, the scattered intensity in the direction (θ_{os}, ϕ_{os}) in region 0 is determined from

$$\begin{aligned} \bar{I}_{os}(\theta_{os}, \phi_{os}) = & \int_0^{2\pi} d\phi' \int_0^{\pi/2} d\theta' \sin \theta' \bar{R}_{01}(\theta_{os}, \phi_{os}; \theta', \phi') \cdot \bar{I}_{oi}(\pi - \theta', \phi') \\ & + \int_0^{2\pi} d\phi' \int_0^{\pi/2} d\theta' \sin \theta' \bar{T}_{10}(\theta_{os}, \phi_{os}; \theta', \phi') \cdot \bar{I}(\theta', \phi', z = 0) \end{aligned} \quad (6)$$

where $\bar{T}_{10}(\theta_{1s}, \phi_{1s}; \theta', \phi')$ represents coupling from region 1 to region 0.

The bistatic scattering coefficient $\gamma_{\beta\alpha}(\theta_{1s}, \phi_{1s}; \theta_{0i}, \phi_{0i})$ is defined as the ratio of the scattered power of polarization β per unit solid angle in the direction (θ_{1s}, ϕ_{1s}) and the intercepted incident power of polarization α in the direction (θ_{0i}, ϕ_{0i}) averaged over 4π radians [Peake, 1959].

$$\gamma_{\beta\alpha}(\theta_{1s}, \phi_{1s}; \theta_{0i}, \phi_{0i}) = 4\pi \frac{\cos \theta_{1s} I_{\alpha\beta s}(\theta_{1s}, \phi_{1s})}{\cos \theta_{0i} I_{\alpha\alpha i}} \quad (7)$$

where $\alpha, \beta = v$ or h with v denoting vertical polarization and h denoting horizontal polarization. In the backscattering direction $\theta_{1s} = \theta_{0i}$ and $\phi_{1s} = \pi - \phi_{0i}$. The backscattering cross sections per unit area are defined to be

$$\sigma_{\beta\alpha}(\theta_{0i}) = \cos \theta_{0i} \gamma_{\beta\alpha}(\theta_{0i}, \pi + \phi_{0i}; \theta_{0i}, \phi_{0i}) \quad (8)$$

10.3 Boundary Conditions

The boundary conditions satisfied by the specific intensities at rough dielectric interfaces are derived in this section. Unlike the planar interface case where the coupling at the boundary is only to the specular reflection and transmission directions, the incident intensity is coupled to all of the reflection and transmission directions. The reflection and transmission matrices are related to the bistatic scattering matrices, which is the generalization of the bistatic scattering coefficients to include the correlation between polarizations of the scattered fields.

Consider a plane wave incident from medium 1 onto medium 2 along the direction \hat{k}_i upon a rough dielectric interface. The electric field of the incident wave is given by

$$\bar{E}_i = \hat{e}_i E_{ci} e^{i\bar{k}_i \cdot \bar{r}} \quad (9)$$

where \bar{k}_i denotes the incident wave vector and \hat{e}_i is the polarization of the electric field vector. The rough surface is characterized by a random height distribution $z = f(\bar{r}_\perp)$ where $f(\bar{r}_\perp)$ is a Gaussian random variable with zero mean, $\langle f(\bar{r}_\perp) \rangle = 0$. The incident field will generate the reflected and transmitted fields in medium 1 and 2, respectively. The solutions to the problem of scattering from a random rough surface have been studied in Chapters 2, 3, and 4. In general, the scattered and transmitted fields for vertical and horizontal polarizations for the incident field with vertical and horizontal polarizations are given by

$$\begin{bmatrix} E_{vs} \\ E_{hs} \end{bmatrix} = \frac{e^{ik_1 r}}{r} \begin{bmatrix} f_{vv}^r(\theta_s, \phi_s; \theta_i, \phi_i) & f_{vh}^r(\theta_s, \phi_s; \theta_i, \phi_i) \\ f_{hv}^r(\theta_s, \phi_s; \theta_i, \phi_i) & f_{hh}^r(\theta_s, \phi_s; \theta_i, \phi_i) \end{bmatrix} \cdot \begin{bmatrix} E_{vi} \\ E_{hi} \end{bmatrix} \quad (10)$$

$$\begin{bmatrix} E_{vt} \\ E_{ht} \end{bmatrix} = \frac{e^{ik_2 r}}{r} \begin{bmatrix} f_{vv}^t(\theta_t, \phi_t; \theta_i, \phi_i) & f_{vh}^t(\theta_t, \phi_t; \theta_i, \phi_i) \\ f_{hv}^t(\theta_t, \phi_t; \theta_i, \phi_i) & f_{hh}^t(\theta_t, \phi_t; \theta_i, \phi_i) \end{bmatrix} \cdot \begin{bmatrix} E_{vi} \\ E_{hi} \end{bmatrix} \quad (11)$$

Now the scattered specific intensities can be expressed in terms of the incident specific intensities.

$$\bar{I}_r = \bar{\bar{R}}_{12} \cdot \bar{I}_i \quad (12)$$

$$\bar{I}_t = \bar{\bar{T}}_{12} \cdot \bar{I}_i \quad (13)$$

where \bar{I}_i , \bar{I}_s , and \bar{I}_t are the column matrices for the specific intensities containing the four Stokes parameters

$$\bar{I}_\alpha = \begin{bmatrix} I_{v\alpha} \\ I_{h\alpha} \\ U_\alpha \\ V_\alpha \end{bmatrix} \quad \alpha = i, r, t \quad (14)$$

and

$$\bar{\bar{R}}_{12}(\theta_s, \phi_s; \theta_i, \phi_i) = \frac{1}{A_s \cos \theta_s} \bar{\bar{L}}^T \quad (15)$$

$$\bar{\bar{T}}_{12}(\theta_t, \phi_t; \theta_i, \phi_i) = \frac{1}{A_s \cos \theta_t} \frac{\eta_1}{\eta_2} \bar{\bar{L}}^T \quad (16)$$

with

$$\bar{\bar{L}}^T = \begin{bmatrix} \langle |f_{vr}^\alpha|^2 \rangle & \langle |f_{vh}^\alpha|^2 \rangle & \text{Re}\langle (f_{vh}^{\alpha*} f_{vr}^\alpha) \rangle & -\text{Im}\langle (f_{vh}^{\alpha*} f_{vr}^\alpha) \rangle \\ \langle |f_{hv}^\alpha|^2 \rangle & \langle |f_{hh}^\alpha|^2 \rangle & \text{Re}\langle (f_{hh}^{\alpha*} f_{hv}^\alpha) \rangle & -\text{Im}\langle (f_{hh}^{\alpha*} f_{hv}^\alpha) \rangle \\ 2\text{Re}\langle (f_{vv}^\alpha f_{hv}^{\alpha*}) \rangle & 2\text{Re}\langle (f_{vh}^\alpha f_{hh}^{\alpha*}) \rangle & \text{Re}\langle (f_{vv}^\alpha f_{hh}^{\alpha*} + f_{vh}^\alpha f_{hv}^{\alpha*}) \rangle & -\text{Im}\langle (f_{vv}^\alpha f_{hh}^{\alpha*} - f_{vh}^\alpha f_{hv}^{\alpha*}) \rangle \\ 2\text{Im}\langle (f_{vv}^\alpha f_{hv}^{\alpha*}) \rangle & 2\text{Im}\langle (f_{vh}^\alpha f_{hh}^{\alpha*}) \rangle & \text{Im}\langle (f_{vv}^\alpha f_{hh}^{\alpha*} + f_{vh}^\alpha f_{hv}^{\alpha*}) \rangle & \text{Re}\langle (f_{vv}^\alpha f_{hh}^{\alpha*} - f_{vh}^\alpha f_{hv}^{\alpha*}) \rangle \end{bmatrix} \quad (17)$$

Thus, the boundary conditions for the specific intensities at a rough interface is given

by

$$\bar{I}_1(\hat{k}_s) = \int_0^{2\pi} d\phi_i \int_0^{\pi/2} d\theta_i \sin \theta_i \bar{\bar{R}}_{12}(\theta_s, \phi_s; \theta_i, \phi_i) \cdot \bar{I}_1(\hat{k}_i) \quad (18)$$

$$\bar{I}_2(\hat{k}_t) = \int_0^{2\pi} d\phi_i \int_0^{\pi/2} d\theta_i \sin \theta_i \bar{\bar{T}}_{12}(\theta_t, \phi_t; \theta_i, \phi_i) \cdot \bar{I}_1(\hat{k}_i) \quad (19)$$

The reflected and transmitted intensities at the directions \hat{k}_s and \hat{k}_t are given by integration of all the scattered intensities which are coupled to that direction from the incident intensity.

The reflection and transmission coupling matrices can also be related to the previously used bistatic scattering coefficients. First, we generalize the definition of bistatic scattering coefficients to include the correlation between polarizations. We define the bistatic scattering matrix $\bar{\bar{\gamma}}$ whose elements are given by

$$\gamma_{\alpha\beta}(\theta_s, \phi_s; \theta_i, \phi_i) = 4\pi \frac{\cos \theta_s I_{\alpha s}(\theta_s, \phi_s)}{\cos \theta_i I_{\beta i}} \quad \alpha, \beta = 1, 2, 3, 4 \quad (20)$$

where

$$\bar{I}_\alpha = \begin{bmatrix} I_{1\alpha} \\ I_{2\alpha} \\ I_{3\alpha} \\ I_{4\alpha} \end{bmatrix} = \begin{bmatrix} I_{v\alpha} \\ I_{h\alpha} \\ U_\alpha \\ V_\alpha \end{bmatrix} \quad \alpha = i, s \quad (21)$$

The previously used bistatic scattering coefficients are

$$\gamma_{vv} = \gamma_{11} \quad \gamma_{vh} = \gamma_{12} \quad \gamma_{hv} = \gamma_{21} \quad \gamma_{hh} = \gamma_{22} \quad (22)$$

The reflection coupling matrix is related to the bistatic scattering matrix as follows:

$$\bar{\bar{R}}_{12}(\theta_s, \phi_s; \theta_i, \phi_i) = \frac{1}{4\pi} \frac{\cos \theta_i}{\cos \theta_s} \bar{\bar{\gamma}}(\theta_s, \phi_s; \theta_i, \phi_i) \quad (23)$$

In a similar manner, we can relate the transmission coupling matrix to the bistatic scattering coefficients for the transmitted intensities:

$$\bar{\bar{T}}_{12}(\theta_t, \phi_t; \theta_i, \phi_i) = \frac{1}{4\pi} \frac{\cos \theta_i}{\cos \theta_t} \bar{\bar{\gamma}}(\theta_t, \phi_t; \theta_i, \phi_i) \quad (24)$$

The explicit expressions for the reflection and transmission matrices, obtained using the scattered and transmitted fields derived by a combination of Kirchhoff approximation and geometrical optics approach, are given in Appendix A. The other solutions for the scattering from a rough dielectric interface, such as small perturbation method (SPM) or modified SPM, can also be used to derive the coupling matrices to be used with the radiative transfer equations.

We also note that the coupling matrices can be broken up into coherent and incoherent components in a manner similar to the breaking up of the bistatic scattering coefficients. The coherent components only couple the incident intensity into the specular reflection and transmission directions while the incoherent components couple to all reflection and transmission directions.

$$\overline{\overline{R}}_{12}(\theta_s, \phi_s; \theta_i, \phi_i) = \overline{\overline{R}}_{12}^c(\theta_s, \phi_s; \theta_i, \phi_i) + \overline{\overline{R}}_{12}^i(\theta_s, \phi_s; \theta_i, \phi_i) \quad (25)$$

$$\overline{\overline{T}}_{12}(\theta_t, \phi_t; \theta_i, \phi_i) = \overline{\overline{T}}_{12}^c(\theta_t, \phi_t; \theta_i, \phi_i) + \overline{\overline{T}}_{12}^i(\theta_t, \phi_t; \theta_i, \phi_i) \quad (26)$$

10.4 Fourier Series Expansion

The radiative transfer equations and the associated boundary conditions can be solved using a numerical approach. We first use a Fourier-series expansion in the azimuthal direction to eliminate the ϕ -dependence from the radiative transfer equations.

We let

$$\bar{I}(\theta, \phi, z) = \sum_{m=0}^{\infty} \left[\bar{I}^{m,c}(\theta, z) \cos m(\phi - \phi_i) + \bar{I}^{m,s}(\theta, z) \sin m(\phi - \phi_i) \right] \quad (27)$$

$$\bar{P}(\theta, \phi; \theta', \phi') = \sum_{m=0}^{\infty} \frac{1}{(1 + \delta_m)\pi} \left[\bar{P}^{m,c}(\theta, \theta') \cos m(\phi - \phi') + \bar{P}^{m,s}(\theta, \theta') \sin m(\phi - \phi') \right] \quad (28)$$

where the superscript m indicates the order of harmonic in the azimuthal direction, the superscripts c and s indicate the cosine and sine dependence, and the Neumann number $\delta_m = 0$ for $m \neq 0$ and $\delta_0 = 1$. Substituting (27) and (28) into the radiative transfer equations, the ϕ' -integration can be carried out. Then, by collecting terms with the same sine or cosine dependence, we obtain a set of equations without the ϕ -dependence [Chapter 7, Section 7.3].

The ϕ -dependence from the boundary conditions can also be eliminated using the Fourier-series expansion. We let

$$\bar{I}_{,\alpha}(\pi - \theta_{,\alpha}, \phi_{,\alpha}) = \bar{I}_{,\alpha} \delta(\cos \theta_{,\alpha} - \cos \theta_{,\alpha i}) \sum_{m=0}^{\infty} \frac{1}{(\delta_m + 1)\pi} \cos m(\phi_{,\alpha} - \phi_{,\alpha i}) \quad (29)$$

and, for $\alpha, \beta = 0, 1, 2$,

$$\bar{R}_{,\alpha\beta}^i(\theta, \phi; \theta', \phi') = \bar{R}_{,\alpha\beta}^i(\theta) \delta(\cos \theta - \cos \theta') \sum_{m=0}^{\infty} \frac{1}{(1 + \delta_m)\pi} \cos m(\phi - \phi') \quad (30a)$$

$$\bar{R}_{,\alpha\beta}^i(\theta, \phi; \theta', \phi') = \sum_{m=0}^{\infty} \frac{1}{(1 + \delta_m)\pi} \left[\bar{R}_{,\alpha\beta}^{m,c}(\theta, \theta') \cos m(\phi - \phi') + \bar{R}_{,\alpha\beta}^{m,s}(\theta, \theta') \sin m(\phi - \phi') \right] \quad (30b)$$

$$\bar{T}_{01}^c(\theta, \phi; \theta', \phi') = \bar{T}_{01}^c(\theta, \phi) \delta(\cos \theta - \cos \theta') \sum_{m=0}^{\infty} \frac{1}{(1 + \delta_m)\pi} \cos m(\phi - \phi') \quad (31a)$$

$$\bar{T}_{01}^i(\theta, \phi; \theta', \phi') = \sum_{m=0}^{\infty} \frac{1}{(1 + \delta_m)\pi} \left[\bar{T}_{01}^{m,c}(\theta, \theta') \cos m(\phi - \phi') - \bar{T}_{01}^{m,s}(\theta, \theta') \sin m(\phi - \phi') \right] \quad (31b)$$

where θ and θ' are related by the Snell's law.

Substituting (29), (30), and (31) into the boundary conditions (4) and (5) and carrying out the $d\phi'$ and $d\phi'_s$ integrations, we obtain the following set of equations. For $0 < \theta < \pi/2$ and $m = 0, 1, 2, \dots$

$$\begin{aligned} \bar{I}^{m,c}(\pi - \theta, z = 0) &= \int_0^{\pi/2} d\theta'_s \sin \theta'_s \left[\bar{T}_{01}^c(\theta, \theta'_s) \cdot \bar{I}_{0s}^{m,c}(\pi - \theta'_s) + \bar{T}_{01}^{m,c}(\theta, \theta'_s) \cdot \bar{I}_{0s}^{m,c}(\pi - \theta'_s) \right] \\ &\quad - \int_0^{\pi/2} d\theta' \sin \theta' \bar{R}_{10}^c(\theta, \theta') \cdot \bar{I}^{m,c}(\theta', z = 0) \\ &\quad + \int_0^{\pi/2} d\theta' \sin \theta' \left[\bar{R}_{10}^{m,c}(\theta, \theta') \cdot \bar{I}^{m,c}(\theta', z = 0) - \bar{R}_{10}^{m,s}(\theta, \theta') \cdot \bar{I}^{m,s}(\theta', z = 0) \right] \quad (32a) \end{aligned}$$

$$\begin{aligned} \bar{I}^{m,s}(\pi - \theta, z = 0) &= \int_0^{\pi/2} d\theta'_s \sin \theta'_s \bar{T}_{01}^{m,s}(\theta, \theta'_s) \cdot \bar{I}_{0s}^{m,c}(\pi - \theta'_s) \\ &\quad + \int_0^{\pi/2} d\theta' \sin \theta' \bar{R}_{10}^c(\theta, \theta') \cdot \bar{I}^{m,s}(\theta', z = 0) \\ &\quad + \int_0^{\pi/2} d\theta' \sin \theta' \left[\bar{R}_{10}^{m,s}(\theta, \theta') \cdot \bar{I}^{m,c}(\theta', z = 0) + \bar{R}_{10}^{m,c}(\theta, \theta') \cdot \bar{I}^{m,s}(\theta', z = 0) \right] \quad (32b) \end{aligned}$$

$$\begin{aligned} \bar{I}^{m,c}(\theta, z = -d) &= \int_0^{\pi/2} d\theta' \sin \theta' \bar{R}_{12}^c(\theta, \theta') \cdot \bar{I}^{m,c}(\pi - \theta', z = -d) \\ &\quad - \int_0^{\pi/2} d\theta' \sin \theta' \left[\bar{R}_{12}^{m,c}(\theta, \theta') \cdot \bar{I}^{m,c}(\pi - \theta', z = -d) - \bar{R}_{12}^{m,s}(\theta, \theta') \cdot \bar{I}^{m,s}(\pi - \theta', z = -d) \right] \quad (33a) \end{aligned}$$

$$\begin{aligned} \bar{I}^{m,s}(\theta, z = -d) &= \int_0^{\pi/2} d\theta' \sin \theta' \bar{R}_{12}^c(\theta, \theta') \cdot \bar{I}^{m,s}(\pi - \theta', z = -d) \\ &\quad + \int_0^{\pi/2} d\theta' \sin \theta' \left[\bar{R}_{12}^{m,s}(\theta, \theta') \cdot \bar{I}^{m,c}(\pi - \theta', z = -d) + \bar{R}_{12}^{m,c}(\theta, \theta') \cdot \bar{I}^{m,s}(\pi - \theta', z = -d) \right] \quad (33b) \end{aligned}$$

where

$$\bar{I}_{\alpha}^{m\epsilon}(\pi - \theta_{\epsilon}) = \bar{I}_{\alpha} \frac{1}{(\delta_m + 1)\pi} \delta(\cos \theta_{\epsilon} - \cos \theta_{\alpha}) \quad (34)$$

We note that the Fourier-series expanded coupling matrices for azimuthally isotropic rough boundaries do not couple the first two Stokes parameters to the last two Stokes parameters. The coupling matrices can be expanded as follows. For $A = R$ or T , and $\alpha, \beta = 0, 1, 2$,

$$\bar{A}_{\alpha\beta}^{m\epsilon} = \begin{bmatrix} A_{\alpha\beta 11}^{m\epsilon} & A_{\alpha\beta 12}^{m\epsilon} & 0 & 0 \\ A_{\alpha\beta 21}^{m\epsilon} & A_{\alpha\beta 22}^{m\epsilon} & 0 & 0 \\ 0 & 0 & A_{\alpha\beta 33}^{m\epsilon} & A_{\alpha\beta 34}^{m\epsilon} \\ 0 & 0 & A_{\alpha\beta 43}^{m\epsilon} & A_{\alpha\beta 44}^{m\epsilon} \end{bmatrix} \quad (35a)$$

$$\bar{A}_{\alpha\beta}^{m\sigma} = \begin{bmatrix} 0 & 0 & A_{\alpha\beta 12}^{m\sigma} & A_{\alpha\beta 14}^{m\sigma} \\ 0 & 0 & A_{\alpha\beta 23}^{m\sigma} & A_{\alpha\beta 24}^{m\sigma} \\ A_{\alpha\beta 31}^{m\sigma} & A_{\alpha\beta 32}^{m\sigma} & 0 & 0 \\ A_{\alpha\beta 41}^{m\sigma} & A_{\alpha\beta 42}^{m\sigma} & 0 & 0 \end{bmatrix} \quad (35b)$$

Thus, the boundary conditions (32) and (33) can be decoupled by defining

$$\bar{I}^{m\epsilon}(\theta, z) = \begin{bmatrix} I_v^{m\epsilon}(\theta, z) \\ I_h^{m\epsilon}(\theta, z) \\ U^{m\epsilon}(\theta, z) \\ V^{m\epsilon}(\theta, z) \end{bmatrix} \quad (36a)$$

$$\bar{I}^{m\sigma}(\theta, z) = \begin{bmatrix} I_v^{m\sigma}(\theta, z) \\ I_h^{m\sigma}(\theta, z) \\ U^{m\sigma}(\theta, z) \\ V^{m\sigma}(\theta, z) \end{bmatrix} \quad (36b)$$

where superscripts ϵ and σ stands for even or odd dependence in the first two Stokes parameters. After carrying out the $d\theta_{\epsilon}$ integration, the decoupled boundary conditions are given by, for $\alpha = e$ or o ,

$$\begin{aligned} \bar{I}^{m\alpha}(\pi - \theta, z = 0) &= \bar{T}_{01}^{m\epsilon}(\theta_{\epsilon}) \cdot \bar{I}_{\alpha}^{m\sigma}(\pi - \theta_{\epsilon}) + \bar{T}_{01}^{m\sigma}(\theta, \theta_{\alpha}) \cdot \bar{I}_{\alpha}^{m\epsilon} \\ &+ \int_0^{\pi/2} d\theta' \sin \theta' \left[\bar{R}_{10}^{m\epsilon}(\theta, \theta') + \bar{R}_{10}^{m\sigma}(\theta, \theta') \right] \cdot \bar{I}^{m\alpha}(\theta', z = 0) \end{aligned} \quad (37a)$$

$$\bar{I}^{m\alpha}(\theta, z = -d) = \int_0^{\pi/2} d\theta' \sin \theta' \left[\bar{R}_{12}^{m\alpha}(\theta, \theta') + \bar{R}_{12}^{m\alpha}(\theta, \theta') \right] \cdot \bar{I}^{m\alpha}(\pi - \theta', z = -d) \quad (37b)$$

where, for $A = R$ or T , and $\alpha, \beta = 0, 1, 2$.

$$\bar{A}_{\alpha\beta}^{m\alpha} = \begin{bmatrix} A_{\alpha\beta 11}^{m\alpha} & A_{\alpha\beta 12}^{m\alpha} & -A_{\alpha\beta 13}^{m\alpha} & -A_{\alpha\beta 14}^{m\alpha} \\ A_{\alpha\beta 21}^{m\alpha} & A_{\alpha\beta 22}^{m\alpha} & -A_{\alpha\beta 23}^{m\alpha} & -A_{\alpha\beta 24}^{m\alpha} \\ A_{\alpha\beta 31}^{m\alpha} & A_{\alpha\beta 32}^{m\alpha} & A_{\alpha\beta 33}^{m\alpha} & A_{\alpha\beta 34}^{m\alpha} \\ A_{\alpha\beta 41}^{m\alpha} & A_{\alpha\beta 42}^{m\alpha} & A_{\alpha\beta 43}^{m\alpha} & A_{\alpha\beta 44}^{m\alpha} \end{bmatrix} \quad (38a)$$

$$\bar{A}_{\alpha\beta}^{m\alpha} = \begin{bmatrix} A_{\alpha\beta 11}^{m\alpha} & A_{\alpha\beta 12}^{m\alpha} & A_{\alpha\beta 13}^{m\alpha} & A_{\alpha\beta 14}^{m\alpha} \\ A_{\alpha\beta 21}^{m\alpha} & A_{\alpha\beta 22}^{m\alpha} & A_{\alpha\beta 23}^{m\alpha} & A_{\alpha\beta 24}^{m\alpha} \\ A_{\alpha\beta 31}^{m\alpha} & A_{\alpha\beta 32}^{m\alpha} & A_{\alpha\beta 33}^{m\alpha} & A_{\alpha\beta 34}^{m\alpha} \\ A_{\alpha\beta 41}^{m\alpha} & A_{\alpha\beta 42}^{m\alpha} & A_{\alpha\beta 43}^{m\alpha} & A_{\alpha\beta 44}^{m\alpha} \end{bmatrix} \quad (38b)$$

and, for $\alpha = e$ or o ,

$$\bar{I}_{\alpha i}^{m\alpha}(\pi - \theta_{\alpha}) = \bar{I}_{\alpha i}^{m\alpha} \frac{1}{(\tilde{\epsilon}_m + 1)\pi} \delta(\cos \theta_{\alpha} - \cos \theta_{\alpha}) \quad (39)$$

with

$$\bar{I}_{\alpha i}^{m\alpha} = \begin{bmatrix} I_{vi} \\ I_{hi} \\ 0 \\ 0 \end{bmatrix} \quad (40a)$$

$$\bar{I}_{\alpha i}^{m\alpha} = \begin{bmatrix} 0 \\ 0 \\ U_i \\ V_i \end{bmatrix} \quad (40b)$$

The radiative transfer equations for the even and odd series can be obtained in a similar manner. We have, for $\alpha = e$ or o and $m = 0, 1, 2, \dots$

$$\cos \theta \frac{d}{dz} \bar{I}^{m\alpha}(\theta, z) = -K_{\alpha} \bar{I}^{m\alpha}(\theta, z) - \bar{K}_{\alpha}(\theta) \cdot \bar{I}^{m\alpha}(\theta, z) + \int_0^{\pi} d\theta' \sin \theta' \bar{P}^{m\alpha}(\theta, \theta') \cdot \bar{I}^{m\alpha}(\theta', z) \quad (41)$$

where $\bar{P}^{m\alpha}(\theta, \theta')$ is defined in a similar manner to (38) [Chapter 7, Section 7.3].

We define m_{max} and m'_{max} to be the number of harmonics that has to be kept in the expansions of the scattering function matrix and the coupling matrices, respectively, such that

$$\bar{P}^{m\alpha}(\theta, \theta') \simeq \bar{P}^{m\alpha}(\theta, \theta') \simeq 0 \quad \text{for } m > m_{max} \quad (42)$$

and

$$\bar{A}_{\alpha\beta}^{m\alpha} \simeq \bar{A}_{\alpha\beta}^{m\alpha} \simeq 0 \quad \text{for } m > m'_{max} \quad (43)$$

Then, for $m > m_{max}$ the radiative transfer equations simplify to

$$\cos \theta \frac{d}{dz} \bar{I}^{m\alpha}(\theta, z) = -K_{\alpha} \bar{I}^{m\alpha} - \bar{K}_{s}(\theta) \cdot \bar{I}^{m\alpha}(\theta, z) \quad (44)$$

where $\alpha = e$ or o . Similarly, for $m > m'_{max}$ the boundary conditions simplify to

$$\bar{I}^{m\alpha}(\pi - \theta, z = 0) = \bar{T}_{01}(\theta_{\alpha}) \cdot \bar{I}_{\alpha}^{m\alpha}(\pi - \theta_{\alpha}) + \bar{R}_{10}(\theta) \cdot \bar{I}^{m\alpha}(\theta, z = 0) \quad (45a)$$

and

$$\bar{I}^{m\alpha}(\theta, z = -d) = \bar{R}_{12}(\theta) \cdot \bar{I}^{m\alpha}(\pi - \theta, z = -d) \quad (45b)$$

where $d\theta'$ integrations are carried out. Thus, for $m > \max\{m_{max}, m'_{max}\}$, we can use the simplified radiative transfer equations and the boundary conditions, given by (44) and (45), to obtain the solutions analytically without resorting to the numerical approach.

10.5 Numerical Solution

The set of decoupled radiative transfer equations without the azimuthal dependence for each harmonic can be solved numerically using the Gaussian quadrature method. The integrals in the radiative transfer equations are replaced by Gaussian quadratures and the resulting system of first-order differential equation with constants coefficients are solved by obtaining eigenvalues and eigenvectors. The numerical solution for the specific intensity is given by [Chapter 7], for each harmonic and for even or odd series,

$$\bar{I}^+ = (\bar{E} + \bar{Q}) \cdot \bar{D}(z) \cdot \bar{x} + (\bar{E} - \bar{Q}) \cdot \bar{U}(z+d) \cdot \bar{y} \quad (46a)$$

$$\bar{I}^- = (\bar{E}' + \bar{Q}') \cdot \bar{D}(z) \cdot \bar{x} + (\bar{E}' - \bar{Q}') \cdot \bar{U}(z+d) \cdot \bar{y} \quad (46b)$$

where \bar{I}^+ and \bar{I}^- represent the upward and downward propagating intensities and \bar{x} and \bar{y} are the unknown constants.

The boundary conditions, which are to be used to determine the unknown constants \bar{x} and \bar{y} , can be obtained by discretizing the boundary conditions given by (37). Following the procedure outlined in the Appendix B, we obtain the following set of equations:

$$\bar{I}^-(z=0) = \bar{R}_{10} \cdot \bar{I}^+(z=0) + \bar{T}_{01} \cdot \bar{I}_{o1}^- \quad (47a)$$

$$\bar{I}^+(z=-d) = \bar{R}_{12} \cdot \bar{I}^-(z=-d) \quad (48a)$$

Substituting in the expressions for the upward and downward propagating intensities into the boundary conditions (54) and (55), we obtain the following set of equations for \bar{x} and \bar{y} :

$$\left[(\bar{E}' + \bar{Q}') - \bar{R}_{10} \cdot (\bar{E} + \bar{Q}) \right] \cdot \bar{x} + \left[(\bar{E}' - \bar{Q}') - \bar{R}_{10} \cdot (\bar{E} - \bar{Q}) \right] \cdot \bar{D}(-d) \cdot \bar{y} = \bar{T}_{01} \cdot \bar{I}_{o1}^- \quad (49a)$$

$$\left[(\bar{E} + \bar{Q}) - \bar{R}_{12} \cdot (\bar{E}' + \bar{Q}') \right] \cdot \bar{D}(-d) \cdot \bar{x} + \left[(\bar{E} - \bar{Q}) - \bar{R}_{12} \cdot (\bar{E}' - \bar{Q}') \right] \cdot \bar{y} = 0 \quad (49b)$$

The above equations can be solved for the constants \bar{x} and \bar{y} for the each cases when the incident intensity is at one of the quadrature angles. Note that in the halfspace random medium case when $d \rightarrow \infty$, $\bar{D} \rightarrow 0$ and the equations for \bar{x} and \bar{y} become decoupled and the matrix equation does not become singular [Fung and Chen, 1981b]. This is due to the form of the solution assumed in (46).

Once the constants \bar{x} and \bar{y} are determined, the scattered intensities from region 1 to region 0, represented by the first term on the right-hand-side of (6), can be determined. We have

$$\begin{aligned} \bar{I}_{os} &= \bar{T}_{10} \cdot \bar{I}^+(z=0) \\ &= \bar{T}_{10} \cdot \left[(\bar{E} + \bar{Q}) \cdot \bar{x} + (\bar{E} - \bar{Q}) \cdot \bar{D}(-d) \cdot \bar{y} \right] \end{aligned} \quad (50)$$

Thus, the complete solution can be obtained by solving the radiative transfer equations using the Gaussian quadrature method for each harmonic as outlined above and reintroducing the azimuthal dependence. The total scattered intensities in region 0 is given by

$$\begin{aligned} \bar{I}_{os}(\phi_o) &= \left\{ \bar{R}'_{01} + \bar{T}'_{10} \cdot \left[\bar{I} - \bar{R}'_{10} \cdot \bar{R}'_{12} \cdot \exp\{-\bar{\mu}^{-1} \cdot \bar{K} \cdot d\} \right]^{-1} \cdot \bar{T}'_{01} \right\} \cdot \bar{I}_{oi} \delta(\phi_o - \phi_{oi}) \\ &+ \sum_{m=0}^{m''_{max}} \left\{ \bar{R}'''_{01} \cdot \bar{I}'''_{oi} \cos m(\phi_o - \phi_{oi}) + \bar{R}'''_{01} \cdot \bar{I}'''_{oi} \sin m(\phi_o - \phi_{oi}) \right. \\ &+ \bar{T}'_{10} \cdot \bar{I}'''_{oi}{}^+(z=0) \cos m(\phi_o - \phi_{oi}) + \bar{T}'_{10} \cdot \bar{I}'''_{oi}{}^+(z=0) \sin m(\phi_o - \phi_{oi}) \\ &+ \left[\bar{T}'''_{10} \cdot \bar{I}'''_{oi}{}^+(z=0) - \bar{T}'''_{10} \cdot \bar{I}'''_{oi}{}^-(z=0) \right] \cos m(\phi_o - \phi_{oi}) \\ &- \bar{T}'_{10} \cdot \left[\bar{I} - \bar{R}'_{10} \cdot \bar{R}'_{12} \cdot \exp\{-\bar{\mu}^{-1} \cdot \bar{K} \cdot d\} \right]^{-1} \cdot \bar{T}'_{01} \cdot \bar{I}'''_{oi} \cos m(\phi_o - \phi_{oi}) \\ &\left. + \left[\bar{T}'''_{10} \cdot \bar{I}'''_{oi}{}^+(z=0) + \bar{T}'''_{10} \cdot \bar{I}'''_{oi}{}^-(z=0) \right] \sin m(\phi_o - \phi_{oi}) \right\} \end{aligned} \quad (51)$$

where $m''_{max} = \max[m_{max}, m'_{max}]$ and for $m > m''_{max}$, we have evaluated the scattered intensities analytically and summed them up. Once the scattered intensities in region 0 are obtained, the bistatic scattering coefficients and the backscattering cross sections can be obtained from (7) and (8). We note that if we are only interested in calculating the scattering intensities for vertically or horizontally polarized intensities, then we only need to calculate the even series. This is because the odd series, represented by (36b), is zero due to the fact the incident intensity for the odd series as given by (40b) is zero.

10.6 Results and Discussion

In this section we illustrate the theoretical results by plotting backscattering cross sections as functions of incident angle and frequency for various cases. In our calculations $n = 16$ is used. The combined volume and rough surface scattering model is illustrated using the geometrical optics solution for the rough surface modified with the shadowing function. In Fig. 10.2, the backscattering cross sections for like-like polarized return σ_{hh} and depolarized return σ_{vh} are plotted as a function of incident angle at 5.0 GHz. The bottom boundary is assumed to be rough with mean square surface slope $s^2 = 0.05$. We note that unlike the case of only volume scattering, which has a fairly smooth angular dependence, we have a peak near nadir. This is due to the contribution from the bottom rough surface. Also, depolarization return for the combined model is higher than the volume scattering model. In the volume scattering case, the depolarization of the backscattered power is due to the second-order and higher-order scattering effects. However, in the presence of a rough boundary, there is the effect of interaction between the rough surface and volume scattering.

In Fig. 10.3, we compare the backscattering cross sections for volume scattering, rough surface scattering, and the combined volume and rough surface scattering. We can see that the backscattering cross section near nadir is dominated by the rough surface scattering whereas for larger angles of incidence volume scattering effects dominate.

In Figs. 10.4 and 10.5, we compare the volume scattering effects and the combined volume and rough surface scattering effects by plotting the backscattering cross sections as a function of frequency. In Fig. 10.4 the angle of incidence is $\theta_i = 4.2^\circ$. At low frequencies the backscattered power due to volume scattering diminishes and the rough

surface effects dominate. As frequency is increased the effect of the bottom rough surface diminishes since the intensities do not penetrate the scattering layer as much as at lower frequencies, and the backscattered power is due to the volume scattering. In Fig. 10.5. we illustrate the same case for the angle of incidence $\theta_i = 32^\circ$. Again, the rough surface scattering dominates at low frequencies. However, the rough surface scattering effect diminishes faster as frequency is increased which is due to the fact that at higher incident angles the intensities have to travel a longer path before being affected by the bottom rough surface.

Appendix A: Expressions for Coupling Matrices obtained using Geometrical Optics Solution

The reflection and transmission coupling matrices at the rough dielectric interface can be obtained using the scattered and the transmitted fields derived by a combination of Kirchhoff approximation and geometrical optics approach. The explicit expressions for the coupling matrices $\overline{\overline{R}}_{12}$ and $\overline{\overline{T}}_{12}$ are given by [Chapter 2, Section 2.5]

$$\overline{\overline{R}}_{12}(\theta_s, \phi_s; \theta_i, \phi_i) = \frac{1}{\cos \theta_s} \frac{|\overline{k}_{1d}|^4}{4|\hat{k}_i \times \hat{k}_s|^4 k_{1dz}^4} \frac{1}{2\pi \varepsilon^2} \exp \left[-\frac{k_{1dx}^2 + k_{1dy}^2}{2k_{1dz}^2 \varepsilon^2} \right] \overline{\overline{C}}_{12}^R(\theta_s, \phi_s; \theta_i, \phi_i) \quad (A1)$$

$$\overline{\overline{T}}_{12}(\theta_t, \phi_t; \theta_i, \phi_i) = \frac{1}{\cos \theta_t} \frac{k_2^2 |\overline{k}_{2d}|^2 (\hat{n} \cdot \hat{k}_t)^2 \eta_1}{|\hat{k}_i \times \hat{k}_t|^4 k_{2dz}^4} \frac{1}{\eta_2} \frac{1}{2\pi \varepsilon^2} \exp \left[-\frac{k_{2dx}^2 + k_{2dy}^2}{2k_{2dz}^2 \varepsilon^2} \right] \overline{\overline{C}}_{12}^T(\theta_t, \phi_t; \theta_i, \phi_i) \quad (A2)$$

where ε^2 is the mean square surface slope

$$\overline{k}_{1d} = \overline{k}_i - \overline{k}_s \quad (A3)$$

$$\overline{k}_{2d} = \overline{k}_i - \overline{k}_t \quad (A4)$$

$$\overline{\overline{C}}_{12}^a = \begin{bmatrix} |f_{vv}^a|^2 & |f_{vh}^a|^2 & \text{Re}(f_{vh}^a f_{vv}^a) & -\text{Im}(f_{vh}^a f_{vv}^a) \\ |f_{hv}^a|^2 & |f_{hh}^a|^2 & \text{Re}(f_{hh}^a f_{hv}^a) & -\text{Im}(f_{hh}^a f_{hv}^a) \\ 2\text{Re}(f_{vv}^a f_{hv}^a) & 2\text{Re}(f_{vh}^a f_{hh}^a) & \text{Re}(f_{vv}^a f_{hh}^a + f_{vh}^a f_{hv}^a) & -\text{Im}(f_{vv}^a f_{hh}^a - f_{vh}^a f_{hv}^a) \\ 2\text{Im}(f_{vv}^a f_{hv}^a) & 2\text{Im}(f_{vh}^a f_{hh}^a) & \text{Im}(f_{vv}^a f_{hh}^a + f_{vh}^a f_{hv}^a) & \text{Re}(f_{vv}^a f_{hh}^a - f_{vh}^a f_{hv}^a) \end{bmatrix} \quad (A5)$$

with

$$f_{vv}^r = (\hat{h}_s \cdot \hat{k}_i)(\hat{h}_i \cdot \hat{k}_s)R_h + (\hat{v}_s \cdot \hat{k}_i)(\hat{v}_i \cdot \hat{k}_s)R_v \quad (A6)$$

$$f_{hv}^r = -(\hat{v}_s \cdot \hat{k}_i)(\hat{h}_i \cdot \hat{k}_s)R_h + (\hat{h}_s \cdot \hat{k}_i)(\hat{v}_i \cdot \hat{k}_s)R_v \quad (A7)$$

$$f_{vh}^r = (\hat{h}_s \cdot \hat{k}_i)(\hat{v}_i \cdot \hat{k}_s)R_h - (\hat{v}_s \cdot \hat{k}_i)(\hat{h}_i \cdot \hat{k}_s)R_v \quad (A8)$$

$$f_{hh}^r = (-\hat{v}_s \cdot \hat{k}_i)(\hat{v}_i \cdot \hat{k}_s)R_h + (\hat{h}_s \cdot \hat{k}_i)(\hat{h}_i \cdot \hat{k}_s)R_v \quad (A9)$$

and

$$f_{iv}^t = (\hat{h}_t \cdot \hat{k}_i)(\hat{h}_i \cdot \hat{k}_t)(1 + R'_h) + (\hat{v}_t \cdot \hat{k}_i)(\hat{v}_i \cdot \hat{k}_t) \frac{\eta_2}{\eta_1} (1 + R'_v) \quad (A10)$$

$$f_{hv}^t = -(\hat{v}_t \cdot \hat{k}_i)(\hat{h}_i \cdot \hat{k}_t)(1 - R'_h) + (\hat{h}_t \cdot \hat{k}_i)(\hat{v}_i \cdot \hat{k}_t) \frac{\eta_2}{\eta_1} (1 + R'_v) \quad (A11)$$

$$f_{vh}^t = -(\hat{h}_t \cdot \hat{k}_i)(\hat{v}_i \cdot \hat{k}_t)(1 + R'_h) + (\hat{v}_t \cdot \hat{k}_i)(\hat{h}_i \cdot \hat{k}_t) \frac{\eta_2}{\eta_1} (1 + R'_v) \quad (A12)$$

$$f_{hh}^t = (\hat{v}_t \cdot \hat{k}_i)(\hat{v}_i \cdot \hat{k}_t)(1 + R'_h) + (\hat{h}_t \cdot \hat{k}_i)(\hat{h}_i \cdot \hat{k}_t) \frac{\eta_2}{\eta_1} (1 + R'_v) \quad (A13)$$

R_v and R_h and R'_v and R'_h are the local reflection coefficients for the vertical and horizontal polarizations evaluated at the stationary phase points (α_s, β_s) and (α'_s, β'_s) , respectively.

As mentioned in Chapter 2, the geometrical optics solution used to derived the boundary conditons for rough dielectric interface satisfies the principle of reciprocity but violates the principle of energy conservation. This is due to the neglect of the effects of multiple scattering and shadowing. The shadowing effects can be incorporated to modify the boundary conditions. Following the same procedure as in Chapter 2, we obtain

$$\overline{\overline{R}}_{12}'''(\hat{k}_s; \hat{k}_i) = S(\hat{k}_s, \hat{k}_i) \overline{\overline{R}}_{12}(\hat{k}_s; \hat{k}_i) \quad (A14)$$

$$\overline{\overline{T}}_{12}'''(\hat{k}_t; \hat{k}_i) = S(\hat{k}_t, \hat{k}_i) \overline{\overline{T}}_{12}(\hat{k}_t; \hat{k}_i) \quad (A15)$$

where $S(\hat{k}_\alpha, \hat{k}_\beta)$ is the probability that a point will be illuminated by rays having the directions \hat{k}_β and $-\hat{k}_\alpha$, given the values of the slope at the point and has been discussed in Section 2.5.

Appendix B: Application of Legendre Quadrature Formula to the Boundary Conditions

The boundary conditions given by (37) can be put into the matrix form using the quadrature formula. In this appendix we will illustrate the application of the Legendre quadrature formula to the boundary conditions. The boundary conditions are approximated in a manner such that the formulation does not have to be changed when applied to the flat surface case.

Consider the following scalar version of the boundary condition at $z = -d$:

$$I(\theta, z = -d) = \int_0^{\pi/2} d\theta' \sin \theta' r_{12}(\theta, \theta') I(\pi - \theta', z = -d) \quad (B1)$$

One way to approximate the above equations is to apply the Gaussian quadrature method. We obtain, for $i, j = 1, 2, \dots, n$,

$$I(\theta_i, z = -d) = \sum_{j=1}^n a_j r_{12}(\theta_i, \theta_j) I(\pi - \theta_j, z = -d) \quad (B2)$$

This approach is justified as long the approximation of changing the integration to the summation is accurate. This means the number of quadrature points n has to be large enough so that the above approximation is valid. Note that as $r_{12}(\theta, \theta')$ becomes more sharply peaked function at the specular direction, the number of quadrature points has to be increased. Thus, it would be difficult to use the above approach for the case of near specular surface. In the limit of specular surface the coupling function is given by

$$r_{12}(\theta, \theta') = r_{12}(\theta) \delta(\cos \theta' - \cos \theta) \quad (B3)$$

and boundary condition simplifies to

$$I(\theta, z = -d) = r_{12}(\theta)I(\pi - \theta, z = -d) \quad (B4)$$

In this limit we note that the number of quadrature points does not have to be large as long as $r_{12}(\theta)$ is a fairly smooth function.

One way to overcome the above problem is to use the Legendre quadrature formula. We let $\mu = \cos \theta$. Then, for $i = 1, 2, \dots, n$ and $j = -n, \dots, -1, 1, 2, \dots, n$,

$$I(\mu_i, z = -d) = \sum_{j=-n}^n w_{ij} I(\mu_j, z = -d) \quad (B5)$$

where

$$w_{ij} = \frac{1}{\Pi'(\mu_j)} \int_0^1 d\mu r_{12}(\mu_i, \mu) \frac{\Pi(\mu)}{\mu - \mu_j} \quad (B6)$$

$$\Pi(\mu) = (\mu - \mu_1)(\mu - \mu_2) \cdots (\mu - \mu_n)(\mu + \mu_1)(\mu + \mu_2) \cdots (\mu + \mu_n) \quad (B7)$$

$$\Pi'(\mu_j) = \left. \frac{d}{d\mu} \Pi(\mu) \right|_{\mu=\mu_j} \quad (B8)$$

$$\mu_j = \cos \theta_j \quad \mu_{-j} = \cos(\pi - \theta_j) \quad (B9)$$

In the above formulation, we note that as $r_{12}(\mu, \mu')$ becomes a sharply peaked function around the specular direction, the number of quadrature angles n does not have to be increased as long as the coefficients w_{ij} are evaluated accurately. In the limit of specular surface, we have

$$w_{ij} = r_{12}(\mu_j) \delta_{ij} \quad (B10)$$

where

$$\delta_{ij} = \begin{cases} 1 & \text{if } i = j \\ 0 & \text{otherwise} \end{cases} \quad (B11)$$

Therefore, in the limit of specular surface, we have

$$I(\theta_i, z = -d) = r_{12}(\theta_i)I(\pi - \theta_i, z = -d) \quad (B12)$$

Thus, if we use the Legendre quadrature formula to discretize the boundary conditions, then as the surface becomes more specular the number of quadrature angles does not have to be increased and also the formulations does not have to be changed.

The boundary condition (B5) can be cast into the following the following matrix equation:

$$\bar{I}^+(z = -d) = \bar{\bar{W}}_{12} \cdot \bar{I}^-(z = -d) + \bar{\bar{U}}_{12} \cdot \bar{I}^+(z = -d) \quad (B13)$$

where

$$\bar{I}^+(z = -d) = \begin{bmatrix} I(\mu_1, z = -d) \\ \vdots \\ I(\mu_n, z = -d) \end{bmatrix} \quad \bar{I}^-(z = -d) = \begin{bmatrix} I(\mu_{-1}, z = -d) \\ \vdots \\ I(\mu_{-n}, z = -d) \end{bmatrix} \quad (B14)$$

$$\bar{\bar{W}}_{12} = \begin{bmatrix} w_{11} & \cdots & w_{1n} \\ \vdots & \vdots & \vdots \\ w_{n1} & \cdots & w_{nn} \end{bmatrix} \quad (B15)$$

$$\bar{\bar{U}}_{12} = \begin{bmatrix} w_{1(-1)} & \cdots & w_{1(-n)} \\ \vdots & \vdots & \vdots \\ w_{n(-1)} & \cdots & w_{n(-n)} \end{bmatrix} \quad (B16)$$

Thus, the appropriate boundary condition is given by

$$\bar{I}^+(z = -d) = \bar{\bar{R}}_{12} \cdot \bar{I}^-(z = -d) \quad (B17)$$

where

$$\bar{\bar{R}}_{12} = [\bar{I} - \bar{\bar{U}}_{12}]^{-1} \cdot \bar{\bar{W}}_{12} \quad (B18)$$

We note that

$$\bar{U}_{12} \simeq 0 \quad (B19)$$

and the coupling matrix is given by

$$\bar{R}_{12} = \bar{W}_{12} \quad (B20)$$

The boundary condition at $z = 0$ is next considered. Unlike the boundary condition at $z = -d$, there is an additional source term, which is the incident intensity being transmitted from the upper region. Consider the following scalar version of the boundary condition at $z = 0$:

$$I(\pi - \theta, z = 0) = g(\theta, \theta_{,i}) + \int_0^{\pi/2} d\theta' \sin \theta' r_{10}(\theta, \theta') I(\theta', z = 0) \quad (B21)$$

where $g(\theta, \theta_{,i})$ represents the incident intensity at $\theta_{,i}$ transmitted from region 0 to region 1. The second term in the left-side of the above equation can be approximated following the same procedure outlined above for the boundary condition at $z = -d$. Thus, we will concentrate on approximating the source term $g(\theta, \theta_{,i})$.

We note that for $g(\theta, \theta_{,i})$ which is a smooth function, there is no problem as long as the number of quadrature angles is sufficiently large. Then, the boundary condition can be discretized in a straightforward manner. In the limit of a specular surface, the source term is given by the delta function and another approach must be used. One way to bypass the problem of discretizing the delta function is to change the source term at the boundary into the source term in the volume by calculating the zeroth-order solution explicitly and using the radiative transfer equations for the higher order terms with the zeroth-order solution acting as the volume source [Fung and Chen,

1981b]. However, this approach requires two different formulations for the rough and planar boundaries. Also, the case of near specular surface where the source term is very sharply peaked in the specular direction cannot be treated easily.

In Chapter 7, we outlined the procedure for discretizing the delta function and keeping the source term at the boundary. This approach also gives the same solution as the other approach of using the volume source terms. We will now generalize that procedure and discretize the sharply peaked incident intensity. Consider an integral given by

$$I = \int_0^{\pi/2} f(\theta, \theta') g(\theta', \theta_{,n}) \quad (B22)$$

where $f(\theta, \theta')$ is a smooth function. Using the Gaussian quadrature method, the integral I is approximated as

$$I \simeq \sum_{j=-n}^{j=n} a_j f(\theta, \theta_j) g_j \quad (B23)$$

Our task is to come up with a set of coefficients g_j , such that the above approximation is accurate for an arbitrary function $g(\theta', \theta_{,n})$. Using the Legendre quadrature formula, the integral I is accurately approximated as

$$I \simeq \sum_{j=-n}^{j=n} f(\theta, \theta_j) w_j \quad (B24)$$

where

$$w_j = \frac{1}{\Pi'(\mu_j)} \int_{-1}^1 d\mu g(\mu, \mu_{,n}) \frac{\Pi(\mu)}{\mu - \mu_j} \quad (B25)$$

Comparing (B24) and (B25), we obtain

$$g_j = \frac{1}{a_j} w_j \quad (B26)$$

If we now let $g(\theta', \theta_{,n}) = \delta(\cos \theta' - \cos \theta_{,n})$ where $\theta_{,n}$ is one of the quadrature angles in region 0, the coefficients w_j is given by

$$w_j = \delta_{j,n} \frac{\epsilon_{,n} \cos \theta_{,n}}{\epsilon'_1 \cos \theta_j} \quad (B27)$$

Thus, the discrete form for the delta function is given by

$$g_j = \delta_{j,n} \frac{1}{a_j} \frac{\epsilon_{,n} \cos \theta_{,n}}{\epsilon'_1 \cos \theta_j} \quad (B28)$$

which is the same as the result given in Chapter 7. If $g(\theta', \theta_{,n})$ is a smooth function, then the coefficients w_j can be approximated as

$$\begin{aligned} w_j &\simeq g(\mu_j, \mu_{,n}) \frac{1}{\Pi'(\mu_j)} \int_{-1}^1 d\mu \frac{\Pi(\mu)}{\mu - \mu_j} \\ &= g(\mu_j, \mu_{,n}) a_j \end{aligned} \quad (B29)$$

Therefore,

$$g_j = g(\mu_j, \mu_{,n}) \quad (B30)$$

which is also a consistent result. Thus, the discretization of the source term by (B25) and (B26) gives the correct results in both limits of very sharply peaked and smooth incident intensities. We also note that

$$w_j \simeq 0 \quad \text{for } j = -1, -2, \dots, -n \quad (B31)$$

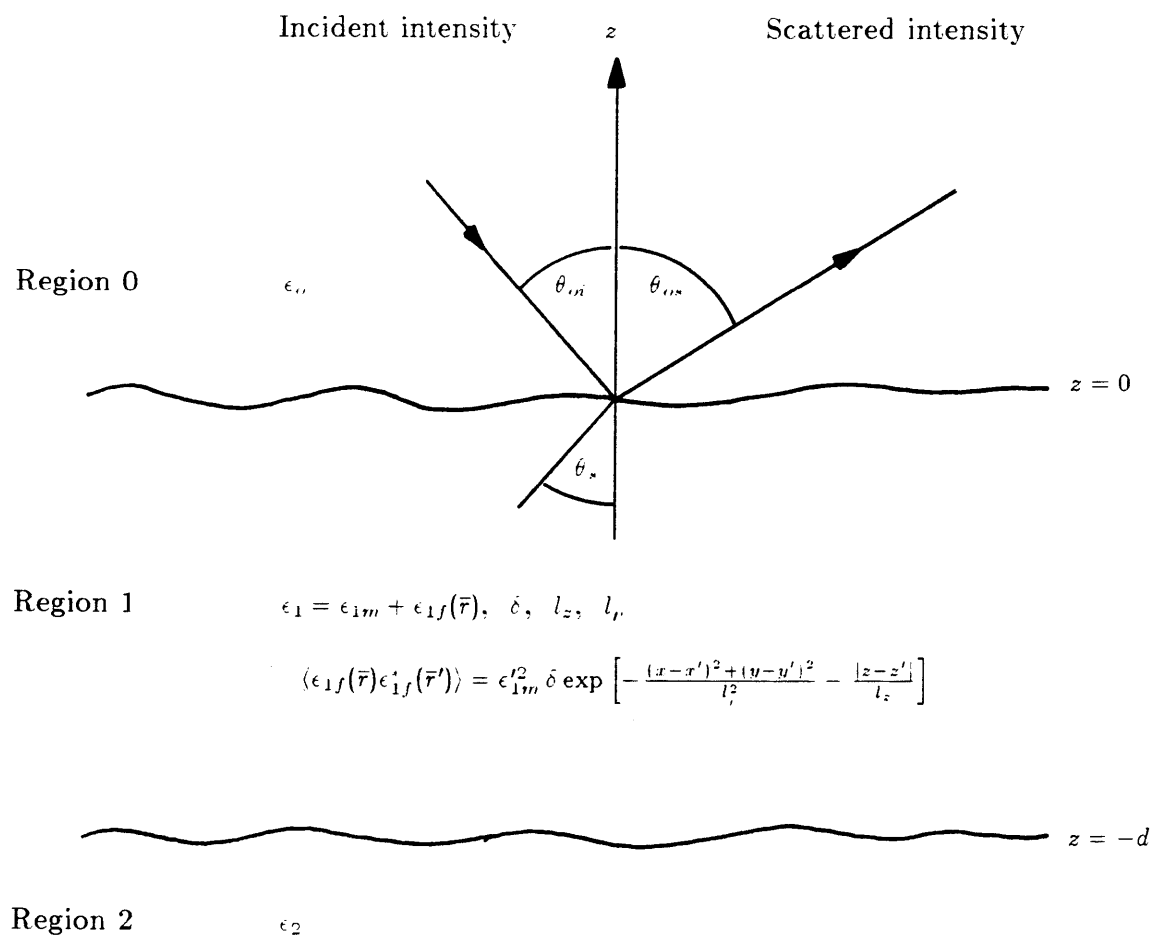


Figure 10.1 Geometrical configuration of the problem.

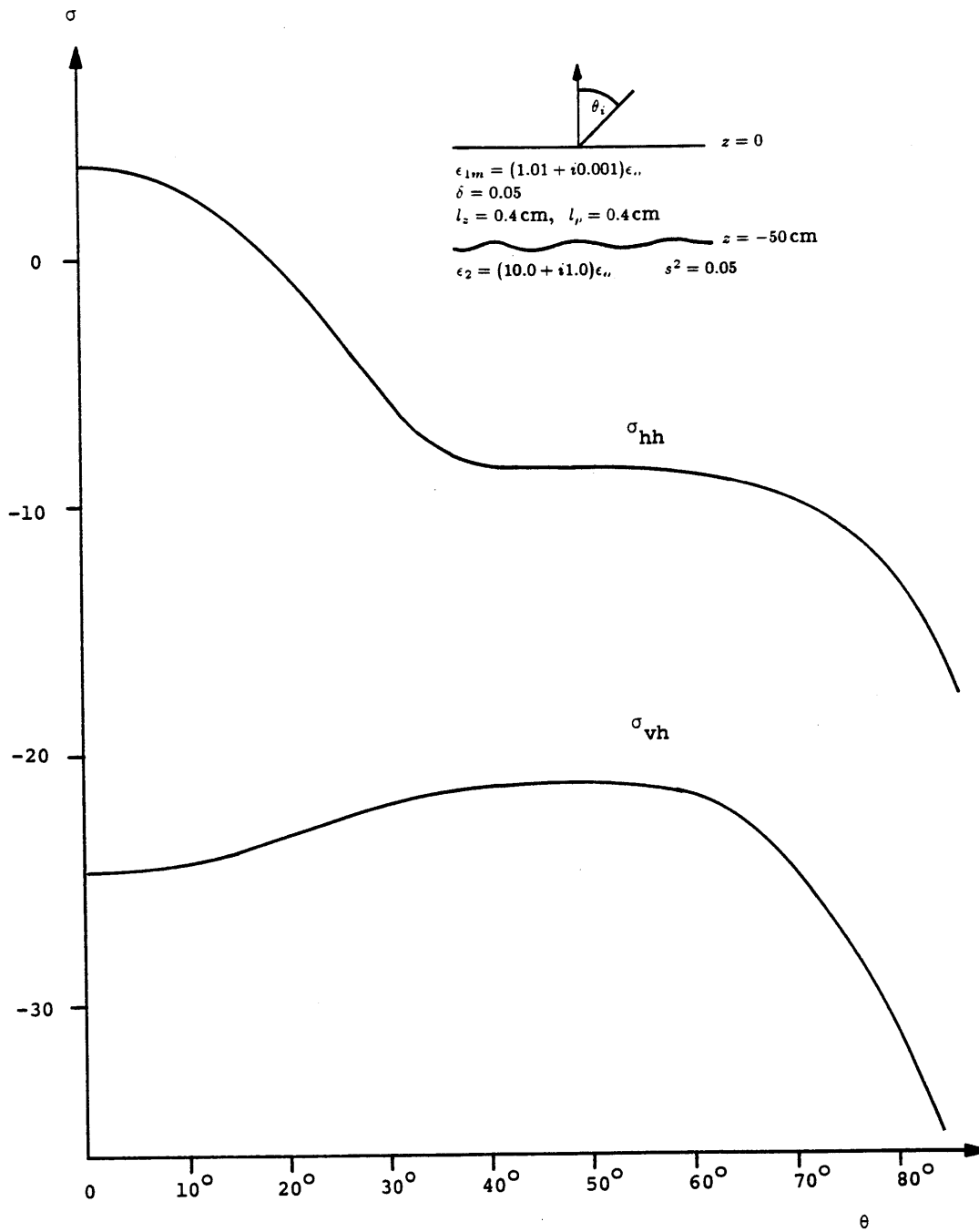


Figure 10.2 Backscattering cross sections as a function of incident angle for rough surface and volume scattering at 5 GHz.

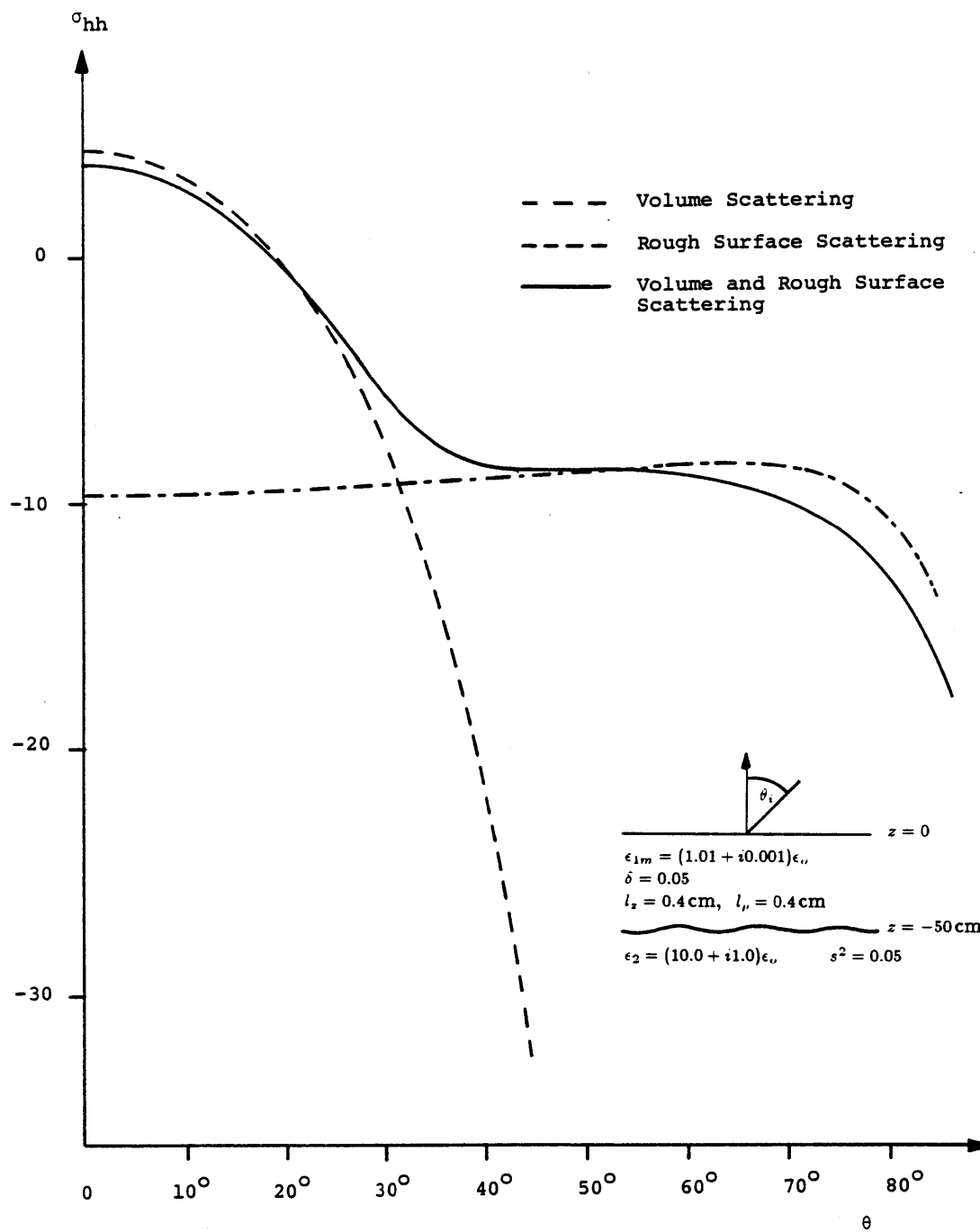


Figure 10.3 Backscattering cross sections as a function of incident angle for volume scattering, rough surface scattering, and combined volume and rough surface scattering at 5 GHz.

Figure 10.4 Backscattering cross sections as a function of frequency for $\theta_i = 4.2^\circ$.

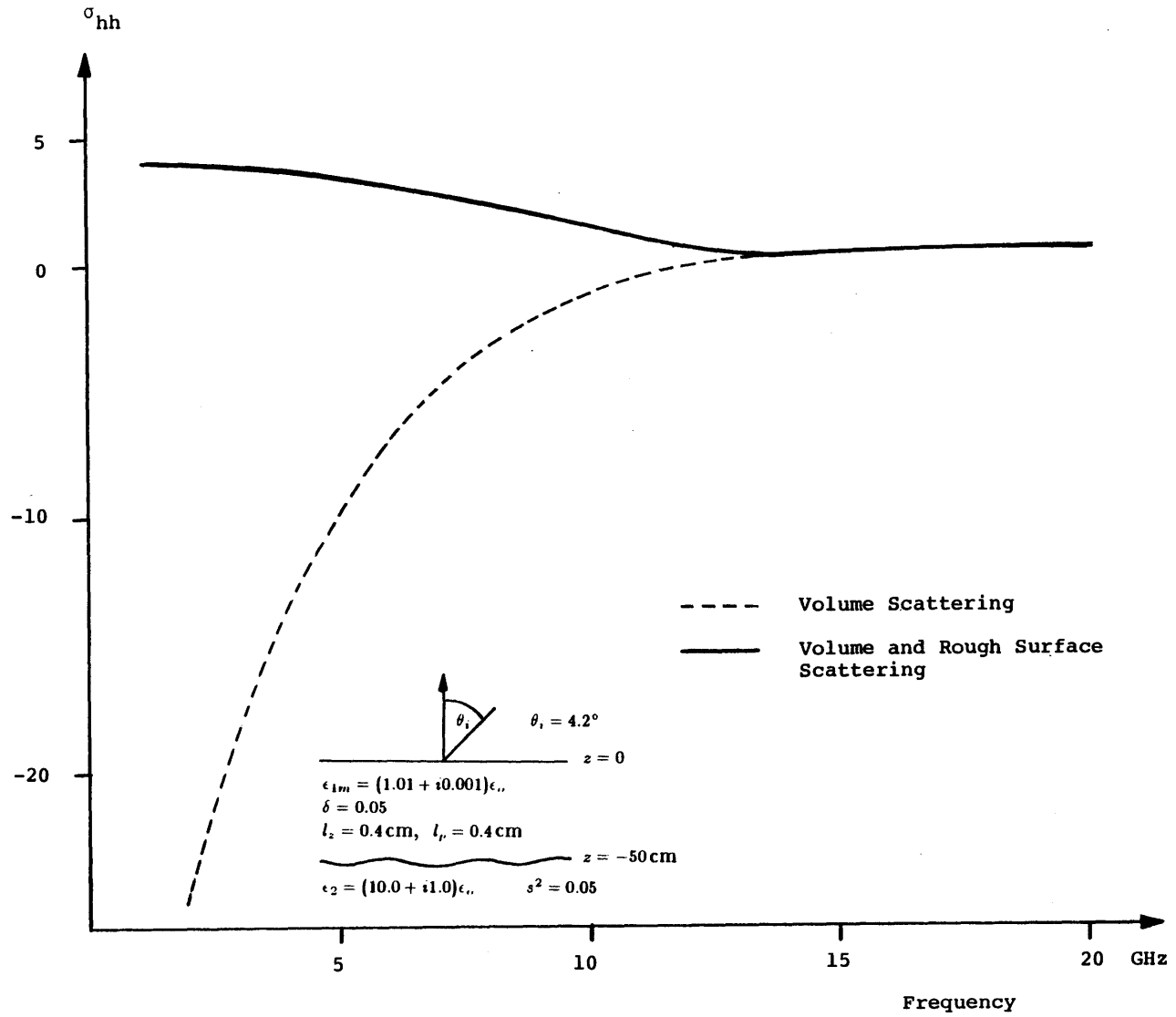
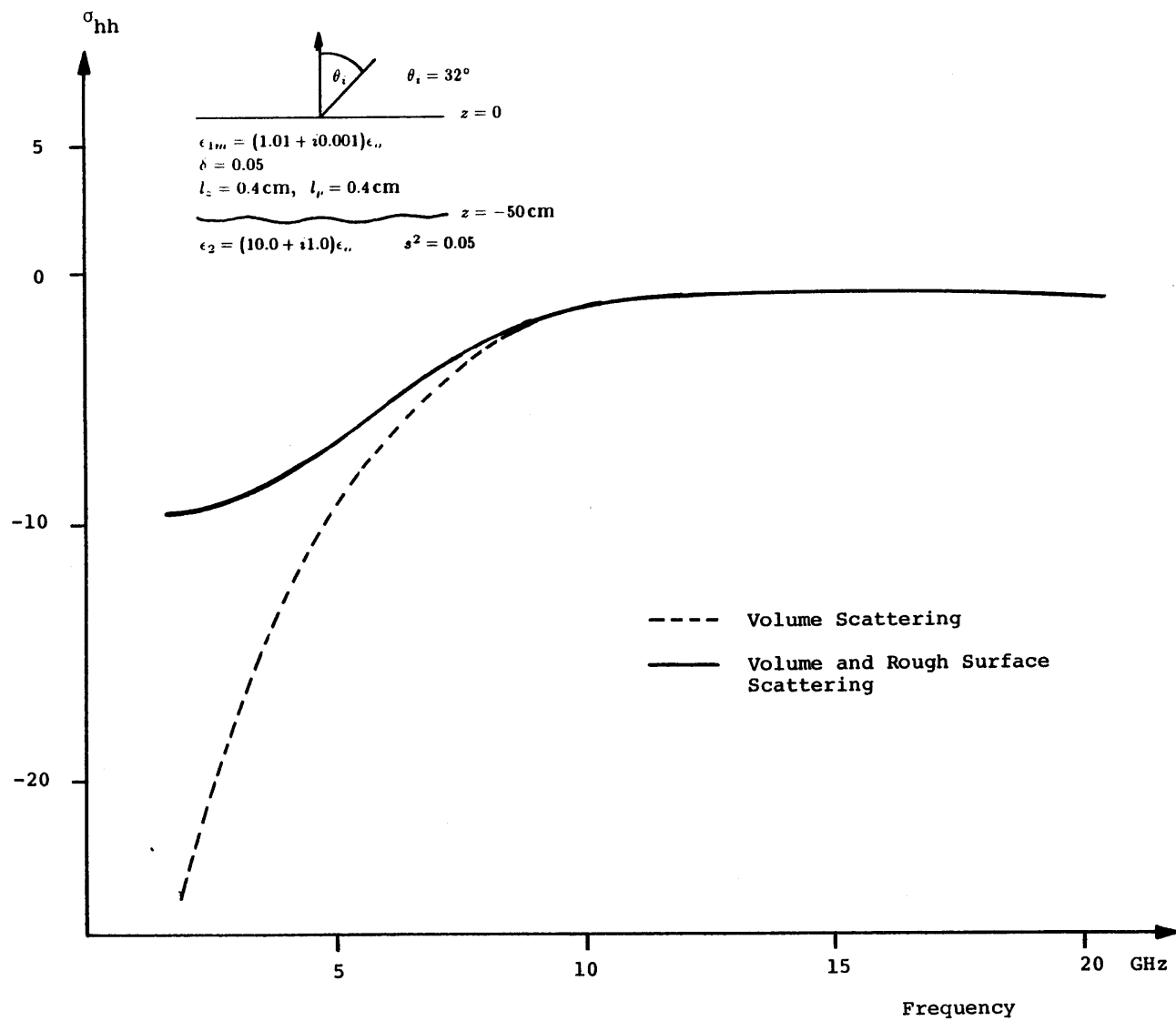


Figure 10.5 Backscattering cross sections as a function of frequency for $\theta_i = 32^\circ$.



CHAPTER 11

Conclusions and Recommendations for Future Studies

In this thesis, various theoretical models have been developed for electromagnetic wave scattering and emission from layered scattering media with applications to microwave remote sensing of earth terrain. In the active and passive microwave remote sensing of earth terrain, scattering effects due to medium inhomogeneities and surface roughness play a dominant role in the determination of brightness temperatures and radar backscattering coefficients. The volume scattering effects have been accounted for by modeling earth terrain either as a random medium or as a homogeneous medium containing discrete scatterers. The rough surface effects have been studied with models of random and periodic rough surfaces. In order to more realistically model earth terrain, a composite model which accounts for volume and rough surface scattering is developed.

The volume scattering effects due to medium inhomogeneities have been studied by characterizing earth terrain with a layered random medium model. The radiative transfer theory is used to calculate the backscattering and bistatic scattering coefficients from a two-layer random medium. Radiative transfer equations are solved numerically using the Fourier series expansion and the Gaussian quadrature method. In order to explain the scattering and emission characteristics of earth terrain which exhibit the effects of layered structure, the results have been generalized to the case

of multi-layered random medium. The complexity of the problem is kept at the same level as the two-layer cases by deriving effective boundary conditions which incorporate all the properties of the medium below that boundary.

The rough surface effects have been studied with the models of random and periodic rough surfaces. The scattering and emission characteristics of randomly rough surface is studied by deriving bistatic scattering coefficients for the reflected and the transmitted waves with the Kirchhoff approach and the small perturbation method. The geometrical optics solution modified to incorporate the shadowing effect is used to study energy conservation and to derive the upper and lower bounds for the emissivities. The small perturbation method is modified with the use of a cumulant technique which is shown to have wider regions of validity. Active remote sensing of plowed fields has been studied with the model of a randomly perturbed quasiperiodic surface and the Kirchhoff approach. The narrow-band Gaussian random variation around the spatial frequency of the sinusoidal variation is used to introduce the quasiperiodicity. It is shown that there is a large difference between the cases where the incident wave vector is parallel or perpendicular to the row direction. When the incident wave vector is perpendicular to the row direction, the maximum value of the backscattering cross section does not necessarily occur at normal incidence. The scattering pattern is interpreted as a convolution of the scattering patterns for the sinusoidal and the random rough surfaces.

The composite model comprising an inhomogeneous layer over a homogeneous halfspace with rough boundaries has been developed to study the scattering and emission characteristics of earth terrain. The radiative transfer theory is used. The random medium and discrete scatterer models are used to incorporate the volume scattering effects. To model rough top and bottom interfaces, the bistatic scattering coefficients

for a randomly rough surface obtained using a combination of Kirchhoff theory and geometrical optics approach are used. Rough surface effects are incorporated into the radiative transfer theory by modifying the boundary conditions. Because the bistatic scattering coefficients for the rough surface violate energy conservation there is ambiguity in the emissivity. However, two alternate formulations are used to calculate the emissivity. By calculating the bistatic scattering coefficients of the scattering layer with rough top and bottom interfaces and integrating over the upper hemisphere an upper limit for the emissivity is obtained by invoking the principle of reciprocity. A lower limit for the emissivity is obtained by directly calculating thermal microwave emission and assuming that the same medium is at a uniform temperature. It has been shown that the backscattering cross section for the angles of incidence near nadir is dominated by the rough surface effects whereas the large angle of incidence behavior is dominated by the volume scattering effects. The rough surface also causes the angular behavior of thermal emission to become flatter and displays smaller differences between horizontal and vertical polarizations due to more coupling of intensities at the boundaries.

The task of developing theoretical models is by no means complete. We have considered primarily the radiative transfer theory which deals with the intensities of the field quantities and neglects the coherent effects. There is a need to develop a more complete theory that accounts for the coherence effects. The interference effects due to the boundaries in the layered structures have been observed to be important in some snow field measurements. Also, the coherence effects due to the conjugate fields is large in the backscattering direction, especially for the depolarized backscattered intensities.

The problem of scattering and emission of electromagnetic waves from rough surfaces remains a challenging problem. The solution which accounts for shadowing and

multiple scattering and satisfies the principles of energy conservation and reciprocity needs to be investigated.

The combined rough surface and volume scattering problem for the anisotropic media still remains to be solved. The volume anisotropy plays a dominant role in the remote sensing of vegetation canopy with row structures or sea ice where the brine inclusions display a preferred direction. The rough surface anisotropy is a dominant effect in the remote sensing of plowed fields.

BIBLIOGRAPHY

- Agarwal, G. S. (1977). "Interaction of electromagnetic waves at rough dielectric surfaces." Phys. Rev. B. **15**, 2371-2383.
- Axline, R. M. and A. K. Fung (1978), "Numerical computation of scattering from a perfectly conducting random surface," IEEE Trans. Ant. Prop., **AP-26**, 482-488.
- Barrick, D. E. (1968), "Relationship between slope probability density function and the physical optics integral in rough surface scattering," Proc. IEEE, **56**, 1728-1729.
- Barrick, D. E. (1970). "Unacceptable height correlation coefficients and the quasispecular component in rough surface scattering," Radio Science, **5**, 647-654.
- Bass, F. G. and I. M. Fuks (1979), Wave Scattering from Statistically Rough Surface. translated by C. B. Vesecky and J. F. Vesecky, Rezon Press, Oxford.
- Batlivala, P. P. and F. T. Ulaby (1976), "Radar look direction and row crops," Photogrammetric Eng. Remote Sens., **42**, 233-238.
- Beckmann, P. (1965), "Shadowing of random rough surfaces," IEEE Trans. Ant. Prop., **AP-14**, 384-388.
- Beckmann, P. and A. Spizzichino (1963), The Scattering of Electromagnetic Waves from Rough Surfaces, MacMillan, New York.
- Blanchard, A. J. and J. W. Rouse, Jr. (1980), "Depolarization of electromagnetic waves scattered from an inhomogeneous half space bounded by a rough surface," Radio Science, **15**, 773-780.
- Blinn, J. C., III, J. E. Conel, and J. G. Quade (1972), "Microwave emission from geological materials: Observations of interference effects," J. Geophys. Res., **77**, 4366-4378.
- Bryan, M. L. and J. R. W. Larson (1975), "The study of fresh-water lake ice using multiplexed imaging radar," J. Glaciology, **14**.
- Burke, H.-h. K. and T. J. Schmugge (1982), "Effects of varying soil moisture contents and vegetation canopies on microwave emissions," IEEE Trans. Geosci. Remote Sensing, **GE-20**, 268-274.
- Burke, W. J., T. Schmugge, and J. F. Paris (1979), "Comparison of 2.8 and 1 - cm microwave radiometer observations over soils with emission model calculations," J. Geophys. Res., **84**, 287-294.
- Burrows, M. L. (1973), "On the composite model for rough surface scattering," IEEE Trans. Ant. Prop., **21**, 241-243.

- Bush, T. F. and F. T. Ulaby (1976), "Radar return from a continuous vegetation canopy," IEEE Trans. Ant. Prop., **AP-24**, 269-276.
- Bush, T. F. and F. T. Ulaby (1978), "An evaluation of radar as a crop classifier," Remote Sensing of Environment, **7** 15-36.
- Campbell, W. J., P. Gloersen, H. J. Zwally, R. O. Ramseyer, and C. Elachi (1980), "Simultaneous passive and active microwave observations of near-shore Beaufort Sea Ice," J. Petrol. Technol., **21**, 1105-1112.
- Chandrasekhar, S. (1960), Radiative Transfer, Dover, New York.
- Chang, T. C., P. Gloersen, T. Schmugge, T. T. Wilhelm, and H. J. Zwally (1976) "Microwave emission from snow and glacier ice," J. Glaciology, **16**, 23-29.
- Chan, H. L. and A. K. Fung (1978), "A numerical study of the Kirchhoff approximation in horizontally polarized backscattering from a random surface," Radio Science, **13**, 811-818.
- Choudhury B., T. J. Schmugge, A. Chang, and R. W. Newton (1979), "Effect of surface roughness on the microwave emission from soils," J. Geophys. Res., **84**.
- Chuang, S. L. and J. A. Kong (1981), "Scattering of waves from periodic rough surface," Proc. IEEE, **69**, 1132-1144.
- Chuang, S. L., J. A. Kong (1982), "Wave scattering from a periodic dielectric surface for a general angle of incidence," Radio Science, **17**, 545-557.
- Chuang, S. L., J. A. Kong, and L. Tsang (1980), "Radiative transfer theory for passive microwave remote sensing of two-layer random medium with cylindrical structures," J. Appl. Phys., **51**, 5588-5593.
- Cumming, W. A. (1952), "The dielectric properties of ice and snow at 3.2 cm," J. Appl. Phys., **23**, 768-773.
- Davenport, W. B., Jr. and W. L. Root (1958). An Introduction to the Theory of Random Signals and Noise, McGraw-Hill, New York.
- DeSanto, J. A. (1974), "Green's function for electromagnetic scattering from a random rough surface," J. Math. Phys., **15**, 283-288.
- DeSanto, J. A. (1983), "Scattering of scalar waves from a rough interface using a singular integral equation," Wave Motion, **73**, 125-135.
- De Loor, G. P., A. A. Jurrins, and H. Gravesteijn (1974), "The radar backscatter from selected agricultural crops," IEEE Trans. Geoscience Electron., **GE-12**, 70-77.
- Dickey, F. M., C. King, J.C. Holtzman, and R. K. Moore (1974), "Moisture dependency of radar backscatter from irrigated and non-irrigated fields at 400 MHz and 13.3 GHz,"

IEEE Trans. Geoscience Electron., **GE-12**, 19-22.

Djermakoye, B. and J. A. Kong (1979), "*Radiative transfer theory for the remote sensing of layered random media*," J. Appl. Phys., **50**, 6600-6604.

Edgerton, A. T., A. Stogryn, and G. Poe (1971), "*Microwave radiometric investigations of snowpacks*," Final Report 1285R-4, Aerojet-General Corp., El Monte, CA.

Elachi, C., M. L. Bryaand W. F. Weeks (1976), "*Imaging radar observations of frozen Arctic lakes*," Remote Sensing of Environment, **5**, 169-175.

England, A. W. (1974), "*Thermal microwave emission from a halfspace containing scatterers*," Radio Science, **9**, 447-454.

England, A. W. (1975), "*Thermal microwave emission from a scattering layer*," J. Geophys. Res., **80**, 4484-4496.

Evans, S. (1965), "*Dielectric properties of ice and snow - a review*," J. Glaciology, **5**, 773-792.

Fenner, R. G., G. F. Pels and S. C. Reid (1980), "*A parametric study of tillage effects on radar backscatter*," Proceedings of the Terrain and Sea Scatter Workshop (TASS), George Washington Univ., Wash., DC.

Fung, A. K. (1979), "*Scattering from a vegetation layer*," IEEE Trans. Geosci. Electro., **GE-17**, 1-5.

Fung, A. K. and H. J. Eom (1981), "*A theory of wave scattering from an inhomogeneous layer with an irregular interface*," IEEE Trans. Ant. Prop., **AP-29**, 899-910.

Fung, A. K. and H. L. Chan, (1969), "*Backscattering of waves by comsite rough surfaces*," IEEE Trans. Ant. Prop., **AP-17**, 590-597.

Fung, A. K. and H. S. Fung (1977), "*Application of first order renormalization method to scattering from a vegetated-like half space*," IEEE Trans. Geoscience Electron., **GE-15**, 189-195.

Fung, A. K. and M. F. Chen (1981a), "*Emission from an inhomogeneous layer with irregular interfaces*," Radio Science, **16**, 289-298.

Fung, A. K. and M. F. Chen (1981b), "*Scattering from a Rayleigh layer with an irregular interface*," Radio Science, **16**, 1337-1347.

Garcia, N. and N. Cabrera (1978), "*New method for solving the scattering of waves from a periodic hard surface: solutions and numerical comparisons with the various formalisms*," Phys. Rev. B, **18**, 576-589.

Garcia, N., V. Celli, N. R. Hill and N. Cabrera (1978), "*Ill-condited matrices in the scattering of waves from hard corrugated surfaces*," Phys. Rev. B, **18**, 5184-5189.

- Gloersen, P., W. Nordberg, T. J. Schmugge, T. T. Wilheit, and W. J. Campbell (1973) *Microwave signatures of first-year and multiyear sea ice,* J. Geophys. Res., **78**, 3564-3572.
- Gray, E. P., R. W. Hart, and R. A. Farrell (1978). "An application of a variational principle for scattering by random rough surfaces," Radio Science, **13**, 333-343.
- Grody, N. C. (1976). "Remote sensing of atmospheric water content from satellites using microwave radiometry," IEEE Trans. Ant. Prop., **AP-24**.
- Gurvich, A. S., V. L. Kalinin, and D. T. Matveyer (1973), "Influence of internal structure of glaciers on their thermal radio emission," Atm. Oceanic Phys. USSR, **9**, 713-717.
- Hoekstra, P. and A. Delaney (1974). "Dielectric properties of soils at UHF and microwave frequencies," J. Geophys. Res., **79**, 1699-1708.
- Hofer, R. and E. Schanda (1978), "Signatures of snow in the 5 to 94 GHz range," Radio science, **13**, 365-369.
- Hofer, R. and W. Good (1979), "Snow parameter determination by multichannel microwave radiometry," Remote Sensing of Environment, **8**, 211-224.
- Holzer, J. A. and C. C. Sung (1978), "Scattering of Electromagnetic waves from a rough surface. II," J. Appl. Phys., **49**, 1002-1011.
- Ishimaru, A. (1978), Wave Propagation and Scattering in Random Media, **1** and **2**, Academic Press, New York.
- Jackson, T. J. and T. J. Schmugge (1981), "Aircraft active microwave measurements for estimating soil moisture," Photogrammetr. Eng. and Remote Sensing, **47**, 801-805.
- Johnson, J. D. and L. D. Farmer (1971), "Use of side-looking airborne radar for sea ice identification," J. Geophys. Res., **76**, 2138-2155.
- Jordan, A. K. and R. H. Lang (1979), "Electromagnetic scattering patterns from sinusoidal surfaces," Radio Science, **14**, 1077-1088.
- Karam, M. A. and A. K. Fung (1982). "Propagation and scattering in multi-layer random media with rough interfaces," Electromagnetics, **2**, 239-256.
- Karam, M. A. and A. K. Fung (1983), "Scattering from randomly oriented circular discs with applications to vegetation," Radio Science, **18**, 565.
- Ketchum, R. D., Jr., and S. G. Tooma, Jr. (1973), "Analysis and interpretation of air-borne multifrequency side-looking radar sea ice imagery," J. Geophys. Res., **3**, 520-538.
- Kodis, R. D. (1966), "A note on the theory of scattering from an irregular surface,"

IEEE Trans. Ant. Prop., **AP-14**, 77-82.

Kong, J. A. (1975), *Theory of Electromagnetic Waves*, Wiley-Interscience New York.

Kong, J. A., ed. (1981), *Research Topics in Electromagnetic Wave Theory*, Wiley-Interscience, New York.

Kong, J. A., R. Shin, J. C. Shiue, and L. Tsang (1979), "*Theory and experiment for passive remote sensing of snowpacks*," J. Geophys. Res., **84**, 5669-5673.

Kong, J. A., S. L. Lin, and S. L. Chuang (1984), "*Microwave thermal emission from periodic surfaces*," IEEE Trans. Geoscience and Remote Sensing, **GE-22**, 377-382.

Kritikos, H. N. and J. Shiue (1979), "*Microwave remote sensing from orbit*," IEEE Spectrum, 34-41.

Kubo, R. (1962), "*Generalized cumulant expansion method*," J. Phys. Soc. Japan., **17**, 1110-1120.

Kunzi, K. F., A. D. Fisher, D. H. Staelin, and J. W. Waters (1976), "*Snow and ice surfaces measured by the Nimbus-5 microwave spectrometer*," J. Geophys. Res., **81**, 4965-4980.

Lane, J. and J. Saxton (1952), "*Dielectric dispersion in pure liquids at very high radio frequencies*," Proc. Roy. Soc., **A213**, 400-408.

Lang, R. H. and J. S. Sidhu (1983), "*Electromagnetic backscattering from a layer of vegetation: a discrete approach*," IEEE Trans. on Geoscience and Remote Sensing, **GE-21**, 62-71.

Lang, R. H. (1981), "*Electromagnetic backscattering from a sparse distribution of lossy dielectric scatterers*," Radio Science, **16**, 15-33.

Leader, J. C. (1971), "*Bidirectional scattering of electromagnetic waves from rough surfaces*," J. Appl. Phys., **42**, 4808-4816.

Leader, J. C. (1975) "*Polarization dependence in EM scattering from Rayleigh scatterers embedded in a dielectric slab. I. Theory*," J. Appl. Phys., **46**, 4371-4385.

Linlor, W. (1980), "*Permittivity and attenuation of wet snow between 4 and 12 GHz*," J. Appl. Phys., **23**, 2811-2816.

Liszka, E. G. and J. J. McCoy (1982), "*Scattering at a rough boundary-extensions of the Kirchhoff approximation*," J. Acoust. Soc. Am., **71**, 1093-1100.

Lynch, P. J. (1970), "*Curvature corrections to rough-surface scattering at high frequencies*," J. Acoust. Soc. Am., **47**, 804-815.

Lynch, P. J. and R. J. Wagner (1968), "*Energy conservation for rough surface scatter-*

ing." J. Acoust. Soc. Am., **47**, 816-821.

Lynch, P. L. and R. J. Wagner (1970). "Rough-surface scattering: Shadowing, multiple scatterer and energy conservation," J. Math. Phys., **11**, 3032-3042.

MacDonald, H. C. and W. P. Waite (1971). "Soil moisture detection with imaging radars." Water Resources Res., **7**, 100-110.

Maradudin, A. A. (1983). "Iterative solutions for electromagnetic scattering by gratings." J. Opt. Soc. Am., **73**, 759-764.

Matzler, C., E. Schanda, and W. Good (1982), "Towards the definition of optimum sensor specifications for microwave remote sensing of snow," IEEE Trans. Geosci. Remote Sensing, **GE-20**, 57-66.

Meier, M. F. and A. T. Edgerton, (1971), "Microwave emission from snow - A progress report," Proc. of the 7th International Sym. On Remote Sensing of Environment, **2**, University of Michigan, Ann Arbor, MI.

Meier, M. F. (1975), "Application of remote sensing techniques to the study of seasonal snow cover," J. Glaciol., **15**, 251-265.

Moore, R. K. and A. K. Fung (1979), "Radar determination of winds at sea," Proc. IEEE, **67**, 1504-1521.

Moore, R. K. (1966), "Radar scatterometry - an active remote sensing tool," Proc. 4th Symp. Rem. Sens. Env., University of Michigan, Ann bor, 3375.

Nakayama, J., H. Ogura, and M. Sakata (1981), "A probabilistic theory of electromagnetic wave scattering from a slightly random rough surface, 1. Horizontal polarization," Radio Science, **16**, 831-845.

Nakayama, J., M. Sakata, and H. Ogu (1981), "A probabilistic theory of electromagnetic wave scattering from a slightly random surface, 2. Vertical polarization," Radio Science, **16**, 847-853.

Newton, R. W. and J. W. Rouse, Jr. (1980), "Microwave radiometer measurements of soil moisture constant," IEEE Trans. Ant. Prop., **AP-28**, 680-686.

Nieto-Vesperinas, M. (1982), "Depolarization of electromagnetic waves scattering from slightly rough random surfaces: A study by means of the extinction theorem," J. Opt. Soc. Am., **72**, 539-547.

Njoku, E. G. and J. A. Kong (1977), "Theory for passive sensing of near-surface soil moisture," J. Geophys. Res., **82**, 3108-3118.

Njoku, E. G. and P. E. O'Neill (1981), "Multifrequency microwave radiometer measurements of soil moisture," IEEE Trans. Geoscience Remote Sensing, **GE-20**, 468-475.

Onstott, R. G., R. K. Moore, and W. F. Weeks (1979), "Surface-based scatterometer results of Arctic sea ice," IEEE Trans. on Geoscience Electronics, **GE-17**, 78-85.

Ozisik, M. N. (1973), Radiative Transfer, Wiley-Interscience, New York

Parashar, S. K., R. M. Haralick, R. K. Moore, and A. W. Biggs (1977), "Radar scatterometer discrimination of sea-ice types," IEEE Trans. Geoscience Electronics, **GE-15**, 83-87.

Peake, W. H. (1959), "Interaction of electromagnetic waves with some natural surfaces," IEEE Trans. Ant. Prop., **AP-7**, Special Supplement, S324-S329.

Rango, A., A. T. C. Chang and J. L. Foster (1979), "The utilization of spaceborne microwave radiometers for monitoring snowpack properties," Nordic Hydrol., **10**, 25-40.

Rice, S. O. (1963), "Reflection of EM waves by slightly rough surfaces," The Theory of Electromagnetic Waves, M. Kline, Ed., Interscience, NY.

Rouse, J. W., Jr. (1969), "Arctic ice type identification by radar," Proc. IEEE, **57**, 605-611.

Sancer, M. I. (1969), "Shadow-corrected electromagnetic scattering from a randomly rough surface," IEEE Trans. Ant. Prop., **17**, 577-585.

Saxton, J. A. and J. A. Lane (1952), "Electrical properties of sea water," Wireless Engineer, **29**, 269.

Schmugge, T. J. (1983), "Remote sensing of soil moisture: Recent advances," IEEE Trans. Geoscience and Remote Sensing, **GE-21**, 336-344.

Schmugge, T. J. and B. J. Choudhury, (1981), "A comparison of radiative transfer models for predicting the microwave emission from soils," Radio Science, **16**, 927-938.

Schmugge, T. J., P. Gloerson, T. Wilheit, and F. Geiger (1974). Remote sensing of soil moisture with microwave radiometers," J. Geophys. Rs., **9**, 317-323.

Semenov, B. (1966). "Approximate computation of scattering electromagnetic waves by rough surface contours," Radio Eng. Electron. Phys., **11**, 1179-1187.

Shen, J. and A. A. Maradudin (1980). "Multiple scattering of waves from random rough surfaces," Phys. Rev. B, **22**, 4234-4240.

Shin, R. T. (1980), "Radiative transfer theory for active remote sensing of layered homogeneous media containing spherical scatterers," M.S. Thesis, MIT.

Shin, R. T. and J. A. Kong (1981), "Radiative transfer theory for active remote sensing of homogeneous layer containing spherical scatterers," J. Appl. Phys., **52**, 4221-4230.

- Shin, R. T. and J. A. Kong (1982). "Theory for thermal microwave emission from a homogeneous layer with rough surfaces containing spherical scatterers" J. Geophys. Res., **87**, 5566-5576.
- Shin, R. T. and J. A. Kong (1984). "Scattering of electromagnetic waves from a randomly perturbed quasiperiodic surface," J. Appl. Phys., **56**, 10-21.
- Shiue, J. C., A. T. C. Chang, H. Boyne, and D. Ellerbruch (1978). "Remote sensing of snowpack with microwave radiometers for hydrologic applications," Proceedings of the 12th International Symposium on Remote Sensing of Environment, **2**, 877-886, Univ. of Michigan, Ann Arbor, MI.
- Smith, B. G. (1967a), "Geometrical shadowing of a random rough surface," IEEE Trans. Ant. Prop., **AP-15**, 668-671.
- Smith, B. G. (1967b), "Lunar surface roughness: Shadowing and thermal emission," J. Geophys. Res., **72**, 4059-4067.
- Staelin, D. H. (1969), "Passive Remote Sensing at Microwave Wavelengths," Proc. IEEE, **57**, 427-459.
- Stiles, W. H. and F. T. Ulaby (1980), "The active and passive microwave response to snow parameters: 1. Wetness," J. Geophys. Res., **85**, 1037-1044.
- Stogryn, A. (1967), "Electromagnetic scattering from rough finitely conducting surfaces." Radio Science, **2**, 415-428.
- Stogryn, A. (1970), "The brightness temperature of a vertically structured medium," Radio Science, **5**, 1397-1406.
- Stogryn, A. (1970), "Electromagnetic scattering by random dielectric constant fluctuations in a bounded medium," Radio Science, **9**, 509-518.
- Stratton, J. A. (1941), Electromagnetic Theory, McGraw-Hill, New York.
- Sung, C. C. and J. A. Holzer (1976). "Scattering of electromagnetic waves from a rough surface," Appl. Phys. Letters, **28**, 429-431.
- Sung, C. C. and W. D. Ekerhardt (1978), "Scattering of an electromagnetic wave from a very rough semi-infinite dielectric plane (exact treatment of the boundary conditions)," J. Appl. Phys., **49**, 994-1001.
- Swift, C. T. (1974), "Microwave radiometer measurements of the Cape Cod Canal," Radio Science, 641-655.
- Tan, H. S., A. K. Fung and H. Eom (1980), "A second order renormalization theory for cross-polarized backscatter from a half space random medium," Radio Science, **15**, 1059-1065.

- Tiuri, M. E. (1982), "Theoretical and experimental studies of microwave emission signatures of snow," IEEE Trans. on Geoscience and Remote Sensing, **GE-20**, 51-57.
- Tomiyasu, K. (1974), "Remote sensing of the earth by microwaves," Proc. IEEE, **62**, 86-92.
- Tooma, S. G., R. A. Mennella, J. P. Hollinger, and R. D. Ketchum, Jr. (1975), "Comparison of sea-ice type identification between airborne dual-frequency passive microwave radiometry and standard laser infrared techniques," J. Glaciology, **15**, 225-239.
- Tsang, L. and J. A. Kong (1975), "The brightness temperature of a half-space random medium with nonuniform temperature profile," Radio Science, **10**, 1025-1033.
- Tsang, L. and J. A. Kong (1976a), "Emissivity of half-space random media," Radio Science, **11**, 593-598.
- Tsang, L. and J. A. Kong (1976b), "Thermal microwave emission from a halfspace random media," Radio Science, **11**, 599-610.
- Tsang, L. and J. A. Kong (1976c), "Microwave remote sensing of a two-layer random medium," IEEE Trans. Ant. Prop., **AP-24**, 283-287.
- Tsang, L. and J. A. Kong (1977a), "Theory for thermal microwave emission from a bounded medium containing spherical scatterers," J. Appl. Phys., **48**, 3593-3599.
- Tsang, L. and J. A. Kong (1977b), "Thermal microwave emission from a random inhomogeneous layer over a homogeneous medium using the method of invariant imbedding," Radio Science, **12**, 185-194.
- Tsang, L. and J. A. Kong (1978), "Radiative transfer theory for active remote sensing of half space random media," Radio Science, **13**, 763-774.
- Tsang, L. and J. A. Kong (1979), "Radiative transfer theory for scattering by layered media," J. Appl. Phys., **50**, 2465-2469.
- Tsang, L. and J. A. Kong (1980a), "Energy conservation for reflectivity and transmissivity at a very rough surface," J. Appl. Phys., **51**, 673-680.
- Tsang, L. and J. A. Kong (1980b), "Thermal microwave emission from a three layer random medium with three dimensional variations," IEEE Trans. Geosci. Electro., **GE-18**, 212-216.
- Tsang, L. and J. A. Kong (1981), "Scattering of electromagnetic waves from random media with strong permittivity fluctuations," Radio Science, **16**, 303-320.
- Tsang, L. and J. A. Kong (1983), "Scattering of electromagnetic waves from a half space of densely distributed dielectric scatterers," Radio Science, **18**, 1260-1272.
- Tsang, L., E. Njoku and J. A. Kong (1975), "Microwave thermal emission from a

stratified medium with nonuniform temperature distribution, J. Appl. Phys. **46**, 5127–5133.

Tsang, L., J. A. Kong and R. W. Newton (1982), “*Application of strong fluctuation random medium theory to scattering of electromagnetic waves from a half space of dielectric mixture.*” IEEE Trans. Ant. Prop., **AP-30**, 292–302.

Tsang, L., J. A. Kong, E. Njoku, D. H. Staelin, and J. Waters (1977), “*Theory for microwave thermal emission from a layer of cloud or rain,*” IEEE Trans. Ant. Prop., **AP-25**, 650–657.

Tsang, L., J. A. Kong and R. T. Shin (1984), “*Radiative transfer theory for active remote sensing of a layer of nonspherical particles,*” Radio Science, **19** 629–642.

Tsang, L., M. C. Kubacsi, and J. A. Kong (1981), “*Radiative transfer theory for active remote sensing of a layer of small ellipsoid scatterers,*” Radio Science, **16**, 321–329.

Tsang, L. and R. W. Newton (1982), “*Microwave emissions from soils with rough surfaces,*” J. Geophysical Research, **87**, 9017–9024.

Ulaby, F. T. (1975), “*Radar response to vegetation,*” IEEE Trans. Ant. Prop., **AP-23**, 36–45.

Ulaby, F. T. and J. E. Bare (1979), “*Look direction modulation function of the radar backscattering coefficient of agricultural fields,*” Photogrammetric Eng. and Remote Sensing, **45**, 1495–1506.

Ulaby, F. T. and P. P. Batlivala (1976a), “*Diurnal variations of radar backscatter from a vegetation canopy,*” IEEE Trans. Ant. Prop., **AP-24**, 11–17.

Ulaby, F. T. and P. P. Batlivala (1976b), “*Optimum radar parameters for mapping soil moisture,*” IEEE Trans. Geosci. Electro., **GE-14**, 81–93.

Ulaby, F. T., T. F. Bush and P. P. Batlivala (1975), “*Radar response to vegetation II: 8-18 GHz band,*” IEEE Trans. Ant. Prop., **AP-23**, 608–618.

Ulaby, F. T., W. H. Stiles, L. F. Dellwig and B. C. Hanson (1977), “*Experiments on the radar backscatter of snow,*” IEEE Trans. Geosci. Electro., **GE-15**, 185–189.

Ulaby, F. T. and W. H. Stiles (1980), “*The active and passive microwave response to snow parameters: 2. Water equivalent of dry snow,*” J. Geophys. Res., **85**, 1045–1049.

Ulaby, F. T., R. K. Moore and A. K. Fung (1981), Microwave Remote Sensing: Active and Passive, **1** and **2**, Addison-Wesley, Reading, MA.

Ulaby, F. T., F. Kouyate, A. K. Fung and A. J. Sieber (1982), “*A backscatter model for a randomly perturbed periodic surface,*” IEEE Trans. Geosci. Remote Sens., **GE-20**, 518–528.

- Valenzuela, G. R. (1967), "*Depolarization of EM waves by slightly rough surfaces,*" IEEE Trans. Ant. Prop., **AP-15**, 552-557.
- Valenzuela, G. R. (1968), "*Scattering of EM waves from a tilted slightly rough surface,*" Radio Science, **3**, 1057-1064.
- Vallese, F. and J. A. Kong (1981), "*Correlation function studies for snow and ice,*" J. Appl. Phys., **52**, 4921-4925.
- Waite, W. P. and H. C. McDonald (1969-70), "*Snow-field mapping with K-band radar,*" Rem. Sen. Environ., **1**, 143-150.
- Wagner, R. J. (1967), "*Shadowing of randomly rough surface,*" J. Acoust. Soc. Am., **41**, 138-147.
- Wang, J. R. and T. J. Schmutge (1980), "*An empirical model for the complex permittivity of soils as a function of water content,*" IEEE Trans. Geoscience Remote Sensing, **GE-18**, 288-295.
- Wang, J. R., P. E. O'Neill, T. J. Jackson, and E. T. Engman (1983), "*Multifrequency measurements of the effects of soil moisture, soil texture and surface roughness,*" IEEE Trans. Geoscience and Remote Sensing, **GE-21**, 44-51.
- Wang, J. R., R. W. Newton, and J. W. Rouse (1980), "*Passive microwave remote sensing of soil moisture: The effect of tilled row structure,*" IEEE Trans. Geosci. Remote Sens., **GE-18**, 296-302.
- Wang, J. R., J. C. Shiue, S. L. Chuang, R. T. Shin and M. Dombrowski (1984), "*Thermal microwave emission from vegetated fields; a comparison between theory and experiment,*" IEEE Trans. on Geoscience and Remote Sensing, **GE-22**, 143-150.
- Waterman, P. C. (1975), "*Scattering by periodic surfaces,*" J. Acoust. S. Am., **57**, 791-802.
- Zipfel, G. C. Jr., and J. A. DeSanto (1972), "*Scattering of a wave from a random rough surface: a diagrammatic approach,*" J. Math. Phys., **13**, 1903-1911.
- Zuniga, M. and J. A. Kong (1980), "*Active remote sensing of random media,*" J. Appl. Phys., **51**, 74-79.
- Zuniga, M. and J. A. Kong (1981), "*Mean dyadic Green's function for a two-layer random medium,*" Radio Science, **16**, 1255-1270.
- Zuniga, M. A. and J. A. Kong (1980), "*Modified radiative transfer theory for a two-layer random medium,*" J. Appl. Phys., **51**, 5228-5244.
- Zuniga, M., J. A. Kong, and L. Tsang (1980), "*Depolarization effects in the remote sensing of random media,*" J. Appl. Phys., **51**, 2315-2325.

Zuniga, M., T. M. Habashy, and J. A. Kong (1979), "Active remote sensing of layered random media," IEEE Trans. Geosci. Electron., **GE-17**, 296-302.

Zwally, H. J. (1977), "Microwave emissivity and accumulation rate of polar firn," J. Glaciology, **18**, 195-215.

BIOGRAPHICAL NOTE

Robert T. Shin was born in Seoul, Korea on January 16, 1955. He received the B.S. and M.S. degrees in electrical engineering in 1977 and 1980, respectively, from the Massachusetts Institute of Technology, Cambridge, MA. In the years as a graduate student, he served both as a research assistant and a teaching assistant.

His research interest is in the area of theoretical model development and data interpretation for microwave remote sensing.

He is a member of Tau Beta Pi and Eta Kappa Nu.